Random geometry and free energy of critical planar lattice models

Mendes Oulamara

université
PARIS-SACLAY

Random geometry and free energy of critical planar lattice models

Géométrie aléatoire et énergie libre de modèles critiques sur réseau planaire

Thèse de doctorat de l'université Paris-Saclay

École doctorale n°574 : mathématiques Hadamard (EDMH)
Spécialité de doctorat: Mathématiques fondamentales
Graduate School : Mathématiques
Référent : Faculté des sciences d'Orsay

Thèse préparée dans le Laboratoire Alexander Grothendieck (Université Paris-Saclay, IHES, CNRS) sous la direction de Hugo Duminil-Copin, Professeur.

Thèse soutenue à Paris-Saclay, le 9 juin 2022, par

Mendes OULAMARA

Composition du jury :

Geoffrey Grimmett Professeur, University of Cambridge	Président
Vincent Beffara Directeur de Recherche, Institut Fourier, Grenoble	Rapporteur & Examinateur
Ron Peled Professeur, Tel Aviv University	Rapporteur & Examinateur
Nicolas Curien Professeur, Université Paris-Saclay	Examinateur
Christophe Garban Professeur, Université Lyon 1	Examinateur
Hugo Duminil-Copin Professeur, IHÉS, Université de Genève	Directeur de thèse

THESE DE DOCTORAT
NNT : 2022UPASM008

université PARIS-SACLAY | ÉCOLE DOCTORALE de mathématiques Hadamard (EDMH)

Titre: Géométrie aléatoire et énergie libre de modèles critiques sur réseau planaire
Mots clés: percolation, universalité, modèle Six-vertex, Incipient Infinite Cluster

Résumé: Dans cette thèses, nous nous intéressons aux conséquences de l'expression de l'énergie libre du modèle six-vertex sur deux modèles planaires, la percolation de Fortuin-Kasteleyn (FK) et la fonction de hauteur du modèle six-vertex. Nous prouvons l'invariance par rotation macroscopique de la percolation FK critique sur le réseau carré pour $q \in [1, 4]$. Pour cela, nous prouvons l'universalité de ce modèle sur les graphes isoradiaux rectangulaires. L'Incipient Infinite Cluster nous permet alors l'étude locale de la géométrie des composantes connexes macroscopiques. Nous démontrons ensuite la délocalisation logarithmique de la fonction de hauteur du modèle six-vertex pour $\mathbf{a} = \mathbf{b} = 1$ et $1 \leq \mathbf{c} \leq 2$. Pour cela, nous construisons une théorie de Russo-Seymmour-Welsh pour ses ensembles de niveau. Dans une section bibliographique, nous exposons le formalisme de lignes de rapidité des graphes isoradiaux et les équations q-Knizhnik–Zamolodchikov.

Title: Random geometry and free energy of critical planar lattice models
Keywords: percolation, universality, six-vertex model, Incipient Infinite Cluster

Abstract: In this thesis, we study the consequences of the expression of the six-vertex model free energy on two planar models, the random cluster model (or Fortuin-Kasteleyn (FK) percolation) and the six-vertex height function. We prove the macroscopic rotational invariance of the critical random cluster model on the square lattice for $q \in [1, 4]$. As an intermediary result, we prove the universality of the model on isoradial rectangular lattices. We use the Incipient Infinite Cluster to study the local geometry of the macroscopic clusters. We prove the logarithmic delocalization of the six-vertex height function with $\mathbf{a} = \mathbf{b} = 1$ and $1 \leq \mathbf{c} \leq 2$. To do so, we construct a Russo-Seymmour-Welsh theory for the levelsets. In a bibliographical section, we expose the rapidity line formalism of isoradial graphs and the q-deformed Knizhnik–Zamolodchikov equations.

université
PARIS-SACLAY

FACULTÉ
DES SCIENCES
D'ORSAY

Fondation mathématique
FMJH
Jacques Hadamard

Remerciements

Quand, en 2018, je cherchais un sujet de thèse, j'avais une idée assez précise du type de mathématiques que je voulais faire, et l'envie de trouver quelqu'un avec qui je m'entendrai bien pour m'encadrer. Je te remercie, Hugo, d'avoir permis à ce plan de se réaliser. Merci pour la grande liberté que tu m'as accordée pendant ma thèse, tout en étant toujours très disponible, réactif et à l'écoute dès que j'en avais besoin. Avec toi, j'ai découvert une façon de faire de la recherche que je croyais réservée aux fictions mathématiques : ces très (très) longues discussions à plusieurs devant un tableau, ces arguments flous qui se clarifient au fil des mois, ces hypothèses audacieuses dont on se rend compte, après un an, qu'elles étaient correctes. J'ai aussi appris à être patient, à passer des semaines, parfois plus, à forger, seul, des arguments sur mon cahier de brouillon. J'ai beaucoup appris et je t'en remercie.

Toute ma gratitude va aux deux rapporteurs de ma thèse, Vincent Beffara et Ron Peled. Lire ou relire des preuves mathématiques est un travail toujours long et laborieux, parfois pénible. Je vous remercie profondément d'avoir accepté cette tâche.

Je remercie également les autres membres de mon jury de thèse. Nicolas Curien, pour m'avoir accueilli toutes les fois où je suis venu suivre des cours ou des séminaires de l'autre côté de l'Yvette. Christophe Garban, pour nos nombreuses rencontres dans les évènements mathématiques, ta sympathie et ta disponibilité sans faille, tes exposés clairs et agréables. Geoffrey Grimmett, pour m'avoir fait découvrir la percolation lors d'un cours à Cambridge en 2015, bien avant que je sache que je ferai une thèse de probabilités.

Parmi les personnes avec qui j'ai pu collaborer tu as, Ioan, une place particulière. Tu as été pour moi comme un second directeur de thèse et les discussions que nous avons eu, ton humilité et ton honnêteté face aux doutes et aux difficultés de la recherche m'ont été d'une aide précieuse pour surmonter les questionnements et autres syndromes de l'imposteur auxquels nous avons tous et toutes à faire face. J'ai aussi beaucoup appris mathématiquement de nos agréables séances de travail à Fribourg, les nombreuses fois où tu m'y as invité.

Cette thèse n'aurait pas été la même sans les probabilistes de l'IHÉS. Merci à Franco et Subhajit de m'y avoir accueilli, d'avoir accompagné les premiers pas de mon séjour ici, de m'avoir introduit à cette communauté de recherche. Merci à Alex Karrila pour nos longues séances de travail à faire des dessins, nous partager l'écriture d'arguments, débattre et essayer de nous accorder sur la meilleure manière de définir tel ou tel objet; mais aussi pour les récitals de guitare et le salmiakki koskenkorva. Je n'oublie pas non plus Pierre-François et nos concours de trottinette, les discussions mathématiques que j'ai eu avec Piet, ni les explications de François sur Yang-Mills, les connexions et les transitions de phase.

J'ai pu aller de nombreuses fois à Genève et j'ai appris à connaître ce groupe de probabilité jumeau. Dima Krachun, nos thèses auront été des parallèles avec de nombreux points d'intersection. Marianna, merci pour l'invitation aux Diablerets et le karaoké. Jhih-Huang, j'admire ton approche courageuse du calcul sur tableau noir.

Les écoles d'été auxquelles j'ai pu participer ont été l'occasion de belles rencontres dont certaines sont devenues des amitiés. Merci à Sébastien Martineau pour nos balades discursives et tes questions "qui n'intéressent personne", à Sébastien Ott pour les intuitions physiques et la lutte contre la gravité, à Alejandro, à Barbara pour le binôme de lecture le plus enthousiasmant que j'ai pu avoir, à Hugo (l'autre) et à Alejandro (l'autre) pour nos discussions non mathématiques.

Je suis reconnaissant envers Sasha de m'avoir donné un avant goût de postdoc par notre collaboration à distance. Merci pour ton accueil extraordinaire à Vienne, ta gentillesse, les heures de dessins au tableau, les balades dans les vignobles. J'espère que tu te plairas à Innsbruck. Merci à Rémy pour nos échanges sur les doutes du doctorat comme sur le BTP, sur les S-embeddings, comme sur la politique algérienne. Il nous reste à faire de la plomberie ensemble un de ces jours. Merci à Paul pour les thés mathématiques que nous avons partagés à Fribourg, et puis tout le reste. Il va bien falloir que l'on reprenne le travail sur les temps de mélange, non ?

Mon séjour à l'IHÉS aurait été plus triste sans ses visiteurs de passage et ses non probabilistes. Merci à Itai pour tes questions et nos discussions, très courtes mais fructueuses, lors des quelques jours que tu as passés ici. Merci à Olivier, Katie et Pierre-Louis de m'avoir initié à la géométrie lors de notre groupe de lecture sur la percolation de graphes hyperboliques. JB, j'ai beaucoup apprécié notre expérience de stage de recherche.

Merci aussi à celles et ceux qui ont fait que ma vie à l'IHÉS ne soit pas que mathématique. Amadou, nos discussions ont grandement égayé les premières années de ma thèse. Maria, les notres ont égayé les dernières. Je remercie également toutes les personnes travaillant à l'institut et, sans vouloir faire de distinction, je me dois tout de même de mentionner ici Corina, Alex, Patrick, Absatou, Hayette, Veronica, Gourab, Luis, Yves...

C'était important pour moi d'enseigner durant ces années et je remercie l'équipe d'enseignement de l'université pour les conditions dans lesquelles j'ai pu faire cela. Merci notamment à Nathanaël Enriquez, dont j'ai eu beaucoup de joie à partager le cours. Merci également à Valérie et toute l'équipe de la MISS pour m'avoir appris à faire de la médiation scientifique auprès de plus jeunes publics.

Ces années de thèse n'auraient pas existé sans toutes celles et ceux qui m'ont amené ici et qui ont été là pour moi. Certaines influences ont été évidentes, d'autres ont résonné bien plus tard, dans tous les cas elles sont multiples. Hors du champs professionnel, l'exhaustivité est difficile alors, contrairement à l'usage commun des remerciements de thèse, je me limiterai ici à d'anonymes collectifs. Merci aux rencontres qui m'ont permis d'être curieux et m'ont appris à être ce que je suis aujourd'hui, dans et hors de l'école. Merci à mes ami·es. Merci à ma famille, à mes parents.

Table des matières

Outlines of the thesis

In Chapter I we introduce, in french, the basics of percolation theory and of the random cluster model on isoradial graphs. We present conjectures related to universality, conformal invariance and the scaling limit. We explain how the work presented in this thesis draws a link between free energy computations and results about the random geometry of, respectively, critical percolation clusters and level set of the height function of the six-vertex model.

In Chapter II, we prove the rotational invariance of the critical random cluster model for $q \in [1, 4]$. We prove a universality result for isoradial rectangular graph using the star-triangle transformation and an exact free-energy computation (that results from the Bethe Ansatz in [DCKK$^+$20b]). The star-triangle transformation enables us to interpolate between different underlying lattices and the free-energy computation is used to show that when doing so, the macroscopic clusters are not deformed. This proof, using a free-energy computation, is the first version of the paper that we cite as [DCKK$^+$20a]. In a newer version that is not exposed in this thesis but that is submitted for publication, we avoid using the Bethe Ansatz: we do not prove a priori that the displacement speed is zero (i.e. Section II.4) and the coupling arguments of Section II.6 yields a bound on $d_{\mathbf{CN}}\left[\phi_{\delta\mathbb{L}(\alpha)}, \phi_{\delta\mathbb{L}(\beta)} \circ M_{\beta,\alpha}^{-1}\right]$ where $M_{\beta,\alpha}$ is some linear map; then results on the structure of the family $(M_{\alpha,\beta})$ enable us to deduce rotational invariance. This is a joint work with Hugo Duminil-Copin, Karol Kozlowski, Dmitry Krachun and Ioan Manolescu.

In Chapter III, we prove the logarithmic delocalization of the six-vertex height function for $\mathbf{a} = \mathbf{b} = 1$ and $1 \leq \mathbf{c} \leq 2$. We do so by using bounds on the free-energy to prove a Russo-Seymmour-Welsh theory for the levelsets of the height function. This is the content of [DCKMO20], which is a joint work with Hugo Duminil-Copin, Alex Karrila and Ioan Manolescu.

In Appendix A, we explain how the existing proofs of existence of the Incipient Infinite Cluster in percolation also apply, up to slight careful modifications, to the random cluster model. In particular, we give a proof of polynomial mixing for the convergence to the IIC measure.

Appendix B is a bibliographical exposition of the "rapidity line" formalism of percolation on isoradial graphs and transformations such as the star-triangle/Yang-Baxter equation. As an application of this formalism, we present the work of [IP12] that establishes the q-deformed Knizhnik-Zamolodchikov equation for passage probabilities of the percolation process on a strip.

I | Introduction *(in french)*

I.1 Du charbon à la percolation

La porosité du charbon

L'histoire de la percolation prend ses racines dans l'industrie du charbon. À partir de la révolution industrielle, l'importance économique de cette source d'énergie a stimulé de nombreuses études sientifiques pour en comprendre la composition et en optimiser l'utilisation. Dans les années 1930 et 1940, l'étude qualitative par des méthodes de chimie organique laisse peu à peu la place à des méthodes physico-chimiques plus quantitatives [vK82].

C'est dans ce contexte qu'est créée en 1938 la British Coal Utilisation Research Association (BCURA), association de recherche financée par les propriétaires de mines de charbon. En 1942, Rosalind Franklin[1], alors diplômée en chimie de l'université de Cambridge, rejoint la BCURA. Elle y est chargée d'entreprendre des recherches sur la densité et la porosité du charbon. Pendant la Seconde Guerre Mondiale, le charbon est alors une ressource d'importance stratégique, non seulement comme combustible (dans la métallurgie notamment), mais aussi comme le constituant essentiel des masques à gaz.

Le charbon est un milieu poreux. Pour mesurer sa densité "réelle", il faut le plonger dans un liquide ou un gaz dont les molécules sont assez fines pour en remplir les pores microscopiques. En essayant de mesurer la densité du charbon à l'aide de différent gaz (hélium, méthanol, hexane, benzène) et en trouvant différentes valeurs selon le gaz utilisé, Rosalind Franklin met en évidence que les pores du charbon sont formés de micro-structures de largeur variables qui discriminent les molécules de gaz selon leur taille : ces pores jouent le rôle d'un tamis moléculaire. Elle découvre également que ces largeurs dépendent de la température de carbonisation à laquelle est produit le charbon. Ces recherches lui permettent de soutenir une thèse de doctorat, et elle quitte la BCURA en 1946. [Har01, ros]

Au milieu des années 1950, Simon Broadbent[2] travaille à la BCURA comme statisticien. Il s'intéresse, entre autres sujets liés au charbon, à la conception des masques à gaz. Il s'agit alors de comprendre la pénétration d'un fluide dans les pores du charbon, modélisés comme un labyrinthe formé de tunnels ouverts ou fermés. En 1954, à l'occasion d'un symposium sur les méthodes Monte Carlo, il questionne John

[1] (1920 - 1958) Elle est principalement connue aujourd'hui pour avoir découvert la structure en double-hélice de l'ADN, découverte qui sera occultée par Watson et Crick.

[2] (1928 - 2002)

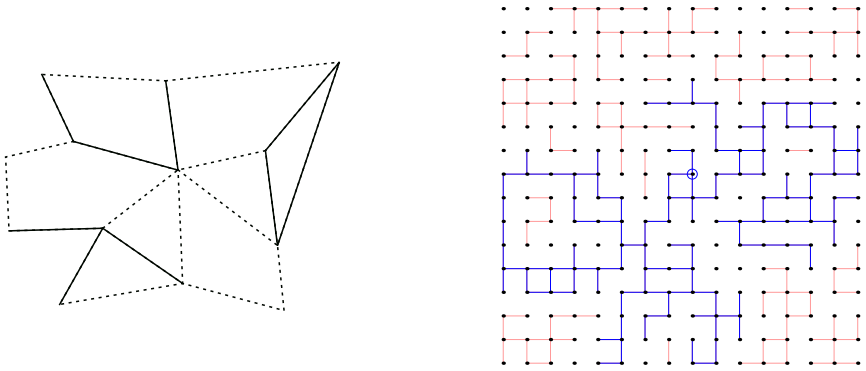

Figure I.1: **À gauche** : Un graphe G où on a tiré une configuration de percolation ω : les arêtes e en pointillé sont fermées ($\omega_e = 0$) et celles en trait plein sont ouvertes ($\omega_e = 1$). Dans cet exemple il y a trois composantes connexes. **À droite** : Une configuration de percolation sur le graphe carré. Seules les arêtes fermées sont représentées. En bleu, la composante connexe du noeud entouré relie le bord gauche au bord droit du carré. Les autres composantes connexes sont représentées en rouge.

Hammersley[3] sur l'utilisation de ces méthodes numériques pour analyser ce modèle [HW80]. Broadbent et Hammersley introduisent dans leur article de 1957 [BH57] un modèle mathématique, la percolation, pour modéliser ce phénomène.

Percolation de Bernoulli

Le modèle de percolation le plus simple à définir est le suivant. On se donne un nombre réel $p \in [0, 1]$ et un graphe $G = (V, E)$ composé d'un ensemble de sommets V reliés entre eux par un ensemble d'arêtes E. Le graphe G modélise un réseau de tunnels. Pour chaque arête e, on tire indépendamment une variable aléatoire ω_e qui vaut 1 avec probabilité p et 0 avec probabité $1 - p$. Si $\omega_e = 1$ on dit que l'arête e est *ouverte*, sinon elle est *fermée*. On appelle ω notre *configuration* aléatoire, qu'on peut voir comme un sous-graphe aléatoire de G (comme le graphe de gauche de la figure I.1).

Les premières propriétés que l'on étudie en percolation sont des propriétés de connectivité. On dit que deux sommets x, y ou deux régions A, B, du graphe G sont *connectées* s'il existe un chemin d'arêtes ouvertes dans ω qui permet de passer de l'une à l'autre (par exemple, les bords de gauche et de droite du graphe carré de la figure I.1). On note alors $x \leftrightarrow y$, ou $A \leftrightarrow B$ pour ces évènements. La *composante connexe* d'un sommet v est l'ensemble des sommets accessibles depuis v par un chemin ouvert dans ω, on la note C_v. Si la taille de C_v est infinie, on dit que v est connecté à l'infini, ce qu'on note $v \leftrightarrow \infty$.

Si le graphe G est infini, on peut aussi s'intéresser à l'évènement où il existe, quelque part dans G, une composante connexe infinie. On note cet évènement $\{\exists \text{c.c.} \infty\}$.

Supposons à partir de maintenant que le graphe G est le graphe carré $\mathbb{Z}^2$ du plan, c'est-à-dire le graphe dont les sommets sont les points de $\mathbb{Z}^2$ et les arêtes relient les

[3] (1920 - 2004)

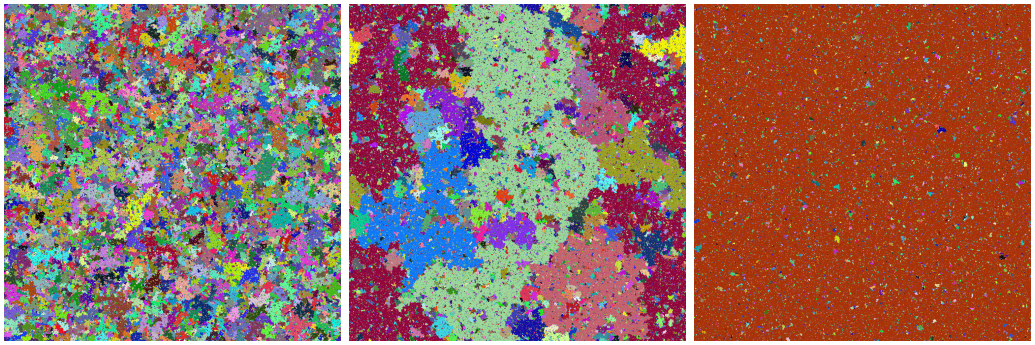

Figure I.2: Percolation de Bernoulli sur une grille carrée périodique de dimension 1000×1000. Chaque composante connexe est coloriée avec une couleur aléatoire. À gauche $p = 0.47$, au centre $p = p_c = 0.5$, à droite $p = 0.53$.

plus proches voisins. Notons 0 le sommet de coordonnées $(0, 0)$. Il est alors possible de montrer ([BH57]) qu'il existe une valeur particulière de p strictement entre 0 et 1, notée p_c et appelée *paramètre critique* qui sépare deux comportements du modèle radicalement différents.

Theorem I.1.1. *Si* $p < p_c$, *alors* $\mathbb{P}_p(\{\exists \text{c.c.} \infty\}) = 0$ *et* $\mathbb{P}(0 \leftrightarrow \infty) = 0$.
Si $p > p_c$, *alors* $\mathbb{P}_p(\{\exists \text{c.c.} \infty\}) = 1$ *et* $\mathbb{P}(0 \leftrightarrow \infty) > 0$.

On dit que ce modèle admet une *transition de phase* à p_c. Pour ce réseau particulier, Kesten a démontré en 1980 [K$^+$80] que $p_c = \frac{1}{2}$. L'ensemble $p \in [0, p_c[$ correspond à la *phase sous-critique*, dans laquelle le réseau aléatoire est essentiellement déconnecté. À l'inverse, dans la phase sur-critique $p \in]p_c, 1]$, la connexion prédomine. Entre les deux, dans la *phase critique* $p = p_c$, les choses sont plus complexes (voir la figure I.2).

On peut se représenter ce modèle de la façon suivante. Le plan correspond à une carte géographique, où les arêtes ouvertes sont des routes sur des zones de terre, et les arête fermées sont des lacs qui bloquent le passage. Le théoreme précédent veut dire visuellement que pour $p < p_c$, il n'y a que des îles, alors que pour $p > p_c$, il existe un continent infini. Plusieurs questions se posent alors : quelle est la forme de ces îles ? Dans le second cas y-a-t-il un océan infini ? Y-a-t-il des îles de toutes tailles ? Toutes ces questions prennent leur sens lorsque l'on s'éloigne de l'image : la maille du réseau devient microscopique et on ne voit plus que les propriétés macroscopiques, c'est-à-dire à grande échelles. On appelle cela prendre la *limite d'échelle*.

En poursuivant la métaphore, dans le cas sur-critique, on ne voit macroscopiquement qu'un continent infini, sans lacs qui disparaissent à mesure qu'on s'éloigne. À l'inverse, dans le cas sous-critique on ne voit qu'un océan infini, dont les îles sont également microscopiques. Autrement dit, dans ces deux cas, la géométrie de la limite d'échelle n'est pas très riche. En revanche, à criticalité, c'est-à-dire $p = p_c$, ce que l'on observe est une coexistence entre connexion et déconnexion, autrement dit terre et eau, à toutes les échelles. Il n'y a alors ni continent infini, ni océan infini, mais des îles, dans des lacs, dans des îles...

Pour un exposé plus détaillé, se réferer à [Gri99, Gri04, DC17].

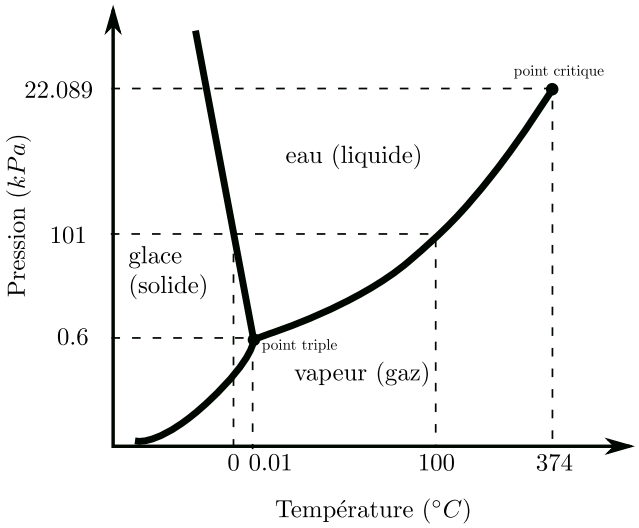

Figure I.3: Diagramme de phase de l'eau en fonction de la pression et de la température.

Physique statistique

La physique statistique est née vers le milieu du XIX^{e} siècle à partir de l'étude de gaz de particules, notamment avec les travaux de Kelvin, Maxwell, Boltzmann.

Si l'on s'intéresse à la trajectoire d'une seule particule dans le vide, par exemple une molécule d'eau, il est possible d'utiliser les équations du mouvement de la mécanique classique pour obtenir l'évolution de sa position et de sa vitesse. Si en revanche on considère simultanément la trajectoire d'un grand nombre de particules, le nombre d'équations à résoudre devient énorme. Par exemple, dans un kilogramme d'eau liquide, il y a de l'ordre de 3×10^{25} molécules d'eau.

Autrement dit, dans un tel *système complexe*, l'état exact du système, appelé *micro-états* (c'est-à-dire la position et la vitesse de chaque particule) ne nous est pas accessible. On décrit alors l'état du système et son évolution par des variables d'états (température, pression, magnétisation...) qui permettent de décrire des *macro-état*, c'est-à-dire des regroupements de micro-états.

La théorie des probabilités intervient à partir de l'une des hypothèses de Boltzmann, qui postule que le système se trouve dans un micro-état aléatoire parmi ceux qui sont accessibles. L'objet de la physique statistique est alors de comprendre le passage des lois qui décrivent les constituants élémentaires (ici le mouvement des particules), à celles décrivant l'évolution macroscopique du système (température, pression...).

Un système macroscopique peut se trouver dans différents états, ou phases. Par exemple, l'eau peut être sous forme solide, liquide ou gazeuse. Or, le passage d'une phase à une autre met en jeu un concept central de la physique statistique, celui de *transition de phase*. c'est-à-dire qu'il existe des seuils critiques des paramètres (température, pression) dont le dépassement fait passer le système d'une phase à une autre très différente. Par exemple, pour l'eau à pression atmosphérique, la température critique d'ébullition, qui est la frontière entre l'etat liquide et l'état gazeux, est de 100°C (voir le diagramme de phases à la figure I.3).

Des phénomènes de transition de phase se retrouvent dans d'autres domaines de la physique que la mécanique statistique des gaz. En 1902, Gibbs formalise les principes de la mécanique statistique [Gib02]. Cette formalisation ouvre la voie à la généralisation de la méthode de la physique statistique à d'autres phénomènes, et en premier lieu à l'étude des transitions de phase dans les matériaux magnétiques.

L'application de la physique statistique à l'étude de la percolation s'inscrit dans ce mouvement. Dans ce modèle, il n'y a pas de particules à proprement parler. Mais ce qui rend applicable ce paradigme est le grand nombre de *degrés de liberté*, c'est-à-dire de variables permettant de décrire l'état du système. Nous l'avons vu, pour un gaz, il faudrait décrire la position et la vitesse de chaque particule. Pour une configuration de percolation, il faudrait décrire le statut (ouvert ou fermé) de chacun des tunnels (ou arête du graphe). Ce grand nombre de degrés de liberté a pour conséquence, à grande échelle, l'existence de plusieurs phases et d'un paramètres critique p_c.

I.2 Universalité

De nombreuses techniques que nous allons utiliser ne sont disponibles qu'en dimension 2, nous nous y limiterons donc. Par ailleurs, dans la suite nous nous plaçons toujours au paramètre critique p_c, c'est-à-dire *à criticalité*.

Nous voulons étudier la géométrie des composantes connexes aléatoires. Dans ce cadre, une idée fondamentale est celle d'*universalité*. En physique statistique, cela désigne le fait que les propriétés macroscopiques du système (c'est-à-dire les propriétés de la limite d'échelle) ne dépendent pas des détails microscopiques du modèle, mais de caractéristiques plus essentielles comme certaines symétries, la dimension... Par exemple, pour la percolation de Bernoulli, on s'attend à ce que la limite d'échelle à criticalité ne dépende pas du graphe que l'on considère.

La première formulation de l'universalité semble avoir été introduite par Kadanoff dans les années 1960 et est justifiée par le formalisme du *groupe de renormalisation*. Cependant, pour la percolation en dimension 2, une autre transformation indique fortement l'existence du phénomène d'universalité. Il s'agit de la transformation triangle étoile. On peut se référer à [Bat19] pour un exposé plus détaillé de l'approche par le groupe de renormalisation, et à [Gri14] pour une autre présentation du contenu de cette section.

Transformation triangle-étoile et universalité

La transformation triangle-étoile apparait en 1899 dans des travaux de Kennelly sur les réseaux de résistances électriques [Ken99a]. Dans un circuit électrique, on peut mesurer la résistance entre deux points. D'après le théorème de Kennelly (figure I.4), si un circuit C contient une "étoile" de résistances R_1, R_2, R_3, alors, si on définit le circuit C' à partir de C en remplaçant l'étoile par un triangle de résistances R'_1, R'_2, R'_3, on obtient un circuit équivalent dans le sens ou la résistance mesurée entre toute paire de points de C ou C' est la même (sauf évidemment au point au milieu de l'étoile, qui n'existe plus dans C').

Cette transformation a été redécouverte pour de nombreux modèles de physique statistique planaire [PAY06, BdT12], d'abord par Onsager et Kramers-Wannier dans

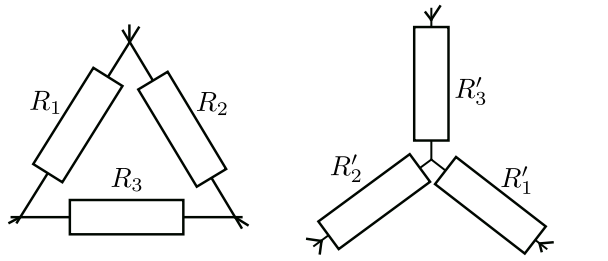

Figure I.4: Transformation triangle-étoile dans un circuit électrique.

l'étude du modèle d'Ising, puis en percolation critique dans plusieurs travaux [ES64, Gri99, GM13a, GM13b, GM14].

Pour étendre la transformation triangle-étoile à la percolation, il est nécessaire de définir le modèle de percolation *non homogène*. Au lieu d'avoir le même paramètre $p \in [0, 1]$ pour chaque arête e, ce paramètre dépend de l'arête. On le note alors p_e.

Contrairement à la transformation des réseaux électriques où aucune condition n'est nécessaire sur les résistances, pour la percolation, on ne peut appliquer la transformation que si les poids p_1, p_2, p_3 des côtés du triangle vérifient

$$p_1 + p_2 + p_3 - p_1p_2p_3 = 1. \tag{I.1}$$

Dans ce cas, la transformation donnée par la figure I.5 préserve les probabilités de connexion $\mathbb{P}(u \leftrightarrow v)$ entre toute paire de sommets u, v du graphe (sauf le sommet v_* au milieu de l'étoile, qui existe dans un graphe et pas dans l'autre). On remarque que la *fonction à deux points* de la percolation est la probabilité $\mathbb{P}(u \leftrightarrow v)$, là où pour les réseaux électriques, il s'agissait de la résistance mesurée entre deux points (et pour les modèles de spin, de la corrélation spin à spin).

L'un des premiers résultats que permet cette transformation est l'équivalence entre la percolation critique sur le réseau triangulaire et sur le réseau hexagonal. En effet, il se trouve que la condition sur les poids permettant d'appliquer la transformation correspond aux poids critiques [GM13a]. Sur la figure I.6, les sommets initialement présents dans le réseau triangulaire ont les mêmes probabilités de connectivité dans le réseau hexagonal. La condition sur les poids permet notamment

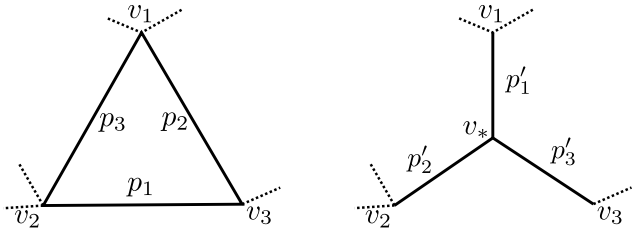

Figure I.5: Transformation triangle-étoile pour la percolation. On a $p'_i = 1 - p_i$ pour $i = 1, 2, 3$.

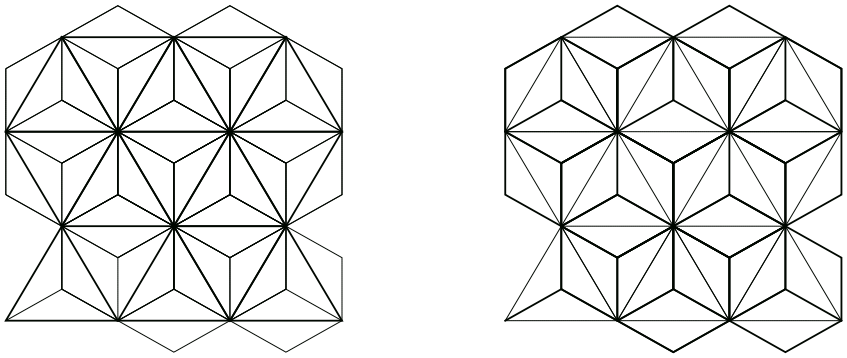

Figure I.6: Équivalence entre la percolation sur les réseaux triangulaire et hexagonal.

de retrouver les paramètres critiques de ces deux réseaux :

$$p_\triangle = 1 - p_\hexagon$$
$$3p_\triangle - p_\triangle^3 = 1$$

d'où $p_\triangle = 2\sin(\pi/18)$ et $p_\hexagon = 1 - 2\sin(\pi/18)$.

Cette transformation montre que les connectivités macroscopiques et la forme des composantes connexes à la limite sont les mêmes dans le réseau hexagonal et le réseau triangulaire. On a pu passer d'un réseau à l'autre car les poids autour de chaque triangle vérifient la condition (I.1). Pour étendre cette preuve d'universalité par transformation triangle-étoile, nous allons définir une classe de réseaux pondérés dont les poids vérifient (I.1).

Graphes isoradiaux

Les graphes isoradiaux sont une classe de graphes plongés dans le plan, qui ont d'abord été introduits pour définir ce que doivent être les fonctions holomorphes discrètes [Duf68, Mer01]. Ils ont été utilisés dans l'étude du modèle d'Ising [CS12] et du modèle de dimère [Ken02, BdT12]. Le modèle de percolation sur les graphes isoradiaux à été défini par Kenyon [Ken03], et la preuve que ce modèle a toutes les caractéristiques de la percolation critique est due à Grimmett et Manolescu [GM14].

Soit $G = (V, E)$ un graphe plongé, c'est-à-dire que la position des sommets V dans le plan est fixée. G est isoradial si chacune de ses faces f peut être inscrite dans un cercle de rayon 1 dont le centre c se situe à l'intérieur de f (voir figure I.7). En reliant les centres des faces aux sommets du graphes, on obtient un pavage de losanges $G^\diamond$.

Chaque arête e est alors inscrite dans un losange, on peut définir l'angle θ_e formé par le losange au sommet adjacent à e. Le poids de percolation que l'on associe à l'arête e est alors défini en fonction de cet angle géométrique, par

$$p_e = \frac{\sin\left(\frac{\theta_e}{3}\right)}{\sin\left(\frac{\theta_e}{3}\right) + \sin\left(\frac{\pi - \theta_e}{3}\right)}. \tag{I.2}$$

On peut vérifier qu'avec ces poids géométriques, tout triangle ou toute étoile vérifie les conditions pour appliquer la transformation triangle-étoile. Cela suggère

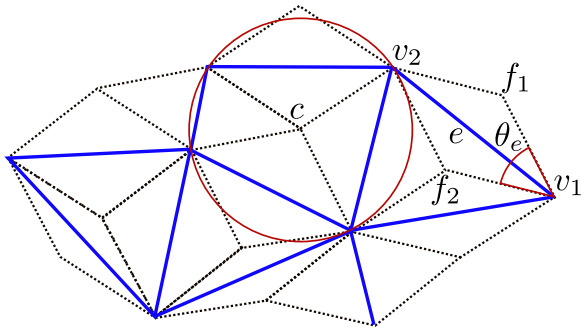

Figure I.7: Exemple de graphe isoradial G, en bleu. Son graphe de losange $G^\diamond$ est en pointillés. Un cercle de centre c circonscrit à l'une des faces est représenté en rouge. Une arête e, d'angle θ_e, est entourée de ses deux sommets primaux v_1, v_2 et duaux f_1, f_2.

une stratégie de preuve pour démontrer l'universalité : partir d'un graphe isoradial G_1, appliquer assez de transformations pour le modifier en un graphe G_2, montrer que la propriété dont on veut montrer l'universalité n'a pas été altérée pendant les transformations. Il s'agit de la stratégie appliquée dans [GM13a, GM13b, GM14], pour montrer la criticalité des poids isoradiaux, et l'universalité de certaines quantités comme les exposants critiques. En revanche, dans ces travaux, le contrôle de la transformation ne permet pas d'en déduire l'universalité d'autres propriétés, comme la forme géométrique macroscopique des composantes connexes. Ceci est l'objet du chapitre II. L'appendice B expose une autre représentation des graphes isoradiaux par des *lignes de rapidité*.

Percolation de Fortuin-Kasteleyn

Nous allons en réalité travailler avec une généralisation du modèle de percolation, la *percolation de Fortuin Kasteleyn* (FK) ou *random cluster model*. Ce modèle permet de relier dans un même paradigme un certain nombre de modèles classiques en physique statistique : modèle d'Ising, de Potts, arbres couvrants, percolation de Bernoulli, modèles de boucles... [Mel19, Figure 23] dresse un panorama des relations entre ces modèles.

L'idée de la percolation FK est de pondérer le nombre de composantes connexes à l'aide d'un paramètre $q > 0$. Ainsi, sur un graphe **fini** $G = (V, E)$, le modèle de percolation FK de paramètres homogènes p, q affecte à chaque configuration de percolation ω le poids

$$w(\omega) = p^{|\omega|_1}(1-p)^{|\omega|_0} q^{k(\omega)}$$

où $|\omega|_1$est le nombre d'arêtes ouvertes, $|\omega|_0$ le nombre d'arêtes fermées et $k(\omega)$ le nombre de composantes connexes. Pour que ces poids donnent une mesure de probabilité, il faut les normaliser par la *fonction de partition*, c'est-à-dire la somme des poids de toutes les configurations :

$$Z = \sum_{\omega \in \{0,1\}^E} w(\omega). \tag{I.3}$$

Pour définir la percolation FK sur un réseau **infini**, comme le réseau carré $\mathbb{Z}^2$, il

faut étudier la limite du modèle lorsqu'on prend des graphes finis G de plus en plus grands, qui tendent vers le réseau infini. La façon de prendre ces graphes finis et les *conditions aux bords* (c'est-à-dire la façon dont on compte les composantes connexes touchant le bord de G) peuvent avoir une influence sur la limite qu'on obtient. Dans quel cas a-t-on une unique mesure de probabilité pour le réseau infini, que l'on appelle *mesure en volume infini* ? Comme pour la percolation de Bernoulli, il existe une transition de phase et trois régimes distincts. Il n'est pas difficile de montrer que la mesure en volume infini est unique dans les régimes sous-critique et sur-critique. À criticalité, sur le réseau carré, d'après [DCST17, DCGH$^+$16] il existe une unique mesure pour $1 \leq q \leq 4$ et plusieurs pour $q > 4$. Dans le premier cas, on parle de transition de phase *continue*, et dans le second de transition de phase *discontinue*. Comme pour la percolation de Bernoulli, il existe des poids isoradiaux permettant d'appliquer la transformation triangle-étoile. Dans [DCLM18], ces résultats sont étendus aux graphes isoradiaux (avec des poids isoradiaux).

Ces poids isoradiaux sont définis de la façon suivante. Pour une arête e d'angle θ_e (cf. Figure I.7), le poids associé est défini, pour $1 \leq q < 4$ par la relation

$$\frac{p_e}{1-p_e} = \sqrt{q}\frac{\sin\left(\frac{1}{\pi}\arccos(\sqrt{q}/2)\theta_e\right)}{\sin\left(\frac{1}{\pi}\arccos(\sqrt{q}/2)(\pi-\theta_e)\right)}$$

et par la limite

$$\frac{p_e}{1-p_e} = 2\frac{\theta_e}{\pi-\theta_e}$$

pour $q = 4$. On remarquera que pour $q = 1$, on retrouve les poids isoradiaux de la percolation de Bernoulli.

Ces poids vérifient alors l'équation suivante qui permet d'appliquer la transformation triangle-étoile à la percolation FK (représentée à la figure I.5 pour $q = 1$). En définissant $y_i = \frac{p_i}{1-p_i}$ et $y'_i = \frac{p'_i}{1-p'_i}$, l'équation s'écrit

$$y_i y'_i = q \tag{I.4}$$

$$y_1y_2y_3 + y_1y_2 + y_2y_3 + y_1y_3 = q. \tag{I.5}$$

Pour $q = 1$, on retrouve l'équation (I.1) ainsi que la relation $p'_i = 1 - p_i$.

Limite d'échelle et invariance conforme

Lorsque l'on fait tendre la maille d'un réseau isoradial vers 0, qu'on le rend microscopique, on s'attend à ce que le processus de percolation FK soit décrit par une limite d'échelle. Pour donner un sens plus précis à cette convergence, nous décrivons deux façons de représenter une configuration de percolation FK qui évacuent le besoin de parler de réseau sous-jacent.

Le première, due à Schramm et Smirnov [SSG11], consiste à décrire la configuration de percolation par ses propriété de connectivité. Un *quad* Q est un domaine du plan avec quatre points a, b, c, d marqués sur son bord. On dit que le quad Q est *croisé* dans une configuration de percolation ω s'il existe un chemin ouvert dans ω, qui reste dans Q et relie les côtés (ab) et (cd) (voir la figure I.8). L'idée est alors de représenter la configuration ω par l'ensemble S de tous les quads croisés dans ω. Cette description ne fait alors plus du tout appel à la notion de réseau sous-jacent.

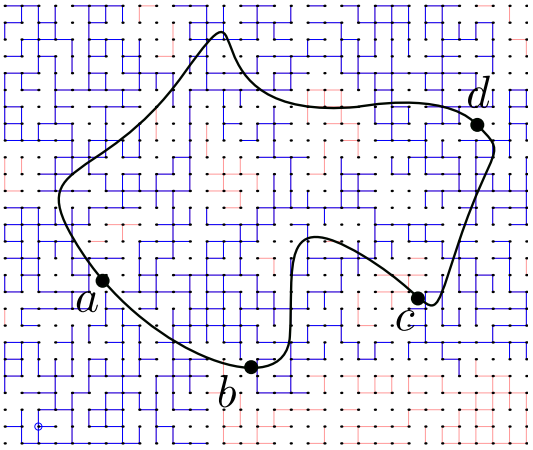

Figure I.8: Un quad Q croisé par la composante connexe représentée en bleu.

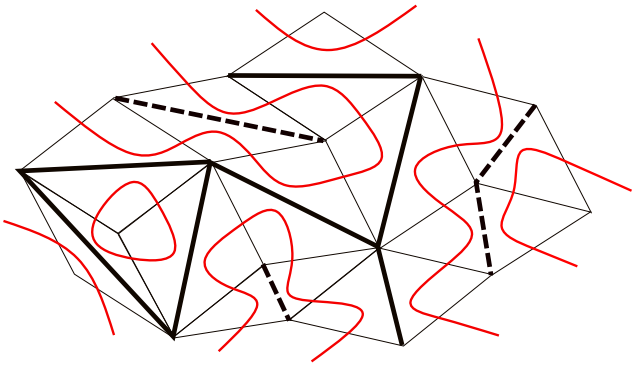

Figure I.9: Une configuration de percolation (en trait gras noir) et sa configuration duale (en pointillé) sur un graphe isoradial représenté par son graphe de losanges (en trait fin noir). Les frontières de ses composantes connexes, séparant les arêtes primales et duale, forment une collection de courbe et de boucles qui ne s'intersectent pas (en rouge).

Il se trouve que la collection de ces ensembles S, que l'on note $\mathcal{H}$, est munie d'une topologie (compacte métrisable) qui permet de donner un sens à l'idée de *limite* : une suite de mesures de probabilités sur $\mathcal{H}$ correspondant à une percolation sur des réseaux de maille de plus en plus petite pourrait alors converger vers une mesure limite sur $\mathcal{H}$. En 2001, Smirnov [Smi01] a démontré que les probabilités de croisement de quad de la percolation de Bernoulli *par site* sur le réseau triangulaire convergent vers une formule explicite, la formule de Cardy. Ce modèle de percolation est un modèle proche de la percolation *par arête* que l'on a décrite.

La seconde, due à Camia et Newman [CN06b], consiste à décrire une configuration ω par une collection de boucles dans le plan consistant en l'ensemble des frontières de ses composantes connexes (voir la figure I.9). En excluant les boucles qui deviennent microscopiques, il est alors possible de définir une distance entre deux collections de boucles, et donc une notion de convergence. Camia et Newman montrent [CN06b, CN07, CN06a] que dans ce formalisme, les frontières de la percolation de Bernoulli par site sur le réseau triangulaire, convergent vers un processus

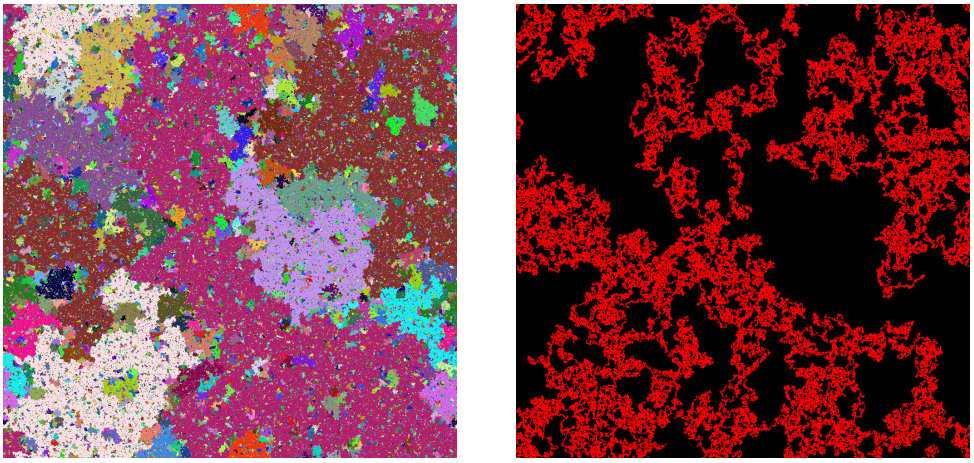

Figure I.10: **À gauche**, des composantes connexes de percolation critique sur une grille périodique 1000×1000. **À droite**, les courbes fractales rouges sont les frontières des composantes connexes. On n'a représenté que les boucles de longueur au moins 10^5.

de courbes aléatoires, qui peut être construit à partir d'un processus continu nommé SLE_6.

Des arguments d'universalité indiquent que la limite d'échelle de la percolation FK doit être invariante par toutes les *transformations conformes*, c'est-à-dire toutes les transformations qui sont localement la composée d'une rotation, d'une translation et d'une dilatation.

Les processus $SLE_\kappa, \kappa \geq 0$ (pour Stochastic Loewner Evolution ou Schramm Loewner Evolution) forment une famille invariante conforme de courbes aléatoires et fractales dans le plan. Elles ont été identifiées par Oded Schramm comme les seules courbes pouvant être des candidates de limite d'échelle des frontières de percolation FK [Sch00]. On s'attend à ce que les collections de boucles correspondant aux frontières de composantes connexes dans un domaine soient décrites par un processus apparenté, nommé CLE_κ. Pour la percolation FK de paramètre $1 \leq q \leq 4$, on conjecture [Wu18] que le paramètre des processus SLE_κ, CLE_κ devant en décrire la limite d'échelle à criticalité satisfait la relation :

$$\kappa = \frac{4\pi}{\arccos(-\sqrt{q}/2)},$$

et on a alors notamment $4 \leq \kappa \leq 6$.

Dans le cas $q = 2$, plusieurs travaux [Smi10, CDCH$^+$14] ont permis de démontrer la convergence des interfaces vers une limite d'échelle décrite par $SLE_{16/3}$. Cette question reste ouverte pour les autres valeurs de q. La figure I.10 représente les interfaces des composantes connexes de percolation pour $q = 1$, qui doivent être décrites par le processus SLE_6 à la limite. Ce sont des courbes fractales qui se touchent elles-mêmes mais ne s'intersectent pas.

I.3 Énergie libre et géométrie

L'énergie libre F est une quantité importante en mécanique statistique et physique de la matière condensée. Originellement définie en thermodynamique à partir d'autres fonctions d'état, elle est exprimable en physique statistique à partir de la fonction de partition :

$$F = -k_B T \log(Z)$$

où k_B est la constante de Boltzmann, T la température, et Z la fonction de partition du système (voir l'équation (I.3)). Dans la suite nous supposerons $k_B T = 1$.

Nous allons faire le lien entre probabilité et fonction de partition. Supposons pour simplifier que l'on considère un modèle de percolation FK sur un graphe fini $G = (V, E)$. Dans ce cas, la probabilité d'un évènement A s'écrit

$$\mathbb{P}(A) = \frac{\sum_{\omega \in A} w(\omega)}{\sum_{\omega \in \{0,1\}^E} w(\omega)}.$$

On reconnait la fonction de partition Z au dénominateur, et en notant Z_A le numérateur, on a

$$\mathbb{P}(A) = \frac{Z_A}{Z} = \exp(F - F_A)$$

où on définit $F_A = -\log(Z_A)$.

Énergie libre des évènements de croisement

Dans les chapitres II et III, nous étudions deux modèles de percolation différents : la percolation FK critique dans le premier cas, et un modèle de percolation des ensembles de niveau d'une fonction de hauteur dans le second. Dans les deux cas, nous aurons besoin d'estimer la probabilité de deux évènements de croisement similaires. Nous décrivons ici cet évènement $E_{N,M,k}$ dans le cadre de la percolation FK.

Soit N, M et $0 \leq k \leq N$ trois entiers. On considère un graphe isoradial cylindrique de périmètre N et de hauteur M. L'évènement $E_{N,M,k}$ se produit si et seulement si il existe k composantes connexes disjointes qui relient le haut et le bas du cylindre (voir la figure I.11).

Soit un réel $0 < \alpha < 1$, on suppose que αN est entier. Nous allons nous intéresser à la quantité, dont on justifiera l'existence et que l'on interprétera comme une énergie, définie par

$$f(\alpha) = \lim_{N \to \infty} \lim_{M \to \infty} -\frac{1}{MN} \log \mathbb{P}(E_{N,M,\alpha N}). \tag{I.6}$$

La théorie de Russo-Seymour-Welsh (RSW), que nous présentons maintenant, nous permettra d'obtenir une première borne sur $f(\alpha)$. Soit R_n un rectangle de dimension $3n \times n$ (voir la figure I.12) et $\mathcal{C}_{R_n}$ l'évènement où R_n est traversé par un chemin ouvert reliant ses bords les plus courts. Alors, la théorie de RSW énonce qu'il existe une constante $c > 0$, qui ne dépend pas de n, telle que

$$\mathbb{P}(\mathcal{C}_{R_n}) \geq c.$$

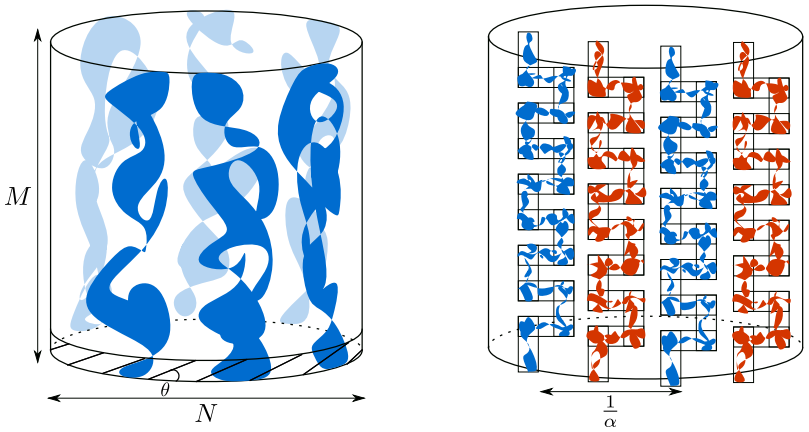

Figure I.11: Représentation de l'évènement $E_{N,M,k}$. **À gauche** : k composantes connexes (en bleu) disjointes traversent le cylindre. Seule la première ligne du graphe isoradial d'angle θ est représentée. **À droite** : Construction de l'évènement $E_{N,M,k}$ en combinant les théorèmes RSW et FKG. Les composantes connexes primales sont en bleu et les duales en rouge.

Le premier résultat de ce type à été démontré pour la percolation de Bernoulli par Russo, Seymour et Welsh [Rus78, SW78], puis étendu à de nombreux modèles de percolation planaire dont la percolation FK sur des graphes isoradiaux [DCLM18]. On peut se référer à [KST20a] pour une recension de ces résultats et une nouvelle version très robuste.

Cette borne sur les probabilités de croisements de quads prend toute sa puissance lorsqu'elle est associée à une autre inégalité, celle de Fortuin-Kasteleyn-Ginibre (FKG) [FKG71]. Celle-ci, valide pour la percolation FK lorsque $q \geq 1$, implique que si l'on sait qu'un chemin est ouvert, cela ne peut qu'augmenter la probabilité qu'un autre chemin soit ouvert. Plus généralement, un *évènement croissant* est un évènement A qui, s'il se produit dans une configuration ω, alors il se produit dans toute autre configuration ω' construite à partir de ω en ouvrant de nouvelles arêtes. L'existence d'un chemin ouvert est un exemple d'évènement croissant. Soit A et B deux évènements croissants, l'inégalité FKG est la suivante :

$$\mathbb{P}(A \cap B) \geq \mathbb{P}(A)\mathbb{P}(B).$$

Soient $R^1, \ldots, R^k$ plusieurs rectangles se recouvrant (comme sur l'une des colonnes bleues de la figure I.11). Soit $\mathcal{C}_A$ l'évènement où tous les rectangles $R^1, \ldots, R^k$ sont croisés par un chemin ouvert. En utilisant les inégalités FKG et RSW, on a donc

$$\mathbb{P}(\mathcal{C}_A) \geq \mathbb{P}(\mathcal{C}_{R^1} \cap \cdots \cap \mathcal{C}_{R^k}) \geq \mathbb{P}(\mathcal{C}_{R^1}) \times \ldots \mathbb{P}(\mathcal{C}_{R^k}) \geq c^k.$$

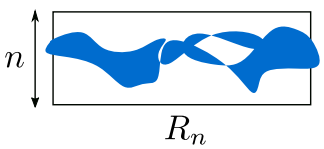

Figure I.12: Le rectangle R_n est croisé par une composante connexe.

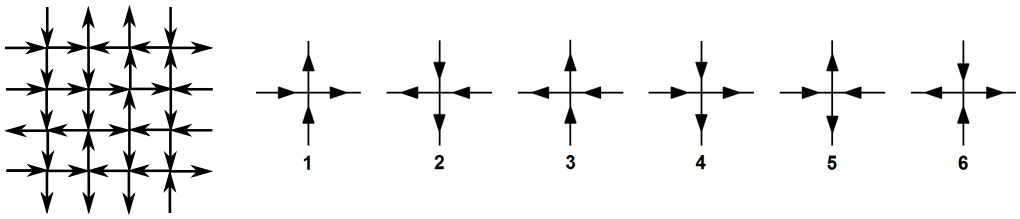

Figure I.13: **À gauche**, une configuration du modèle six-vertex sur une portion du réseau carré. **À droite**, les 6 orientations possibles autour d'un sommet.

Ces deux inégalités permettent donc de "jouer aux LEGOs" en construisant des composantes connexes de diverses formes, et en donnant une borne inférieure sur leur probabilité d'existence.

La figure I.11 montre comment ces techniques donnent une borne sur la probabilité de l'évènement $E_{N,M,\alpha N}$. On utilise aussi les inégalités RSW et FKG pour les *chemins duaux* (en rouge sur la figure), c'est-à-dire l'absence de connexion. Il y a de l'ordre de $\alpha N \times \alpha M$ rectangles, la borne obtenue est donc

$$\mathbb{P}(E_{N,M,\alpha N}) \geq c^{\alpha^2 MN},$$

ce qui se traduit pour l'énergie libre par

$$f(\alpha) \leq c'\alpha^2 \tag{I.7}$$

pour une certaine constante $c' > 0$.

Énergie libre du modèle six-vertex

Il est possible d'obtenir une estimation beaucoup plus fine de l'énergie libre et exploitant le lien entre la percolation FK et un autre modèle de physique statistique, le modèle six-vertex. Introduit originellement par Pauling pour modéliser la glace [Pau35], il s'est trouvé être l'un des modèles les plus étudiés en physique statistique planaire, d'une part pour ses relations à de nombreux autres modèles, d'autre part pour son *intégrabilité*, c'est-à-dire la possibilité de calculer exactement certaines quantités comme la fonction de partition. Pour un exposé des différentes notions d'intégrabilité et de leur sens en physique statistique, on peut se référer à [Mel19, Section I.3].

Le modèle est défini sur un graphe $G = (V, E)$ qu'on suppose être une partie finie du graphe carré $\mathbb{Z}^2$. Une configuration σ est la donnée d'une orientation des arêtes de E, telle que chaque sommet ayant quatre arêtes adjacentes en ait deux entrantes et deux sortantes. Il y a six possiblités d'orientation autour de chaque sommet, représentées sur la figure I.13, auquelles on associe des poids $\mathbf{a}, \mathbf{b}, \mathbf{c} > 0$. Le poids d'une configuration est alors égale au produit des poids de ses sommets.

$$w_{6V}(\sigma) = \mathbf{a}^{n_1+n_2}\mathbf{b}^{n_3+n_4}\mathbf{c}^{n_5+n_6}$$

où n_i est le nombre de sommets de type i. On peut alors définir la fonction de partition comme la somme de tous les poids $Z_{6V} = \sum_\sigma w_{6V}(\sigma)$, et la mesure de probabilité par $\mathbb{P}_{6V}(\sigma) = \frac{w_{6V}(\sigma)}{Z}$.

On va considérer ce modèle sur un graphe carré cylindrique de dimension $M \times N$ (similaire à celui de la figure I.11). On dénote toujours par Z_{6V} la fonction de partition, et pour $0 < k < N$, on définit $Z_{6V}(k)$ comme la somme des poids des configurations ayant, à la base du cylindre, k flèches de plus vers le haut que vers le bas. On définit alors

$$f_{6V}(\alpha) = \lim_{N\to\infty} \lim_{M\to\infty} -\frac{1}{MN} \log \frac{Z_{6V}(\alpha N)}{Z_{6V}}. \tag{I.8}$$

Dans [DCKK$^+$20b], la valeur de cette quantité a pu être calculée, et pour $-1 \leq \Delta < 1$, on a :

$$f_{6V}(\alpha) = C(\Delta)\sin(\theta)\alpha^2$$

où $C(\Delta)$ est une constante explicite qui ne dépend que de $\Delta := \frac{\mathbf{a}^2+\mathbf{b}^2-\mathbf{c}^2}{\mathbf{ab}}$ et θ est une fonction de $\mathbf{a}, \mathbf{b}, \mathbf{c}$ (explicitée à l'équation (II.4)).

Or, il existe une correspondance entre le modèle six-vertex décrit ici, et le modèle de percolation FK de la figure I.11, où θ est l'angle du plongement isoradial et $\Delta = -\sqrt{q}/2$. Il s'agit de la construction de Baxter-Kelland-Wu [BKW76]. On peut alors en déduire une égalité des énergies libres (pour plus de détails, voir [DCGH$^+$16, Section 3.3]), c'est-à-dire que pour $1 \leq q \leq 4$,

$$f(\alpha) = f_{6V}(\alpha) = C(\Delta)\sin(\theta)\alpha^2.$$

De l'énergie libre à la géométrie

Cette égalité sera utilisée dans les chapitres II et III. Le but du chapitre II est de montrer l'invariance par rotation de la percolation FK. Nous ne prouvons pas qu'il existe une limite d'échelle à criticalité (au sens de Schramm-Smirnov ou Camia-Newman) mais si il y en a une, alors elle est invariante par les rotations, qui sont un sous-ensemble des transformations conformes du plan.

Pour quantifier ce résultat, nous utilisons deux distances entre les configurations, $d_{\mathbf{CN}}$ et $d_{\mathbf{SS}}$ qui métrisent les topologies de Camia-Newman et Schramm-Smirnov évoquées plus haut. La mesure de percolation FK critique sur la grille d'échelle δ restreinte au domaine Ω est notée $\phi^0_{\Omega_\delta}$, et $\phi^0_{(e^{-i\theta}\Omega)_\delta}$ dénote sa rotation d'angle θ. Le résultat s'énonce ainsi :

Theorem I.3.1 (Invariance par rotation de la percolation FK critique)**.** *Fixons $q \in [1,4]$ et un domaine simplement connexe du plan Ω ayant un bord C^1. Pour tout $\varepsilon > 0$, il existe $\delta_0 = \delta_0(q,\varepsilon,\Omega) > 0$ tel que pour tout $\theta \in (\varepsilon, \pi-\varepsilon)$ et $\delta \leq \delta_0$, il existe un couplage $\mathbb{P}$ entre $\omega_\delta \sim \phi^0_{\Omega_\delta}$ et $\omega'_\delta \sim \phi^0_{(e^{-i\theta}\Omega)_\delta}$ tel que*

$$\mathbb{P}[d_{\mathbf{SS}}(\omega_\delta, e^{i\theta}\omega'_\delta) > \varepsilon] < \varepsilon,$$
$$\mathbb{P}[d_{\mathbf{CN}}(\omega_\delta, e^{i\theta}\omega'_\delta) > \varepsilon] < \varepsilon.$$

Pour cela, nous prouvons un résultat d'universalité en utilisant la stratégie basée sur la transformation triangle-étoile indiquée précédemment : on transforme étape par étape un réseau isoradial rectangulaire d'angle θ en un autre réseau isoradial rectangulaire d'angle $\pi/2$. On montre alors que les composantes connexes ne changent pas de forme macroscopique au cours du processus. Pour montrer cette

invariance, nous utilisons entre autre que l'expression exacte de l'énergie libre ne dépend que de la longueur euclidienne (via le facteur $\sin\theta$) et ne "voit" donc pas le graphe sous-jacent.

Theorem I.3.2 (Universalité de la percolation FK sur les graphes isoradiaux rectangulaires)**.** *Soit $q \in [1,4]$ et $\varepsilon > 0$, il existe $\delta_0 = \delta_0(q,\varepsilon) > 0$ tel que pour tout $\delta < \delta_0$ et $\theta \in (\varepsilon, \pi - \varepsilon)$, il existe un couplage $\mathbf{P}_{\theta,\delta,\varepsilon}$ entre $\omega \sim \phi_{\delta\mathbb{L}(\theta)}$ et $\omega' \sim \phi_{\delta\mathbb{L}(\frac{\pi}{2})}$ tel que*

$$\mathbf{P}_{\theta,\delta,\varepsilon}[d_{\mathbf{CN}}(\omega,\omega') > \varepsilon] < \varepsilon,$$
$$\mathbf{P}_{\theta,\delta,\varepsilon}[d_{\mathbf{SS}}(\omega,\omega') > \varepsilon] < \varepsilon.$$

Dans le chapitre III, nous étudions la *fonction de hauteur* du modèle six-vertex. À partir d'une configuration six-vertex sur un graphe carré, on peut définir sa fonction de hauteur en assignant à chaque face une valeur entière telle que, lorsque l'on traverse une arête du graphe, la valeur augmente de 1 ou diminue de 1 selon que l'arête traversée est orientée vers la droite ou vers la gauche (par rapport au déplacement, voir la figure I.14). La fonction de hauteur peut alors être vue comme un modèle de surface aléatoire où l'on indique l'altitude de chaque point d'un domaine du plan.

Fixons un domaine D du plan, fixons la valeur de la fonction de hauteur sur le bord à 0 ou 1. On peut alors s'intéresser aux fluctuations de la hauteur d'un point x du domaine, que l'on note $h(x)$. Par exemple, la figure I.14 représente une telle fonction de hauteur sur un domaine carré. Le théorème que l'on démontre à propos de ces fluctuations peut s'énoncer de la façon suivante :

Theorem I.3.3 (Variance logarithmique dans un domaine du plan)**.** *Fixons $\mathbf{a} = \mathbf{b} = \mathbf{1}$ et $1 \leq \mathbf{c} \leq 2$. Il existe $c, C > 0$ tel que pour tout domaine discret D, toute condition au bord admissible ξ sur ∂D, et toute face x de $D \setminus \partial D$, si l'on note $\max_{y\in\partial D} |\xi(y)| =: \ell$, alors*

$$c \log d(x, \partial D) - 4\ell^2 \leq \mathrm{Var}_D^{\xi}(h(x)) \leq C \log d(x, \partial D) + 4\ell^2.$$

Pour montrer ce résultat sur les fluctuations, nous démontrons un résultat de type RSW pour les ensembles de niveau de la fonction de hauteur. On dit que deux régions sont connectées par l'ensemble de niveau $\{h \geq k\}$ si il existe un chemin de faces dont la hauteur est supérieure à k qui connecte les deux régions (voir la figure I.14).

Dans l'équation (I.7), nous avons vu que RSW implique une borne quadratique sur l'énergie libre. Dans ce chapitre, l'idée est de faire le chemin inverse : partir de l'expression exacte de l'énergie libre, qui est quadratique, et en déduire un résultat de type RSW.

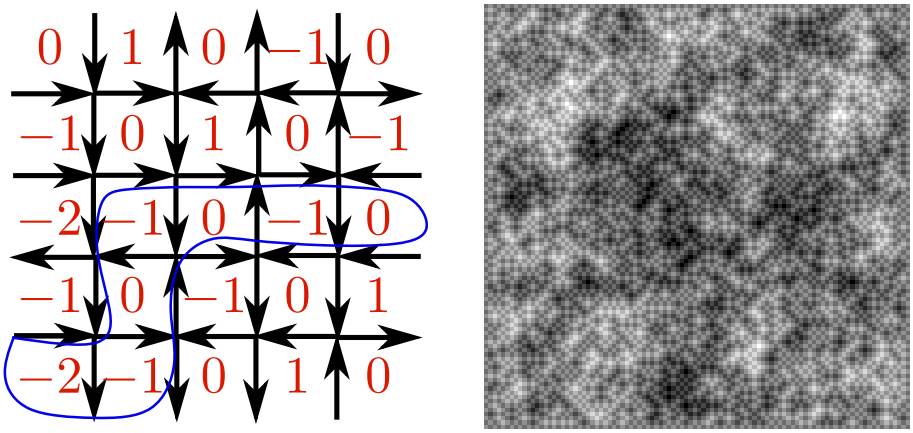

Figure I.14: **À gauche**, une configuration six-vertex et une fonction de hauteur correspondante. La grille est croisée de gauche à droite par un ensemble de niveau $\{h \leq 0\}$. **À droite**, une simulation de la fonction de hauteur du modèle six-vertex avec $\mathbf{a} = \mathbf{b} = \mathbf{c} = 1$ sur une grille 100×100. Les hauteurs sur le bord du carré sont égales à 0 ou 1, et s'étendent dans la grille entre -3 (en noir) et 4 (en blanc).

II | Rotational invariance in critical planar lattice models

Joint work with Hugo Duminil-Copin, Karol Kozlowski, Dmitry Krachun, Ioan Manolescu.

II.1 Introduction

II.1.1 Motivation

Physical systems undergoing a continuous phase transition have been the focus of much attention in the past seventy years, both on the physical and the mathematical sides. Since Onsager's revolutionary solution of the 2D Ising model, mathematicians and physicists tried to understand the delicate features of the critical phase of these systems. In the sixties, the arrival of the renormalization group (RG) formalism (see [Fis98] for a historical exposition) led to a generic (non-rigorous) deep understanding of continuous phase transitions. The RG formalism suggests that "coarse-graining" renormalization transformations correspond to appropriately changing the scale and the parameters of the model under study. The large scale limit of the critical regime then arises as the fixed point of the renormalization transformations.

A striking consequence of the RG formalism is that the assumption that the critical fixed point is unique leads to the prediction that the scaling limit at the critical point must satisfy translation, rotation and scale invariance, which allows one to deduce some information about correlations. In [Pol70], Polyakov outlined a set of arguments pointing towards a much stronger invariance of statistical physics models at criticality: since the scaling limit field theory is a local field, it should be invariant under any map which is locally a composition of translation, rotation and homothety, which leads to postulate full conformal invariance. In [BPZ84b, BPZ84a], Belavin, Polyakov and Zamolodchikov went even further by considering massless field theories that enjoy full conformal invariance from the very start, a fact which allowed them to derive explicit expressions for their correlation functions, hence giving birth to conformal field theories. Once conformal invariance is proved, a whole world of new techniques becomes available thanks to Conformal Field Theory and the Schramm-Loewner Evolution [Law08], and it is therefore a problem of fundamental importance to prove conformal invariance of the scaling limits of lattice models.

Proving conformal invariance is quite difficult for most lattice models. The examples of models for which such a statement has been obtained can be counted on the fingers of one's hand: site Bernoulli percolation on the triangular lattice [Smi01, CN06b, CN07] (respectively for Cardy's formula, SLE(6) convergence, and CLE(6)

convergence), Ising and FK-Ising models [Smi10, CS12, HS13, CHI15, CDCH$^+$14, BH19] (respectively for the fermionic observables in FK-Ising, in Ising, the energy and the spin fields, SLE convergence, and CLE convergence), uniform spanning trees [Sch00], dimers [Ken00], level lines of the discrete GFF [SS09].

In all the mentioned cases, the proof relied under one form or another, on discrete holomorphic observables satisfying some discrete version of conformally covariant boundary value problems. Mathematicians were therefore able to prove conformal invariance directly, bypassing the road suggested by physicists consisting in first proving scaling and rotation invariance (translation invariance is obvious), and then deducing from it conformal invariance. Unfortunately, today's mathematicians' strategy is very dependent on discrete properties of the system, which explains why we are currently limited to very few instances of proofs of conformal invariance.

In this paper, we perform one step towards the strategy inspired by Field Theory and prove rotational invariance of the large-scale properties of a number of planar models at their critical point. Our strategy is quite general and applies to a number of integrable planar systems. Namely, we treat the case of the random-cluster model (also called Fortuin-Kasteleyn percolation), the Potts models, as well as the six-vertex model. We believe that the reasoning has also applications for the Askhin-Teller model and certain loop models. The proof will proceed by focusing on the random-cluster model and then extending its rotational invariance to other planar lattice models using known mapping between the models.

II.1.2 Definition of the random-cluster model and distance between percolation configurations

As mentioned in the previous section, the model of central interest in this paper is the random-cluster model, introduced by Fortuin and Kasteleyn around 1970 [FK72, For71], which we now define. For background, we direct the reader to the monograph [Gri04] and to the lecture notes [DC17] for an exposition of the most recent results.

Consider the square lattice $(\mathbb{Z}^2, \mathbb{E})$, that is the graph with vertex-set $\mathbb{Z}^2 = \{(n, m) : n, m \in \mathbb{Z}\}$ and edges between nearest neighbours. In a slight abuse of notation, we write $\mathbb{Z}^2$ for the graph itself. Consider a finite subgraph G of the square lattice with vertex-set V and edge-set E. For instance, think of $G = \Lambda_n$ as being the subgraph of $\mathbb{Z}^2$ spanned by the vertex-set $\{-n, \dots, n\}^2$ (we will use the notation Λ_n throughout the paper). A percolation configuration ω on G is an element of $\{0, 1\}^E$. An edge e is *open* (in ω) if $\omega_e = 1$, otherwise it is *closed*. A configuration ω can be seen as a subgraph of G with vertex-set V and edge-set $\{e \in E : \omega_e = 1\}$. When speaking of connections in ω, we view ω as a graph. A *cluster* is a connected component of ω.

Definition II.1.1. The random-cluster measure on G with edge-weight $p \in [0, 1]$, cluster-weight $q > 0$, and free boundary conditions is given by

$$\phi^0_{G,p,q}[\omega] := \frac{p^{|\omega|}(1-p)^{|E|-|\omega|}q^{k(\omega)}}{Z^0_{\mathrm{RCM}}(G, p, q)}, \tag{II.1}$$

where $|\omega| := \sum_{e \in E} \omega_e$ is the number of open edges, $k(\omega)$ is the number of connected components of the graph, and $Z^0_{\mathrm{RCM}}(G, p, q)$ is a normalising constant called the *partition function* chosen in such a way that $\phi^0_{G,p,q}$ is a probability measure.

For $q \geq 1$, the family of measures $\phi^0_{G,p,q}$ converges weakly as G tends to the whole square lattice to an infinite-volume measure $\phi^0_{p,q}$ on $\{0,1\}^{\mathbb{E}}$. The random-cluster model undergoes a phase transition [BDC12, DCRT19] at a critical parameter

$$p_c = p_c(q) = \frac{\sqrt{q}}{1+\sqrt{q}}$$

in the sense that the $\phi^0_{p,q}$-probability that there exists an infinite cluster is 0 if $p < p_c(q)$, and is 1 if $p > p_c(q)$.

It was also proved in [DCGH$^+$16, DCST17] that the phase transition is continuous (i.e. that the probability that 0 is connected to infinity is tending to 0 as $p \searrow p_c$) if and only if $q \leq 4$ (see also [RS20] for a short proof of discontinuity of the phase transition when $q > 4$). In the whole paper we restrict our attention to the range $q \in [1,4]$. For this reason,

fix $q \in [1,4]$ and $p = p_c(q)$ and drop them from notation.

We will be interested in measuring how close the large scale properties of two random percolation configurations really are. In order to do that, we introduce a rescaling of the lattice and define the random-cluster model on subgraphs of $\delta\mathbb{Z}^2$ with $\delta > 0$. To highlight on which lattice we are working, we will consistently use the subscript δ to refer to a percolation configuration on a subgraph of the lattice $\delta\mathbb{Z}^2$, and write ω_δ for such a configuration. When Ω is a simply connected domain of $\mathbb{R}^2$, write Ω_δ for the intersection of Ω with $\delta\mathbb{Z}^2$.

In [CN06b], Camia and Newman introduced a convenient way of measuring the geometry of large clusters in a percolation configuration in the plane. Let $\mathfrak{C} = \mathfrak{C}(\Omega)$ be the collection of sets $\mathcal{F} = \mathcal{F}_0 \sqcup \mathcal{F}_1$ of two locally finite families $\mathcal{F}_0$ and $\mathcal{F}_1$ of non-self-crossing loops in some simply connected domain Ω that do not intersect each other (even between loops in $\mathcal{F}_0$ and $\mathcal{F}_1$). Define the metric on $\mathfrak{C}$,

$$d_{\mathbf{CN}}(\mathcal{F},\mathcal{F}') \leq \varepsilon \iff \left(\begin{array}{c} \forall i \in \{0,1\}, \forall \gamma \in \mathcal{F}_i \text{ with } \gamma \subset B(0,1/\varepsilon), \exists \gamma' \in \mathcal{F}'_i, d(\gamma,\gamma') \leq \varepsilon \\ \text{and similarly when exchanging } \mathcal{F}' \text{ and } \mathcal{F} \end{array} \right),$$

where, for two loops γ_1 and γ_2, we set

$$d(\gamma_1,\gamma_2) := \inf \sup_{t \in \mathbb{S}^1} |\gamma_1(t) - \gamma_2(t)|,$$

with the infimum running over all continuous one-to-one parametrizations of the loops γ_1 and γ_2 by $\mathbb{S}^1$.

Another way of encoding the geometry of large clusters was proposed by Schramm and Smirnov in [SSG11]. In order to define it formally, let a *quad* Q be the image of an homeomorphism from $[0,1]^2$ to $\mathbb{C}$, and let a,b,c,d be the images of the corners of $[0,1]^2$. A *crossing* of Q is a continuous path in Q going from (ab) to (cd). Let $\mathcal{Q}$ be the set of quads, endowed with the distance between quads given by

$$d_{\mathcal{Q}}(Q,Q') := d(\partial Q, \partial Q') + |a-a'| + |b-b'| + |c-c'| + |d-d'|.$$

Call $S \subset \mathcal{Q}$ *hereditary* if whenever $Q \in S$, every quad Q' that is such that any crossing of Q contains a crossing of Q' must also belong to S. Let $\mathfrak{H} = \mathfrak{H}(\Omega)$ be the set of closed hereditary subsets of $\mathcal{Q}$. Endow $\mathfrak{H}$ with the smallest topology generated by the sets of the type $\{Q \in S\}_{Q \in \mathcal{Q}}$ and $\{S \cap U = \emptyset\}_{U \text{ open set in } \mathcal{Q}}$. The set $\mathfrak{H}$ with this topology is metrizable, and we denote the metric (whose definition is implicit) by $d_{\mathbf{SS}}(\cdot,\cdot)$.

A configuration ω can be identified with the (automatically hereditary) set $S \in \mathfrak{H}$ containing all the quads that are crossed by an open path in ω (seen as a continuous path in the plane). Similarly, ω can be seen as an element of $\mathfrak{C}$ by considering the loop representation of the model obtained as follows (see Section II.3.2 for details): to each ω is associated a *dual configuration* ω^* on the dual graph, as well as a *loop configuration* $\overline{\omega}$ on the medial graph, corresponding basically to the boundaries between the primal and dual clusters. Then, we say that a loop is in $\mathcal{F}_1$ if it is the exterior boundary of a primal cluster, and in $\mathcal{F}_0$ if it is the exterior boundary of a dual cluster. Whether ω is seen as an element of $\mathfrak{H}$ or $\mathfrak{C}$ will depend on the context (it will always be clear which identification is used, if any).

II.1.3 Main results for the random-cluster model

Below, we state results in simply connected domains Ω with a C^1-smooth boundary, meaning that $\partial\Omega$ can be parametrized by a C^1-function whose differential does not vanish at any point[1]. By taking the limit as Ω tends to $\mathbb{R}^2$ of the results below, we also obtain the statement for the unique infinite-volume measure[2].

We will identify the rotation by the angle α with the multiplication by $e^{i\alpha}$. Below, $X \sim \mu$ means a random variable X with law μ.

The main theorem of our paper is the following.

Theorem II.1.2 (Rotation invariance of critical random-cluster model)**.** *Fix $q \in [1,4]$ and a simply connected domain Ω with a C^1-smooth boundary. For every $\varepsilon > 0$, there exists $\delta_0 = \delta_0(q,\varepsilon,\Omega) > 0$ such that for every $\alpha \in (\varepsilon, \pi - \varepsilon)$ and $\delta \le \delta_0$, there exists a coupling $\mathbb{P}$ between $\omega_\delta \sim \phi^0_{\Omega_\delta}$ and $\omega'_\delta \sim \phi^0_{(e^{-i\alpha}\Omega)_\delta}$ such that*

$$\mathbb{P}[d_{\mathbf{SS}}(\omega_\delta, e^{i\alpha}\omega'_\delta) > \varepsilon] < \varepsilon,$$
$$\mathbb{P}[d_{\mathbf{CN}}(\omega_\delta, e^{i\alpha}\omega'_\delta) > \varepsilon] < \varepsilon.$$

This theorem has a number of applications for the random-cluster model. First, the definition of the Schramm-Smirnov topology implies, in particular, that crossing probabilities are invariant under rotation in the following sense. For a quad Q, let $\{\omega \in \mathcal{C}(Q)\}$ be the event that Q is crossed in the percolation configuration ω.

Corollary II.1.3 (Rotation invariance of crossing probabilities)**.** *Fix $q \in [1,4]$ and a simply connected domain Ω with a C^1-smooth boundary. For every $\varepsilon > 0$ small enough, there exists $\delta_0 = \delta_0(q,\varepsilon,\Omega) > 0$ such that for every quad Q with ε-neighborhood contained in Ω, every $\alpha \in (\varepsilon, \pi - \varepsilon)$, and every $\delta < \delta_0$,*

$$|\, \phi^0_{(e^{i\alpha}\Omega)_\delta}[\mathcal{C}(e^{i\alpha}Q)] - \phi^0_{\Omega_\delta}[\mathcal{C}(Q)] \,| \le \varepsilon.$$

Furthermore, the condition that Ω contains the ε-neighborhood of Q can be replaced[3] *by $\Omega \supset Q$ when $1 \le q < 4$.*

[1] Such a condition may be relaxed to cover any Jordan domain, yet we postpone such considerations to a later article to focus on the most interesting aspects of the problem at hand (which are already encompassed in the present framework).

[2] In fact, the proof will consist in first obtaining an infinite-volume version and then deducing from it the finite volume one.

[3] We also believe the result to be true for $q = 4$, but in this case both quantities may tend to zero (under certain conditions) as δ tends to 0.

We turn to "pointwise correlations". For points $x_1, \dots, x_n$ and a partition $\mathcal{P}$ of $\{x_1, \dots, x_n\}$, let $\mathcal{E}(\mathcal{P}, x_1, \dots, x_n)$ be the event that x_i and x_j are connected if and only if they belong to the same element of $\mathcal{P}$. The following corollary will be useful when studying spin-spin correlations in the Potts model.

Corollary II.1.4 (Rotation invariance of connectivity correlations)**.** *Fix $q \in [1, 4]$ and a simply connected domain Ω with a C^1-smooth boundary. For every $\varepsilon > 0$ and n, there exists $\delta_0 = \delta_0(q, n, \varepsilon, \Omega) > 0$ such that for every $\alpha \in (\varepsilon, \pi - \varepsilon)$ and $\delta \leq \delta_0$, every $x_1, \dots, x_n \in \Omega_\delta$ at a distance at least ε of each other and of the boundary of Ω, and every partition $\mathcal{P}$ of $\{x_1, \dots, x_n\}$,*

$$|\phi^0_{(e^{i\alpha}\Omega)_\delta}[\mathcal{E}(\mathcal{P}, e^{i\alpha}x_1, \dots, e^{i\alpha}x_n)] - \phi^0_{\Omega_\delta}[\mathcal{E}(\mathcal{P}, x_1, \dots, x_n)]| \leq \varepsilon\, \phi^0_{\Omega_\delta}[\mathcal{E}(\mathcal{P}, x_1, \dots, x_n)],$$

where we use, in a slight abuse of notation, $e^{i\alpha}x_i$ to denote a vertex x of $(e^{i\alpha}\Omega)_\delta$ within a distance δ of the image of x_i under the rotation by the angle α.

Remark II.1.5. We may also study the edge-density variables $\epsilon^\Omega_e := \omega_e - \phi^0_\Omega[\omega_e]$ and prove some rotation invariance for these variables. Obtaining this result requires some standard coupling argument that we postpone to a forthcoming paper in which we will prove additional properties of the near-critical regime of the model related to these edge-density variables.

II.2 Proof Roadmap

In this section, we outline the proof of Theorem II.1.2 and introduce several key concepts and results. This roadmap is essential for navigating the rest of the paper; the other parts of the paper may be read separately. Let us mention that all the results in the introduction are deduced from Theorem II.1.2 in fairly straightforward ways in Section II.7.

The main idea will be to couple the random-cluster model on the square lattice with a random-cluster model on a rotated rectangular lattice (meaning a lattice whose faces are rectangles) which has the line $e^{i\alpha/2}\mathbb{R}$ as axis of symmetry, in such a way that the Camia-Newman and Schramm-Smirnov distances between the two configurations are small. Then, one may couple the original model with the model on the rectangular lattice with this additional symmetry, use this symmetry, and then couple the obtained configuration with the original model, in such a way that the distance between the starting and final configurations is small with probability very close to one. This will therefore prove that the symmetry in question is an approximate symmetry of the original model. Together with the symmetries with respect to horizontal lines, this will imply the approximate rotational symmetry. In order to implement the scheme, we need a few additional notions.

II.2.1 Random-cluster model on isoradial rectangular graphs.

An *isoradial graph* $\mathbb{L}$ is a planar graph embedded in the plane in such a way that (i) every face is inscribed in a circle of radius 1 and (ii) the center of each circumcircle is contained in the corresponding face, see Fig. II.1. We sometimes call the embedding *isoradial* (note that it is a property of the embedding and that the graph can have several isoradial embeddings). Isoradial graphs were introduced by Duffin

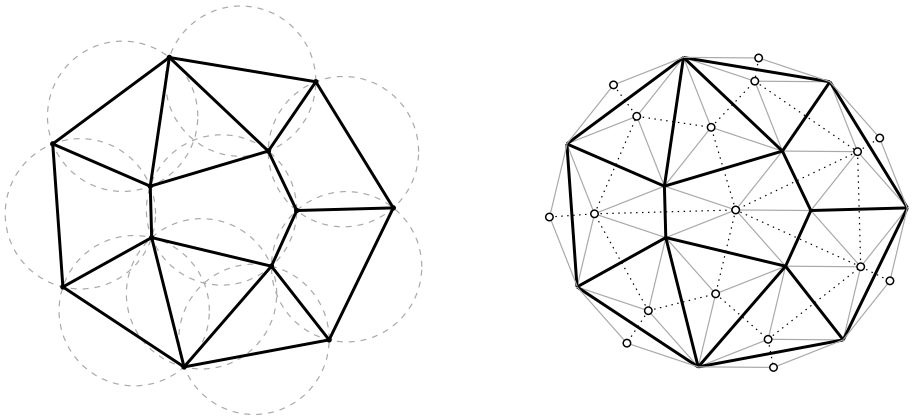

Figure II.1: The black graph is (a finite part of) an isoradial graph. All its faces can be inscribed into circumcircles of radius one. The centers of the inscribing circles have been drawn in white; the dual edges are in dotted lines. The diamond graph is drawn in gray in the right picture.

in [Duf68] in the context of discrete complex analysis, and later appeared in the physics literature in the work of Baxter [Bax78], where they are called Z-invariant graphs. The term isoradial was only coined later by Kenyon, who studied discrete complex analysis on these graphs [Ken02]. Since then, isoradial graphs have been studied extensively; we refer to [CS12, KS05, Mer01] for literature on the subject.

Given an isoradial graph $\mathbb{L}$ (which we call the *primal graph*), we can construct its *dual graph* $\mathbb{L}^*$ as follows: the vertex-set is given by the circumcenters of faces of $\mathbb{L}$, and the edges connect vertices that correspond to faces of $\mathbb{L}$ that share an edge. The *diamond graph* associated to $\mathbb{L}$ has vertex-set given by the vertices of $\mathbb{L}$ and $\mathbb{L}^*$, and edge-set given by the pairs (x, u) with $x \in \mathbb{L}$ and each $u \in \mathbb{L}^*$ which is the center of a face adjacent to x. All edges of the diamond graph are of length 1, and the diamond graph is a rhombic tiling of the plane. See Figure II.1 for an illustration.

A track of $\mathbb{L}$ is a bi-infinite sequence of adjacent faces $(r_i)_{i\in\mathbb{Z}}$ of the diamond graph, with the edges shared by each r_i and r_{i+1} being parallel. The angle formed by any such edge with the horizontal axis is called the *transverse angle* of the track.

Isoradial graphs considered in this paper are of a very special type, see Figure II.2. They will all be isoradial embeddings of the square lattice; moreover we assume that all diamonds have bottom and top edges that are horizontal. A consequence of this assumption is that the diamond graph can be partition into *(horizontal) tracks* t_i with a constant transverse angle α_i. When the sequence of track angles is $\boldsymbol{\alpha} = (\alpha_i)_{i\in\mathbb{Z}} \in (0, \pi)^{\mathbb{Z}}$, denote the graph by $\mathbb{L}(\boldsymbol{\alpha})$. When $\alpha_i = \alpha$ for every i, simply write $\mathbb{L}(\alpha)$ and call such lattices *rectangular lattices*. Note that $\mathbb{L}(\alpha)$ is a rotated version of a rectangular lattice that has $e^{i\alpha/2}\mathbb{R}$ as axis of symmetry. In particular, $\mathbb{L}(\frac{\pi}{2})$ is simply a rescaled and rotated (by an angle of $\pi/4$) version of $\mathbb{Z}^2$.

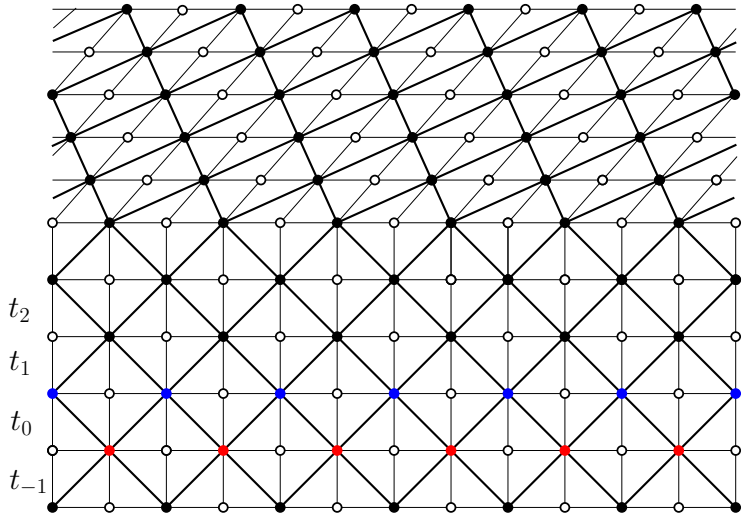

Figure II.2: An example of a graph $\mathbb{L}(\boldsymbol{\alpha})$, where α_i is equal to $\frac{\pi}{2}$ for $i \leq 3$, and α above. The diamond graph is drawn in light black lines, the white points refer to the vertices of the dual lattice, and the black points and the stronger black lines refer to the primal lattice. One sees that both the lower and upper parts are portions of a rotated rectangular lattice, and that below this rectangular lattice is simply the square lattice. The vertices of t_0^- are drawn in red, and those of t_0^+ in blue.

II.2.2 Universality among isoradial rectangular graphs and a first version of the coupling.

As described in Section II.3, isoradial graphs $\mathbb{L}(\boldsymbol{\alpha})$ are associated to a canonical set of edge-weights, therefore producing random-cluster measures $\phi_{\delta\mathbb{L}(\boldsymbol{\alpha})}$ on $\delta\mathbb{L}(\boldsymbol{\alpha})$. The next theorem states that the behaviour on different rectangular isoradial graphs is universal. In a way, this is the cornerstone of the paper.

Theorem II.2.1 (Universality of critical random-cluster models on rectangular graphs)**.** *For $q \in [1,4]$ and $\varepsilon > 0$, there exists $\delta_0 = \delta_0(q,\varepsilon) > 0$ such that for every $\delta < \delta_0$ and $\alpha \in (\varepsilon, \pi - \varepsilon)$, there exists a coupling $\mathbf{P}_{\alpha,\delta,\varepsilon}$ between $\omega \sim \phi_{\delta\mathbb{L}(\alpha)}$ and $\omega' \sim \phi_{\delta\mathbb{L}(\frac{\pi}{2})}$ such that*

$$\mathbf{P}_{\alpha,\delta,\varepsilon}[d_{\mathbf{CN}}(\omega,\omega') > \varepsilon] < \varepsilon,$$
$$\mathbf{P}_{\alpha,\delta,\varepsilon}[d_{\mathbf{SS}}(\omega,\omega') > \varepsilon] < \varepsilon.$$

This result states the universality of the scaling limit among rectangular lattices. It will be shown in Section II.7 that it implies Theorem II.1.2. Even though we already mentioned it before, let us recall that the proof will consist in using this theorem to relate the model on $\delta\mathbb{L}(\frac{\pi}{2})$ to the one on $\delta\mathbb{L}(\alpha)$, then use the reflection with respect to $e^{i\alpha/2}\mathbb{R}$, and finally use again the theorem to relate back the new graph to the model on a rotated version of $\delta\mathbb{L}(\frac{\pi}{2})$.

To describe the coupling of Theorem II.2.1, let us first ignore the rescaling by δ and simply work with $\delta = 1$. The coupling $\mathbf{P}_{\alpha,\delta,\varepsilon}$ will then simply be the push forward by the map $x \mapsto \delta x$ of a coupling between configurations in $\mathbb{L}(\alpha)$ and $\mathbb{L}(\frac{\pi}{2})$.

A naive and simplified version of the coupling can be described fairly easily. We do it now. The construction is based on exchanging tracks by successive applications of the star-triangle transformation. Below, let $\mathbf{T}_i$ be the track-exchange operator (constructed in Section II.3.5) exchanging the tracks t_i and t_{i-1}. This track exchange is seen as a random map on configurations, and a deterministic one on lattices; it maps $\mathbb{L}(\boldsymbol{\alpha})$ to $\mathbb{L}(\boldsymbol{\alpha}')$ where $\boldsymbol{\alpha}'$ is obtained from $\boldsymbol{\alpha}$ by exchanging α_i and α_{i-1}. It also maps configurations on $\mathbb{L}(\boldsymbol{\alpha})$ to possibly random configurations in $\mathbb{L}(\boldsymbol{\alpha}')$ by applying successive star-triangle operations. One of its most important features is that the push-forward of $\phi_{\mathbb{L}(\boldsymbol{\alpha})}$ by $\mathbf{T}_i$ is $\phi_{\mathbb{L}(\boldsymbol{\alpha}')}$. For readers who are not familiar with these notions, everything is detailed in Section II.3.5.

Coupling: version 1

1) Let $\mathbb{L}^{(0)}$ be the lattice with angles

$$\alpha_j = \alpha_j(\alpha, N) := \begin{cases} \alpha & \text{if } j \geq N, \\ \frac{\pi}{2} & \text{if } j < N. \end{cases}$$

and sample $\omega_\delta^{(0)} \sim \phi_{\mathbb{L}^{(0)}}$.

2) Recursively for $0 \leq t < T := 2N \times \lceil 2N/\sin\alpha \rceil$, define

$$j(t) := N + (2N+1)\lfloor t/(2N) \rfloor - t$$

and

$$\mathbb{L}^{(t+1)} := \mathbf{T}_{j(t)}(\mathbb{L}^{(t)}),$$
$$\omega^{(t+1)} := \mathbf{T}_{j(t)}(\omega^{(t)}).$$

Since the track-exchange operator $\mathbf{T}_{j(t)}$ preserves the law of the random-cluster model, we have that

$$\omega^{(t)} \sim \phi_{\mathbb{L}^{(t)}} \qquad \text{for every } t.$$

Also, note that $\omega^{(0)}$ and $\omega^{(T)}$ are not quite sampled according to $\phi_{\mathbb{L}(\pi/2)}$ and $\phi_{\mathbb{L}(\alpha)}$, but the law of the restriction to the strip $\mathbb{R} \times [-N, N]$ is the same on $\mathbb{L}^{(0)}$ and $\mathbb{L}(\frac{\pi}{2})$ (resp. $\mathbb{L}^{(T)}$ and $\mathbb{L}(\alpha)$) due to classical properties of the track-exchange operator (see Remark II.3.12 for a more precise statement).

The problem with this first version of the coupling is that it lacks ergodic properties that are essential to our proof (or at least it is not straightforward to prove them). We therefore introduce below a slightly modified version of the coupling where the configuration is resampled at each step, just keeping some relevant information on $\omega^{(t)}$. Which relevant information will be dictated by the following paragraph.

II.2.3 The homotopy topology and the second and third versions of the coupling.

The track-exchange operator behaves well with respect to certain properties of the collection of loops in the percolation configuration, among which the inclusion between large loops/clusters and the homotopy class of large loops in punctured planes. We will therefore work with the interpretation of configurations as collection of loops $\mathcal{F} = (\mathcal{F}_0, \mathcal{F}_1)$, but with a different distance than the Camia-Newman one.

For $\eta > 0$ and a loop γ, let $[\gamma]_\eta$ be its cyclic homotopy class in $\mathbb{R}^2 \setminus \mathbb{B}_\eta$, where $\mathbb{B}_\eta := \eta\mathbb{Z}^2 \cap [-1/\eta, 1/\eta]^2$. The homotopy classes will be encoded by reduced words, see Section II.5.1 for a detailed definition (for an explanation of why we chose to work with homotopy classes rather than the maybe more intuitive inclusion, see Figure II.3). Introduce the distance defined by

$$d_{\mathbf{H}}[\mathcal{F}, \mathcal{F}'] \leq \eta \iff \left(\begin{array}{l} \forall i \in \{0,1\}, \forall \gamma \in \mathcal{F}_i \text{ surrounding at least 2 but not all points in } \mathbb{B}_\eta \\ \exists \gamma' \in \mathcal{F}'_i \text{ s.t. } [\gamma]_\eta = [\gamma']_\eta, \text{ and similarly when exchanging } \mathcal{F} \text{ and } \mathcal{F}' \end{array} \right).$$

This distance controls the Camia-Newman and Schramm-Smirnov distances, as stated in the next theorem.

Theorem II.2.2 (Correspondence between different topologies)**.** *Fix $q \in [1,4]$. For every $\kappa > 0$, there exist $\eta = \eta(q,\kappa) > 0$ and $\delta_0 = \delta_0(\kappa,\eta) > 0$ such that for every $\delta < \delta_0$, and every $\alpha \in (0,\pi)$, if $\mathbf{P}$ denotes a coupling between $\omega_\delta \sim \phi^0_{\delta\mathbb{L}(\pi/2)}$ and $\omega'_\delta \sim \phi^0_{\delta\mathbb{L}(\alpha)}$,*

$$\mathbf{P}[d_{\mathbf{H}}[\omega_\delta, \omega'_\delta] \leq \eta \text{ and } d_{\mathbf{SS}}[\omega_\delta, \omega'_\delta] \geq \kappa] \leq \kappa,$$
$$\mathbf{P}[d_{\mathbf{H}}[\omega_\delta, \omega'_\delta] \leq \eta \text{ and } d_{\mathbf{CN}}[\omega_\delta, \omega'_\delta] \geq \kappa] \leq \kappa.$$

It may at first sight look strange that the shape of a large loop is well determined by its homotopy class. Indeed, one may produce arbitrarily large loops that have trivial homotopy. Yet, recall that percolation clusters are typically fractal, and that it is therefore unlikely that large parts of their contour do not contribute to the complexity of their homotopy class. For instance, one may easily see that it is very unlikely that a large loop is homotopically (almost) trivial.

With this theorem in our hands, we can reformulate Theorem II.2.1 into the following theorem.

Theorem II.2.3 (Universality of critical random-cluster models on rectangular graphs)**.** *For $q \in [1,4]$ and $\varepsilon > 0$, there exists $\delta_0 = \delta_0(q,\varepsilon) > 0$ such that for every $\delta < \delta_0$ and $\alpha \in (\varepsilon, \pi - \varepsilon)$, there exists a coupling $\mathbf{P}_{\alpha,\delta,\varepsilon}$ between $\omega \sim \phi_{\delta\mathbb{L}(\alpha)}$ and $\omega' \sim \phi_{\delta\mathbb{L}(\frac{\pi}{2})}$ such that*

$$\mathbf{P}_{\alpha,\delta,\varepsilon}[d_{\mathbf{H}}(\omega, \omega') > \varepsilon] < \varepsilon.$$

The trivial proof below justifies that we henceforth focus on deriving Theorem II.2.3.

Proof of Theorem II.2.1. Theorems II.2.3 and II.2.2 combine to give Theorem II.2.1. □

The fact that we are only interested in the homotopy classes of loops suggests that we may allow ourselves to resample the configuration at every step only keeping non-trivial homotopy classes in mind. This naturally leads to the next coupling (notations are the same as in the previous section).

Below, introduce the multiset $[\cdot]_{\eta,i}(\omega)$ gathering[4] the homotopy classes in $\mathbb{R}^2 \setminus N\mathbb{B}_\eta$ (here homotopy class is meant in the sense of Remark II.5.2) of the loops in $\mathcal{F}_i(\omega)$ (when ω is seen as an element of the Camia-Newman space) that surround at least two but not all points in $N\mathbb{B}_\eta$.

Coupling: second version

1) Sample $\omega^{(0)} \sim \phi_{\mathbb{L}^{(0)}}$.

2) Recursively for $0 \leq t < T$, given $\omega^{(t)}$,

- Sample $\omega^{(t+1/2)} \sim \phi_{\mathbb{L}^{(t)}}[\,\cdot\,|([\cdot]_{\eta,0},[\cdot]_{\eta,1})(\omega^{(t+1/2)}) = ([\cdot]_{\eta,0},[\cdot]_{\eta,1})(\omega^{(t)})]$,
- Sample $\omega^{(t+1)} := \mathbf{T}_{j(t)}(\omega^{(t+1/2)})$.

The construction still guarantees that $\omega^{(t)}$ has law $\phi_{\mathbb{L}^{(t)}}$ at each time step. Furthermore, the resampling trick keeps only the homotopy classes of loops in mind, while guaranteeing sufficient refreshment at each step. The problem with this second coupling is that we actually mislead the reader into believing that the track-exchange preserves in a reasonable fashion the homotopy classes of large loops.

What is true is that it preserves the homotopy "between loops". As a consequence, it is in fact more convenient to consider the homotopy classes of large loops in ω not with respect to points in $N\mathbb{B}_\eta$, but rather with respect to certain clusters, which we will call "marked nails" (see Section II.6 for a formal definition). At this point we do not enter into precise considerations concerning these nails, but simply mention that they will be mesoscopic clusters of ω which are close to the points in $N\mathbb{B}_\eta$. It will be crucial to control how the positions of these nails evolve during the process. At this stage, and in order not to complicate the discussion too much, let us informally consider $\mathcal{H}_{\text{intro}}(\omega)$ to be the information of the *position of the marked nails*, as well as the *homotopy classes* in $\mathbb{R}^2 \setminus \{\text{marked nails}\}$ of the loops in $\mathcal{F}(\omega)$ surrounding at least 2 and not all marked nails (we will see how to make formal sense of these notions in Section II.6).

Coupling: third version

1) Sample $\omega_\delta^{(0)} \sim \phi_{\mathbb{L}^{(0)}}$.

2) Recursively for $0 \leq t < T$, given $\omega^{(t)}$,

- Sample $\omega^{(t+1/2)} \sim \phi_{\mathbb{L}^{(t)}}[\,\cdot\,|\mathcal{H}_{\text{intro}}(\omega^{(t+1/2)}) = \mathcal{H}_{\text{intro}}(\omega^{(t)})]$,

[4]Formally, it is a function from the set of homotopy classes into non-negative integers.

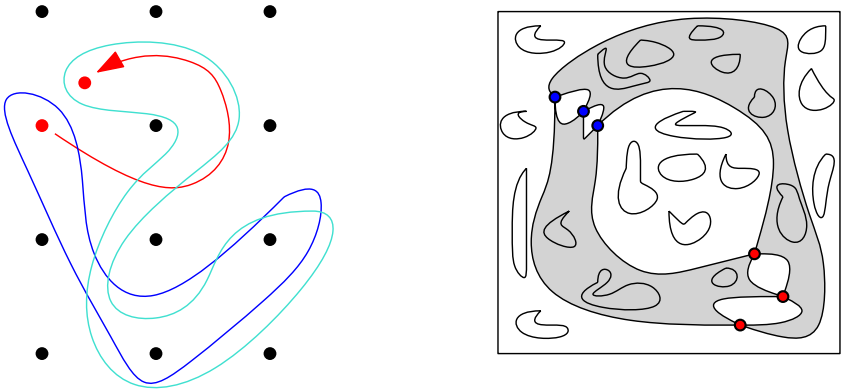

Figure II.3: On the left, an example of a transformation of the red points that continuously transforms a blue loop with a certain homotopy class into another blue loop with a different homotopy class. It is therefore crucial to encode homotopy classes in a coherent way, which will be done in Section II.5.1. Also, on the right, a justification of why we did not choose to keep track of a simpler property of loops, namely, the inclusion between loops. In the picture, the two loops created by opening one of the blue dots, or one of the red dots, have the same inclusion properties with respect to other loops, but have very different large scale connectivity properties (in particular they are far apart in Camia-Newman and Schramm-Smirnov distances). They do however have different homotopy classes with respect to other loops.

- Sample $\omega^{(t+1)} := \mathbf{T}_{j(t)}(\omega^{(t+1/2)})$.

The true coupling will be made completely explicit in Section II.6, in particular with a precise definition of the formal equivalent $\mathcal{H}(\omega)$ of $\mathcal{H}_{\text{intro}}(\omega)$. The coupling will be close (but not quite the same) to this one. There will be small technicalities related to the definition of marked nails, but all of this will be treated carefully in Section II.6, and the fourth version of the coupling defined there will be the final one.

The true (and interesting) challenge with this third coupling is to manage to relate the homotopy classes in $\mathbb{R}^2 \setminus \{\text{marked nails}\}$ to those in $\mathbb{R}^2 \setminus \mathbb{B}_\eta(N)$. Indeed, the coupling will perfectly preserve the former, but these homotopy classes relate to homotopy classes of $\mathbb{R}^2 \setminus \mathbb{B}_\eta(N)$ only if the marked nails are not moving too much. The main part of the proof of Theorem II.2.3 will be to show that this is indeed the case.

In order to do that, we will approximately write the global displacement of extrema for the nails as a sum of independent increments whose laws are dictated by the action of a track-exchange on Incipient Infinite Clusters with three-arms in half-planes. More precisely, fix $\alpha, \beta \in (0, \pi)$. Introduce the *(half-plane three-arm) Incipient Infinite Cluster (IIC) on* $\mathbb{L}(\beta)$ defined informally by the formula

$$\mathfrak{M}[\cdot] = \phi_{\mathbb{L}(\beta)}[\,\cdot\,|\text{lmax}(\infty) = 0],$$

where $\text{lmax}(\infty)$ is the left-most highest vertex on the infinite cluster (the condi-

tioning is degenerate, but can be made sense of, see the proper definition in Section II.3.4).

Then, consider a series of track exchanges bringing down a track of angle α from $+\infty$ to $-\infty$. We will prove that the average height of the highest vertex on the infinite cluster after this series of track exchanges is 0. In other words, the "drift" induced by passing down a track of angle α through an environment of tracks of angle β is zero.

This result will then be combined with the fact that highest points of nails look like highest points of the infinite cluster in the half-plane three arm IIC to prove that extremal coordinates of large clusters do not move much throughout the coupling described above. To complete this, soft arguments will enable us to extend this property to extrema in the other directions.

To conclude this part, let us mention that the original idea of [GM13a, GM13b, GM14] was to prove that macroscopic clusters of Bernoulli percolation do not move too fast when applying the track exchanges to transform one isoradial graph into another[5]. In this paper, we refine the argument by studying the drift of large clusters through the track-exchange coupling and by extending it to general random-cluster models. In order to prove that this speed is zero, we use the integrability of the six-vertex model on the torus.

II.2.4 Harvesting integrability on the torus

For a vertex v, let v^+ be the vertex on the top left of v. We will see in Section II.6 that proving that the drift is zero in the previous section will be related to the following result.

Fix $\alpha, \beta \in (0, \pi)$. Consider the graphs $\mathbb{L}_i = \mathbb{L}_i(\alpha, \beta)$ defined by $\alpha_j = \beta$ for $j \neq i$, and $\alpha_i = \alpha$. Let $\mathbb{\Phi}_i^2$ be the *2-rooted (half-plane three-arm) Incipient Infinite Cluster on* $\mathbb{L}_i$ defined as the random-cluster model on $\mathbb{L}_i$ conditioned on having an infinite cluster and having $\mathrm{lmax}(\infty)$ equal to 0 or 0^+ (see Section II.3.4 for a formal definition).

Theorem II.2.4. *For every $q \in [1, 4]$ and $\alpha, \beta \in (0, \pi)$,*

$$\mathbb{\Phi}_1^2[\mathrm{lmax}(\infty) = 0^+] = \frac{\sin\alpha}{\sin\alpha + \sin\beta} = \mathbb{\Phi}_0^2[\mathrm{lmax}(\infty) = 0]. \tag{II.2}$$

To prove this result, we work on the torus. For positive integers N, M with N even, let $\mathbb{T}_i(N, M)$ be the $N \times 2M$ torus with $2M$ horizontal tracks $t_{1-M}, \dots, t_M$ with angle equal to α for t_i and β for t_j with $j \neq i$. Let t_j^- (resp. t_j^+) denote the set of vertices on the bottom (resp. top) of the track t_j. Also, let $\phi_{\mathbb{T}_i(N,M)}$ be the random-cluster measure on $\mathbb{T}_i(N, M)$.

Fix $z_{-1}, z_0, z_1, x_1, \dots, x_k$ distinct vertices found on $t_{1-M}^-(= t_M^+)$ in that order. Let $y_1, \dots, y_k$ be the vertices of t_M^- such that $x_i = y_i^+$. Define the event (see Figure II.4):

$$E(k) = E(k, z_{-1}, z_0, z_1, x_1, \dots, x_k, y_1, \dots, y_k, N, M)$$

that

[5] In these papers, the notion of speed was not introduced nor proved to exist, but in the language of this paper, the results of [GM13a, GM13b, GM14] state that the absolute value of the speed is strictly smaller than 1 for Bernoulli percolation.

(i) the only edges that are open in t_M are the edges linking x_i and y_i,
(ii) there are k disjoint clusters connecting x_i to y_i for $1 \leq i \leq k$ in $\mathbb{T}_i(N,M) \setminus t_M$ (note that these clusters are also disjoint in $\mathbb{T}_i(N,M)$),
(iii) z_{-1} is connected to z_1 but not to z_0 or to any of the x_i among $x_1, \dots, x_k$.

Roughly speaking, the event states that there exists k disjoint clusters "winding" vertically around the torus, along with a separate cluster forming an arch above z_0. The role of this event will be explained after Theorem II.2.7.

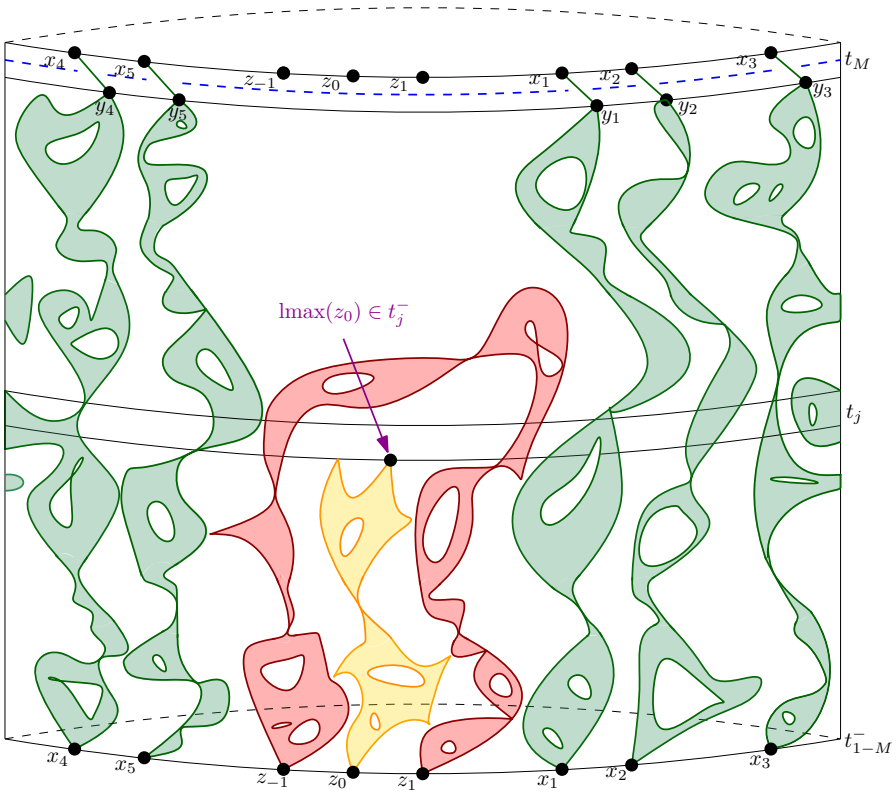

Figure II.4: A picture of the event $E_j(k)$. Note that we are on a torus, hence $t_{1-M}^- = t_M^+$.

If $\mathrm{lmax}(z_0)$ denotes the left-most highest vertex of the cluster of z_0, set, for $-M < j \leq M$,

$$E_j(k) := E(k) \cap \{\mathrm{lmax}(z_0) \in t_j^-\}. \tag{II.3}$$

The interest of these events comes from the following proposition combining two tools from exact integrability: the commutation of transfer matrices and the asymptotic behaviour of the Perron-Frobenius eigenvalues of the transfer matrix of the six-vertex model. More precisely, let $V_N(q,\theta)$ be the transfer matrix of the six-vertex on a torus of width N, with weights a, b, c given, if $\zeta \in [0, \pi/2]$ satisfies $\sqrt{q}/2 = \cos\zeta$, by the formulae

$$a \sin\tfrac{\zeta}{2} = \sin(1 - \tfrac{\theta}{\pi})\zeta \qquad b \sin\tfrac{\zeta}{2} = \sin\tfrac{\theta\zeta}{\pi} \qquad c = 2\cos\tfrac{\zeta}{2}. \tag{II.4}$$

Let $\lambda_N^{(k)}(\theta)$ be the Perron-Frobenius eigenvalue of the block of the transfer matrix with $N/2+k$ up arrows (and therefore $N/2-k$ down arrows) per row. To better grasp the signs in the next statements, note that $\lambda_N^{(k)}(\theta)$ is non-increasing in k.

Proposition II.2.5. *For every $\alpha, \beta \in (0,\pi)$ and every $N \geq 2k$,*

$$\lim_{M\to\infty} \frac{\phi_{\mathbb{T}_1(N,M)}[E_1(k)]}{\phi_{\mathbb{T}_1(N,M)}[E_0(k)]} = \frac{\lambda^{(k)}(\beta)}{\lambda^{(k+3)}(\beta)} \times \frac{1-\lambda_N^{(k+3)}(\alpha)/\lambda_N^{(k)}(\alpha)}{1-\lambda_N^{(k+3)}(\beta)/\lambda_N^{(k)}(\beta)},$$
$$\lim_{M\to\infty} \frac{\phi_{\mathbb{T}_0(N,M)}[E_1(k)]}{\phi_{\mathbb{T}_0(N,M)}[E_0(k)]} = \frac{\lambda^{(k+3)}(\alpha)}{\lambda^{(k)}(\alpha)} \times \frac{1-\lambda_N^{(k+3)}(\beta)/\lambda_N^{(k)}(\beta)}{1-\lambda_N^{(k+3)}(\alpha)/\lambda_N^{(k)}(\alpha)}.$$

This proposition combines very well with the following probabilistic estimate.

Proposition II.2.6. *For every $\alpha, \beta \in (0, \frac{\pi}{2})$, there exist $C, \eta > 0$ such that for $i = 0, 1$ and every $k \leq N/2$,*

$$\big| \lim_{M\to\infty} \phi_{\mathbb{T}_i(N,M)}[E_1(k) | E_1(k) \cup E_0(k)] - \mathfrak{h}_i^2[\mathrm{lmax}(\infty) = 0^+] \big| \leq C\Big(\frac{\lambda_N^{(k)}(\beta)}{\lambda_N^{(k+3)}(\beta)} - 1\Big)^{\eta}.$$

To interpret this proposition, think of a value of k for which $\lambda_N^{(k)}(\beta)/\lambda_N^{(k+3)}(\beta)$ is close to 1, which should be the case when N/k is large. By the definition of the events $E_0(k)$ and $E_1(k)$, there are k clusters crossing the torus from bottom to top, with an additional cluster finishing either on t_0^- or $t_1^-(=t_0^+)$. One expects the different clusters to be typically distant of roughly N/k. In particular, one may predict that none of the clusters of the x_i or $z_{\pm 1}$ comes close (meaning much closer than N/k) to the maximum of the cluster of z_0. Proving the separation property will not be straightforward, and will constitute the heart of the proof of this proposition. Now, the convergence of finite volume measures with proper conditioning to $\mathfrak{h}_i^2$ would imply that near the top of the cluster, the measure $\phi_{\mathbb{T}_i}[\,\cdot\,|E_1(k) \cup E_0(k)]$ can be coupled with $\mathfrak{h}_i^2$ with probability close to 1 when N/k is very large.

These two propositions will combine with the following statement from [DCKK$^+$20b, Thm. 22] on the behaviour of the eigenvalues for the six-vertex model's transfer matrix, to prove Theorem II.2.4.

Theorem II.2.7. *For every $\theta \neq \pi/2$ and $\Delta \in (-1,0)$, there exists $C = C(\Delta) < \infty$ such that, for every N, k large enough,*

$$\tfrac{1}{N} \log \lambda_N^{(k)}(\theta) = F(a,b,c) - C(\Delta) \sin\theta (1+o(1)) (\tfrac{k}{N})^2 + O(\tfrac{1}{kN}), \tag{II.5}$$

where $o(1)$ is a quantity tending to zero as k/N tends to 0.

The reason for working with the events $E_j(k)$ rather than the simpler event $\{\mathrm{lmax}(z_0) \in t_j^-\}$ is now apparent: the asymptotic in (II.5) is most meaningful when $N = o(k^3)$, so that the $O(\frac{1}{kN})$ becomes insignificant compared to the middle term. The arch formed by the cluster of $z_{\pm 1}$ is not strictly necessary, but will simplify the proof of Proposition II.2.6.

A finer asymptotic for $\frac{1}{N}\log\lambda_N^{(1)}(\theta)$ would allow one to circumvent the introduction of $E(k)$, and would eliminate all difficulties from the proof of Proposition II.2.6. Unfortunately, at the time of wiring, no such asymptotic is available.

Organization In Section II.3, we recall some background on the random-cluster model on isoradial graphs and prove several technical facts that will be used later in the paper. In Section II.4, we show Theorem II.2.4 via Propositions II.2.5 and II.2.6. Section II.5 proves Theorem II.2.2. In Section II.6, we explain how Theorem II.2.3 is derived. Finally, in Section II.7, we show Theorem II.1.2 as well as its direct applications.

II.3 Preliminaries

II.3.1 Definition of the random-cluster model

For a graph $G = (V, E)$ included in an isoradial graph $\mathbb{G} = (\mathbb{V}, \mathbb{E})$ with vertex-set V and edge-set E, *boundary conditions* ξ on G are given by a partition of the set ∂G of vertices in V incident to a vertex in $\mathbb{V} \setminus V$. We say that two vertices of G are *wired together* if they belong to the same element of the partition ξ. Recall that a *cluster* is a connected component of ω.

In the paper, we will always work with the random-cluster model on an isoradial graph with specific weights, called *isoradial weights*, associated with this graph, given by

$$p_e := \begin{cases} \dfrac{\sqrt{q}\sin(r(\pi-\theta_e))}{\sin(r\theta_e)+\sqrt{q}\sin(r(\pi-\theta_e))} & \text{if } q<4, \\ \dfrac{2\pi-2\theta_e}{2\pi-\theta_e} & \text{if } q=4, \\ \dfrac{\sqrt{q}\sinh(r(\pi-\theta_e))}{\sinh(r\theta_e)+\sqrt{q}\sinh(r(\pi-\theta_e))} & \text{if } q>4, \end{cases} \tag{II.6}$$

(the last case is not relevant to this paper, see below) where $r := \frac{1}{\pi}\cos^{-1}\left(\frac{\sqrt{q}}{2}\right)$ for $q \le 4$ and the same formula with cosh instead of cos for $q > 4$, and $\theta_e \in (0, \pi)$ is the angle subtended by e (see Figure II.5).

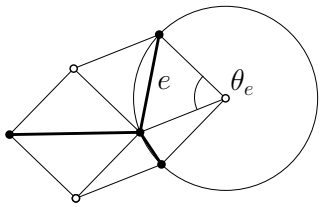

Figure II.5: The edge e and its subtended angle θ_e; bold edges are those of $\mathbb{G}$, thin ones are those of the diamond graph.

Definition II.3.1. The random-cluster measure with isoradial edge-weights and cluster-weight $q > 0$ on a finite graph G with boundary conditions ξ is given by

$$\phi^{\xi}_{G,q}[\omega] := \frac{q^{k(\omega^\xi)}}{Z^{\xi}_{\mathrm{RCM}}(G,q)} \prod_{e\in E} p_e^{\omega_e}(1-p_e)^{1-\omega_e}, \tag{II.7}$$

where $k(\omega^\xi)$ is the number of connected components of the graph ω^ξ which is obtained from ω by identifying wired vertices together, and $Z^{\xi}_{\mathrm{RCM}}(G,q)$ is a normal-

ising constant called the *partition function* chosen in such a way that $\phi^{\xi}_{G,q}$ is a probability measure.

Two specific families of boundary conditions will be of special interest to us. On the one hand, the *free* boundary conditions, denoted 0, correspond to no wirings between boundary vertices. On the other hand, the *wired* boundary conditions, denoted 1, correspond to all boundary vertices being wired together.

We will also consider the random-cluster model on infinite isoradial graphs $\mathbb{G}$ with free boundary conditions obtained by taking the limit of the measures with free boundary conditions on larger and larger finite graphs G tending to $\mathbb{G}$. Set $\phi_{\mathbb{G},q}$ for the measure in infinite volume, which, as shows in [DCLM18] is unique for $1 \leq q \leq 4$.

The choice of the isoradial parameters is such that the model is critical. This result was obtained in the case of the square lattice in [BDC12] and for isoradial graphs in [DCLM18] (see also the anterior paper [BDCS15] for the case $q > 4$).

As we will always fix isoradial weights and $q \in [1, 4]$, we remove their dependency from the notation.

II.3.2 Elementary properties of the random-cluster model

We will use the following standard properties of the random-cluster model. They can be found in [Gri04], and we only recall them briefly below.

Monotonic properties. Fix G as above. An event A is called *increasing* if for any $\omega \leq \omega'$ (for the partial ordering on $\{0,1\}^E$ given by $\omega \leq \omega'$ if $\omega_e \leq \omega'_e$ for every $e \in E$), $\omega \in A$ implies that $\omega' \in A$. Fix $q \geq 1$ and some boundary conditions $\xi' \geq \xi$, where $\xi' \geq \xi$ means that any wired vertices in ξ are also wired in ξ'. Then, for every increasing events A and B,

$$\phi^{\xi}_{G}[A \cap B] \geq \phi^{\xi}_{G}[A]\phi^{\xi}_{G}[B], \tag{FKG}$$

$$\phi^{\xi'}_{G}[A] \geq \phi^{\xi}_{G}[A]. \tag{CBC}$$

The inequalities above will respectively be referred to as the *FKG inequality* and the *comparison between boundary conditions*.

Spatial Markov property. For any configuration $\omega' \in \{0,1\}^E$ and any $F \subset E$,

$$\phi^{\xi}_{G}[\cdot_{|F} \,|\, \omega_e = \omega'_e, \forall e \notin F] = \phi^{\xi'}_{H}[\cdot], \tag{SMP}$$

where H denotes the graph induced by the edge-set F, and ξ' are the boundary conditions on H defined as follows: x and y on ∂H are wired if they are connected in $(\omega'_{|E\setminus F})^{\xi}$.

A direct consequence of the spatial Markov property is the *finite-energy property* guaranteeing that conditioned on the states of all the other edges in a graph, the probability that an edge is open is between $p/(p + q(1-p))$ and p.

Dual model. Define (see Figure II.6) the dual graph $G^* = (V^*, E^*)$ of G as follows: place dual sites at the centers of the faces of G (the external face, when considering a graph in the plane, must be counted as a face of the graph), and for every edge $e \in E$, place a dual edge between the two dual sites corresponding to faces bordering e. When the graph is isoradial, we make the following choice for the position of dual vertices in V^*: the vertex v^* corresponding to a face of G is placed at the center of the corresponding circumcircle. The dual of an isoradial graph is by construction an isoradial graph.

Given a subgraph configuration ω, construct a configuration ω^* on G^* by declaring any edge of the dual graph to be open (resp. closed) if the corresponding edge of the primal lattice is closed (resp. open) for the initial configuration. The new configuration is called the *dual configuration* of ω. The dual model on the dual graph given by the dual configurations then corresponds to a random-cluster measure with isoradial weights and dual boundary conditions. We do not want to discuss too much the details of how dual boundary conditions are defined (we refer to [Gri04] for details and to [DCLM18] for the isoradial setting) and we simply observe that the dual of free boundary conditions are the wired ones, and vice versa.

Loop model. The loop representation of a configuration on G is supported on the *medial graph* of G defined as follows (see Figure II.6). For an isoradial lattice $\mathbb{G}$, let $\mathbb{G}^\diamond$ be the graph with vertex-set given by the midpoints of edges of $\mathbb{G}$ and edges between pairs of nearest vertices. For future reference, note that the faces of $\mathbb{G}^\diamond$ contain either a vertex of $\mathbb{G}$ or one of $\mathbb{G}^*$, and that it is the dual of the diamond graph. Let $G^\diamond$ be the subgraph of $\mathbb{G}^\diamond$ spanned by the edges of $\mathbb{G}^\diamond$ adjacent to a face corresponding to a vertex of G.

Let ω be a configuration on G; recall its dual configuration ω^*. Draw self-avoiding paths on $G^\diamond$ as follows: a path arriving at a vertex of the medial lattice always takes a turn at vertices so as not to cross the open edges of ω or ω^*. The loop configuration $\overline{\omega}$ thus defined is formed of disjoint loops. Together these form a partition of the edges of $G^\diamond$.

Let us conclude this section by mentioning that we will (almost) always consider $\mathbb{G} = \mathbb{L}(\boldsymbol{\alpha})$.

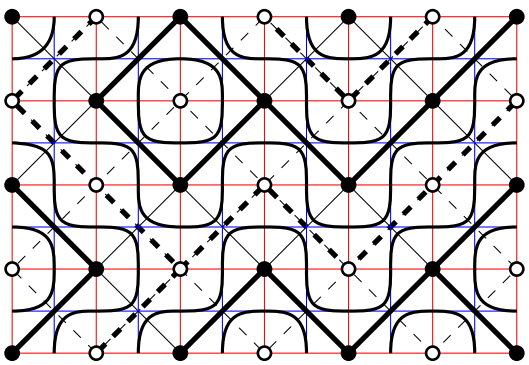

Figure II.6: We depicted in black, dotted black, red and blue respectively the primal, dual, diamond and medial lattices. The primal configuration ω is in bold and the dual one ω^* in dashed bold. Finally, the loop configuration $\overline{\omega}$ is in black.

II.3.3 Uniform bounds on crossing probabilities

As it is often the case when investigating the critical behaviour of lattice models, we will rely on uniform crossing estimates in rectangles, as well as estimates on certain universal and non-universal critical exponents. Such crossing estimates initially emerged in the study of Bernoulli percolation in the late seventies under the coined name of Russo-Seymour-Welsh theory [Rus78, SW78].

Recall the following definition: for a quad Q, let $\mathcal{C}(Q)$ be the event that Q is crossed in the percolation configuration ω (when ω is seen as an element of the Schramm-Smirnov set $\mathfrak{H}$, this corresponds to the event $\omega \in Q$).

Theorem II.3.2. *For $1 \leq q \leq 4$ and $\rho, \varepsilon > 0$, there exists $c = c(\rho, \varepsilon) > 0$ such that for every $n \geq 1$, every $\boldsymbol{\alpha} = (\alpha_i : i \in \mathbb{Z})$ with $\varepsilon \leq \alpha_i \leq \pi - \varepsilon$ for every $i \in \mathbb{Z}$, every $\Omega \subset \mathbb{R}^2$ containing the εn neighborhood of $R := [0, \rho n] \times [0, n]$), and every boundary conditions ξ,*

$$c \leq \phi^{\xi}_{\mathbb{L}(\boldsymbol{\alpha})\cap\Omega}[\mathcal{C}(R)] \leq 1 - c. \tag{RSW}$$

Proof. This result is a direct consequence of [DCLM18, Thm. 1.1]. While that paper studies doubly-periodic isoradial graphs, the techniques in it extend to our framework with rectangular-type tracks with angles $\alpha_i \in (\varepsilon, \pi - \varepsilon)$ for every $i \in \mathbb{Z}$ (this condition guarantees a uniform bounded angle property; see comments below [DCLM18, Thm. 1.2]). □

Remark II.3.3. We will repeatedly use this theorem as well as a number of its classical applications. We are aware that some proofs may be difficult to read for somebody not familiar with Russo-Seymour-Welsh type arguments. We tried to be complete but succinct, as there is a clear trade-off in the proofs below between providing a large amount of detail on classical RSW machinery, and putting emphasis on the novel arguments in this paper. We refer to the large literature on the RSW theory to see some of the classical arguments we will use in this article.

We now discuss some consequences of the above. The previous theorem has classical applications for the probability of so-called arm events. Below, $\Lambda_n \subset \mathbb{G}$ is the subgraph of $\mathbb{G}$ induced by vertices in $[-n, n]^2 \subset \mathbb{R}^2$. A self-avoiding path of type 0 or 1 connecting the inner to the outer boundary of an annulus $\Lambda_R \setminus \Lambda_{r-1}$ is called an *arm*. We say that an arm is *of type* 1 if it is composed of primal edges that are all open in ω, and *of type* 0 if it is composed of dual edges that are all open in ω^*. For $k \geq 1$ and $\sigma \in \{0, 1\}^k$, define $A_\sigma(r, R)$ to be the event that there exist k *disjoint* arms from $\partial\Lambda_r$ to $\partial\Lambda_R$ which are of type $\sigma_1, \ldots, \sigma_k$, when indexed in counterclockwise order. We also introduce $A^X_\sigma(r, R)$ to be the same event as $A_\sigma(r, R)$, except that the paths must lie in the lower half-plane $\mathbb{H}^- := \mathbb{R} \times (-\infty, 0]$ if $X = \mathrm{T}$, upper-half-plane $\mathbb{H}^+ := \mathbb{R} \times [0, +\infty)$ if $X = \mathrm{B}$, and left half-plane $\mathbb{L}(\boldsymbol{\alpha}) \cap ((\infty, 0] \times \mathbb{R})$ if $X = \mathrm{R}$.

Finally, let $A^{\mathrm{TR}}_{010}(r, R)$ be the event that there are three arms (two of type 0 and one of type 1) in the quarter plane $[-\infty, 0]^2$, and $A^X_{010}(r, R) \circ A_1(r, R)$ the event that there are three arms in the corresponding half-plane, plus an additional disjoint arm of type 1 in the plane.

We will need the following two estimates.

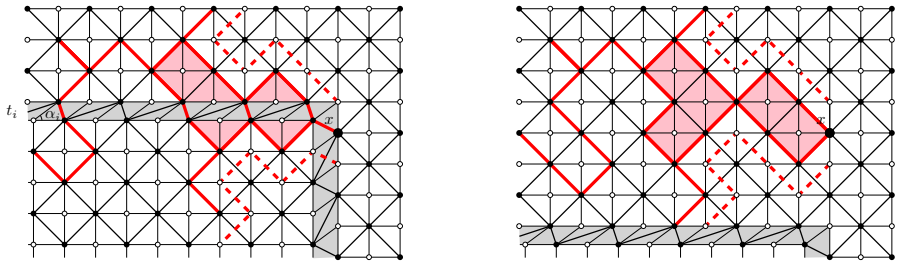

Figure II.7: On the left is an isoradial lattice in the left half-plane, almost identical to $\mathbb{L}(\boldsymbol{\alpha})$. The three arm events for any point on the vertical axis have the same probability in the left and right graphs.

Proposition II.3.4 (Estimates on certain arm events)**.** *For every $\varepsilon > 0$, there exist $c, C \in (0, \infty)$ such that for every $1 \leq q \leq 4$, every $R \geq r \geq 1$ and every $\boldsymbol{\alpha}$ with $\alpha_i \in (\varepsilon, \pi - \varepsilon)$ for every $i \in \mathbb{Z}$,*

$$\phi_{\mathbb{L}(\boldsymbol{\alpha})}[A_1(r,R)] \leq C(r/R)^c, \tag{II.8}$$
$$\phi_{\mathbb{L}(\boldsymbol{\alpha})}[A^{\mathrm{T}}_{010}(r,R)] \leq C(r/R)^2, \tag{II.9}$$
$$\phi_{\mathbb{L}(\boldsymbol{\alpha})}[A^{\mathrm{B}}_{010}(r,R)] \leq C(r/R)^2, \tag{II.10}$$
$$\phi_{\mathbb{L}(\boldsymbol{\alpha})}[A^{\mathrm{R}}_{010}(r,R)] \leq C(r/R)^{1+c}, \tag{II.11}$$
$$\phi_{\mathbb{L}(\boldsymbol{\alpha})}[A^{\mathrm{TR}}_{010}(r,R)] \leq C(r/R)^{2+c}, \tag{II.12}$$
$$\phi_{\mathbb{L}(\boldsymbol{\alpha})}[A^{\mathrm{T}}_{010}(r,R) \circ A_1(r,R)] \leq C(r/R)^{2+c}. \tag{II.13}$$

Furthermore, if α_i is equal to $\pi/2$ except for one value of i, then we also have

$$\phi_{\mathbb{L}(\boldsymbol{\alpha})}[A^{\mathrm{R}}_{010}(r,R)] \leq C(r/R)^2, \tag{II.14}$$
$$\phi_{\mathbb{L}(\boldsymbol{\alpha})}[A^{\mathrm{R}}_{010}(r,R) \circ A_1(r,R)] \leq C(r/R)^{2+c}. \tag{II.15}$$

Proof. The first bound can be obtained from (RSW) using standard techniques from Bernoulli percolation.

For the second and third ones, the case of the square lattice is also a direct consequence of (RSW) and standard techniques of Bernoulli percolation. Transferring the estimates to $\mathbb{L}(\boldsymbol{\alpha})$ can be done using the techniques in [DCLM18, Theorem 1.4]).

The argument involving [DCLM18, Theorem 1.4] only allows one to access exponents for half-planes delimited by straight tracks, but does not apply to arm exponents in the left half-plane of $\mathbb{L}(\boldsymbol{\alpha})$. Nevertheless, the special condition on the lattice allows one to obtain (II.14) via a simple trick. Indeed, assuming that $\alpha_i < \pi/2$, consider the isoradial graph on the left of Figure II.7. Applying repeated star-triangle transformations (see also Figure II.27 for the exact procedure), the probability of a half-plane three arm event for any vertex on the vertical axis may be shown to be the same in the left and right lattices of Figure II.7, and ultimately be equal to the corresponding probability in the square lattice. Thus, (II.14) follows from the result for the square lattice.

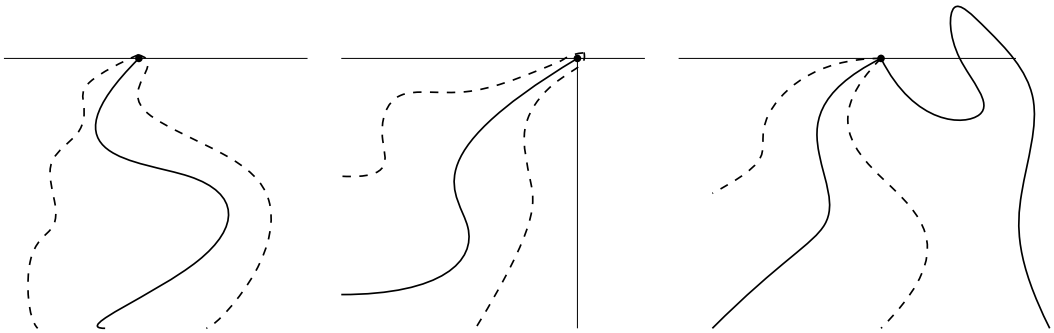

Figure II.8: On the left, an instance of $A^{\mathrm{T}}_{010}(0,R)$ where the primal path is depicted by a bold path, and the dual ones by dashed paths. In the middle, an instance of $A^{\mathrm{TR}}_{010}(0,R)$. On the right, $A^{\mathrm{T}}_{010}(0,R) \circ A_1(0,R)$.

For (II.11), note that the classical argument for Bernoulli percolation for the two-arm event in the half-plane immediately implies that

$$\phi_{\mathbb{L}(\boldsymbol{\alpha})}[A^{\mathrm{R}}_{01}(r,R)] \leq C(r/R). \tag{II.16}$$

Therefore, (II.11) follows by conditioning on the first two arms, and then using (RSW) and the comparison between boundary conditions to bound the probability of the third arm.

For (II.12), one may use (RSW) to prove that

$$\phi_{\mathbb{L}(\boldsymbol{\alpha})}[A^{\mathrm{TR}}_{010}(r,R)] \leq C(r/R)^c \phi_{\mathbb{L}(\boldsymbol{\alpha})}[A^{\mathrm{T}}_{010}(r,R)] \leq C(r/R)^{2+c}.$$

For (II.13), one can condition on the first three arms, and then use (II.8) and the comparison between boundary conditions to bound the probability of the fourth arm. □

A second consequence of (RSW) that we will repeatedly use is the mixing property.

Proposition II.3.5 (Mixing property)**.** *For every $\varepsilon > 0$, there exist $C_{\mathrm{mix}}, c_{\mathrm{mix}} \in (0,\infty)$ such that for every $\boldsymbol{\alpha}$ with $\alpha_i \in (\varepsilon, \pi-\varepsilon)$ for every $i \in \mathbb{Z}$, every $r \leq R/2$, every event A depending on edges in Λ_r, and every event B depending on edges outside Λ_R, we have that*

$$\left|\phi_{\mathbb{L}(\boldsymbol{\alpha})}[A \cap B] - \phi_{\mathbb{L}(\boldsymbol{\alpha})}[A]\phi_{\mathbb{L}(\boldsymbol{\alpha})}[B]\right| \leq C_{\mathrm{mix}}(r/R)^{c_{\mathrm{mix}}} \phi_{\mathbb{L}(\boldsymbol{\alpha})}[A]\phi_{\mathbb{L}(\boldsymbol{\alpha})}[B].$$

Proof. The argument follows the same lines as for the square lattice, see e.g. [DCM20, Proposition 2.9]. □

The previous properties imply the following, which we will use repeatedly.

Proposition II.3.6 (Crossing in annulus with adverse boundary conditions)**.** *There exists $c > 0$ such that for every $r \leq R/2$, every $\Omega \subset \mathbb{L}(\boldsymbol{\alpha})$ with $\alpha_i \in (\varepsilon, \pi-\varepsilon)$ for every $i \in \mathbb{Z}$, and every boundary conditions ξ inducing free boundary conditions on $\partial\Omega \cap (\Lambda_R \setminus \Lambda_r)$,*

$$\phi^{\xi}_{\Omega}[\Lambda_r \longleftrightarrow \partial\Lambda_R] \leq (r/R)^c.$$

Proof. The comparison between boundary conditions implies that

$$\phi_{\mathbb{L}(\boldsymbol{\alpha})}[\Lambda_r \longleftrightarrow \partial\Lambda_R] \leq \phi^1_{\Lambda_R\setminus\Lambda_r}[\Lambda_r \longleftrightarrow \partial\Lambda_R].$$

Now, the mixing property together with (II.8) conclude the proof. □

Finally, we will also use the following easy claim.

Proposition II.3.7 (Tight number of macroscopic clusters in a box)**.** *For $\varepsilon > 0$, there exist $c, C \in (0,\infty)$ such that for every $N \geq 0$ and every $\boldsymbol{\alpha}$ with $\alpha_i \in (\varepsilon, \pi-\varepsilon)$ for every $i \in \mathbb{Z}$,*

$$\phi_{\mathbb{L}(\boldsymbol{\alpha})}[\exp(c\mathbf{N}_\varepsilon)] \leq C, \tag{II.17}$$

where $\mathbf{N}_\varepsilon$ be the number of clusters of diameter at least εN intersecting Λ_N.

Proof. The claim follows if we can show that for some constant $c_0 > 0$, we have that for every $k \geq 0$,

$$\phi_{\mathbb{L}(\boldsymbol{\alpha})}[\mathbf{N}_\varepsilon \geq k+1 | \mathbf{N}_\varepsilon \geq k] \leq 1 - c_0.$$

Index the vertices in the box one by one and let $\mathcal{C}_i$ be the cluster of the i-th vertex (it is equal to the clusters $\mathcal{C}_j$ for every j such that the j-th vertex belongs to $\mathcal{C}_i$). Let $\mathbf{i}$ be the smallest index i such that there are k clusters of diameter at least εN among $\mathcal{C}_j$ for $1 \leq j \leq i$. Conditioned on $\mathcal{C}_1, \dots, \mathcal{C}_{\mathbf{i}}$, the boundary conditions outside of the union of these clusters are free within the box. One easily deduces from (RSW) and the comparison between boundary conditions that the probability that there is an additional cluster of diameter at least εN is smaller than $1 - c_0$, hence concluding the proof of the proposition. □

II.3.4 Incipient Infinite Clusters with three arms in the half-plane

In this section, we introduce the Incipient Infinite Cluster (IIC) measures with three arms in the half-plane. Let $\alpha, \beta \in (0,\pi)$ be two angles. Recall the definitions of $\mathbb{L}(\beta)$ and $\mathbb{L}_i(\alpha,\beta)$. Below, we use the shorthand notation $\mathbb{L} := \mathbb{L}(\beta)$ and $\mathbb{L}_i := \mathbb{L}_i(\alpha,\beta)$ and embed the lattices in such a way that the origin 0 is a vertex of the graph. Let $\mathrm{lmax}(v)$ be the left-most highest vertex of the cluster of v.

Theorem II.3.8. *For every $\alpha, \beta \in (0,\pi)$, there exist a measure $\mathbb{\Phi}$ on $\mathbb{L}(\beta)$ and measures $\mathbb{\Phi}_i$ and $\mathbb{\Phi}_i^2$ on $\mathbb{L}_i$ for every $i \in \mathbb{Z}$ such that for every event A depending on finitely many edges,*

$$\begin{aligned}
\mathbb{\Phi}[A] &= \lim_{R\to\infty} \phi^0_{\mathbb{L}}[A | 0 \longleftrightarrow \partial\Lambda_R, \mathrm{lmax}(0) = 0],\\
\mathbb{\Phi}_i[A] &= \lim_{R\to\infty} \phi^0_{\mathbb{L}_i}[A | 0 \longleftrightarrow \partial\Lambda_R, \mathrm{lmax}(0) = 0],\\
\mathbb{\Phi}_i^2[A] &= \lim_{R\to\infty} \phi^0_{\mathbb{L}_i}[A | \{0 \longleftrightarrow \partial\Lambda_R, \mathrm{lmax}(0) = 0\} \cup \{0^+ \leftrightarrow \partial\Lambda_R, \mathrm{lmax}(0^+) = 0^+\}].
\end{aligned}$$

Proof. The proof of this theorem follows the same lines as the construction of the IIC for Bernoulli percolation once one has (RSW). We omit the details here and refer to [BS17, GPS18, Jár03, Kes86]. □

We also mention a mixing property. We state it in the way which is closest to applications.

Proposition II.3.9 (Mixing property for IIC)**.** *For every $\varepsilon > 0$, there exist $C, c > 0$ such that for every $\alpha, \beta \in (\varepsilon, \pi - \varepsilon)$, every $r \leq R/2$, every event A depending on Λ_r, every $\Omega \supset [-R, R]^2$, every $I \subset \partial\Omega$, every $x \in \partial\Omega \setminus I$, and every boundary conditions ξ, we have that*

$$|\mathbb{\Phi}[A] - \phi^{\xi}_{\Omega\cap\mathbb{L}}[A | x \overset{I}{\not\leftrightarrow}, \mathrm{lmax}(x) = 0]| \leq C(r/R)^c,$$
$$|\mathbb{\Phi}_i[A] - \phi^{\xi}_{\Omega\cap\mathbb{L}_i}[A | x \overset{I}{\not\leftrightarrow}, \mathrm{lmax}(x) = 0]| \leq C(r/R)^c,$$
$$\left|\mathbb{\Phi}^2_i[A] - \phi^{\xi}_{\Omega\cap\mathbb{L}_i}[A \middle| x \overset{I}{\not\leftrightarrow}, \mathrm{lmax}(x) \in \{0, 0^+\}]\right| \leq C(r/R)^c.$$

Proof. As before, we refer to [BS17, GPS18, Jár03, Kes86] for details. □

We also introduce the measures Ψ_i where the conditioning is over the right-most bottom-most vertex of the cluster being 0. It also coincides with the symmetry with respect to the origin of the measure $\mathbb{\Phi}_{-i}$ defined on $\mathbb{L}_{1-i}(\pi-\alpha, \pi-\beta)$. The measures Ψ_i satisfy properties corresponding to the properties above.

Finally, we introduce $\mathbb{\Psi}$ to be the measure obtained as the limit as $R \to \infty$ of measures on $\mathbb{L}_0$ conditioned on the events that 0 is connected to $\partial\Lambda_R$ and is not connected to the right of the vertical line $\{(x, y) \in \mathbb{R}^2 : x = 0\}$. Again, the properties of the measures $\mathbb{\Phi}_i$ extend to this measure.

II.3.5 The star-triangle and the track-exchange transformations

In this section, we present the track-exchange transformation. In order to do it, we first introduce the star-triangle transformation and then define the track-exchange transformation as the result of a sequence of star-triangle transformations.

Star-triangle transformation The *star-triangle transformation*, also known as the *Yang-Baxter relation*, was first discovered by Kennelly in 1899 in the context of electrical networks [Ken99b]. Then, it became a key relation in different models of statistical mechanics [Bax82, Ons44] indicative of the integrability of the system. We do not plan to do a full review on this transformation (see for instance [DCLM18] for more details) and focus directly on the context of the random-cluster model on isoradial graphs with isoradial edge-weights.

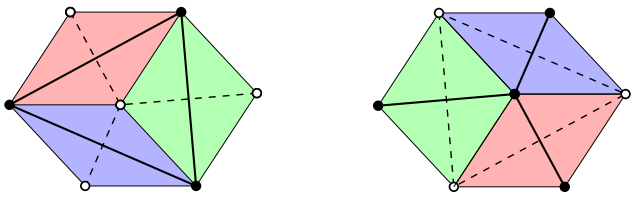

Figure II.9: The three diamonds together with the drawing, on the left, of the triangle (in which case the dual graph in dashed has a star) and, on the right, of the star (in which case the dual graph has a triangle).

First of all, note that for any triangle ABC contained in an isoradial graph, there exists a unique choice of point O (namely the orthocenter) such that, if the triangle ABC is replaced by the star $ABCO$, the resulting graph is also isoradial. Conversely, for every star $ABCO$ in an isoradial graph, the graph obtained by removing this

star and putting the triangle ABC is isoradial. This process of changing the graph is called the *star-triangle transformation*. Note that triangles and stars of isoradial graphs correspond to hexagons formed of three rhombi in the diamond graph. Thus, when three such rhombi are encountered in a diamond graph, they may be permuted as in Figure II.9 using a star-triangle transformation.

The star-triangle transformation was first used to prove that the laws of connections between vertices of a graph G with a triangle ABC and the graph G' obtained from G with the star $ABCO$ instead of ABC are the same, except for the additional vertex O in G'. The fact that the star-triangle transformation can be used to construct a coupling between the random-cluster models on G and G' was proved in several places, see for instance [DCLM18]. The first observation that this could be done goes back to the work of [GM13a, GM13b, GM14], even though the identification that the star-triangle transformation was preserving the partition functions of models on isoradial graphs with isoradial weights goes long back.

Definition II.3.10 (Star-triangle coupling)**.** Consider a graph G containing a triangle ABC and let G' be the graph with the star $ABCO$ instead. Introduce the *star-triangle coupling* between $\omega \sim \phi^{\xi}_{G}$ and $\omega' \sim \phi^{\xi}_{G'}$ defined as follows (see Figure II.10):

- For every edge e which does not belong to $ABCO$, $\omega'_e = \omega_e$,
- If two or three of the edges of ABC are open in ω, then all the edges in $ABCO$ are open in ω',
- If exactly one of the edges of ABC is open in ω, say BC, then the edges BO and OC are open in ω', and the third edge of the star is closed in ω',
- If no edge of ABC is open in ω, then ω'_{OABC} has
  - no open edge with probability equal to $\frac{1-p_{OA}}{p_{OA}}\frac{1-p_{OB}}{p_{OB}}\frac{1-p_{OC}}{p_{OC}}$,
  - the edge OA is open and the other two closed with probability $q\frac{1-p_{OB}}{p_{OB}}\frac{1-p_{OC}}{p_{OC}}$,
  - similarly with cyclic permutations for B and C.

Let us make a few observations concerning the coupling. First, note that the transformation uses extra randomness in one case and that it is not a deterministic matching of the different configurations. Second, the coupling preserves the connectivity between the vertices, except at the vertex O. Third, in the coupling, given ω', the edges of ABC in ω are sampled as follows:

- If there is one or zero edge of $ABCO$ that is open in ω', then none of the edges in ABC is open in ω,
- If exactly two of the edges in $ABCO$ are open in ω', say AO and BO, then the edge AB is the only edge of ABC that is open in ω,
- If all the edges of $ABCO$ are open in ω', then
  - all the edges of ABC are open in ω with probability $\frac{1}{q}\frac{p_{AB}}{1-p_{AB}}\frac{p_{BC}}{1-p_{BC}}\frac{p_{CA}}{1-p_{CA}}$,
  - AB and BC are open and CA is closed with probability equal to $\frac{1}{q}\frac{p_{AB}}{1-p_{AB}}\frac{p_{BC}}{1-p_{BC}}$,
  - similarly with cyclic permutations.

Track-exchange operator The previous star-triangle operator gives rise to a track-exchange operator defined as follows. For $\mathbb{L} = \mathbb{L}(\boldsymbol{\alpha})$ and $i \in \mathbb{Z}$, let $\mathbb{L}' = \mathbb{L}(\boldsymbol{\alpha}')$ be the lattice obtained by exchanging the tracks t_i and t_{i-1} that is exchanging α_i and

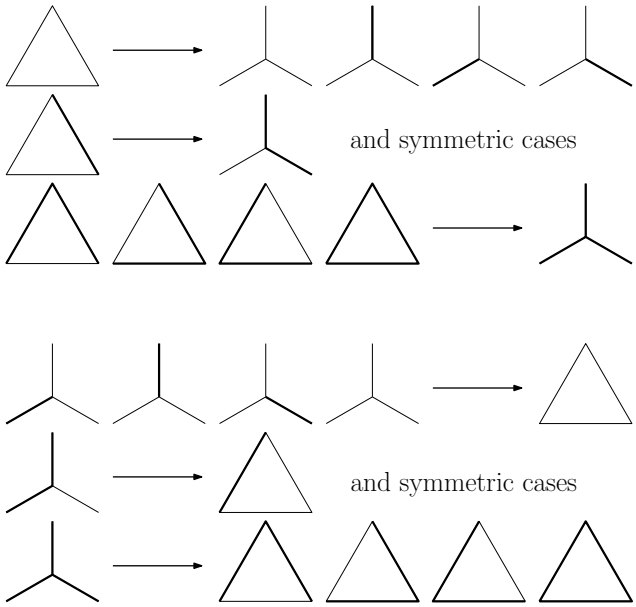

Figure II.10: A picture of the possible transformations in the star-triangle coupling (the probabilities in the case of multiple outcomes are described in the definition). We also pictured the reverse map.

α_{i-1} in the sequence $\boldsymbol{\alpha}$. Index the vertices of t_{i-1}^- from left to right by $(x_k : k \in \mathbb{Z})$ and assume that $\alpha_{i-1} > \alpha_i$. Also, let $\mathbb{L}_k$ be the isoradial graph, see Figure II.12, obtained by

- taking the same diamonds as $\mathbb{L}$ (or equivalently $\mathbb{L}'$) on t_j with $j \notin \{i-1, i\}$;
- taking the same diamonds as $\mathbb{L}$ on the part of t_{i-1} and t_i on the right of x_k;
- taking the same diamonds as $\mathbb{L}'$ on the part of t_{i-1} and t_i on the left of x_k;
- adding a diamond above x_k to complete the gap.

Note that the properties above determine all the diamonds in $\mathbb{L}_k$, and that there is only one diamond in $\mathbb{L}_k$ which does not belong to either $\mathbb{L}$ or $\mathbb{L}'$. Denote this diamond by $\Diamond$. We now define an operator sending configurations on $\mathbb{L}$ to configurations on $\mathbb{L}'$, that gives a formal meaning to the intuitive idea of inserting $\Diamond$ at the position $+\infty$ and using the star-triangle transformation to exchange the tracks by moving $\Diamond$ step by step to $-\infty$.

Let ω be some configuration on $\mathbb{L}$ and define for every $k \in \mathbb{Z}$ the configuration $\tilde{\omega}_k$ on $\mathbb{L}_k$ coinciding with ω on the diamonds common to $\mathbb{L}_k$ and $\mathbb{L}$ (i.e. outside t_{i-1}, t_i and on the left of x_k), and defined arbitrarily otherwise. Denote $\tilde{\omega}_k^k := \tilde{\omega}_k$ and for every $j < k$, define inductively $\tilde{\omega}_k^j$ to be the result of the star-triangle transformation mapping a configuration on $\mathbb{L}_{j+1}$ to a configuration on $\mathbb{L}_j$, applied to $\tilde{\omega}_k^{j+1}$. Define $\omega_k := \lim_{j\to-\infty} \tilde{\omega}_k^j$, which is a configuration on $\mathbb{L}'$. Now remark the important fact that if we have three integers $k, k' \geq j$ such that $\tilde{\omega}_k^j$ and $\tilde{\omega}_{k'}^j$ coincide on $\Diamond$, then the (local) outcome of the star-triangle transformation from $\tilde{\omega}_k^j$ and $\tilde{\omega}_{k'}^j$ will be the same (as long as it uses the same external randomness). More generally, applying all the subsequent steps we see that ω_k and $\omega_{k'}$ coincide on the part of $t_{i-1} \cup t_i$ that is to the left of x_j. Finally, notice that some configurations on

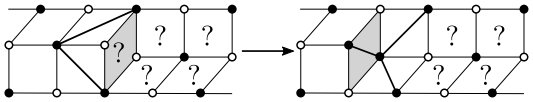

Figure II.11: An example where the configuration on the two diamonds left of the grey diamond ◊ determines the configuration on ◊ after the star-triangle transformation, irrespectively of the configuration on or right of ◊.

the two diamonds left of ◊ in $\mathbb{L}_k$ fix deterministically the state of ◊ in $\mathbb{L}_{k-1}$ after a star-triangle transformation (e.g. see Figure II.11). Denote by F_k this event. If F_k occurs for ω, then for all $k', k'' > k$, it also does by definition for $\omega_{k'}$ and $\omega_{k''}$, and therefore $\omega_{k'}$ and $\omega_{k''}$ coincide left of x_k. This leads to the following definition.

Definition II.3.11 (Track exchange by star-triangle transformation)**.** If $\alpha_{i-1} > \alpha_i$, and ω is a percolation configuration on $\mathbb{L}$ such that $\omega \in F_k$ occurs for an infinite number of indices $k > 0$, define the track-exchange operator $\mathbf{T}_i$ by $\mathbf{T}_i(\omega) = \lim_{k\to-\infty} \omega_k$, where ω_k is defined as in the previous paragraph.

We will only work with measures (random cluster measures, IIC measures) that verify some finite energy property so that F_k occurs for an infinite number of $k < 0, k > 0$ almost surely. Hence the operator $\mathbf{T}_i$ is well defined on almost all configurations ω.

If $\alpha_i > \alpha_{i-1}$, we construct $\mathbf{T}_i$ similarly by inverting the left and the right, and $-\infty$ and $+\infty$.

It should be noted that the mixing properties of the random-cluster model implies that the random-cluster measure on $\mathbb{L}$ is the limit of the random-cluster measures on $\mathbb{L}_k$ and therefore, if ω is distributed according to $\phi_{\mathbb{L}}$, then $\mathbf{T}_i(\omega)$ has law $\phi_{\mathbb{L}'}$. Let us also insist on the fact that $\mathbf{T}_i$ is not a deterministic map, as at each step where a star-triangle operator is used, there is extra randomness in the outcome of the transformation.

We finish this section by an important proposition.

Proposition II.3.12. *If $\boldsymbol{\alpha}$ and $\boldsymbol{\beta}$ satisfy $\alpha_i = \beta_i$ for $a \le i \le b$, the law of ω restricted to the strip between t_a^- and t_b^+ as well as the law of the homotopy classes of loops in ω with respect to points in this strip is the same in $\phi_{\mathbb{L}(\boldsymbol{\alpha})}$ and $\phi_{\mathbb{L}(\boldsymbol{\beta})}$.*

Proof. As a sequence of star-triangle transformations, the track-exchange operator preserves the connection properties of the vertices that are not on the tracks which are exchanged. From this, one may deduce that for every event A involving only edges inside the strip, or only the homotopy classes mentioned above,

$$\phi_{\mathbb{L}(\boldsymbol{\alpha})}[A] = \lim_{R\to\infty} \phi_{\mathbb{L}(\boldsymbol{\alpha}(R))}[A] = \lim_{R\to\infty} \phi_{\mathbb{L}(\boldsymbol{\beta}(R))}[A] = \phi_{\mathbb{L}(\boldsymbol{\beta})}[A],$$

where

$$\boldsymbol{\alpha}(R) := \begin{cases} \alpha_i & \text{if } |i| \le R, \\ \beta_{i-R+b} & \text{if } i > R, \\ \beta_{R-i+a} & \text{if } i < -R, \end{cases} \quad \text{and} \quad \boldsymbol{\beta}(R) := \begin{cases} \beta_i & \text{if } |i| \le R, \\ \alpha_{i-R+b} & \text{if } R < i < 2R - b, \\ \alpha_{R-i+a} & \text{if } -2R + a < i < -R, \\ \beta_i & \text{otherwise.} \end{cases}$$

(In the first and last inequalities, we use the measurability and the uniqueness of the infinite-volume measure, and in the second one the track-exchange operator.) □

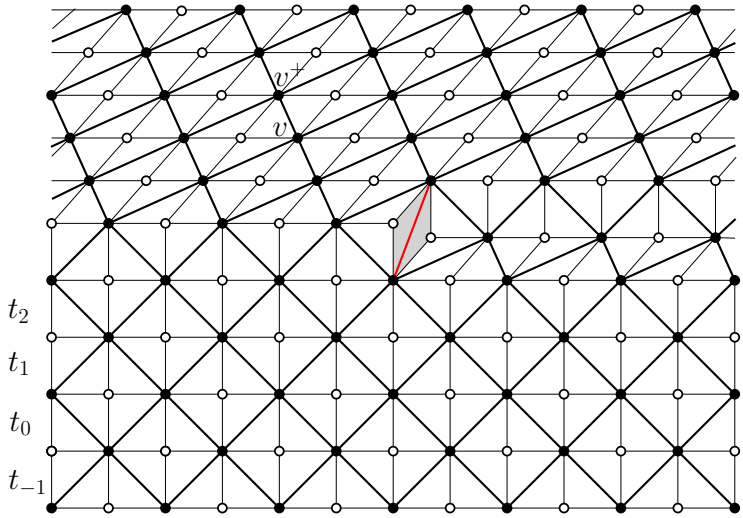

Figure II.12: An example of a graph $\mathbb{L}_k$ for $k = 4$. What happens between tracks t_2 and t_5 is a mixture of the isoradial lattice $\mathbb{L}$ with angles $\pi/2$ for $i \leq 3$ and α for $i \geq 4$, and $\mathbb{L}'$ is obtained by exchanging the tracks 4 and 5. The only diamond that does not belong to $\mathbb{L}$ or $\mathbb{L}'$ is in gray.

II.4 Probabilities in 2-rooted IIC: proof of Theorem II.2.4

The goal of this section is to prove Theorem II.2.4. As mentioned in the introduction, the main steps will be Propositions II.2.5 and II.2.6. We prove these two statements in Sections II.4.1 and II.4.2 respectively. The proof of Theorem II.2.4 is postponed to Section II.4.3 (recall that it relies on Theorem II.2.7, which was obtained in [DCKK$^+$20b]).

II.4.1 Harvesting exact integrability: Proof of Proposition II.2.5

Below, for an event E and i, M, N, introduce the convenient notation

$$Z_{\mathbb{T}_i(N,M)}[E] := Z^{\xi}_{\mathrm{RCM}}(\mathbb{T}_i(N,M), q)\phi^{\xi}_{\mathbb{T}_i(N,M),q}[E].$$

We divide the proof in two lemmata. The first one uses an aspect of the commutation of transfer matrices. To be more precise, we will use a result of [PR15, Theorem 1.3] which is written for Bernoulli percolation but works with almost no change for the random cluster model, proving the existence of a (track-exchange) map $\widetilde{\mathbf{T}}_i : \Omega_{\mathbb{T}_i(N,M)} \to \Omega_{\mathbb{T}_{i-1}(N,M)}$ (slightly different from our track-exchange maps) between percolation configurations on the tori, such that,

(a) For any $\omega \in \Omega_{\mathbb{T}_i(N,M)}$, $\widetilde{\mathbf{T}}_i(\omega)$ and ω coincide outside of $t_{i-1} \cup t_i$;
(b) For any $x, y \notin t_i^-$, x and y are connected in ω if and only if they are in $\widetilde{\mathbf{T}}_i(\omega)$;
(c) For every event E, $Z_{\mathbb{T}_i(N,M)}[\widetilde{\mathbf{T}}_i^{-1}(E)] = Z_{\mathbb{T}_{i-1}(N,M)}[E]$.

Let us mention that with a little bit of work one can also simply use the star-triangle transformation, or the commutation of transfer matrices to produce a more abstract proof.

Recall the definition of $E_j(k)$ from the introduction.

Lemma II.4.1. *For every k, N, M, we have that*

(i) For fixed j, $i \mapsto Z_{\mathbb{T}_i(N,M)}[E_j(k)]$ is constant for $i > j$ and similarly for $i < j$,
(ii) $Z_{\mathbb{T}_1(N,M)}[E_0(k) \cup E_1(k)] = Z_{\mathbb{T}_0(N,M)}[E_0(k) \cup E_1(k)]$.

Proof. We use the track-exchange map mentioned above. The connectivity preservation (a) and (b) imply that ω belongs to $E_j(k) \cup E_{j+1}(k)$ (resp. $E_j(k)$ for $j \neq i$) if and only if $\widetilde{\mathbf{T}}_i(\omega)$ does. Therefore, (c) implies the lemma. □

The second lemma harvests the transfer matrix formalism to get an explicit formula for the probability of events $E_j(k)$ in terms of eigenvalues of the transfer matrix. Below, we use the following connection between the eigenvalues of the transfer matrix of the six-vertex model and the partition function of the random-cluster model obtained via the Baxter-Kelland-Wu coupling [BKW76] (see also [DCGH$^+$16, Section 3.3.] for details). Let $\mathbb{T}(N, M)$ be the N by $2M$ torus with tracks of angle β only and introduce the notation $Z_{\mathbb{T}(N,M)}[E]$ in the same way as for $\mathbb{T}_i(N, M)$. Consider the event $G(k)$ that there exist exactly k disjoint clusters wrapping around the torus in the vertical direction. Then[6]

$$Z_{\mathbb{T}(N,M)}[G(k)] = C(q, N, M)(1 + o_M(1)) \cdot (q/4)^k \cdot \lambda_N^{(k)}(\beta)^{2M}, \tag{II.18}$$

$$Z_{\mathbb{T}_i(N,M)}[G(k)] = C(q, N, M)(1 + o_M(1)) \cdot (q/4)^k \cdot \lambda_N^{(k)}(\alpha)\lambda_N^{(k)}(\beta)^{2M-1}, \tag{II.19}$$

where $C(q, N, M) := q^{NM/2}/(1 + \sqrt{q})^{2MN}$ and $o_M(1)$ is a quantity tending to 0 as M tends to infinity.

[6]To be precise, [DCGH$^+$16] proves an inequality only, but an equality is easily derived. Indeed, to explain the first formula, recall from [DCGH$^+$16] that the weight of each random cluster configuration ω may be written as the sum over all orientations of its loop configuration of the weight of the ensuing oriented loop configuration. The latter is the product over each oriented loop of $e^{+i\zeta}$, $e^{-i\zeta}$ or $\sqrt{q}/2$ depending whether the oriented loop is retractable and oriented counter-clockwise, clockwise or non-retractable, respectively, with $\zeta = \arccos\sqrt{q/2}$. Notice now that for $\omega \in G(k)$, there exist at least $2k$ non-retractable loops winding vertically around the torus; all but an exponentially small proportion of $Z_{\mathbb{T}(N,M)}[G(k)]$ actually comes from configuration with exactly $2k$ non-retractable loops, and we will ignore all other contributions as they can be incorporated in the $o_M(1)$. For each such configuration, rather than orienting all loops in one of two directions, consider the two possible orientations only for retractable loops and orient all vertically-winding loops upwards. When summing the weights of resulting oriented loop configurations, we obtain the partition function of the six vertex model on the torus with exactly $N/2+k$ up-arrows on each row (up to the multiplicative factor $C(q, N, M)$). This may be written using the transfer matrix as $\lambda_N^{(k)}(\beta)^{2M}(1 + o_M(1))$. The factor $(2/\sqrt{q})^{2k}$ in the formula for $Z_{\mathbb{T}(N,M)}[G(k)]$ accounts for the arbitrary choice of orientation of the vertically-winding loops. The same explanation applies for the second formula, with the only difference coming from the computation of the partition function in the six-vertex model.

Lemma II.4.2. *For every $k, N, \alpha, \beta \in (0,\pi)$, there exists $C_N^{(k)}(\alpha,\beta) \in (0,\infty)$ such that*

$$\lim_{M\to\infty} \frac{Z_{\mathbb{T}_i(N,M)}[E_j(k)]}{Z_{\mathbb{T}_0(N,M)}[E_0(k)]} = \Big[\frac{\lambda_N^{(k+3)}(\beta)}{\lambda_N^{(k)}(\beta)}\Big]^j \times \begin{cases} C_N^{(k)}(\alpha,\beta)\frac{\lambda_N^{(k)}(\alpha)}{\lambda_N^{(k)}(\beta)} & \text{if } i > j, \\ 1 & \text{if } i = j, \\ C_N^{(k)}(\alpha,\beta)\frac{\lambda_N^{(k+3)}(\alpha)}{\lambda_N^{(k+3)}(\beta)} & \text{if } i < j. \end{cases} \quad \text{(II.20)}$$

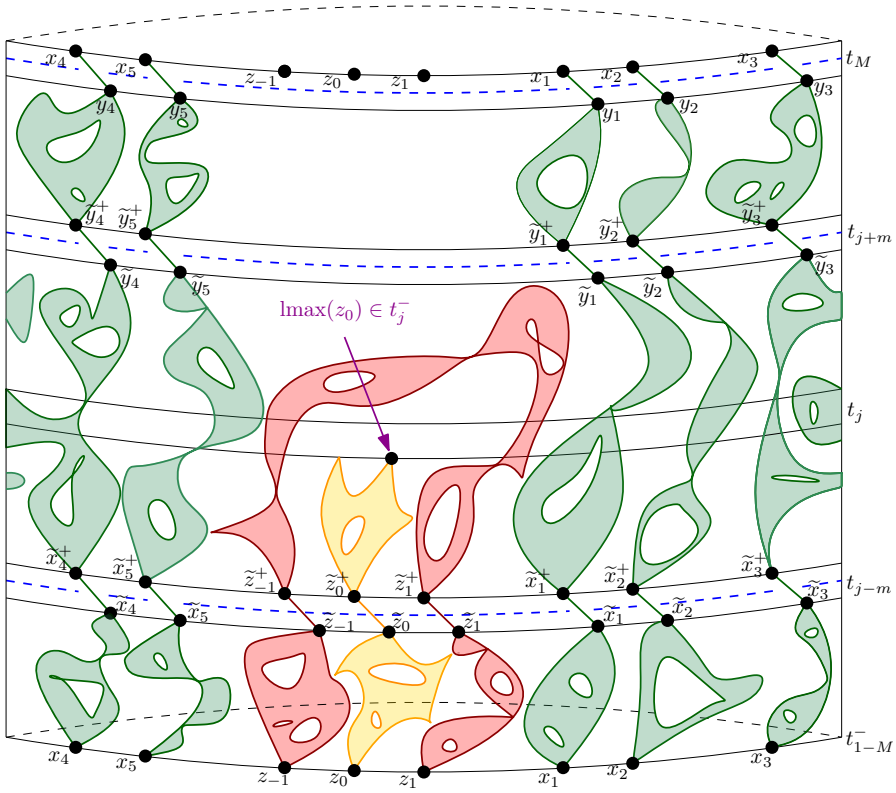

Figure II.13: A picture of the event $E_j(k,m)$ (except that the minimality of m is not really explicitly depicted). Compared to Figure II.4, additional conditions are forced on the tracks t_{j-m} and t_{j+m} and what happens in between.

Proof. We start with the case $i = j$. For $1 \le m \le M/3$ with $M - j - m$ even, let $E_j(k,m) \subset E_j(k)$ be the event (see Figure II.13) that

- all the edges of t_{j+m} are closed except the edges from $\widetilde{y}_1, \dots, \widetilde{y}_k$ to $\widetilde{y}_1^+, \dots, \widetilde{y}_k^+$, where the former are the vertical translates on t_{j+m}^- of the vertices $y_1, \dots, y_k$ used in the definition of $E(k)$,
- all the edges of t_{j-m} are closed except the edges from $\widetilde{x}_1, \dots, \widetilde{x}_k, \widetilde{z}_{-1}, \widetilde{z}_0, \widetilde{z}_1$ to $\widetilde{x}_1^+, \dots, \widetilde{x}_k^+, \widetilde{z}_{-1}^+, \widetilde{z}_0^+, \widetilde{z}_1^+$, where the latter are the vertical translates on t_{j-m}^- of the vertices $x_1, \dots, x_k, z_{-1}, z_0, z_1$ used in the definition of $E(k)$,
- $E_j(k)$ occurs and $\widetilde{x}_i$ and $\widetilde{y}_i$ are connected to x_i (and therefore y_i) for $1 \le i \le k$, and $\widetilde{z}_i$ to z_i for $-1 \le i \le 1$,

- m is the smallest integer satisfying the three first properties.

With this definition, we can now proceed as follows. On the one hand, let $Z_j(k,m) = Z(k,m)$ (it does not depend on j by vertical translation invariance) be the sum of the random-cluster weights (counted as there would be free boundary conditions) of configurations ω on $t_{j-m+1} \cup \cdots \cup t_{j+m-1}$ that are compatible with the occurrence of $E_j(k,m)$. Then, if $M^+ := \frac{1}{2}(M-j-m)$ and $M^- := \frac{1}{2}(M+j-m)$, we find that

$$Z_{\mathbb{T}_j(N,M)}[E_j(k,m)] = Z(k,m) Z_{\mathbb{T}(N,M^+)}[F(k)] Z_{\mathbb{T}(N,M^-)}[F(k+3)],$$

where $F(\ell)$ is the event that the conditions (i) and (ii) of the definition of $E(\ell)$ occur. Now, the existence of a thermodynamical limit (as M tends to infinity) implies that for fixed ℓ,

$$Z_{\mathbb{T}(N,M^\pm)}[F(\ell)] = C_N^{(\ell)}(\beta)(1+o_M(1)) Z_{\mathbb{T}(N,M^\pm)}[G(\ell)].$$

Therefore, (II.18) and the two previous displayed equations give that uniformly in $1 \le m \le M/3$,

$$\lim_{M\to\infty} \frac{Z_{\mathbb{T}_j(N,M)}[E_j(k,m)]}{Z_{\mathbb{T}_0(N,M)}[E_0(k,m)]} = \Big[\frac{\lambda_N^{(k+3)}(\beta)}{\lambda_N^{(k)}(\beta)}\Big]^j.$$

The claim follows by summing over m and observing that the finite-energy property implies the existence of $c = c(N) > 0$ such that for every m,

$$\phi_{\mathbb{T}_j(N,M)}\big[\bigcup_{1\le m'\le m} E_j(k,m') \big| E_j(k)\big] \ge 1 - \exp[-cm]. \tag{II.21}$$

We now turn to the case $i > j$. We first use Lemma II.4.1(i) to "push the track of angle α up to macroscopic distance", meaning that we observe that for $M/2 > j$,

$$Z_{\mathbb{T}_i(N,M)}[E_j(k)] = Z_{\mathbb{T}_{M/2}(N,M)}[E_j(k)].$$

As before, we can fix m and run the same argument to get that for some constant $Z'(k,m)$ and with $i' := M/2 - j - m$,

$$\begin{aligned} &Z_{\mathbb{T}_{M/2}(N,M)}[E_j(k,m)] \\ &\qquad = (1+o_M(1)) C_N^{(k)}(\beta) C_N^{(k+3)}(\beta) Z'(k,m) Z_{\mathbb{T}_{i'}(N,M^+)}[G(k)] Z_{\mathbb{T}(N,M^-)}[G(k+3)] \\ &\qquad = (1+o_M(1)) \frac{Z'(k,m)}{Z(k,m)} \frac{Z_{\mathbb{T}_{i'}(N,M^+)}[G(k)]}{Z_{\mathbb{T}(N,M^+)}[G(k)]} Z_{\mathbb{T}_0(N,M)}[E_0(k,m)]. \end{aligned}$$

We wish to highlight the fact that the constants $C_N^{(\ell)}(\beta)$ involved in the previous equation are the same as for $i = j$, as the track of angle α is at a distance larger than $M/2 - m$ of the m-th track (this quantity tends to infinity as M tends to infinity), but that the constant $Z'(k,m)$ is a priori different from $Z(k,m)$ (it is a sum on the same configurations but the track t_j has an angle of α instead of β, hence some edge-weights are different).

Using (II.19) instead of (II.18) to estimate $Z_{\mathbb{T}_{i'}(N,M^+)}[F(k)]$, we infer that the second ratio converges to $\lambda_N^{(k)}(\alpha)/\lambda_N^k(\beta)$. We obtain the result by summing over m. Indeed, we may use again a uniform bound that is similar to (II.21) and observe

that the case $i = j$ immediately implies that $\phi_{\mathbb{T}_0(N,M)}[E_0(k,m)|E_0(k)]$ converges as M tends to infinity. Note that

$$C_N^{(k)}(\alpha,\beta) := \sum_m \frac{Z'(k,m)}{Z(k,m)} \lim_{M\to\infty} \phi_{\mathbb{T}_0(N,M)}[E_0(k,m)|E_0(k)].$$

Using this definition of the constant and applying the same reasoning for $i < j$ concludes the proof. □

We are now in a position to prove Proposition II.2.5.

Proof of Proposition II.2.5. Lemma II.4.2 (for $i, j = 0, 1$) and Lemma II.4.1(ii) imply that

$$C_N^{(k)}(\alpha,\beta)\frac{\lambda_N^{(k)}(\alpha)}{\lambda_N^{(k)}(\beta)} + \frac{\lambda_N^{(k+3)}(\beta)}{\lambda_N^{(k)}(\beta)} = 1 + C_N^{(k)}(\alpha,\beta)\frac{\lambda_N^{(k+3)}(\alpha)}{\lambda_N^{(k)}(\beta)},$$

which gives

$$C_N^{(k)}(\alpha,\beta) = \frac{\lambda_N^{(k)}(\beta) - \lambda_N^{(k+3)}(\beta)}{\lambda_N^{(k)}(\alpha) - \lambda_N^{(k+3)}(\alpha)}.$$

Plugging this formula into Lemma II.4.2 gives

$$\lim_{M\to\infty} \frac{\phi_{\mathbb{T}_1}[E_1(k)]}{\phi_{\mathbb{T}_1}[E_0(k)]} = \frac{\lambda_N^{(k)}(\beta)}{\lambda_N^{(k+3)}(\beta)} \times \frac{1}{C_N^{(k)}(\alpha,\beta)\frac{\lambda_N^{(k)}(\alpha)}{\lambda_N^{(k)}(\beta)}} = \frac{\lambda_N^{(k)}(\beta)}{\lambda_N^{(k+3)}(\beta)} \times \frac{1 - \lambda_N^{(k+3)}(\alpha)/\lambda_N^{(k)}(\alpha)}{1 - \lambda_N^{(k+3)}(\beta)/\lambda_N^{(k)}(\beta)}.$$

Similarly,

$$\lim_{M\to\infty} \frac{\phi_{\mathbb{T}_0}[E_1(k)]}{\phi_{\mathbb{T}_0}[E_0(k)]} = \frac{\lambda_N^{(k+3)}(\alpha)}{\lambda_N^{(k)}(\beta)} \times C_N^{(k)}(\alpha,\beta) = \frac{\lambda_N^{(k+3)}(\alpha)}{\lambda_N^{(k)}(\alpha)} \times \frac{1 - \lambda_N^{(k+3)}(\beta)/\lambda_N^{(k)}(\beta)}{1 - \lambda_N^{(k+3)}(\alpha)/\lambda_N^{(k)}(\alpha)}.$$

□

II.4.2 Separation of interfaces: Proof of Proposition II.2.6

In this section, $\mathbf{\Gamma}$ is the left-most boundary of the cluster of z_1. For $r > 0$ and $a \le b$ in $\mathbb{Z}$, introduce two events

$$\begin{aligned} \mathrm{Iso}(r) &:= \{\mathbf{\Gamma} \cap \Lambda_r(\mathrm{lmax}(z_0)) = \emptyset\}, \\ E_{[a,b]}(k) &:= \bigcup_{a\le j\le b} E_j(k). \end{aligned}$$

The following proposition states a form of typical isolation of clusters.

Proposition II.4.3 (Isolation of the top of the cluster of z_0)**.** *For every $\varepsilon > 0$, there exist $C, \eta > 0$ such that for every $\alpha, \beta \in (\varepsilon, \pi - \varepsilon)$, $i, j \in \mathbb{Z}$, $k \le N$, and $13r \le s \le N$, we have that for M large enough,*

$$\phi_{\mathbb{T}_i(N,M)}[E_j(k) \setminus \mathrm{Iso}(r)|E_{[j-s,j]}(k)] \le \frac{Cr^\eta}{s^{1+\eta}}. \tag{II.22}$$

Before focusing on this proposition, let us explain how it combines with the mixing of the 2-rooted IIC (Proposition II.3.9) to imply Proposition II.2.6. The key observation is that when $\mathrm{Iso}(r)$ occurs, one may sample everything but the cluster of z_0, and then sample the cluster of z_0 in such a way that near its maximum, the configuration looks like a 2-rooted IIC (since this maximum is far from the other clusters).

Proof of Proposition II.2.6. The result is trivial when $\lambda_N^{(k)}(\beta)/\lambda_N^{(k+3)}(\beta) - 1$ is large as we may choose C in such a way that the right-hand side is larger than 1. We will therefore assume in the proof that it is small. We will also omit integer approximations. For a vertex v, define the event

$$E_v(k) := E(k) \cap \{\mathrm{lmax}(z_0) = v\}.$$

We can write

$$\phi_{\mathbb{T}_i(N,M)}[E_1(k)|E_{[0,1]}(k), \mathrm{Iso}(r)] = \frac{\sum_{v\in t_0^-} \phi_{\mathbb{T}_i(N,M)}[E_{v^+}(k)|\mathrm{Iso}(r)]}{\sum_{v\in t_0^-} \phi_{\mathbb{T}_i(N,M)}[E_{v^+}(k) \cup E_v(k)|\mathrm{Iso}(r)]}. \quad \text{(II.23)}$$

Fix some $v \in t_0^-$. On the event $\mathrm{Iso}(r)$, one may explore the clusters of the x_i's and $\mathbf{\Gamma}$ and use the spatial Markov property to sample the cluster of z_0. The mixing property of the 2-rooted IIC given by Proposition II.3.9 thus implies that

$$|\phi_{\mathbb{T}_i(N,M)}[E_{v^+}(k)|E_v(k) \cup E_{v^+}(k), \mathrm{Iso}(r)] - \mathfrak{M}_i^2[\mathrm{lmax}(\infty) = 0^+]| \le Cr^{-\eta}. \quad \text{(II.24)}$$

Proposition II.4.3 gives that for every choice of s, for M large enough,

$$\begin{aligned}\phi_{\mathbb{T}_i(N,M)}[\mathrm{Iso}(r)^c|E_{[0,1]}(k)] &\le \phi_{\mathbb{T}_i(N,M)}[\mathrm{Iso}(r)^c|E_1(k)] + \phi_{\mathbb{T}_i(N,M)}[\mathrm{Iso}(r)^c|E_0(k)] \\ &\le \frac{Cr^\eta}{s^{1+\eta}}\Big(\frac{\phi_{\mathbb{T}_i(N,M)}[E_{[1-s,1]}(k)]}{\phi_{\mathbb{T}_i(N,M)}[E_1(k)]} + \frac{\phi_{\mathbb{T}_i(N,M)}[E_{[-s,0]}(k)]}{\phi_{\mathbb{T}_i(N,M)}[E_0(k)]}\Big).\end{aligned}$$

Using Lemma II.4.2 and taking the limsup as M tends to infinity implies that

$$\limsup_{M\to\infty} \phi_{\mathbb{T}_i(N,M)}[\mathrm{Iso}(r)^c|E_{[0,1]}(k)] \le \frac{2Cr^\eta}{s^{1+\eta}} \sum_{u=0}^{s} \Big(\frac{\lambda_N^{(k)}(\beta)}{\lambda_N^{(k+3)}(\beta)}\Big)^u \le \frac{2Cr^\eta}{s^{1+\eta}} \frac{\Big(\frac{\lambda_N^{(k)}(\beta)}{\lambda_N^{(k+3)}(\beta)}\Big)^{s+1}}{\frac{\lambda_N^{(k)}(\beta)}{\lambda_N^{(k+3)}(\beta)} - 1}. \quad \text{(II.25)}$$

Combining (II.23), (II.24), and (II.25) for

$$s := \Big\lfloor \frac{1}{\log[\lambda_N^{(k)}(\beta)/\lambda_N^{(k+3)}(\beta)]} \Big\rfloor \qquad \text{and} \qquad r := \lfloor \sqrt{s} \rfloor$$

(one has $r \le s/13$ since we assume the ratio of eigenvalues is close to 1) gives the result by possibly changing the value of C. □

We now focus on Proposition II.4.3. In the rest of this section, we fix i, j, and $k \leq N \leq M$ as well as $13r \leq s \leq N$. We drop the dependency in these parameters when it cannot lead to any confusion. In particular, we write

$$E := E_{[j-s,j]}(k)$$

and

$$\phi := \phi_{\mathbb{T}_i(N,M)}[\,\cdot\,|\text{edges of } t_M \text{ that are open are exactly the } \{x_i, y_i\} \text{ for } 1 \leq i \leq k].$$

We first prove, in Lemma II.4.4, a bound for the probability that a vertex x is equal to $\mathrm{lmax}(z_0)$ while being not isolated, conditionally on the event that the cluster of z_0 intersects a box of size s centered around x (in fact around a vertex y near x). Then we prove, in Lemma II.4.5, that conditionally on $E_{[j-s,j]}(k)$, the number of disjoint boxes of size s centered on a vertex of t_j^- intersected by the cluster of z_0 is bounded in expectation. The proposition then follows by combining the two lemmata (see below for a formal proof).

Lemma II.4.4. *There exist uniform constants $c, \eta > 0$ such that for every two vertices $x, y \in t_j^-$ such that $d(x, y) \leq s/4$,*

$$\phi[x = \mathrm{lmax}(z_0), \mathrm{Iso}(r)^c | E, z_0 \leftrightarrow \Lambda_s(y)] \leq \frac{Cr^\eta}{s^{2+\eta}}. \tag{II.26}$$

Proof. Fix $x, y \in t_j^-$ as in the statement. Let $\mathbf{C}$ be the union of the clusters of $x_1, \ldots, x_k$, and $\mathbf{C}_0$ be the cluster of z_0 in $\mathbb{T}_i \setminus \Lambda_s(y)$. Introduce the events

$$F := E \cap \{z_0 \longleftrightarrow \Lambda_s(y)\},$$
$$\mathrm{Risk}_x := \{d(x, \mathbf{\Gamma}) \leq r\} \cap \{x \text{ is below } \mathbf{\Gamma}\},$$

where by "below" we mean in the connected component of z_0 in the graph $\mathbb{T}_i \setminus (\mathbf{\Gamma} \cup t_M^-)$.

We have that

$$\begin{aligned}\phi[x = \mathrm{lmax}(z_0), \mathrm{Iso}(r)^c | F] &= \phi[x = \mathrm{lmax}(z_0), \mathrm{Risk}_x | F] \\ &= \phi[x = \mathrm{lmax}(z_0) | \mathrm{Risk}_x, F]\phi[\mathrm{Risk}_x | F]. \end{aligned} \tag{II.27}$$

We now bound separately the two probabilities of the last product.

Claim 1. *There exists $C_0 > 0$ independent of everything such that*

$$\phi[x = \mathrm{lmax}(z_0) | \mathrm{Risk}_x, F] \leq C_0 s^{-2}. \tag{II.28}$$

Proof. Let $\mathbf{C}_{\mathbf{\Gamma}}$ be the union (see Figure II.14) of the clusters intersecting $\mathbf{\Gamma}$ in $\omega \setminus \Lambda_{s/2}(y)$. Introduce the random variable $\mathcal{A} := (\mathbf{C}, \mathbf{\Gamma}, \mathbf{C}_0, \mathbf{C}_{\mathbf{\Gamma}})$. The following inequality will imply (II.28): for every $A = (\mathcal{C}, \Gamma, \mathcal{C}_0, \mathcal{C}_\Gamma)$,

$$\phi[x = \mathrm{lmax}(z_0), \mathrm{Risk}_x, F | \mathcal{A} = A] \leq C_0 s^{-2} \phi[\mathrm{Risk}_x, F | \mathcal{A} = A]. \tag{II.29}$$

Indeed, it suffices to sum the above over all possible realizations A of $\mathcal{A}$. We now prove (II.29).

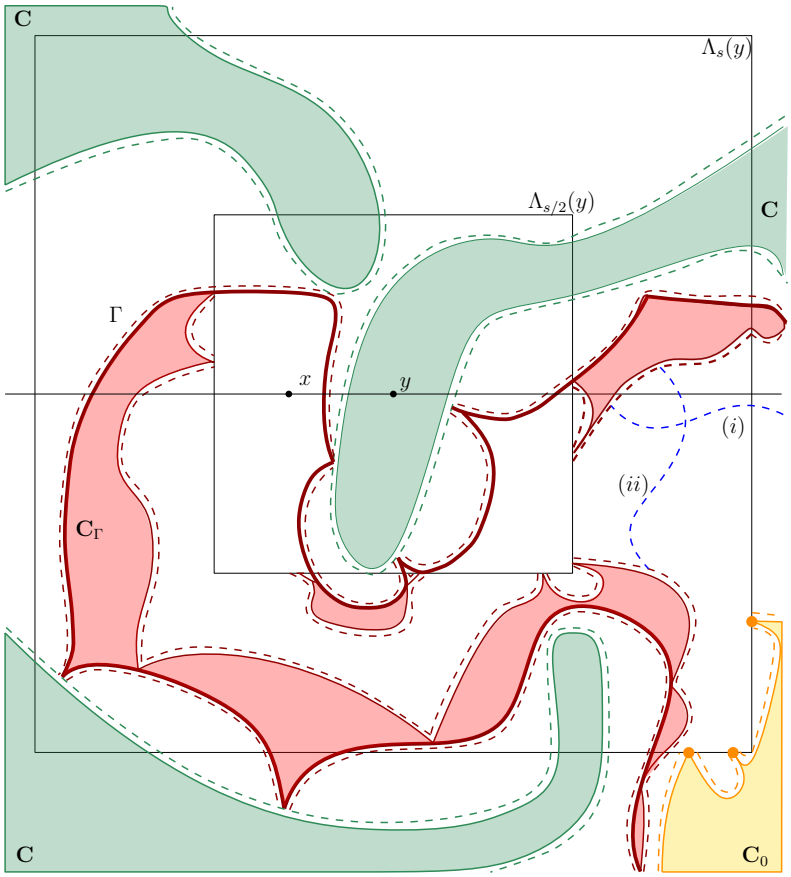

Figure II.14: The conditioning on $(\mathbf{C}, \mathbf{\Gamma}, \mathbf{C_0}, \mathbf{C_\Gamma})$. The plain lines correspond to open paths, and the dashed ones to closed ones, or more precisely to open paths in the dual configuration ω^*. We kept the same color code as in Figure II.13. Green clusters are the clusters of $x_1, \dots, x_k$ and depict $\mathbf{C}$. The red ones depict $\mathbf{\Gamma}$ (in bold) and $\mathbf{C_\Gamma}$ (they are connected to z_{-1} and z_1). These induce wired boundary conditions on the part of $\Omega \cap \Lambda_{s/2}(y)$ below Γ, and free boundary conditions outside of $\Lambda_{s/2}(y)$. Finally, the yellow part is $\mathbf{C}_0$, i.e. the cluster of z_0 outside of $\Lambda_s(y)$. We also depicted (i) and (ii) in blue.

Below, we set Ω to be the set of edges below $\mathbf{\Gamma}$ whose state is not deterministically fixed on the event $\{\mathcal{A} = A\}$. We may assume without loss of generality that the probability on the left is strictly positive otherwise there is nothing to prove. Under this condition, $\mathrm{Risk}_x \cap \{z_0 \longleftrightarrow \Lambda_s(y)\}$ already happens (since it is measurable in terms of $(\Gamma, \mathcal{C}_0)$). As a consequence, the following two conditions are sufficient (but not necessary) for E to happen:

(i) z_0 is not connected to t_j^+ in $\mathbb{T}_i \setminus \Lambda_{s/2}(y)$,
(ii) $\partial\Lambda_s(y)$ is not connected to $\partial\Lambda_{s/2}(y)$ in Ω.

Indeed, we must guarantee that z_0 is not connected to $z_{\pm 1}$ (or equivalently to Γ), and that the highest-most vertex of the cluster of z_0 is strictly below t_j^+. The conditioning on $\mathcal{A} = A$ implies that the only way for z_0 to be connected to Γ is via a path intersecting $\partial\Lambda_{s/2}(y)$. Since we only conditioned on $\mathbf{C}_0 = \mathcal{C}_0$, i.e. on the cluster of z_0 *outside* $\Lambda_s(y)$, the condition (ii) is sufficient to prevent the occurrence of a connection between z_0 and Γ. Moreover, (ii) ensures that z_0 is not connected to $\Lambda_{s/2}(y)$. Once this is guaranteed, (i) suffices to ensure that z_0 is disconnected from t_j^+.

Since the boundary conditions induced by $\mathcal{A} = A$ are free on the part of $\partial\Omega$ strictly inside $\Lambda_s(y) \setminus \Lambda_{s/2}(y)$, Proposition II.3.6 shows that (ii) happens with probability larger than some universal constant $c_0 > 0$. Since both events in (i) and (ii) are decreasing, the FKG inequality implies that

$$\phi[\mathrm{Risk}_x, F | \mathcal{A} = A] \geq \phi[(i), (ii) | \mathcal{A} = A] \geq c_0 \phi[(i) | \mathcal{A} = A]. \tag{II.30}$$

Conversely, on $\{\mathcal{A} = A\}$, for $x = \mathrm{lmax}(z_0)$ to occur, (i) must occur together with

(iii) The half-plane three-arm event with type 010 in Ω to distance $s/4$ of x.

This gives

$$\begin{aligned}\phi[x = \mathrm{lmax}(z_0), \mathrm{Risk}_x, F | \mathcal{A} = A] &\leq \phi[(iii), (i) | \mathcal{A} = A] \\ &= \phi[(iii) | (i), \mathcal{A} = A] \phi[(i) | \mathcal{A} = A] \\ &\leq \tfrac{1}{c_0} \phi[(iii) | (i), \mathcal{A} = A] \phi[\mathrm{Risk}_x, F | \mathcal{A} = A]\end{aligned} \tag{II.31}$$

(in the last line we used (II.30)). Thus, to prove (II.29) it suffices to show that

$$\phi[(iii) | (i), \mathcal{A} = A] \leq C_1 s^{-2}.$$

In order to see that, we claim the following. For every n, every Ω' containing 0, and every boundary conditions ξ for which all the vertices of $\partial\Omega' \cap \Lambda_n$ are wired together,

$$\phi^{\xi}_{\Omega'}[A^{\mathrm{T}}_{010}(0, n)] \leq C_2 \phi_{\mathbb{L}(\beta)}[A^{\mathrm{T}}_{010}(0, n/2)] \leq C_3 n^{-2} \tag{II.32}$$

(the last inequality follows from Proposition II.3.4). Note that this inequality would imply the result. Indeed, if $\mathcal{A} = A$ and (i) occurs, the remaining unexplored edges in $\Lambda_{s/2}(y)$ that are in the connected component of x are bordered, strictly inside $\Lambda_{s/2}(y)$, by Γ only, which is wired by definition.

We will now conclude the proof of the claim by showing (II.32). Notice that this is a general property independent of the setting used in the claim. Fix Ω' and

some boundary conditions ξ. By spatial Markov property, we may condition on everything outside Λ_n and assume without loss of generality that $\Omega' \subset \Lambda_n$. To get (II.32), let $\mathbf{C}(0)$ be the cluster of 0 in Ω' (without considering the connection due to boundary conditions). Let ψ be the boundary conditions on Λ_n corresponding to ξ on $(\partial\Omega') \setminus \Lambda_{n-1}$, and wired for all the other vertices of $\partial\Lambda_n$. For every realization $\mathcal{C}(0) \subset \Omega'$ of $\mathbf{C}(0)$ for which $A^{\mathrm{T}}_{010}(0,n)$ occurs, the spatial Markov property and the FKG inequality imply

$$\begin{aligned}\phi^{\xi}_{\Omega'}[\mathbf{C}(0)=\mathcal{C}(0)] &= \phi^{\psi}_{\Lambda_n}[\mathbf{C}(0)=\mathcal{C}(0)|\omega_{|\Lambda_n\setminus\Omega'}=1]\\ &= \frac{\phi^{\psi}_{\Lambda_n}[\omega_{|\Lambda_n\setminus\Omega'}=1|\mathbf{C}(0)=\mathcal{C}(0)]}{\phi^{\psi}_{\Lambda_n}[\omega_{|\Lambda_n\setminus\Omega'}=1]}\phi^{\psi}_{\Lambda_n}[\mathbf{C}(0)=\mathcal{C}(0)]\\ &= \frac{\phi^{\psi}_{\Lambda_n}[\omega_{|\Lambda_n\setminus\Omega'}=1|\omega_{|\partial_e\mathcal{C}(0)}=0]}{\phi^{\psi}_{\Lambda_n}[\omega_{|\Lambda_n\setminus\Omega'}=1]}\phi^{\psi}_{\Lambda_n}[\mathbf{C}(0)=\mathcal{C}(0)] \le \phi^{\psi}_{\Lambda_n}[\mathbf{C}(0)=\mathcal{C}(0)],\end{aligned}$$

where $\partial_e\mathcal{C}(0)$ is the edge-boundary composed of the edges in Λ_n with one endpoint in and the other outside $\mathcal{C}(0)$. Summing over the $\mathcal{C}(0)$ included in Ω', we obtain that

$$\phi^{\xi}_{\Omega'}[A^{\mathrm{T}}_{010}(0,n)] \le \phi^{\psi}_{\Lambda_n}[A^{\mathrm{T}}_{010}(0,n)].$$

Comparing the later to the full space is now a simple use of the mixing property (Proposition II.3.5):

$$\phi^{\psi}_{\Lambda_n}[A^{\mathrm{T}}_{010}(0,n)] \le \phi^{\psi}_{\Lambda_n}[A^{\mathrm{T}}_{010}(0,n/2)] \le C_{\mathrm{mix}}\phi^{0}_{\mathbb{L}(\beta)}[A^{\mathrm{T}}_{010}(0,n/2)].$$

The previous inequalities imply (II.32) and therefore conclude the proof. □

We now turn to the bound on the second term of (II.27). Introduce

$$G := F \cap \{z_0 \overset{\Lambda}{\not\longleftrightarrow}_{s/2} (y)\} \cap \{z_1 \longleftrightarrow z_{-1} \text{ in } \mathbb{T} \setminus \Lambda_{s/3}(y)\}.$$

Claim 2. *There exists $C_1 > 0$ independent of everything such that*

$$\phi[\mathrm{Risk}_x|F] \le C_1\phi[\mathrm{Risk}_x|G]. \tag{II.33}$$

Proof. We reuse the notation from Claim 1. We only need to prove that for every A,

$$\phi[\mathrm{Risk}_x, F|\mathcal{A}=A] \le C\phi[\mathrm{Risk}_x, G|\mathcal{A}=A]. \tag{II.34}$$

Fix A and note that we may focus on A for which the left-hand side is strictly positive. Now, for such values of A, $\mathrm{Risk}_x \cap G$ occurs if the following sufficient conditions do:

(*i*) z_0 is not connected to t_j^+ in $\mathbb{T}_i \setminus \Lambda_{s/2}(y)$;
(*ii*) $\partial\Lambda_s(y)$ is not connected to $\partial\Lambda_{s/2}(y)$ in $\omega \cap \Omega$;
(*iv*) $\partial\Lambda_{s/2}(y)$ and $\partial\Lambda_{s/3}(y)$ are not connected in $\omega^* \cap \Omega$.

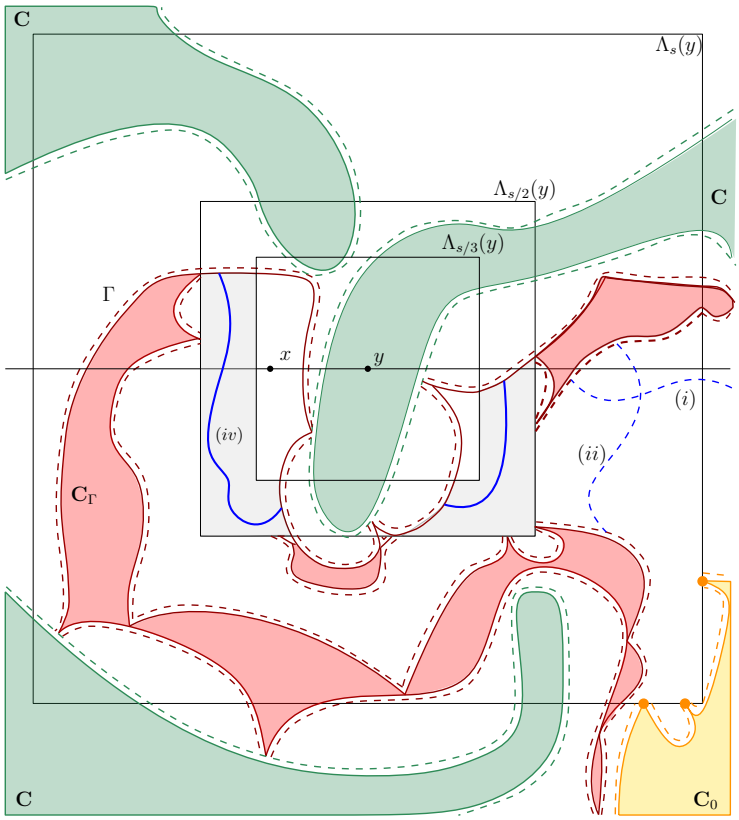

Figure II.15: The picture is almost the same as in the previous one, except we depicted (iv) instead of (iii).

Conditions (i) and (ii) are the same as in Claim 1. They ensure that F and $z_0 \overset{\partial}{\leftrightarrow} \Lambda_{s/2}(y) \cup t_j^+$ occur. Condition (iv) ensures that, when $\mathbf{\Gamma}$ visits $\Lambda_{s/3}(x)$, there exists a path between z_{-1} and z_1 that by-passes $\Lambda_{s/3}(x)$.

Using the previous claim, we already know that

$$\phi[(i),(ii)|\mathcal{A}=A] \geq c_0 \phi[(i)|\mathcal{A}=A].$$

Also, since the boundary conditions induced by $\{\mathcal{A}=A\} \cap (ii)$ on vertices in $\partial\Omega \cap \Lambda_{s/2}(y)$ are wired (see Figure II.15), we deduce from Proposition II.3.6 applied to the dual model that

$$\phi[(iv)|(i),(ii),\mathcal{A}=A] \geq c_0.$$

Combining the previous two displayed inequalities implies that

$$\phi[\mathrm{Risk}_x, G|\mathcal{A}=A] \geq \phi[(i),(ii),(iv)|\mathcal{A}=A] \geq c_0^2 \phi[(i)|\mathcal{A}=A].$$

Since (i) is needed for F to occur, we find

$$\phi[(i)|\mathcal{A}=A] \geq \phi[\mathrm{Risk}_x, F|\mathcal{A}=A]$$

and therefore (II.34) follows from the last two displayed equations. This concludes the proof of the claim. □

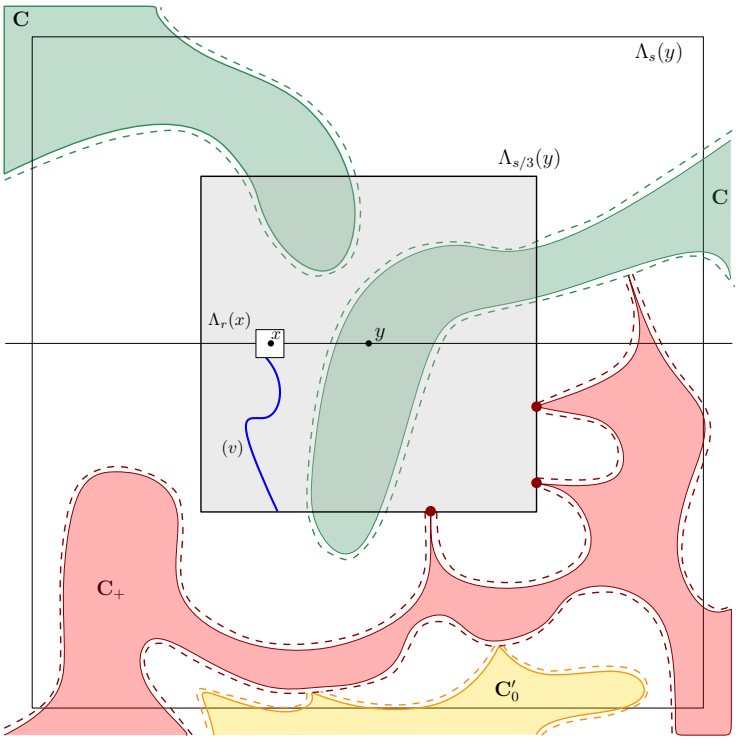

Figure II.16: The conditioning on $(\mathbf{C}, \mathbf{C}'_\mathbf{0}, \mathbf{C}_+)$. Note that the boundary conditions in the remaining set Ω are free within $\Lambda_{s/3}(y)$. In fact, the only points that are wired on $\partial\Omega$ are the vertices of $\mathbf{C}_+$ on the boundary of $\partial\Lambda_{s/3}(y)$ (the red bullets on the picture). In blue, the path that must exist for (v) to occur. Note that since $r < s/13$, the distance between $\Lambda_r(x)$ and $\partial\Lambda_{s/3}(y)$ is larger than $s/3 - |x-y| - r \geq s/156$.

Claim 3. *There exist $c_2, C_2 > 0$ independent of everything such that for every $r \leq s/13$ and every M large enough,*

$$\phi[\mathrm{Risk}_x | G] \leq C_2 (r/s)^{c_2}. \tag{II.35}$$

Proof. Recall the definition of $\mathbf{C}$ and introduce the clusters $\mathbf{C}'_0$ of z_0 in $\mathbb{T}_i$ and $\mathbf{C}_+$ of z_1 in $\mathbb{T}_i \setminus \Lambda_{s/3}(y)$. Consider the random variable $\mathcal{B} := (\mathbf{C}, \mathbf{C}'_0, \mathbf{C}_+)$. Since G is $\mathcal{B}$-measurable, it suffices to show that for every $B = (\mathcal{C}, \mathcal{C}'_0, \mathcal{C}_+)$ for which G occurs,

$$\phi[\mathrm{Risk}_x, G | \mathcal{B} = B] \leq C_2 (r/s)^{c_2} \tag{II.36}$$

and to sum the previous inequality over all possible B.

Fix B as above. Below, we set Ω to be the set of edges whose states are not deterministically fixed on the event $\{\mathcal{B} = B\}$. Note that for Risk_x to occur, there must exist (see Figure II.16)

(v) an open path in Ω from $\partial\Lambda_{s/3}(y)$ to $\partial\Lambda_r(x)$.

Since the boundary conditions induced by $\{\mathcal{B} = B\}$ on the part of $\partial\Omega$ strictly inside $\Lambda_{s/3}(y)$ are free, Proposition II.3.6 implies that

$$\phi[\mathrm{Risk}_x | \mathcal{B} = B] \leq \phi[(v) | \mathcal{B} = B] \leq C_2 (\tfrac{r}{s})^{c_2}.$$

This concludes the proof of (II.36) and of the claim. □

Plugging Claims 1, 2 and 3 into (II.27) concludes the proof of the lemma. □

We now deal with the second lemma, which states a bound on the probability that two boxes of size s centered on vertices in t_j^- are connected to z_0 in terms of the probability that one of them is. Below, $|\cdot|$ denotes the Euclidean distance.

Lemma II.4.5. *There exists a uniform constant $C > 0$ such that for every $x, y \in t_j^-$,*

$$\phi[z_0 \leftrightarrow \Lambda_s(x), z_0 \leftrightarrow \Lambda_s(y), E] \leq C(\tfrac{s}{|y-x|})^2 \max_{z\in\{x,y\}} \phi[z_0 \leftrightarrow \Lambda_s(z), E].$$

Proof. Assume that $|x-y| \geq 13s$ otherwise one may simply set $C = 16$ to guarantee the inequality. Set $L := \lfloor |x-y|/3 \rfloor$. Let $\mathbf{C}$ and $\mathbf{\Gamma}$ be defined as in the proof of Lemma II.4.4, and write $\mathcal{D} := (\mathbf{C}, \mathbf{\Gamma})$. We will prove that for every possible realization $D = (\mathcal{C}, \Gamma)$ of $\mathcal{D}$,

$$\begin{aligned}\phi[z_0 \leftrightarrow \Lambda_s(x), &z_0 \leftrightarrow \Lambda_s(y), E|\mathcal{D} = D] \\ &\leq C(\tfrac{s}{|y-x|})^2 \Big(\phi[z_0 \leftrightarrow \Lambda_s(x), E|\mathcal{D} = D] + \phi[z_0 \leftrightarrow \Lambda_s(y), E|\mathcal{D} = D]\Big),\end{aligned} \tag{II.37}$$

which implies the claim by summing over all possible D.

From now on, fix a realization D for which the left-hand side is strictly positive. Let Ω be the set below $\mathbf{\Gamma}$. Consider the family of arcs $\ell_{x,i}$ (indexed by i) of $\Omega \cap \partial\Lambda_L(x)$ disconnecting z_0 in Ω from at least one vertex in $\Lambda_s(x)$. Since $\mathbf{\Gamma}$ is a path, any $z \in \Lambda_s(x) \cap \Omega$ is separated from z_0 by at least one such arc. Let $P_{x,i}$ be the region of $\Omega \setminus \ell_{x,i}$ separated from z_0, see Figure II.17. Introduce the events

$$H_{x,i} := \{\exists z \in \Lambda_s(x) \cap P_{x,i} : z \longleftrightarrow z_0\} \cap \{\exists z' \in \Lambda_s(y) \setminus P_{x,i} : z' \longleftrightarrow z_0\} \cap E$$

and $H_{y,j}$ defined in a similar fashion by considering arcs of $\Omega \cap \partial\Lambda_L(y)$, with the roles of x and y exchanged.

We claim that

$$\{z_0 \longleftrightarrow \Lambda_s(x), z_0 \longleftrightarrow \Lambda_s(y), E\} \subset \Big(\bigcup_i H_{x,i}\Big) \cup \Big(\bigcup_j H_{y,j}\Big). \tag{II.38}$$

Indeed, assume that the event on the left holds true and consider the regions $P_{u,k}$ with $u \in \{x, y\}$ for which there exists $z \in \Lambda_s(u) \cap P_{u,k}$ with $z \longleftrightarrow z_0$. There exists at least one $P_{u,k}$ with this property. Fix a region $P_{u,k}$ with the property above, and which is minimal among such regions for the inclusion. For simplicity, assume $u = x$. The first condition is ensured by the choice of $P_{x,k}$, and E occurs by assumption. The only way for $H_{x,k}$ to fail is if the second condition does, which implies the existence of $z' \in \Lambda_s(y) \cap P_{x,k}$ which is connected to z_0. Now, if we take $P_{y,j}$ to be the minimal (for the inclusion again) region containing z', we have $P_{y,j} \subsetneq P_{x,k}$, which contradicts the minimality of $P_{x,k}$.

We now prove the following claim.

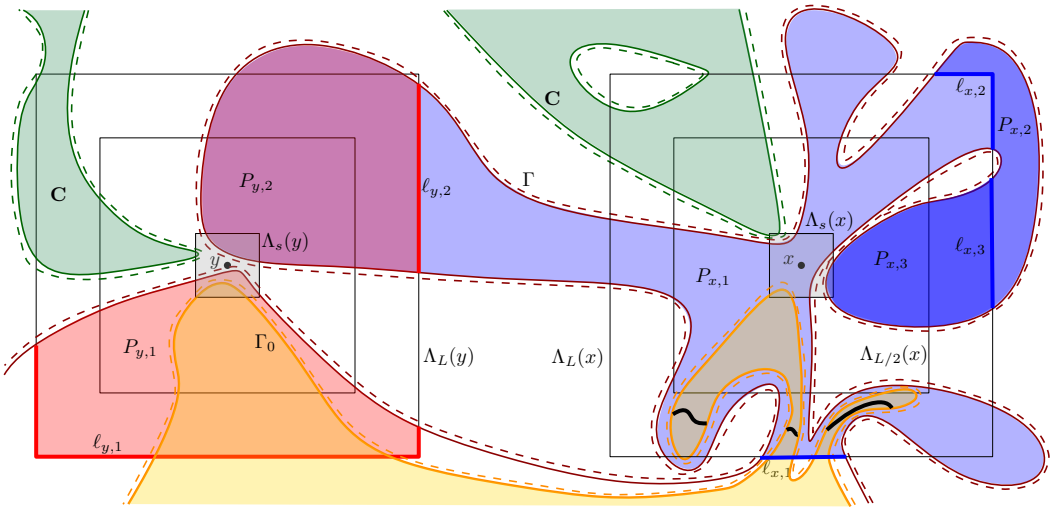

Figure II.17: We depicted in green (for $\mathbf{C}$) and dark red (for $\mathbf{\Gamma}$) the event $\mathcal{D} = D$. We also listed the arcs $\ell_{x,i}$ and $\ell_{y,i}$, as well as the domains $P_{x,i}$ enclosed by them. Note that the domains can be included into each other: here $P_{y,2}$ and $P_{x,2}$ are included in $P_{x,1}$, and $P_{x,3}$ is itself included in $P_{x,2}$. In yellow, the path Γ_0 contains a vertex in $\Lambda_s(y)$ and a vertex in $\Lambda_s(x)$. In the picture, $H_{x,1}$ occurs. Then, if the bold black paths are open, z_0 is connected to $\Lambda_s(y)$ outside of $P_{x,1} \cap \Lambda_{s/2}(x)$ by following $\mathbf{\Gamma}_0$ and shortcutting any visit of $\mathbf{\Gamma}_0$ to $\Lambda_{L/2}(x)$ via the black paths.

Claim. *There exists a universal constant $C_0 > 0$ such that*

$$\phi[H_{x,i} | \mathcal{D} = D] \leq C_0 \phi_{\mathbb{Z}^2}[E_{x,i}] \phi[z_0 \leftrightarrow \Lambda_s(y), E | \mathcal{D} = D], \tag{II.39}$$

where $E_{x,i}$ is the event that $\Lambda_s(x) \cap P_{x,i}$ contains a vertex z which is connected to $\partial\Lambda_{L/4}(x)$ but not to $\partial P_{x,i} \cup t_j^+$.

Proof. Introduce the event $H'_{x,i}$ that $H_{x,i}$ occurs and there exists $z' \in \Lambda_s(y) \setminus P_{x,i}$ which is connected to z_0 *outside* of $P_{x,i} \cap \Lambda_{L/2}(x)$. There exists $c_0 > 0$ such that

$$\phi[H'_{x,i} | \mathcal{D} = D] \geq c_0 \phi[H_{x,i} | \mathcal{D} = D]. \tag{II.40}$$

Indeed, consider the outer boundary $\mathbf{\Gamma}_0$ of the cluster of z_0. By definition on $H_{x,i}$, $\mathbf{\Gamma}_0$ must contain a vertex $z \in \Lambda_s(x) \cap P_{x,i}$ and a vertex $z' \in \Lambda_s(y) \setminus P_{x,i}$. As a consequence, $H'_{x,i}$ occurs as soon as there is no crossing in ω^* from $\partial\Lambda_{L/2}(x)$ to $\partial\Lambda_L(x)$ in the interior of $\mathbf{\Gamma}_0$, see Figure II.17 and its caption for more details. Since conditioning on $\mathbf{\Gamma}_0$ induces wired boundary conditions on its interior, the probability of this event is bounded from below by some universal constant $c_0 > 0$ by Proposition II.3.6.

Now, following a reasoning similar to Claim 1 of the previous lemma – here $\mathbf{C}_0$ becomes the cluster of z_0 outside $P_{x,i} \cap \Lambda_{L/2}(x)$ (which, on the event $H'_{x,i}$, necessarily contains a vertex in $\Lambda_s(y)$), and $\mathbf{C}_{\mathbf{\Gamma}}$ the union of the clusters of $\mathbf{\Gamma}$ outside of $P_{x,i} \cap \Lambda_{L/4}(x)$ – we obtain that

$$\phi[H'_{x,i} | \mathcal{D} = D, z_0 \text{ connected to } \Lambda_s(y) \text{ but not to } t_j^+ \text{ in } \Omega \setminus \Lambda_{L/2}(x)] \leq C_1 \phi_{\mathbb{Z}^2}[E_{x,i}]. \tag{II.41}$$

The two inequalities together give the result. □

We are ready to conclude. Write $\mathbf{N}$ for the number of disjoint clusters (in $\Lambda_{L/4}(x)$) from $\Lambda_s(x)$ to $\partial\Lambda_{L/4}(x)$ that are contained in the lower half-plane. By exploring the clusters one by one we obtain easily from (RSW) and the comparison between boundary conditions that there exist $c_2, C_2 \in (0,\infty)$ such that for every $k \geq 0$,

$$\phi_{\mathbb{Z}^2}[\mathbf{N} > k] \leq C_2(s/L)^{2+c_2 k}.$$

We deduce that

$$\sum_i \phi_{\mathbb{Z}^2}[E_{x,i}] \leq \phi[\mathbf{N}] \leq C_3(s/L)^2.$$

Summing over i the estimate provided by the claim and using the previous inequality gives

$$\phi\Big[\bigcup_i H_{x,i} \big| \mathcal{D} = D\Big] \leq C_4(s/L)^2 \phi[z_0 \leftrightarrow \Lambda_s(y), E | \mathcal{D} = D]. \tag{II.42}$$

A similar estimate holds for the union of the $H_{y,j}$. Together with (II.38), this gives (II.37) and therefore the claim. □

We are now in a position to prove Proposition II.4.3.

Proof of Proposition II.4.3. Without loss of generality, we may assume that 4 divides s which divides N (otherwise the proof can be trivially adapted). Let Y be a set of vertices $y \in t_j^-$ at a distance $s/4$ of each other. For any vertex $x \in t_j^-$, define $[x]$ to be the vertex $y \in Y$ closest to x.

On the one hand, using the inclusion of events, we get that

$$\begin{aligned}\phi[E_0(k), \mathrm{Iso}(r)^c | E] &\leq \sum_{x \in t_j^-} \phi[x = \mathrm{lmax}(z_0), z_0 \leftrightarrow \Lambda_s([x]), \mathrm{Iso}(r)^c | E] \\ &= \sum_{y \in Y} \sum_{\substack{x \in t_j^- \\ [x]=y}} \phi[x = \mathrm{lmax}(z_0), z_0 \leftrightarrow \Lambda_s(y), \mathrm{Iso}(r)^c | E].\end{aligned}$$

Now, Lemma II.4.4 and the fact that there are at most s vertices x satisfying $[x] = y$ for every fixed $y \in Y$ give

$$\sum_{\substack{x \in t_j^- \\ [x]=y}} \phi[x = \mathrm{lmax}(z_0), z_0 \leftrightarrow \Lambda_s(y), \mathrm{Iso}(r)^c | E] \leq \frac{C r^\eta}{s^{1+\eta}} \phi[z_0 \leftrightarrow \Lambda_s(y) | E].$$

It remains to bound the sum over $y \in Y$ of $\phi[z_0 \leftrightarrow \Lambda_s(y) | E]$ by a uniform constant.

To do that, observe that the Cauchy-Schwarz inequality and Lemma II.4.5 give

$$\begin{aligned}\Big(\sum_{y\in Y}\phi[z_0\leftrightarrow\Lambda_s(y)|E]\Big)^2 &\le \sum_{y,z\in Y}\phi[z_0\leftrightarrow\Lambda_s(y),z_0\leftrightarrow\Lambda_s(z)|E]\\ &\le C\sum_{y\in Y}\phi[z_0\leftrightarrow\Lambda_s(y)|E]\\ &\quad + C\sum_{y\neq z\in Y}(\tfrac{s}{|z-y|})^2\Big[\phi[z_0\leftrightarrow\Lambda_s(y)|E]+\phi[z_0\leftrightarrow\Lambda_s(z)|E]\Big]\\ &\le C'\sum_{y\in Y}\phi[z_0\leftrightarrow\Lambda_s(y)|E],\end{aligned}$$

which implies that the sum is at most C', and therefore concludes the proof. □

II.4.3 Proof of Theorem II.2.4

We prove the first identity (the second follows from the same argument). It suffices to show that

$$\frac{\mathfrak{h}_1^2[\mathrm{lmax}(\infty)=0^+]}{\mathfrak{h}_1^2[\mathrm{lmax}(\infty)=0]}=\frac{\sin\alpha}{\sin\beta}.$$

First of all, as seen in Theorem II.3.8, for every $\varepsilon>0$, there exists $R>0$ such that for every $\alpha,\beta\in(\varepsilon,\pi-\varepsilon)$ and $q\in[1,4]$, for every event A,

$$|\mathfrak{h}_1^2[A]-\phi^0_{\mathbb{L}_1}[A|\{0\leftrightarrow\partial\Lambda_R,\mathrm{lmax}(0)=0\}\cup\{0^+\leftrightarrow\partial\Lambda_R,\mathrm{lmax}(0^+)=0^+\}]|\le\varepsilon.$$

The convergence in Theorem II.3.8 is uniform in $q\in[1,4]$ and $\alpha,\beta\in(\varepsilon,\pi-\varepsilon)$ (as shown by Proposition II.3.9). Also, the eigenvalues $\lambda_N^{(k)}(\theta)$ are continuous in θ and q. As a consequence, we only need to prove the claim for $\alpha,\beta\neq\pi/2$ and $1\le q<4$.

We now focus on this case. Applying Propositions II.2.5 and II.2.6 gives that

$$\Big|\frac{\mathfrak{h}_1^2[\mathrm{lmax}(\infty)=0^+]}{\mathfrak{h}_1^2[\mathrm{lmax}(\infty)=0]}-\frac{\lambda^{(k)}(\beta)}{\lambda^{(k+3)}(\beta)}\times\frac{1-\lambda_N^{(k+3)}(\alpha)/\lambda_N^{(k)}(\alpha)}{1-\lambda_N^{(k+3)}(\beta)/\lambda_N^{(k)}(\beta)}\Big|\le C\Big(\frac{\lambda_N^{(k)}(\beta)}{\lambda_N^{(k+3)}(\beta)}-1\Big)^\eta. \tag{II.43}$$

Below, $o(1)$ denotes a quantity tending to 0 as N tends to infinity. Theorem II.2.7 implies that for $k\in[N^{1/2},2N^{1/2}]$,

$$\frac{1-\lambda_N^{(k+3)}(\alpha)/\lambda_N^{(k)}(\alpha)}{1-\lambda_N^{(k+3)}(\beta)/\lambda_N^{(k)}(\beta)}=\frac{\log\lambda_N^{(k)}(\alpha)-\log\lambda_N^{(k+3)}(\alpha)}{\log\lambda_N^{(k)}(\beta)-\log\lambda_N^{(k+3)}(\beta)}+o(1)$$

and

$$\frac{\lambda_N^{(k)}(\beta)}{\lambda_N^{(k+3)}(\beta)}=1+o(1)$$

so (II.43) implies that

$$\frac{\mathfrak{h}_1^2[\mathrm{lmax}(\infty)=0^+]}{\mathfrak{h}_1^2[\mathrm{lmax}(\infty)=0]}=\frac{\log\lambda_N^{(k)}(\alpha)-\log\lambda_N^{(k+3)}(\alpha)}{\log\lambda_N^{(k)}(\beta)-\log\lambda_N^{(k+3)}(\beta)}+o(1). \tag{II.44}$$

At this stage, we use Theorem II.2.7 one more time to notice that

$$\frac{\log \lambda_N^{(N^{1/2})}(\alpha) - \log \lambda_N^{(2N^{1/2})}(\alpha)}{\log \lambda_N^{(N^{1/2})}(\beta) - \log \lambda_N^{(2N^{1/2})}(\beta)} = \frac{\sin \alpha}{\sin \beta} + o(1).$$

We deduce that there exists k_- between $N^{1/2}$ and $2N^{1/2}$ such that

$$\frac{\log \lambda_N^{(k_-)}(\alpha) - \log \lambda_N^{(k_-+3)}(\alpha)}{\log \lambda_N^{(k_-)}(\beta) - \log \lambda_N^{(k_-+3)}(\beta)} \geq \frac{\sin \alpha}{\sin \beta} - o(1)$$

and similarly k_+ such that

$$\frac{\log \lambda_N^{(k_+)}(\alpha) - \log \lambda_N^{(k_++3)}(\alpha)}{\log \lambda_N^{(k_+)}(\beta) - \log \lambda_N^{(k_++3)}(\beta)} \leq \frac{\sin \alpha}{\sin \beta} + o(1).$$

Applying (II.44) to k_+ and k_- and letting N tend to infinity concludes the proof.

II.5 Homotopy distance: proof of Theorem II.2.2

II.5.1 Encoding of homotopy classes

In the introduction, we were not precise in the way we compute homotopy classes. We now remedy this approximation. Recall that $\mathbb{B}_\eta := \eta\mathbb{Z}^2 \cap [-1/\eta, 1/\eta]^2$. Consider the set of *oriented edges* $\vec{E}$:

$$\vec{E} := \{(x, y) : x, y \in \mathbb{B}_\eta : \|x - y\|_2 = \eta\}.$$

Below, we see an oriented edge (x, y) as a segment joining the endpoints x and y with an orientation from x to y.

Let $\mathcal{W}$ be the set of finite words on the alphabet $\vec{E}$ and denote the empty word by $\emptyset$. Define the "cyclic" equivalence relation $\sim$ on $\mathcal{W}$ by $(u_i)_{1\leq i\leq p} \sim (v_j)_{1\leq j\leq q}$ if and only if $p = q$ and there exists $k \in [1, p]$ such that $u_1 \dots u_p = v_k \dots v_p v_1 \dots v_{k-1}$. Define the set of *cyclic words* as the quotient $\mathcal{CW} := \mathcal{W}/\sim$.

We also wish to work with a reduced representation of cyclic words. Let $\preceq$ be the (smallest) order relation on $\mathcal{CW}$ such that for any word $u = u_1 \cdots u_p$, any integer $1 \leq k < p$ (resp. $1 \leq k \leq p$) such that $u_{k+1} = (x, y)$ and $u_k = (y, x)$, and $v = u_1 \cdots u_{k-1} u_{k+2} \cdots u_p$, we have $v \preceq u$. It is straightforward to check that there exists a smallest $\underline{u} \preceq u$ for every u. We call this the *reduced word of* u.

Definition II.5.1 (Homotopy classes)**.** For a non-self-intersecting smooth loop $\gamma \subset \mathbb{R}^2 \setminus \mathbb{B}_\eta$, let $u = \mathbf{u}(\gamma)$ be the *word associated to* γ defined as follows: orient the loop counterclockwise, fix $a \in \gamma$ not on an oriented edge[7], and let $\mathbf{u}(\gamma) = u_1 \cdots u_k$, where u_i is the i-th (when going counter-clockwise along the curve starting from a) oriented edge (x, y) crossed by γ in such a way that x is on the left of the crossing and y on the right. Then, the *homotopy class* $[\gamma]_\eta$ of γ is the reduced word $\underline{u}(\gamma)$.

[7]Changing a will correspond to a rerooting of the loop and will lead to the same cyclic word.

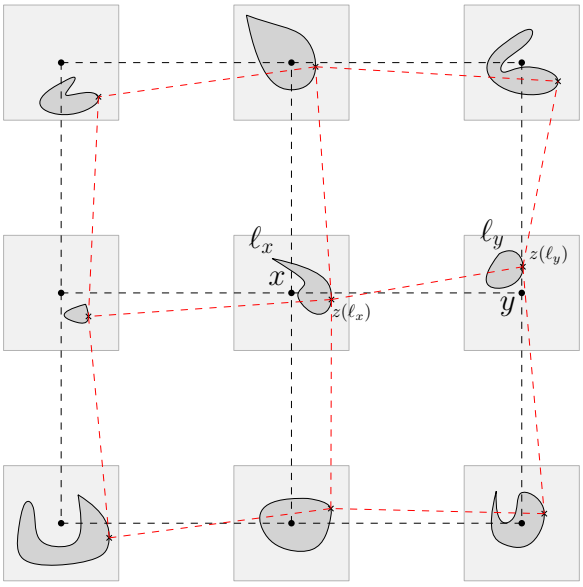

Figure II.18: In dashed black, the segments corresponding to the oriented edges in $\mathbb{B}_\eta$. Also, the crosses correspond to the points $z(\ell_x)$ for the loops. Finally, the associated segments are depicted in dashed red.

Remark II.5.2. The previous definitions are sufficient for the proof of Theorem II.2.2. In preparation for the proof of Theorem II.2.3 in the next section, we explain how homotopy classes in other spaces considered in this paper are encoded. Consider a collection of non-self-intersecting loops $(\ell_x : x \in \mathbb{B}_\eta)$ satisfying that the right-most point $z(\ell_x)$ in ℓ_x (if there is more than one such point, consider the lowest one) belongs to $B(x, \frac{1}{4}\eta)$ for every $x \in \mathbb{B}_\eta$. We wish to compute homotopy classes in the space $\mathbb{R}^2 \setminus \cup_{x\in\mathbb{B}_\eta} \ell_x$ in a way that is consistent with the definition of $[\cdot]$ above. Define the segment (x, y) for x and y neighbors to be the oriented segment from $z(\ell_x)$ to $z(\ell_y)$. Encode the homotopy classes of loops in $\mathbb{R}^2 \setminus \cup_{x\in\mathbb{B}_\eta} \ell_x$ using reduced words in the same way as above with segments between $z(\ell_x)$ and $z(\ell_y)$ playing the role of the segment between x and y in the case of $\mathbb{R}^2 \setminus \mathbb{B}_\eta$.

II.5.2 Proof of Theorem II.2.2

Proof of Theorem II.2.2. We show the result for the Camia-Newman distance. The version of the result for the Schramm-Smirnov distance follows readily from known implications between the former and the latter (see e.g. [CN06b, Theorem 7]). In this proof, fix $\kappa, \eta, \delta > 0$ such that

$$\kappa > 12\sqrt{2}\eta \geq 1000\delta.$$

Below, a word $v = v_1 \cdots v_\ell \in \mathcal{W}$ is a *subword* of $u \in \mathcal{CW}$ if there exists k such that $v_i = u_{k+i}$ for all $1 \leq i \leq \ell$. We extend the order relation to non-cyclic words and can therefore talk of $\underline{v}$. Also, we call $\mathrm{diam}(v)$ the maximal Euclidean distance between two centers of edges in $\{v_1, \ldots, v_k\}$ and say that v *intersects* $B(0, 1/\kappa)$ if it contains a letter which is incident to a point of $\mathbb{B}_\eta \cap B(0, 1/\kappa)$. With these

definitions, introduce the events

$$\text{Normal}(\kappa,\eta) := \left\{ \begin{array}{c} \nexists \text{ a loop } \gamma \text{ such that } \mathbf{u}(\gamma) \text{ contains a subword } v \\ \text{intersecting } B(0,1/\kappa) \text{ with } \underline{v} = \emptyset \text{ and } \text{diam}(v) \geq \frac{1}{3}\kappa \end{array} \right\},$$

$$\text{Dense}(\eta) := \{\text{every face of } \eta\mathbb{Z}^2 \cap B(0,1/\eta) \text{ contains a loop in } \mathcal{F}_0 \text{ and one in } \mathcal{F}_1\}.$$

Now, consider $\omega_\delta \sim \phi_{\delta\mathbb{L}(\alpha)}$ and $\overline{\omega}'_\delta$ of $\omega_\delta \sim \phi_{\delta\mathbb{L}(\pi/2)}$ and let $\mathcal{F}_i(\omega_\delta)$ and $\mathcal{F}_i(\omega'_\delta)$ be the collections of loops (primal or dual depending on i) in $\overline{\omega}_\delta$ and $\overline{\omega}'_\delta$ respectively.

Claim 1. *For every $\kappa > 12\sqrt{2}\eta$, one has*

$$\{d_{\mathbf{H}}(\omega_\delta,\omega'_\delta) \leq \eta\} \cap \{\omega_\delta,\omega'_\delta \in \text{Normal}(\kappa,\eta) \cap \text{Dense}(\eta,\delta)\} \subset \{d_{\mathbf{CN}}(\omega_\delta,\omega'_\delta) \leq \kappa\}. \tag{II.45}$$

Proof. Consider a loop $\gamma \in \mathcal{F}_i(\omega_\delta)$ that is included in $B(0,1/\kappa)$, we need to prove that there exists $\gamma' \in \mathcal{F}_i(\omega'_\delta)$ such that $d(\gamma',\gamma) \leq \kappa$. Since the same can be done for $\mathcal{F}_i(\omega'_\delta)$, this will conclude the proof of (II.45).

Write $\boldsymbol{u}(\gamma) = \underline{u}_1 v^1 \underline{u}_2 v^2 \cdots \underline{u}_k v^k$, where $\underline{u}_i$ are the letters of $\underline{u} = [\gamma]_\eta$ and $v^1,\dots,v^k$ are words satisfying $\underline{v}^1 = \cdots = \underline{v}^k = \emptyset$ (such a decomposition exists but may not be unique). We justify in the next paragraph that $\omega_\delta \in \text{Normal}(\kappa,\eta)$ implies that $d(\gamma,\boldsymbol{\gamma}) \leq \kappa/2$ for *any* non-self-crossing smooth curve $\boldsymbol{\gamma}$ satisfying $\mathbf{u}(\boldsymbol{\gamma}) = [\gamma]_\eta = \underline{u}$.

To prove that $d(\gamma,\boldsymbol{\gamma}) \leq \kappa/2$, consider a parametrization of γ on $[0,1]$ and let t_i be the first time $t \geq t_{i-1}$ such that $\gamma(t_i) \in \underline{u}_i$ (where we consider $t_0 = 0$) and parametrize $\boldsymbol{\gamma}$ on $[0,1]$ in such a way that $\boldsymbol{\gamma}(t_i) \in \underline{u}_i$. Then, we claim that for every $t \in [0,1]$, $|\gamma(t) - \boldsymbol{\gamma}(t)| \leq \kappa/2$. Indeed, we know that for $t_i \leq t < t_{i+1}$, $\boldsymbol{\gamma}(t)$ belongs to the face of $\eta\mathbb{Z}^2$ that contains $\underline{u}_i$ and $\underline{u}_{i+1}$ and $\gamma(t)$ belongs to one of the faces bordering $\underline{u}_i$, $\underline{u}_{i+1}$, or one of the letters in v^i. Now, the diameter of v^i is smaller than $\kappa/3$, and we therefore deduce that $\gamma(t)$ is within distance $\kappa/3 + 2\sqrt{2}\eta \leq \kappa/2$ of $\boldsymbol{\gamma}(t)$, hence $d(\gamma,\boldsymbol{\gamma}) \leq \kappa/2$.

We are now ready to conclude. Assume first that γ surrounds at most one point $x \in \mathbb{B}_\eta$. Then, $[\gamma]_\eta$ is either the empty word, or a word made of four letters corresponding to edges incident to x. As a consequence, we may choose $\boldsymbol{\gamma}$ with a diameter which is smaller than $2\sqrt{2}\eta$ and such that $u(\boldsymbol{\gamma}) = [\gamma]_\eta$. Also, since $\omega'_\delta \in \text{Dense}(\eta)$, there exists a loop $\gamma' \in \mathcal{F}_i(\omega'_\delta)$ included in one of the faces intersected by $\boldsymbol{\gamma}$. We obtain immediately that $d(\boldsymbol{\gamma},\gamma') \leq 2\sqrt{2}\eta$ and therefore $d(\gamma,\gamma') \leq \kappa/2 + 2\sqrt{2}\eta \leq \kappa$.

Let us now assume that γ surrounds at least two points in $\mathbb{B}_\eta$. Being included in $B(0,1/\kappa)$, γ cannot surround all the points in $\mathbb{B}_\eta$. The fact that $d_{\mathbf{H}}(\omega_\delta,\omega'_\delta) \leq \eta$ thus implies the existence of $\gamma' \in \mathcal{F}'_i$ such that $[\gamma]_\eta = [\gamma']_\eta$. Since γ' must intersect $B(0,1/\kappa)$ as well, and ω_δ and ω'_δ are in $\text{Normal}(\kappa,\eta)$, we obtain that $d(\gamma,\boldsymbol{\gamma}) \leq \kappa/2$ and $d(\gamma',\boldsymbol{\gamma}) \leq \kappa/2$ for every $\boldsymbol{\gamma}$ with $u(\boldsymbol{\gamma}) = [\gamma]_\eta = [\gamma']_\eta$. The triangular inequality gives that $d(\gamma',\gamma) \leq \kappa$. This concludes the proof. □

We now turn to another claim.

Claim 2. *There exist $c, C \in (0,\infty)$ such that for every β,*

$$\phi_{\delta\mathbb{L}(\beta)}[\text{Normal}(\kappa,\eta)] \geq 1 - \tfrac{C}{\eta^2\kappa^2}\exp[-c\kappa/\eta]. \tag{II.46}$$

Proof. Let $A(\kappa,\eta)$ be the event that there exists a crossing of the rectangle $R := [0,\kappa/3]\times[0,\kappa/12]$ whose cluster in the strip $\mathbb{R}\times[0,\kappa/12]$ surrounds no vertex in $\eta\mathbb{Z}^2$. We claim the existence of $c>0$ such that

$$\phi_{\delta\mathbb{L}(\beta)}[A(\kappa,\eta)] \leq C\exp[-c\kappa/\eta]. \tag{II.47}$$

To prove (II.47), let $\mathbf{N}$ be the number of clusters that contain a vertical crossing of R and for $i \leq \mathbf{N}$, call Γ_i the right-boundary of the i-th cluster $\mathcal{C}_i$ in R crossing R when starting counting clusters from the right. Let Ω_i be the set of vertices in $\mathbb{R}\times[0,\kappa/12]$ on the left of (and including) Γ_i (see Figure II.19 for a picture). Note that Γ_i is measurable in terms of the edges on Γ_i or on its right, and that it induces wired boundary conditions on Γ_i for the measure in Ω_i. Let X_i be a maximal set of vertices in $\Omega_i \cap \eta\mathbb{Z}^2$ that are at a distance at least 4η of each other[8], but at a distance at most η of Γ_i. Note that one may easily construct such a set of cardinality at least $\lfloor\kappa/(48\eta)\rfloor - 1$. Then, for every $x \in X_i$, by (RSW) there exists an open path disconnecting $\Lambda_\eta(x)$ from $\partial\Lambda_{2\eta}(x)$ in Ω_i with probability larger than $c_0>0$, even when we enforce free boundary conditions on $\partial\Lambda_{2\eta}(x)$. The comparison between boundary conditions thus implies that

$$\phi_{\delta\mathbb{L}(\beta)}[\nexists x \in X_i \text{ surrounded by } \mathcal{C}_i|\Gamma_i] \leq (1-c_0)^{|X_i|} \leq (1-c_0)^{\lfloor\kappa/(48\eta)\rfloor-1}.$$

It remains to sum over i and use that $\phi_{\delta\mathbb{L}(\beta)}[\mathbf{N}] \leq C_0$ (Proposition II.3.7) to get (II.47):

$$\phi_{\delta\mathbb{L}(\beta)}[A(\kappa,\eta)] \leq (1-c_0)^{\lfloor\kappa/(48\eta)\rfloor-1}\phi_{\delta\mathbb{L}(\beta)}[\mathbf{N}] \leq C_0(1-c_0)^{\lfloor\kappa/(48\eta)\rfloor-1}.$$

We are now in a position to conclude. Consider the square box $B_1 := [-\kappa/24,\kappa/24]^2$ as well as the rectangle $R_1^R := [\kappa/12,\kappa/6]\times[-\kappa/6,\kappa/6]$ and its rotations R_1^T, R_1^L, and R_1^B by angles $\pi/2$, π, and $3\pi/2$, respectively. Also, consider a collection of translates $(B_i,R_i^R,R_i^T,R_i^L,R_i^B)$ of $(B_1,R_1^R,R_1^T,R_1^L,R_1^B)$ such that the boxes B_i cover $B(0,1/\eta-\kappa/3)$. Note that the probability that a translate/rotation/dual of $A(\kappa,\eta)$ occurs for some $R_i^\#$ is bounded by the right-hand side of (II.47). Write A_{global} for the event that the rotation/translation of A or its dual occurs for some $R_i^\#$. The union bound implies that

$$\phi_{\delta\mathbb{L}(\beta)}[A_{\text{global}}(\kappa,\eta)] \leq \frac{C_1}{\eta^2\kappa^2}(1-c_0)^{\lfloor\kappa/(48\eta)\rfloor-1}.$$

We next prove that $\text{Normal}(\kappa,\eta)$ occurs as soon as $A_{\text{global}}(\kappa,\eta)$ does.

To see this, assume $\text{Normal}(\kappa,\eta)$ fails and consider a loop γ and a subword v of $u(\gamma)$ with $\underline{v}=\emptyset$ of maximal diameter among the subwords intersecting $B(0,1/\kappa)$. The first and last letters of v must necessarily border the same face f. Consider two times s and t such that $\gamma(s),\gamma(t)\in f$ and $\gamma([s,t])$ has v as an encoding word, and

[8]This is a technical statement enabling to use the comparison between boundary conditions "independently" in each of the boxes $\Lambda_{2\eta}(x)$.

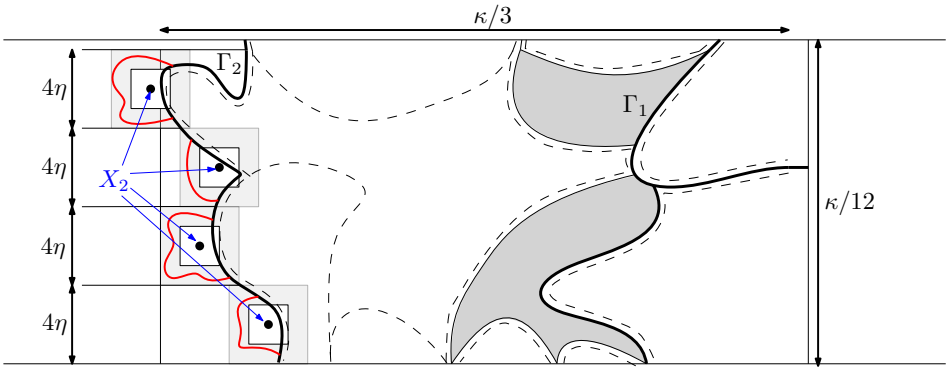

Figure II.19: An example with two clusters crossing. Note that the set X_i does not have to be included in the rectangle R. A way to construct a large set of points with the properties of X_i is to choose for each $1 \leq j < \lfloor \kappa/48\eta \rfloor - 1$, on each line $\{(x,y) \in \mathbb{R}^2 : y = (2j+1)\eta\}$, a vertex of Ω_i which is at a distance smaller than η of Γ_i.

close $\gamma([s,t])$ into a non-self-crossing loop $\ell(\gamma)$ by going from $\gamma(s)$ to $\gamma(t)$ inside the face f. Note that f must intersect a box B_i, and that $\ell(\gamma)$ must cross one of the four rectangles $R_i^{\#}$ around it. Now, outside of f, $\ell(\gamma)$ is identical to γ so it has either primal edges of ω_δ bordering it on its interior or dual edges. In the former case, the non occurrence of $A(\kappa,\eta)$ for the rectangle mentioned above implies that $\ell(\gamma)$ must necessarily surround a point in $\mathbb{B}_\eta$, which contradicts the fact that $\underline{v} = \emptyset$. In the latter case, the non occurrence of the dual of $A(\kappa,\eta)$ implies the same claim. □

We are now in a position to conclude the proof of the theorem. Claim 1 implies that

$$\begin{aligned}\mathbf{P}[d_{\mathbf{H}}(\omega_\delta,\omega'_\delta) \leq \eta, d_{\mathbf{CN}}(\omega_\delta,\omega'_\delta) > \kappa] \leq \phi_{\delta\mathbb{L}(\alpha)}[\mathrm{Normal}(\kappa,\eta)^c] + \phi_{\delta\mathbb{L}(\pi/2)}[\mathrm{Normal}(\kappa,\eta)^c] \\ + \phi_{\delta\mathbb{L}(\alpha)}[\mathrm{Dense}(\eta)^c] + \phi_{\delta\mathbb{L}(\pi/2)}[\mathrm{Dense}(\eta)^c].\end{aligned}$$

Now, Claim 2 applied to β equal to α or $\frac{\pi}{2}$ gives

$$\phi_{\delta\mathbb{L}(\alpha)}[\mathrm{Normal}(\kappa,\eta)^c] + \phi_{\delta\mathbb{L}(\pi/2)}[\mathrm{Normal}(\kappa,\eta)^c] \leq \tfrac{1}{2}\kappa,$$

provided $\eta = \eta(\kappa) > 0$ is chosen small enough.

Finally, since any vertex with four closed edges incident to it gives rise to a small loop in $\mathcal{F}_1$, and similarly for $\mathcal{F}_0$ when considering the dual graph, the finite-energy property immediately implies that

$$\phi_{\delta\mathbb{L}(\alpha)}[\mathrm{Dense}(\eta)^c] + \phi_{\delta\mathbb{L}(\pi/2)}[\mathrm{Dense}(\eta)^c] \leq \frac{2C}{\eta^2}\exp[-c(\eta/\delta)^2] \leq \tfrac{1}{2}\kappa,$$

provided $\delta = \delta(\eta)$ small enough. The last three displayed inequalities conclude the proof of the theorem. □

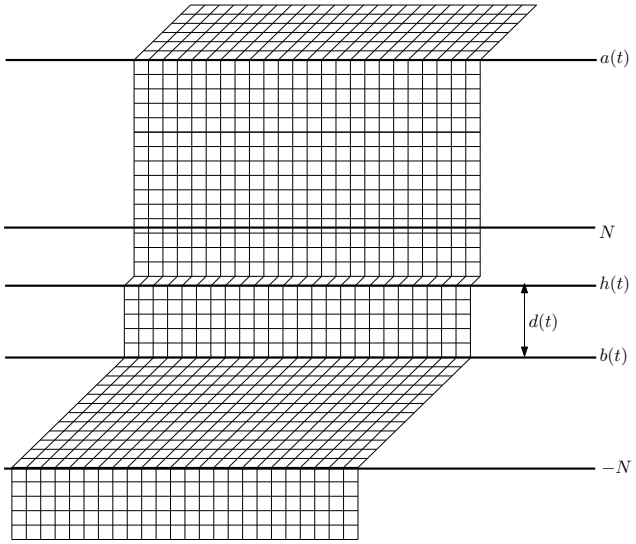

Figure II.20: The quantities $h(t)$, $a(t)$, $b(t)$ and $d(t)$. One may deduce from the picture that $\lfloor t/(2N) \rfloor = 12$ as there are 12 tracks of angle α stacked above level $-N$.

II.6 Universality in isoradial rectangular graphs: proof of Theorem II.2.3

The section is divided in six subsections. In the first one, we recall the setting of the proof and introduce some convenient notation. In the second one, we define the notion of nails, give a precise definition of $\mathcal{H}$, and introduce the formal definition of our coupling. The third one explains how one can couple the increments of the maximal coordinates of nails with independent increments that have the law of increments in a track-exchange on the IIC. In the fourth subsection, we will explore the combination of several increments into so-called compounded steps corresponding to bringing down one track from its starting to its ending position. The fifth subsection shows that the speed that can be associated to the evolution of a compounded step is approximately zero. Finally, the last subsection contains the proof of the theorem.

II.6.1 Setting of the proof

Below, fix $\alpha \in (0, \pi/2)$ (the case $\alpha > \pi/2$ can be obtained by a global reflection with respect to the y-axis). We further assume, except when otherwise stated, that

$$\cos \alpha \notin \mathbb{Q}. \tag{II.48}$$

This assumption plays an implicit role in the definition of the coupling, and is essential in the proof of Proposition II.6.14, see Remark II.6.15.

Also, let $0 < \varepsilon \ll \eta \ll 1$ be fixed along the whole section (they will be chosen appropriately in the proof of the theorem at the end of the section). Set

$$\mathbb{B}_\eta(N) := \eta N \mathbb{Z}^2 \cap [-N, N]^2$$

(note that it is not quite the blow up by a factor N of $\mathbb{B}_\eta$) and

$$T := 2N \times \lceil 2N/\sin\alpha \rceil.$$

As in Section II.2, $\mathbb{L}^{(0)}$ is the isoradial lattice with angles

$$\alpha_j = \alpha_j(\alpha, N) := \begin{cases} \alpha & \text{if } j \geq N, \\ \frac{\pi}{2} & \text{if } j < N. \end{cases}$$

Recall the successive transformations $\mathbf{T}_{j(t)}$ of the lattice described in Section II.2: at time $0 \leq t < T$, the track to be descended is $t_{j(t)}$ with

$$j(t) := N + (2N+1)\lfloor t/(2N) \rfloor - t.$$

and the graph $\mathbb{L}^{(t)}$ obtained from the graph $\mathbb{L}^{(0)}$ by applying successively the maps $\mathbf{T}_{j(s)}$ for $0 \leq s < t$.

We use the following four convenient quantities (see Figure II.20):

$$\begin{aligned} h(t) &:= \text{the second coordinate of the horizontal line } t^-_{j(t)} \text{ in } \mathbb{L}^{(t)}, \\ a(t) &:= h(2N\lfloor t/(2N) \rfloor) + \sin\alpha, \\ b(t) &:= h(2N\lfloor t/(2N) \rfloor - 1) + \sin\alpha - 1 \text{ if } t > 2N \text{ and } := -N \text{ if } t \leq 2N, \\ d(t) &:= \min\{h(t) - b(t), a(t) - h(t)\}. \end{aligned}$$

Note that $b(t)$ is the top of the track of angle α below $t_{j(t)}$ (except when $t < 2N$ in which case we set it to be $-N$ by convention), and $a(t)$ is the bottom of the track of angle α above $t_{j(t)}$.

II.6.2 Definition of nails, marked nails, and the coupling P

Recall the definition, for a (primal) cluster $\mathcal{C}$ in a configuration ω, of $\mathrm{T}(\mathcal{C})$, $\mathrm{B}(\mathcal{C})$ and $\mathrm{R}(\mathcal{C})$, which are respectively the maximal second, minimal second and maximal first coordinates of a vertex in $\mathcal{C}$. Define $\mathrm{Vspan}(\mathcal{C}) := \mathrm{T}(\mathcal{C}) - \mathrm{B}(\mathcal{C})$.

Definition II.6.1 (Nail)**.** For $x = (x_1, x_2) \in \mathbb{B}_\eta(N)$ and a configuration ω, call a (primal) cluster $\mathcal{C}$ of ω on some $\mathbb{L}^{(t)}$ a *nail (near x)* if

$$\mathrm{Vspan}(\mathcal{C}) \geq \varepsilon N \qquad \text{and} \qquad \max\{|\mathrm{T}(\mathcal{C}) - x_2|, |\mathrm{B}(\mathcal{C}) - x_2|, |\mathrm{R}(\mathcal{C}) - x_1|\} \leq \sqrt{\eta\varepsilon} N.$$

We now define the coupling of the measures $\phi_{\mathbb{L}^{(t)}}$ for $0 \leq t \leq T$.

Step 0 of the coupling P. Sample $\omega^{(0)} \sim \phi_{\mathbb{L}^{(0)}}$.

Index the nails near all points in $\mathbb{B}_\eta$ in $\omega^{(0)}$ by integers $1, \ldots, M = M(\omega^{(0)})$, and let $\mathcal{C}(\omega^{(0)}, i)$ be the nail indexed by i. Define $I^{(0)} := \{1, \ldots, M\}$. Write $\mathrm{T}^{(0)}$, $\mathrm{B}^{(0)}$ and $\mathrm{R}^{(0)}$ for the functions from $I^{(0)}$ into $\mathbb{R}$ giving, for every $i \in I^{(0)}$ and $A \in \{\mathrm{T}, \mathrm{B}, \mathrm{R}\}$, $A^{(0)}(i) := A(\mathcal{C}(\omega^{(0)}, i))$. Also set $\mathrm{Vspan}(i) := \mathrm{Vspan}(\mathcal{C}(\omega^{(0)}, i))$.

For each $x = (x_1, x_2) \in \mathbb{B}_\eta(N)$, choose, if it exists, $i_x \in I^{(0)}$ such that

$$\mathrm{Vspan}(i_x) \geq 2\varepsilon N \qquad \text{and} \qquad \max\{|\mathrm{T}(i_x) - x_2|, |\mathrm{B}(i_x) - x_2|, |\mathrm{R}(i_x) - x_1|\} \leq (\sqrt{\eta\varepsilon} - \varepsilon) N \tag{II.49}$$

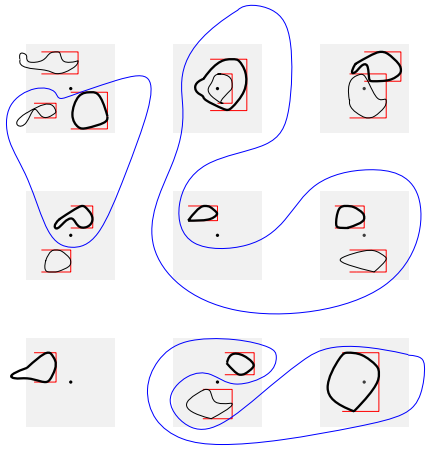

Figure II.21: In black, the nails (i.e. the elements indexed by $I(\omega)$) and in bold black the marked nails. The red segments depict the information provided by $(\mathrm{T}^{(t)}, \mathrm{B}^{(t)}, \mathrm{R}^{(t)})$. The blue loops are the loops surrounding at least two marked nails, i.e. the loops contributing to $[\cdot]_{\bullet,0}$ and $[\cdot]_{\bullet,1}$. The grey area are the boxes $\Lambda_{\sqrt{\varepsilon\eta}N}(x)$, which one should think of potentially much bigger than the minimal size $O(\varepsilon N)$ of nails, but much smaller than the minimal distance ηN between vertices of $\mathbb{B}_\eta(N)$.

(if there is more than one, pick the smallest such integer). Call $\mathcal{C}(\omega^{(0)}, i_x)$ the *marked nail near* x. Let $I_\bullet \subset I^{(0)}$ be the indexes corresponding to the marked nails near each $x \in \mathbb{B}_\eta(N)$, with the understanding that there may be some x for which there is no such marked nail (we will see later in this section that, with a very large probability, there is a marked nail near every $x \in \mathbb{B}_\eta(N)$).

Finally, if there exists a marked nail near every $x \in \mathbb{B}_\eta$, introduce the two multi-sets[9] $[\cdot]^{(0)}_{\bullet,0}$ and $[\cdot]^{(0)}_{\bullet,1}$ gathering the homotopy classes (in the sense of Remark II.5.2) in the full plane minus the marked nails $\mathbb{R}^2 \setminus \{\mathcal{C}(\omega, i) : i \in I_\bullet\}$ of the loops in $\mathcal{F}_0(\omega^{(0)})$ and $\mathcal{F}_1(\omega^{(0)})$ that surround at least two but not all marked nails. At this stage, we insist on the fact that $[\cdot]^{(0)}_{\bullet,0}$ and $[\cdot]^{(0)}_{\bullet,1}$ are multisets as there may be more than one loop in $\omega^{(0)}$ of a given homotopy class. If there exists $x \in \mathbb{B}_\eta$ that does not have a marked nail near it, simply set $[\cdot]^{(0)}_{\bullet,0} = [\cdot]^{(0)}_{\bullet,1} = \emptyset$.

To lighten the notation, we write

$$\mathcal{H}^{(0)} := (I^{(0)}, \mathrm{T}^{(0)}, \mathrm{B}^{(0)}, \mathrm{R}^{(0)}, [\cdot]^{(0)}_{\bullet,0}, [\cdot]^{(0)}_{\bullet,1}).$$

Fix now $0 \le t < T$ and assume that $\omega^{(t)}$ and $\mathcal{H}^{(t)} = (I^{(t)}, \mathrm{T}^{(t)}, \mathrm{B}^{(t)}, \mathrm{R}^{(t)}, [\cdot]^{(t)}_{\bullet,0}, [\cdot]^{(t)}_{\bullet,1})$ have been constructed (for the latter, the way it is given in terms of $\omega^{(t)}$ is explained for $t+1$ below), where

- $I^{(t)}$ is a subset of $\mathbb{Z}_{>0}$,
- $\mathrm{T}^{(t)}, \mathrm{B}^{(t)}, \mathrm{R}^{(t)}$ are functions from $I^{(t)}$ to $\mathbb{R}$,

[9] Formally, these are functions from the set of homotopy classes, or in our case of reduced words, into non-negative integers.

- $[\cdot]^{(t)}_{\bullet,0}$ and $[\cdot]^{(t)}_{\bullet,1}$ are multisets with elements in homotopy classes in $\mathbb{R}^2 \setminus \{\mathcal{C}(\omega^{(t)}, i) : i \in I_\bullet\}$ if $I_\bullet \subset I^{(t)}$, and equal to $\emptyset$ otherwise.

Step t to $t+\frac{1}{2}$ of the coupling P. Sample $\omega^{(t+1/2)} \sim \phi_{\mathbb{L}^{(t)}}[\,\cdot\,|\mathcal{H} = \mathcal{H}^{(t)}]$,

where $\omega \in \{\mathcal{H} = H\}$ (with $H = (I, \mathrm{T}, \mathrm{B}, \mathrm{R}, [\cdot]_{\bullet,0}, [\cdot]_{\bullet,1})$ a possible realization of $\mathcal{H}^{(t)}$) denotes the event that

(i) there exists an indexation of the nails in ω by I (call $\mathcal{C}(\omega, i)$ the nail indexed by $i \in I$);
(ii) $A(\mathcal{C}(\omega, i)) = A(i)$ for every $i \in I$ and $A \in \{\mathrm{T}, \mathrm{B}, \mathrm{R}\}$;
(iii) if $I_\bullet \subset I$, the further requirement that $[\cdot]_{\bullet,0}$ and $[\cdot]_{\bullet,1}$ are giving the homotopy classes of the loops of ω that surround at least two but not all marked nails.

Step $t+\frac{1}{2}$ to $t+1$ of the coupling P. Set $\omega^{(t+1)} := \mathbf{T}_{j(t)}(\omega^{(t+1/2)})$ (remember that $\mathbf{T}_{j(t)}$ is a map sending a configuration to a *random* configuration).

Due to the previous step, $\omega^{(t+1/2)}$ necessarily satisfies the event $\{\mathcal{H} = \mathcal{H}^{(t)}\}$. Consider the indexation of the nails of $\omega^{(t+1/2)}$ by $I^{(t)}$ given by (i) and write $\mathcal{C}(\omega^{(t+1/2)}, i)$ for the nail indexed by i.

Since the track-exchange map $\mathbf{T}_{j(t)}$ is obtained as a sequence of star-triangle transformations, one can check that a nail $\mathcal{C}(\omega^{(t+1/2)}, i)$ is transformed into a cluster $\mathcal{C}$ in $\omega^{(t+1)}$. If $\mathcal{C}$ is still a nail in $\omega^{(t+1)}$, include i in $I^{(t+1)}$ and define $A^{(t+1)}(i) = A(\mathcal{C})$ for $A \in \{\mathrm{T}, \mathrm{B}, \mathrm{R}\}$. If this is not the case, then do not include i in $I^{(t+1)}$. Finally, for each "new" nail $\mathcal{C}'$ in $\omega^{(t+1)}$, i.e. a nail that was not in $\omega^{(t+1/2)}$, pick an integer i that was not used in any of the $I^{(s)}$ for $s \le t$ and include it in $I^{(t+1)}$. As before, let $A^{(t+1)}(i) = A(\mathcal{C}')$ for $A \in \{\mathrm{T}, \mathrm{B}, \mathrm{R}\}$. Note that nails may appear or disappear when applying $\mathbf{T}_{j(t)}$ since extrema of clusters may move during the star-triangle transformations, which may alter the validity of the conditions of being a nail.

If $I_\bullet \subset I^{(t+1)}$, define $[\cdot]^{(t+1)}_{\bullet,0}$ and $[\cdot]^{(t+1)}_{\bullet,1}$ to be the multisets giving the homotopy classes in $\mathbb{R}^2 \setminus \{\mathcal{C}(\omega^{(t+1)}, i) : i \in I_\bullet \cap I^{(t+1)}\}$ of the loops surrounding at least two but not all marked nails. Otherwise, set $[\cdot]^{(t+1)}_{\bullet,0} = [\cdot]^{(t+1)}_{\bullet,1} = \emptyset$.

Set

$$\mathcal{H}^{(t+1)} := (I^{(t+1)}, \mathrm{T}^{(t+1)}, \mathrm{B}^{(t+1)}, \mathrm{R}^{(t+1)}, [\cdot]^{(t+1)}_{\bullet,0}, [\cdot]^{(t+1)}_{\bullet,1}).$$

From now on, call $\mathbf{P}$ the coupling thus obtained.

Remark II.6.2. Let us mention that a marked nail can disappear at some time t, meaning that some $i \in I_\bullet$ can be in $I^{(t)}$ but not in $I^{(t+1)}$, but no new marked nail may appear. The disappearance of a marked nail affects significantly the notion of homotopy and we stop keeping track of it (hence the convention of denoting $[\cdot]^{(t)}_{\bullet,0} = [\cdot]^{(t)}_{\bullet,1} = \emptyset$ and to consider it as an empty condition in (iii) of the definition of $\mathcal{H} = \mathcal{H}^{(t)}$). We will see that the condition (II.49) on our marked nails guarantees a posteriori that the marked nails do not disappear during the whole process with high probability. We will also see that $[\cdot]^{(t)}_{\bullet,0}$ and $[\cdot]^{(t)}_{\bullet,1}$ are preserved, and therefore equal to their values at time 0.

II.6.3 Controlling one single time step using IIC increments

In this section, we wish to connect our configurations $(\omega^{(t)} : 0 \leq t < T)$ with IIC measures in order to be able to control the displacements of the nails during the process. We therefore "decorate" our coupling by enhancing it with additional configurations sampled according to IIC measures.

Recall the lattice $\mathbb{L}^{(i)}$ with horizontal tracks of angle β except for t_i which has angle α. In this section, β is fixed to be $\pi/2$. Recall also the IIC measures Ⓣ_i, Ψ_i and Ⓡ defined on $\mathbb{L}^{(i)}$ and $\mathbb{L}^{(0)}$ respectively.

Let us give ourselves i.i.d. families of random variables $\omega^{(t)}_{A,j}$ indexed by $0 \leq t < T$, $j \in \mathbb{Z}$, and $A \in \{\mathrm{T}, \mathrm{B}, \mathrm{R}\}$, with laws Ⓣ_j, Ψ_j, and Ⓡ if $A = \mathrm{T}, \mathrm{B}, \mathrm{R}$ respectively (when $A = \mathrm{R}$ there is no need for a subscript j but we will use this convenient "unified" notation).

We also give ourselves independent $\{0,1\}$-valued random variables $X^{(t)}_H(i)$, indexed by all possible values $H = (I, \mathrm{T}, \mathrm{B}, \mathrm{R}, [\cdot]_{\bullet,0}, [\cdot]_{\bullet,1})$ of $\mathcal{H}^{(t)}$ and $i \in I$, satisfying

$$\mathbf{P}[X^{(t)}_H(i) = 1] = \phi_{\mathbb{L}^{(t)}}[(\mathrm{R}(i), h(t)) \in \mathcal{C}(\omega, i) \,|\, \mathcal{H} = H]$$

(it is possible that $(\mathrm{R}(i), h(t))$ is not a vertex of $\mathbb{L}^{(t)}$, in which case $X^{(t)}_H(i)$ is 0 almost surely). To get an intuition on these variables, in the coupling below, the fact that $X^{(t)}_{\mathcal{H}^{(t)}}(i)$ is equal to 1 will detect whether the cluster $\mathcal{C}(\omega, i)$ has a right extremum on $t^-_{j(t)}$.

We are now ready to define the coupling of the process $(\omega^{(t)} : 0 \leq t < T)$ with the random variables introduced above. Below, the steps 0 and $t + 1/2$ to $t + 1$ are done exactly as in the previous section. We therefore focus on the steps t to $t + 1/2$. We will sample $\omega^{(t+1/2)}$ from $\omega^{(t)}$ in a few steps, coupled to the variables introduced in the two last paragraphs. Nevertheless, notice that the law of $\omega^{(t+1/2)}$ given $\omega^{(t)}$ is the same as in the previous section. For this reason, we keep denoting this bigger coupling $\mathbf{P}$.

For $0 \leq t < T$ and a nail $\mathcal{C}$, call a vertex $x \in \mathbb{L}^{(t)}$ a

- *Top t-extremum* (of $\mathcal{C}$) if $x \in t^-_{j(t)} \cup t^-_{j(t)-1}$ and its second coordinate equals $\mathrm{T}(\mathcal{C})$,
- *Bottom t-extremum* (of $\mathcal{C}$) if $x \in t^-_{j(t)} \cup t^-_{j(t)+1}$ and its second coordinate equals $\mathrm{B}(\mathcal{C})$,
- *Right t-extremum* (of $\mathcal{C}$) if $x \in t^-_{j(t)}$ and its first coordinate equals $\mathrm{R}(\mathcal{C})$,
- *Fake right t-extremum* (of $\mathcal{C}$) if $x \in t^-_{j(t)}$, its first coordinate is strictly larger than $\mathrm{R}(\mathcal{C}) - \cos\alpha$, *and* the vertex of $\mathcal{C}$ with maximal first coordinate is *below* $b(t)$.

We also use *vertical t-extremum* to denote a top or bottom t-extremum.

Remark II.6.3. Note that for $A(\mathcal{C})$ to be possibly modified by the track-exchange, there must exist a A t-extremum or fake right t-extremum in the case $A = \mathrm{R}$.

Complete description of the coupling P from time t to $t+1/2$

Fix $0 \le t < T$ and assume that $I_\bullet$, $\omega^{(t)}$, and $\mathcal{H}^{(t)}$ have been defined. We divide the construction of $\omega^{(t+1/2)}$ in four cases; which case applies is determined by $\mathcal{H}^{(t)}$.

Case 0: Two distinct nails contain vertical t-extrema. In such case, sample $\omega^{(t+1/2)}$ as in previous section independently of the variables $\omega^{(t)}_{A,j}$ and $X^{(t)}_H$.

Case 1: A unique nail contains a vertical t-extremum and it is a top one. Let i be the index of this nail. Proceed as follows:

Step 1. Sample the random variable $\mathbf{x}$ in such a way that for every $x \in \mathbb{L}^{(t)}$,

$$\mathbf{P}[\mathbf{x} = x] = \phi_{\mathbb{L}^{(t)}}[\mathrm{lmax}(\mathcal{C}(\omega, i)) = x | \mathcal{H} = \mathcal{H}^{(t)}].$$

Step 2. Sample ω according to

$$\phi_{\mathbb{L}^{(t)}}[\,\cdot\,|\mathrm{lmax}(\mathcal{C}(\omega, i)) = \mathbf{x}, \mathcal{H} = \mathcal{H}^{(t)}]$$

and sample $\omega^{(t+1/2)} = \omega$ on the set $\Omega(\mathbf{x}, \omega)$ of edges outside of $\Lambda_{d(t)^{1/3}}(\mathbf{x})$ that are connected in ω to the complement of $\Lambda_{d(t)^{1/2}}(\mathbf{x})$ (see Figure II.25).

Step 3. Sample $(\omega^{(t+1/2)}, \omega^{\mathrm{T}}_{h(t)-T^{(t)}(i)})$ (for the first one we only need to sample the remaining edges) using the coupling between

$$\phi_{\mathbb{L}^{(t)}}[\,\cdot\,|\mathrm{lmax}(\mathcal{C}(\omega^{(t+1/2)}, i)) = \mathbf{x}, \mathcal{H} = \mathcal{H}^{(t)}, \omega^{(t+1/2)}_{|\Omega(\mathbf{x}, \omega^{(t+1/2)})}] \quad \text{and} \quad \mathfrak{M}_{j(t)-T^{(t)}(i)}$$

which is maximizing the probability that $\omega^{(t+1/2)}$ and the translate of $\omega^{(t)}_{\mathrm{T}, j(t)-T^{(t)}(i)}$ by $\mathbf{x}$ coincide on $\Lambda_{d(t)^{1/4}}(\mathbf{x})$.

Case 2: A unique nail contains a vertical t-extremum and it is a bottom one. Proceed exactly as in the previous step with B instead of T and Ψ instead of $\mathfrak{M}$.

Case 3: No nail contains a vertical t-extremum. Proceed as follows,

Step -1. Couple[a] in the best possible way the random variables

$$X^{(t)} := (X^{(t)}_{\mathcal{H}^{(t)}}(i) : i \in I^{(t)}) \qquad \text{and} \qquad \widetilde{X}^{(t)} = (\widetilde{X}^{(t)}(i) : i \in I^{(t)}),$$

where $\widetilde{X}^{(t)}$ has the law of the random variable $(\mathbf{1}[(\mathrm{R}(i), h(t)) \in \mathcal{C}(\omega, i)] : i \in I^{(t)})$ with $\omega \sim \phi_{\mathbb{L}^{(t)}}[\,\cdot\,|\mathcal{H} = \mathcal{H}^{(t)}]$.

Step 0. If $X^{(t)} \neq \widetilde{X}^{(t)}$ or $\sum_{i\in I^{(t)}} \widetilde{X}^{(t)}(i) \neq 1$, sample independently the random variables $\omega_{A,j}^{(t)}$ and the random variable

$$\omega^{(t+1/2)} \sim \phi_{\mathbb{L}^{(t)}}[\,\cdot\,|\mathcal{H} = \mathcal{H}^{(t)}, X = \widetilde{X}^{(t)}],$$

where the event $X = \widetilde{X}^{(t)}$ means that $(\mathrm{R}(i), h(t))$ belongs to the nail indexed by i if and only if $\widetilde{X}^{(t)}(i) = 1$.

Step 1. Otherwise, set $\mathbf{x} := (\mathrm{R}^{(t)}(i), h(t))$ with i the integer such that $\widetilde{X}^{(t)}(i) = 1$.

Step 2–3. Proceed as in Case 1 with R instead of T and $\nRightarrow$ instead of Φ, except that we further condition at each step on $X = \widetilde{X}^{(t)}$.

[a]Note that $X^{(t)}$ and $\widetilde{X}^{(t)}$ have the same marginal laws, but that in the former the random variables $X^{(t)}_{\mathcal{H}^{(t)}}(i)$ are independent, while in the latter they are not.

Remark II.6.4. We will see in the next section that Case 0 occurs very rarely, hence we do not bother coupling efficiently the true configuration with an IIC configuration in this case. In Step 3 of Case 1, it could be that the best coupling is terrible due to the fact that $\omega^{(t+1/2)}$ does something strange on $\Omega(\mathbf{x}, \omega^{(t+1/2)})$. Yet, this will be shown to occur with only small probability and the best coupling guarantees equality of the two configurations with very large probability. Finally, in Step 0 of Case 3, the best coupling (which depends on $\mathcal{H}^{(t)}$) is typically making the two random variables equal. We will see that in this case there is typically a single i for which $X^{(t)}(i) = 1$.

We now turn to an important proposition describing the increments $A^{(t+1)}(i) - A^{(t)}(i)$ for the nails $i \in I^{(t)}$ in terms of increments of IIC variables, called the *IIC displacement random variables*.

Definition II.6.5 (IIC displacements)**.** Sample a configuration according to Φ_j, apply $\mathbf{T}_j$, and call $\delta_j^{\mathrm{IIC}}\mathrm{T}$ the maximal y-coordinate of a vertex of the incipient infinite cluster after the transformation. Similarly, sample a configuration according to Ψ_j, apply $\mathbf{T}_j$, and call $\delta_j^{\mathrm{IIC}}\mathrm{B}$ the maximal y-coordinate of a vertex of the incipient infinite cluster after the transformation. Finally, sample a configuration according to $\nRightarrow$, apply $\mathbf{T}_0$, and call $\delta^{\mathrm{IIC}}\mathrm{R}$ the maximal x-coordinate of a vertex of the incipient infinite cluster after the transformation.

Remark II.6.6. The effect of a track exchange on the top and right of a cluster is described in Figures II.22 and II.23. Notice that $\delta_1^{\mathrm{IIC}}\mathrm{T} \in \{0, \sin\alpha\}$, $\delta_0^{\mathrm{IIC}}\mathrm{T} \in \{-1, \sin\alpha - 1\}$, and $\delta_j^{\mathrm{IIC}}\mathrm{T} = 0$ for other values of j. Similarly, $\delta_0^{\mathrm{IIC}}\mathrm{B} \in \{\sin\alpha, \sin\alpha - 1\}$, $\delta_{-1}^{\mathrm{IIC}}\mathrm{B} \in \{0, -1\}$, and $\delta_j^{\mathrm{IIC}}\mathrm{B} = 0$ for other values of j. For the right, note that $\delta^{\mathrm{IIC}}\mathrm{R} \in \{0, -1, \cos\alpha - 1, \cos\alpha\}$.

Remark II.6.7. The effect of a track exchange implies that $\mathrm{T}^{(t+1)}(i) - \mathrm{T}^{(t)}(i)$ and $\mathrm{B}^{(t+1)}(i) - \mathrm{B}^{(t)}(i)$ belong to $\{-1, \sin\alpha - 1, 0, \sin\alpha\}$. For $\mathrm{R}^{(t+1)}(i) - \mathrm{R}^{(t)}(i)$, the situation is more complicated since there may be a fake right t-extremum, whose coordinate is therefore not equal to $\mathrm{R}(\mathcal{C}(\omega^{(t+1/2)}, i))$, that jumps right and after the transformation has a first coordinate equal to $\mathrm{R}(\mathcal{C}(\omega^{(t+1)}, i))$. Nevertheless, one always has $|\mathrm{R}^{(t+1)}(i) - \mathrm{R}^{(t)}(i)| \leq 1$.

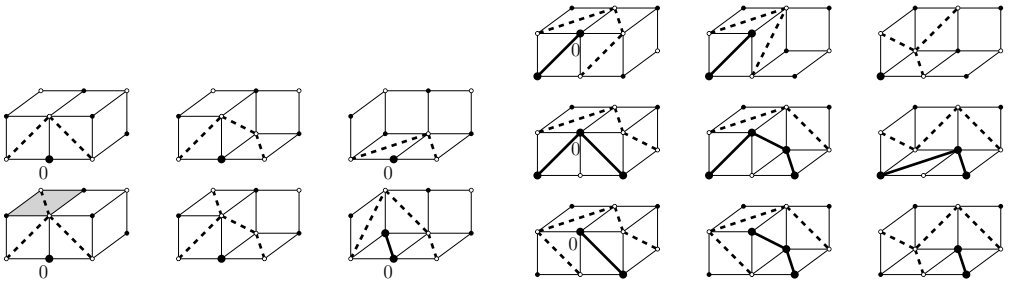

Figure II.22: Different environments around 0 picked according to the incipient infinite cluster measures with a track of angle α at height 1 (left) and 0 (right). The bold edges and points are part of the incipient infinite clusters. The different outcomes of the transformations give different top-most points for the infinite cluster. *Left two diagrams:* Two possible outcomes of the track-exchange $\mathbf{T}_1$ corresponding to $\delta_1^{\mathrm{IIC}}\mathrm{T} = 0$ and $\delta_1^{\mathrm{IIC}}\mathrm{T} = \sin\alpha$. The first outcome occurs certainly when the gray rhombus contains a primal edge, and with positive probability when it contains a dual one; in the latter case, the second outcome is also possible.
Right three diagrams: Three possible outcomes of the track-exchange $\mathbf{T}_0$ corresponding to $\delta_0^{\mathrm{IIC}}\mathrm{T} = -1$ and $\delta_0^{\mathrm{IIC}}\mathrm{T} = \sin\alpha - 1$, respectively. The first outcome occurs only when the edge below and to the left of 0 is the unique open edge adjacent to 0.

Let $\delta_j^{\mathrm{IIC}}A^{(t)}$ be the displacement constructed out of the IIC configuration $\omega_{A,j}^{(t)}$ by applying $\mathbf{T}_{j(t)}$. Note that the $\delta_j^{\mathrm{IIC}}A^{(t)}$ form families of i.i.d. random variables with law $\delta_j^{\mathrm{IIC}}A$. For $i \in I^{(t)}$, define the random variables

$$\begin{aligned}
\delta^{\mathrm{err}}\mathrm{T}^{(t)}(i) &:= \mathrm{T}^{(t+1)}(i) - \mathrm{T}^{(t)}(i) - \delta^{\mathrm{IIC}}_{h(t)-T^{(t)}(i)}\mathrm{T}^{(t)}(i),\\
\delta^{\mathrm{err}}\mathrm{B}^{(t)}(i) &:= \mathrm{B}^{(t+1)}(i) - \mathrm{B}^{(t)}(i) - \delta^{\mathrm{IIC}}_{h(t)-B^{(t)}(i)}\mathrm{B}^{(t)}(i),\\
\delta^{\mathrm{err}}\mathrm{R}^{(t)}(i) &:= \mathrm{R}^{(t+1)}(i) - \mathrm{R}^{(t)}(i) - X^{(t)}_{\mathcal{H}^{(t)}}(i)\,\delta^{\mathrm{IIC}}\mathrm{R}^{(t)}(i).
\end{aligned}$$

We are now ready to present the main statement of this section.

Proposition II.6.8 (Properties of the coupling)**.** *For $\varepsilon, \eta > 0$, the coupling $\mathbf{P}$ satisfies the following properties:*

(o) for every $0 \le t \le T$, $\omega^{(t)} \sim \phi_{\mathbb{L}^{(t)}}$;

(i) $([\cdot]^{(t)}_{\bullet,0}, [\cdot]^{(t)}_{\bullet,1}) = ([\cdot]^{(0)}_{\bullet,0}, [\cdot]^{(0)}_{\bullet,1})$ for every $t < \tau$, where $\tau := \inf\{t > 0 : I_\bullet \not\subset I^{(t)}\}$;

(ii) for every $t \ge 0$, the variables $(\delta_j^{\mathrm{err}}A^{(s)}(i), \delta_j^{\mathrm{IIC}}A^{(s)}(i), X_H^{(s)}(i) : A, i, j, H, s < t)$ are independent of the $(\delta_j^{\mathrm{IIC}}A^{(t)}(i), X_H^{(t)}(i) : A, i, j, H)$;

(iii) there exist $C, c \in (0, \infty)$ such that for every $t \ge 0$,

$$\mathbf{E}[\mathrm{Err}^{(t)}] \le \frac{C}{d(t)N^c},$$

where $\mathrm{Err}^{(t)} := \sum_{i \in I^{(t)}} M^{(t)}(i)$ with $M^{(t)}(i) := |\delta^{\mathrm{err}}\mathrm{T}^{(t)}(i)| + |\delta^{\mathrm{err}}\mathrm{B}^{(t)}(i)| + |\delta^{\mathrm{err}}\mathrm{R}^{(t)}(i)|$.

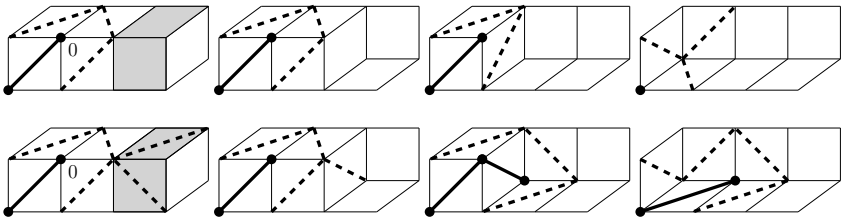

Figure II.23: When performing a track exchange between t_0 and t_{-1}, the vertex 0 is modified locally so that the coordinate of the right-most point in $t_0^- \cup t_{-1}^-$ moves by either -1 (first line) or $\cos\alpha$ (second line). The first outcome occurs certainly when both gray rhombi contain primal edges, and with positive probability otherwise; the second outcome may only occur when at least one of the two gray rhombi contains a dual edge. When the second outcome occurs, $\delta^{\mathrm{IIC}}\mathrm{R} = \cos\alpha$. For the first outcome, $\delta^{\mathrm{IIC}}\mathrm{R}$ may take values 0, $\cos\alpha - 1$, or -1. The first two values appear if the incipient infinite cluster contains a vertex below 0 with first coordinate 0, or one above 0, with first coordinate $\cos\alpha - 1$, respectively. The same outcomes occur for any environment in t_0 and t_{-1} to the left of 0.

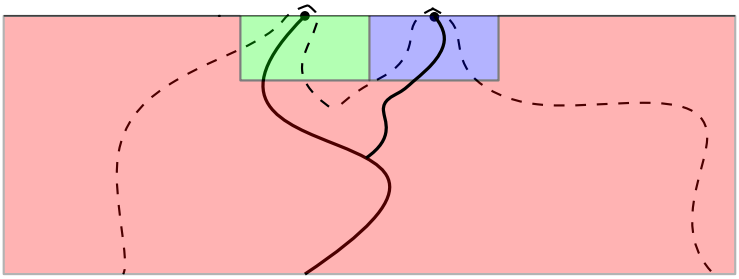

Figure II.24: We depicted the example of a nail having two top t-extrema.

Remark II.6.9. Let us mention that we expect the bound of (iii) to be valid with N^{1+c} instead of $d(t)N^c$ in the denominator. The reason for the appearance of $d(t)$ is due to the fact that we do not, at this stage, know how to prove (II.14) for generic sequences of angles $\boldsymbol{\alpha}$. In retrospect, our rotation invariance result shows that (II.14) does hold for arbitrary sequences, but only post factum.

The rest of the subsection is dedicated solely to proving Proposition II.6.8. This proof is tedious, but does not involve particularly innovative ideas (the heavy lifting was done when properly defining the coupling). In the first reading, one may skip the proof and focus on the next sections first.

Before diving into the proof of this proposition, let us start with a lemma. Define

$\mathrm{BAD}_1(t) := \{\text{a nail contains a vertical and a right } t\text{-extremum}\}$,

$\mathrm{BAD}_2(t) := \{\text{a nail contains two vertical } t\text{-extrema } x, y \text{ satisfying } |x-y| \geq d(t)^{1/5}\}$,

$\mathrm{BAD}_3(t) := \{\text{two nails contain a } t\text{-extremum}\}$,

$\mathrm{BAD}_4(t) := \{\text{a nail contains a fake right } t\text{-extremum}\}$,

$$\mathrm{BAD}_5(t) := \left\{ \begin{array}{c} \text{a nail } i \text{ contains a right } t\text{-extremum and a vertex } (x_1,x_2) \\ \text{with } \mathrm{R}^{(t)}(i)-1 < x_1 < \mathrm{R}^{(t)} \text{ and } |x_2 - h(t)| \geq d(t)^{1/5} \end{array} \right\}.$$

Lemma II.6.10. *There exist $C, c \in (0,\infty)$ such that for every $0 \leq t < T$ and $1 \leq i \leq 4$,*

$$\phi_{\mathbb{L}^{(t)}}[\mathrm{BAD}_i(t)] \leq \frac{C}{d(t)N^c}.$$

Proof. We divide into the different events $\mathrm{BAD}_i(t)$.

Bound on the probability of $\mathrm{BAD}_1(t)$. Assume that the vertical t-extremum is a top t-extremum (the bottom case is treated similarly) and let x be the right t-extremum of the nail. In this case, there must be a three-arm event in the bottom-left quarterplane translated by x, and going from $\Lambda_1(x)$ to $\partial\Lambda_{\varepsilon N}(x)$. We therefore deduce from (II.12) that the probability of this is bounded by $C/(\varepsilon N)^{2+c}$. Summing over $O(N)$ possible values of x – recall that since it is a right t-extremum, x is within a distance $\sqrt{\varepsilon\eta}N$ of one of the points in $\mathbb{B}_\eta(N)$ – gives the required bound.

Bound on the probability of $\mathrm{BAD}_2(t)$. In this case, the two t-extrema are either both in the top direction, or both in the bottom one (since $\mathrm{Vspan} \geq \varepsilon N > 1 + \sin\alpha$ for N large enough). Let us assume it is the former that happens and let x and y be the two t-extrema. We assume that x is on the left of y. Also, note that they have to be exactly at the same height as they belong to the same nail. The following must therefore occur (see Figure II.24 for a picture):

- a 3-arm event in the half-plane below x from x to $\partial\Lambda_{|x-y|/2}(x)$;
- a 3-arm event in the half-plane below y from y to $\partial\Lambda_{|x-y|/2}(y)$;
- a 3-arm event in the half-plane below x from $\Lambda_{2|x-y|}(x)$ to $\partial\Lambda_{\varepsilon N}(x)$ (this may be an empty condition if $|x-y| \geq \frac{1}{2}\varepsilon N$);
- a 1-arm event from $\Lambda_{\varepsilon N}(x)$ to Λ_N in $\mathbb{Z}\times[-N,N]$ (this last condition is only relevant in case $x \notin \Lambda_N$, which may occur since nails may be very long in the left direction, and have maxima far on the left of Λ_N – obviously, this is atypical, but should be taken care of nonetheless).

We deduce from (II.9) that

$$\phi_{\mathbb{L}^{(t)}}[x,y \text{ top } t\text{-extrema of the same nail}] \leq \frac{C}{|x-y|^4}\Big(\frac{|x-y|}{\varepsilon N}\Big)^2 \exp\big(-\frac{c|x|}{N}\big). \tag{II.50}$$

Summing over x and y at a distance $d(t)^{1/4}$ of each other (with y on the right of x and left of the right-side of Λ_N) gives that

$$\phi_{\mathbb{L}^{(t)}}[\mathrm{BAD}_2(t)] \leq \frac{C'}{\varepsilon^2 N d(t)^{1/4}}. \tag{II.51}$$

Bound on the probability of $\mathrm{BAD}_3(t)$**.** Assume that x and y are the right t-extrema of two different nails. The cases of the top or bottom t-extrema are actually simpler to handle (and they give better bounds).

First, assume that $|x-y| \le 2d(t)$ and that y is on the right of x. In this case, for x and y to be right t-extrema of their respective nails, there must be

- a 3-arm event in the half-plane on the left of x from x to $\partial\Lambda_{|x-y|/2}(x)$;
- a 3-arm event in the half-plane on the left of y from y to $\partial\Lambda_{|x-y|/2}(y)$;
- a 5-arm event in the half-plane on the left of y from $\Lambda_{2|x-y|}(y)$ to $\partial\Lambda_{d(t)}(y)$ (this may be an empty condition if $|x-y| \ge d(t)/2$);
- a 3-arm event[10] in the half-plane on the left of y from $\Lambda_{d(t)}(y)$ to $\partial\Lambda_{\varepsilon N/2}(y)$.

Using (II.14) (twice), (II.15), and (II.11), we deduce that

$$\phi_{\mathbb{L}^{(t)}}[x,y \text{ right } t\text{-extrema of distinct nails}] \le \frac{C}{|x-y|^4}\Big(\frac{|x-y|}{d(t)}\Big)^{2+c_0}\Big(\frac{2d(t)}{\varepsilon N}\Big)^{1+c_1}. \tag{II.52}$$

Now, assume $|x-y| > 2d(t)$ and assume that y is right of x. In this case, for x and y to be at the right-most ends of their respective nails, there must be

- a 3-arm event in the half-plane on the left of x from x to $\partial\Lambda_{d(t)}(x)$;
- a 3-arm event in the half-plane on the left of y from y to $\partial\Lambda_{d(t)}(y)$;
- a 3-arm event in the half-plane on the left of x from $\Lambda_{d(t)}(x)$ to $\partial\Lambda_{|x-y|/2}(x)$;
- a 3-arm event in the half-plane on the left of y from $\Lambda_{d(t)}(y)$ to $\partial\Lambda_{|x-y|/2}(y)$;
- a 3-arm event[11] in the half-plane on the left of y from $\Lambda_{2|x-y|}(y)$ to $\partial\Lambda_{\varepsilon N/2}(y)$ (this condition is empty if $|x-y| \ge \varepsilon N/4$).

Using (II.14) (twice) and (II.11) (three times), we deduce that

$$\phi_{\mathbb{L}^{(t)}}[x,y \text{ right } t\text{-extrema of distinct nails}] \le \frac{C}{d(t)^4}\Big(\frac{d(t)}{|x-y|}\Big)^{2+2c_1}\Big(\frac{2|x-y|}{\varepsilon N}\Big)^{1+c_1}. \tag{II.53}$$

Let us now sum on y and then on x to obtain

$$\begin{aligned}
&\phi_{\mathbb{L}^{(t)}}[\text{two distinct nails in } I^{(t)} \text{ contain a right } t\text{-extremum}]\\
&\quad\le 2CN\Big[\sum_{k=1}^{2d(t)}\frac{1}{k^4}\Big(\frac{k}{d(t)}\Big)^{2+c_0}\Big(\frac{d(t)}{\varepsilon N}\Big)^{1+c_1} + \sum_{k=2d(t)}^{2N}\frac{1}{d(t)^4}\Big(\frac{d(t)}{k}\Big)^{2+2c_1}\Big(\frac{k}{\varepsilon N}\Big)^{1+c_1}\Big]\\
&\quad\le \frac{C_1}{d(t)^{1+c_0}}\Big(\frac{d(t)}{\varepsilon N}\Big)^{c_1} + \frac{C_2}{d(t)^2}\Big(\frac{d(t)}{\varepsilon N}\Big)^{c_1} \le \frac{C_3}{d(t)(\varepsilon N)^{c_3}},
\end{aligned}$$

where we choose $c_3 := \min\{c_0, c_1\}$.

Doing the same with other types of t-extrema implies the bound for $\mathrm{BAD}_3(t)$.

[10] In fact even a 5-arm event occurs up to $\partial\Lambda_{\varepsilon N/2-|x-y|}(y)$. Also, once this is observed, one may wonder why we distinguish between the third and fourth bullets since in both cases a 5-arm event occurs. The reason comes from the fact that the estimate used in both cases is not quite the same, since one occurs in an area with all but one track having a transverse angle equal to $\frac{\pi}{2}$, while the second occurs in a "mixed" lattice.

[11] Again, there is even a 5-arm event up to $\partial\Lambda_{\varepsilon N/2-|x-y|}(y)$.

Bound on the probability of $\mathrm{BAD}_4(t)$**.** For x to be a fake right t-extremum of a nail $\mathcal{C}$, there must exist $y = (y_1, y_2) \in \mathcal{C}$ with $y_2 \le b(t)$ and $y_1 = \mathrm{R}(\mathcal{C})$. As a consequence, there must be

- a 3-arm event in the half-plane on the left of x from x to $\partial\Lambda_{d(t)/2}(x)$;
- a 3-arm event in the half-plane on the left of x from $\Lambda_{d(t)/2}(x)$ to $\partial\Lambda_{|x-y|/2}(x)$;
- a 3-arm event in the half-plane on the left of y from y to $\partial\Lambda_{|x-y|/2}(y)$;
- a 3-arm event in the half-plane on the left of y from $\Lambda_{2|x-y|}(y)$ to $\partial\Lambda_{\varepsilon N/2}(x)$.

If we denote $E(x,y)$ the previous event, we deduce that

$$\phi_{\mathbb{L}^{(t)}}[E(x,y)] \le \frac{C}{d(t)^2}\Big(\frac{d(t)}{|x-y|}\Big)^{1+c_1}\Big(\frac{2}{|x-y|}\Big)^{1+c_1}\Big(\frac{4|x-y|}{\varepsilon N}\Big)^{1+c_1}. \tag{II.54}$$

Summing over y and then over x gives,

$$\phi_{\mathbb{L}^{(t)}}[\mathrm{BAD}_4(t)] \le \sum_{x,y}\phi_{\mathbb{L}^{(t)}}[E(x,y)] \le \sum_x \frac{C}{d(t)}\frac{C_2}{N^{1+c_1}} \le \frac{C_3}{d(t)N^{c_1}}. \tag{II.55}$$

Bound on the probability of $\mathrm{BAD}_5(t)$**.** The bound follows from a combination of the arguments for $\mathrm{BAD}_2(t)$ and $\mathrm{BAD}_4(t)$. We leave it to the reader. □

Proof of Proposition II.6.8. By construction of the coupling, (o) and (ii) are trivial.

Property (i) follows from the locality of the star-triangle operations and the common way of measuring $([\cdot]^{(t)}_{\bullet,0}, [\cdot]^{(t)}_{\bullet,1})$. Indeed, since $[\cdot]^{(t-1)}_{\bullet,0} = [\cdot]^{(t-1/2)}_{\bullet,0}$ by definition of $\omega^{(t-1/2)}$, it suffices to check that $[\cdot]^{(t-1/2)}_{\bullet,0} = [\cdot]^{(t)}_{\bullet,0}$. Now, $I_\bullet \subset I^{(s)}$ for every $s \le t$ so there are nails near every $x \in \mathbb{B}_\eta(N)$. Recall the definition of oriented edges (x,y) from Section II.5.1. Since the star-triangle transformations modify the lowest right-most point of marked nails of $\omega^{(t-1/2)}$, but do so only locally, while preserving the connections outside of $t^-_{j(t)}$, we immediately get that the reduced words are not modified by the track-exchange, and therefore $[\cdot]^{(t-1/2)}_{\bullet,0} = [\cdot]^{(t)}_{\bullet,0}$.

We therefore focus on proving (iii). We divide the analysis of $\mathrm{Err}^{(t)}$ depending on the case used for the coupling. Below, constants c_i, C_i are universal and independent of everything else except ε and η.

Error in Case 0 If Case 0 holds, then $\omega^{(t)} \in \mathrm{BAD}_3(t)$. Due to the coupling generated by the track-exchange, the displacement of any t-extremum is at most 1 so all variables $\delta^{\mathrm{err}}A^{(t)}(i)$ are deterministically bounded by 2. Thus, Markov's inequality implies that for every $\lambda \ge 0$,

$$\mathbf{E}[\mathrm{Err}^{(t)}\mathbf{1}_{\text{Case 0}}] \le 6\mathbf{E}[|I^{(t)}|\mathbf{1}_{\omega^{(t)}\in\mathrm{BAD}_3(t)}] \le 6\lambda\mathbf{P}[\omega^{(t)} \in \mathrm{BAD}_3(t)] + 6\mathbf{P}[|I^{(t)}| > \lambda].$$

Lemma II.6.10 and Proposition II.3.7 imply that by choosing λ to be a large multiple of $\log N$, we obtain

$$\mathbf{E}[\mathrm{Err}^{(t)}\mathbf{1}_{\text{Case 0}}] \le \frac{C_2}{d(t)N^{c_2}}.$$

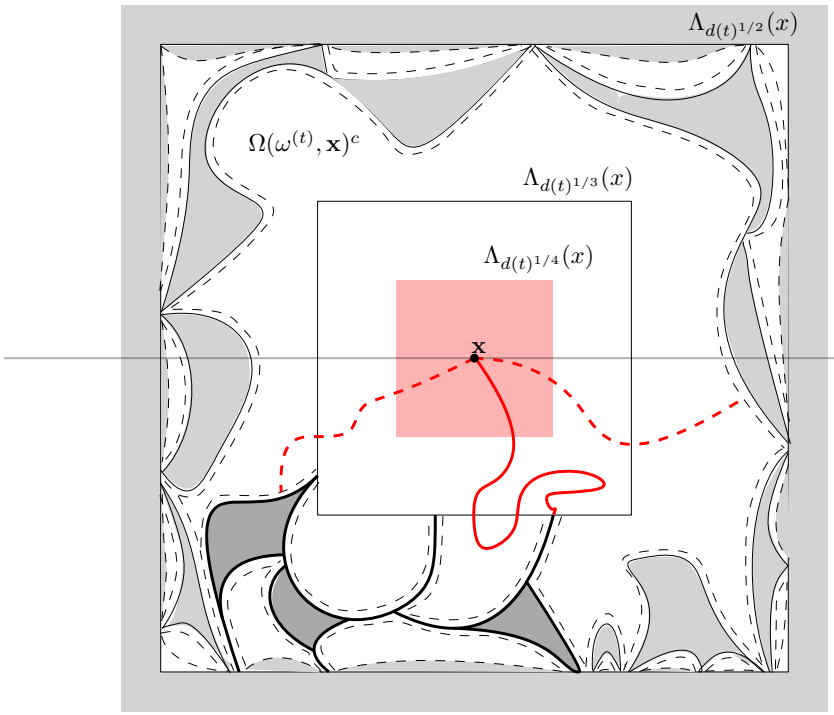

Figure II.25: A picture of the set $\Omega(\omega^{(t+1/2)}, x)$ (in grey). The dark grey cluster is the unique cluster of the annulus crossing from inside to outside. Everything outside $\Lambda_{d(t)^{1/2}}(x)$ is included in $\Omega(\omega^{(t+1/2)}, x)$. The red part is the place where we try to couple as best as possible $\omega^{(t+1/2)}$ and $\mathbf{x} + \omega^{(t)}_{\mathrm{T}, j(t)-T^{(t)}(i)}$. In the proof of Proposition II.6.8, note that when applied to $\omega^{(t+1/2)} \in E(x)$ (which means that there exists a unique cluster crossing the annulus), all the conditions on the t-extrema of other nails and homotopy classes of loops are not impacted by what happens inside $\Omega(\omega^{(t+1/2)}, \mathbf{x})^c$. As a consequence, there is a "screening" property and the conditioning inside is simply the existence of the red arms, meaning that $\mathbf{x}$ is equal to the left-most top-most vertex in the cluster that is crossing the annulus.

Error in Cases 1 and 2 We deal with Case 1 as Case 2 can be treated in the same way. Since $\mathbf{x}$ can take values $x \in S^{(t)}$ only, and that by (II.9),

$$\phi_{\mathbb{L}^{(t)}}[\mathrm{lmax}(\mathcal{C}(\omega, i)) = x, \mathbf{x} = x, \mathcal{H} = \mathcal{H}^{(t)}] \leq \frac{C_3}{N^2} \exp[-c_3 \tfrac{|x|}{N}], \tag{II.56}$$

(as in the bound of the probability of $\mathrm{BAD}_2(t)$, we need to account for the possibility that x is far on the left of Λ_N), it suffices to show that

$$\mathbf{P}[\mathrm{Err}^{(t)} \neq 0 | \omega^{(t+1/2)} \in \{\mathrm{lmax}(\mathcal{C}(\omega, i)) = x, \mathbf{x} = x, \mathcal{H} = \mathcal{H}^{(t)}\}]$$

is small and to plug it in (II.56) above. Then, summing over x and applying a manipulation similar to Case 0 will conclude the proof.

For (A, i) in $\{(\mathrm{B}, i), i\} \cup \{(\mathrm{T}, i), i \neq \mathbf{i}\}$, with $\mathbf{i}$ the unique integer such that $\mathcal{C}(\omega, \mathbf{i})$ contains a top t-extremum, we immediately find that

$$\delta^{\mathrm{err}} A^{(t)}(i) = A^{(t+1)}(i) - A^{(t)}(i) = \delta^{\mathrm{IIC}} A^{(t)}(i) = 0.$$

Therefore, the errors can only come from the evolution of $\mathrm{T}^{(t)}(\mathbf{i})$ and the $\mathrm{R}^{(t)}(i)$ for $i \in I^{(t)}$. We treat the case $A = \mathrm{T}$ and $A = \mathrm{R}$ separately.

Below, we fix x and set $\omega^{\mathrm{T}} := \omega^{(\mathrm{T})}_{h(t) - \mathrm{T}^{(t)}(i)}$.

Error from the top t-extremum We start with $|\delta^{\mathrm{err}} \mathrm{T}^{(t)}(\mathbf{i})|$, which can come from a number of facts (see Figure II.26):

(i) $\omega^{(t+1/2)}$ and $x + \omega^{\mathrm{T}}$ are not equal on $\Lambda_{d(t)^{1/4}}(x)$;
(ii) there is another top t-extremum in $\mathcal{C}(\omega^{(t+1/2)}, \mathbf{i})$ at a distance at least $d(t)^{1/5}$ of x;
(iii) there are two top t-extrema in ω^{T} at a distance at least $d(t)^{1/5}$ of each other.
(iv) $\omega^{(t+1/2)}$ and $x + \omega^{\mathrm{T}}$ are equal on $\Lambda_{d(t)^{1/4}}(x)$ but the track-exchange operators outputs on $\Lambda_{d(t)^{1/5}}(x)$ are different in $\omega^{(t+1/2)}$ and ω^{T};

Indeed, if none of (i)–(iv) occurs, then (i) gives that $\omega^{(t+1/2)}$ and $x + \omega^{\mathrm{T}}$ coincide on $\Lambda_{d(t)^{1/4}}(x)$, (iv) guarantees that the result of the track-exchange output is the same in $\Lambda_{d(t)^{1/5}}(x)$. Finally, the absence of other top t-extrema in either $\omega^{(t+1/2)}$ and ω^T guarantees that the change of height is measured by what happens within $\Lambda_{d(t)^{1/5}}(x)$.

Subcase (i). Let $E(x)$ be the event that there is a unique cluster in $\omega^{(t+1/2)}$ crossing the annulus $\Lambda_{d(t)^{1/2}}(x) \setminus \Lambda_{d(t)^{1/3}}(x)$ from outside to inside. Note that this event is measurable in terms of $\omega^{(t+1/2)}$ restricted to $\Omega(x, \omega^{(t+1/2)})$. Furthermore, observe that this event has a "screening effect" (see Figure II.25) implying

$$\phi_{\mathbb{L}^{(t)}}[\,\cdot\,|\mathrm{lmax}(\mathcal{C}(\omega, \mathbf{i})) = x, \mathbf{x} = x, \mathcal{H} = \mathcal{H}^{(t)}, \omega^{(t+1/2)}_{|\Omega(x, \omega^{(t+1/2)})}] = \phi^{\xi}_{\Omega(x, \omega^{(t+1/2)})^c}[\,\cdot\,|\mathrm{lmax}(\mathcal{C}) = x],$$

where ξ are the boundary conditions induced by $\omega^{(t+1/2)}$ on the graph $\mathbb{L}^{(t)} \setminus \Omega(x, \omega^{(t+1/2)})$, and $\mathcal{C}$ is the unique cluster crossing the annulus $\Lambda_{d(t)^{1/2}}(x) \setminus \Lambda_{d(t)^{1/3}}(x)$.

Therefore, the mixing property of the IIC given by Proposition II.3.9 implies that on $\omega^{(t+1/2)} \in E(x)$, the coupling does not give equality with probability at most $C_3 d(t)^{-c_3}$. Combined with (II.56) (and using $|\delta^{\mathrm{err}}\mathrm{T}^{(t)}| \leq 2$), we deduce that

$$\begin{aligned}
&\mathbf{E}[|\delta^{\mathrm{err}}\mathrm{T}^{(t)}(\mathbf{i})|\mathbf{1}_{(i),\mathrm{lmax}(\mathcal{C}(\omega^{(t+1/2)},\mathbf{i}))=x}] \\
&\leq \frac{2C_3}{d(t)^{c_3}}\mathbf{P}[\mathrm{lmax}(\mathcal{C}(\omega^{(t+1/2)},\mathbf{i})) = x] + 2\mathbf{P}[\mathrm{lmax}(\mathcal{C}(\omega^{(t+1/2)},\mathbf{i})) = x, \omega^{(t+1/2)} \notin E(x)] \\
&\leq \frac{C_4}{N^2 d(t)^{c_4}} \exp[-c|x|/N],
\end{aligned}$$

where in the last inequality we used (II.9) and (II.13).

Subcase (ii). In this case, $\omega^{(t+1/2)}$ belongs to $\mathrm{BAD}_2(t)$ so Lemma II.6.10 gives

$$\mathbf{E}[|\delta^{\mathrm{err}}\mathrm{T}^{(t)}(\mathbf{i})|\mathbf{1}_{(ii)}] \leq 2\phi_{\mathbb{L}^{(t)}}[\mathrm{BAD}_2(t)] \leq \frac{C_5}{d(t)N^{c_5}}$$

(we directly provided the estimate summed over x in this case as it follows from the statement of Lemma II.6.10).

Subcase (iii). First, since by construction ω^{T} is independent of the event $\omega^{(t+1/2)} \in \{\mathrm{lmax}(\mathcal{C}(\omega, i)) = x, \mathbf{x} = x, \mathcal{H} = \mathcal{H}^{(t)}\}$, it suffices to prove that

$$\mathbf{P}[\omega^{\mathrm{T}} \text{ contains a top } t\text{-extremum outside } \Lambda_{d(t)^{1/5}}] \leq \frac{C_6}{d(t)^{1/4}}.$$

To see this, simply sum over $y \in \mathbb{Z} \setminus \Lambda_{d(t)^{1/4}}$ the probability of y being a top t-extremum, which can easily be proved to be of order $C_7/|y|^2$. We conclude that

$$\mathbf{P}[|\delta^{\mathrm{err}}\mathrm{T}^{(t)}(\mathbf{i})|\mathbf{1}_{(iii),\mathrm{lmax}(\mathcal{C}(\omega^{(t+1/2)},\mathbf{i}))=x}] \leq \frac{C_8}{N^2 d(t)^{1/4}} \exp[-c|x|/N].$$

Subcase (iv). To be in this case, it must be that in the intersection of the annulus $\Lambda_{d(t)^{1/4}}(x) \setminus \Lambda_{d(t)^{1/5}}(x)$ with $t^-_{j(t)} \cup t^-_{j(t)-1}$ on the left and the right of x, there is no pair of closed edges on top of each other since the existence of such edges decouple the star-triangle transformations on their left and right as seen in the paragraph above Definition II.3.11. We deduce that

$$\mathbf{E}[|\delta^{\mathrm{err}}\mathrm{T}^{(t)}(\mathbf{i})|\mathbf{1}_{(iv),\mathrm{lmax}(\mathbf{i})=x}] \leq \frac{C_8 \exp[-c_8 d(t)^{1/4}]}{N^2} \exp[-c|x|/N].$$

Error from the right t-extrema On the one hand, there can exist $i \in I^{(t)}$ such that $\mathrm{R}^{(t+1)}(i) \neq \mathrm{R}^{(t)}(i)$. Yet, this can occur only when some $\mathcal{C}(\omega^{(t+1/2)}, i)$ contains a right t-extremum, i.e. when $\omega^{(t+1/2)} \in \mathrm{BAD}_1(t) \cup \mathrm{BAD}_3(t)$. On the other hand, there can exist i such that $X^{(t)}_{\mathcal{H}^{(t)}}(i) = 1$ and $\delta^{\mathrm{IIC}}\mathrm{R}^{(t)}(i) \neq 0$. Yet, the probability that $X^{(t)}_{\mathcal{H}^{(t)}}(i) = 1$ is such that

$$\mathbf{P}[X^{(t)}_{\mathcal{H}^{(t)}}(i) = 1|\mathcal{H}^{(t)}] \leq \mathbf{P}[\omega^{(t+1/2)} \in \mathrm{BAD}_1(t) \cup \mathrm{BAD}_3(t)|\mathcal{H}^{(t)}].$$

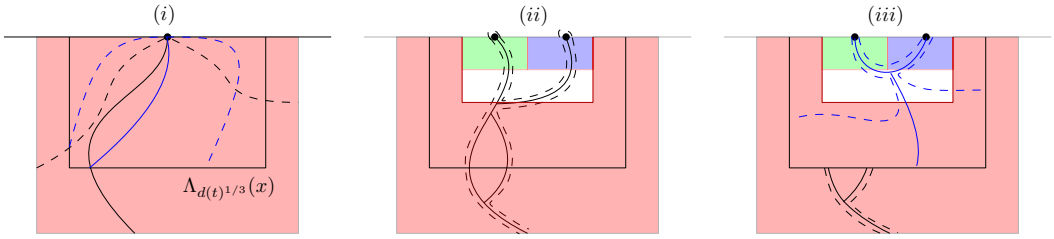

Figure II.26: The different cases zoomed at a distance $d(t)^{1/2}$ around $\mathbf{x}$. The configuration $\omega^{(t+1/2)}$ is depicted in black, and $\mathbf{x}+\omega^{(t)}_{\mathrm{T},j}$ in blue.

By proceeding in the same way as in Case 0, and using Lemma II.6.10, we deduce that

$$\mathbf{E}\Big[\Big(\sum_{i\in I^{(t)}}|\delta^{\mathrm{err}}\mathrm{R}^{(t)}(i)|\Big)\mathbf{1}_{\text{Case 1}}\Big]\leq 2\mathbf{E}[|I^{(t)}|\mathbf{1}_{\omega^{(t+1/2)}\in \mathrm{BAD}_1(t)\cup\mathrm{BAD}_3(t)}]\leq \frac{C_9}{d(t)N^{c_9}}$$

(again here we directly give the summed error as it is provided by Lemma II.6.10).

Error in Case 3 In Case 3, no error is made for T and B, and we only need to control the error due to movements of $\mathrm{R}^{(t)}(i)$. Also, the error strictly after Step 0 can be treated in exactly the same way as in Case 1. Indeed, any such error either implies the occurrence of $\mathrm{BAD}_5(t)$ or is generated by the configuration in the box of size $d(t)$ around $\mathbf{x}$, in which case we use (II.14) instead of (II.9) as for Case 1.

The only new type of errors we need to control are those in Case 0, and they are of three types:

(i) $X^{(t)}$ and $\widetilde{X}^{(t)}$ do not couple,
(ii) $X^{(t)}=\widetilde{X}^{(t)}$ but there is no i with $\widetilde{X}^{(t)}(i)=1$,
(iii) $X^{(t)}=\widetilde{X}^{(t)}$ but there are two i with $\widetilde{X}^{(t)}(i)=1$.

We divide our analysis between the different cases.

Subcase (i). For every $i\in I^{(t)}$, $X^{(t)}(i)$ and $\widetilde{X}^{(t)}(i)$ have the same law. Using the inclusion-exclusion principle, we see that for the best coupling between the two random variables, we have that

$$\mathbf{P}[X^{(t)}(i)\neq\widetilde{X}^{(t)}(i)|\mathcal{H}^{(t)}]\leq C_{13}\mathbf{P}[|\widetilde{X}^{(t)}|\geq 2|\mathcal{H}^{(t)}].$$

Yet, using an argument similar to Case 2, we find that

$$\begin{aligned}\mathbf{E}\Big[\mathrm{Err}^{(t)}\mathbf{1}_{\text{Case 2},X^{(t)}\neq\widetilde{X}^{(t)}}\Big]&\leq 2\mathbf{E}[|I^{(t)}|\mathbf{1}(X^{(t)}\neq\widetilde{X}^{(t)})]\\&\leq 2C_{13}\mathbf{E}[|I^{(t)}|\mathbf{1}(|\widetilde{X}^{(t)}|\geq 2)]\\&=2C_{13}\mathbf{E}[|I^{(t)}|\mathbf{1}(\omega^{(t+1/2)}\in\mathrm{BAD}_3(t))]\end{aligned}$$

(the last equality is due to the fact that $\omega^{(t+1/2)}\in\{X=\widetilde{X}^{(t)}\}$). Then, we conclude using Lemma II.6.10 as before.

Subcase (ii). In this case, $\delta^{\mathrm{IIC}}\mathrm{R}^{(t)}(i) = 0$ for every $i \in I^{(t)}$. Yet, for $\mathrm{R}^{(t+1)}(i)$ to be different from $\mathrm{R}^{(t)}(i)$, it must be that $\mathcal{C}(\omega^{(t+1/2)}, i)$ contains a fake right t-extremum (as it does not contain a right t-extremum on the event $X = \widetilde{X}^{(t)}$). Therefore, $\omega^{(t+1/2)}$ must contain a fake right t-extremum, i.e. that $\omega^{(t+1/2)} \in \mathrm{BAD}_4(t)$. We deduce the result from Lemma II.6.10.

Subcase (iii). In this case, $\omega^{(t+1/2)}$ must contain two right t-extrema. Therefore, $\omega^{(t+1/2)} \in \mathrm{BAD}_3(t)$ again and the proof follows from Lemma II.6.10 and an argument similar to Case 0. □

II.6.4 Compounded time steps

We now group steps into so-called *compounded time steps* corresponding to the action of a single track going down from its initial position to its final one. More precisely, for $0 \le k < \lceil 2N/\sin\alpha \rceil$ we study the steps $t \in [\tau_k, \tau_{k+1})$, where $\tau_k := 2kN$ (it will be important that the time steps correspond to the action of the same track of angle α, here the $(k+1)$-st one) to be pushed down.

First, introduce the *speeds* of the IIC in each direction, a notion which will be useful in the next sections. Note that the definition below does not immediately seem to be connected to the speed of a process. We will see later that it will in fact correspond to the speed (or "drift") of extrema of nails when bringing tracks down.

Definition II.6.11 (Speed in each direction)**.** Define

$$v_{\mathrm{T}} := \sin\alpha - \frac{\mathbf{P}[\delta_1^{\mathrm{IIC}}\mathrm{T} = 0]}{\mathbf{P}[\delta_0^{\mathrm{IIC}}\mathrm{T} = \sin\alpha - 1]} \qquad v_{\mathrm{B}} := \sin\alpha - \frac{\mathbf{P}[\delta_0^{\mathrm{IIC}}\mathrm{B} = \sin\alpha - 1]}{\mathbb{P}[\delta_{-1}^{\mathrm{IIC}}\mathrm{B} = 0]},$$

$$v_{\mathrm{R}} := \frac{\mathbf{E}[\delta^{\mathrm{IIC}}\mathrm{R}]}{\mathbf{P}[\delta^{\mathrm{IIC}}\mathrm{R} \in \{0, -1\}]}.$$

For $i \in I^{(\tau_k)}$, introduce the random time at which i ceases to be the index of a nail:

$$\tau_{\mathrm{end}}(i) := \min\{s : i \notin I^{(s)}\}$$

(it is equal to T if such an s does not exist). Let $\mathcal{F}_k$ be the σ-algebra containing all the variables

$$(\omega^{(s)} : s \le \tau_k)\ ,\ (\omega^{(s+1/2)} : s < \tau_k)\ ,\ (X_H^{(s)}(i) : s < \tau_k)\ ,\ (\delta_j^{\mathrm{IIC}} A^{(s)}(i) : s < \tau_k).$$

Recall the definition of $M^{(s)}(i)$ from the previous section.

Proposition II.6.12 (Compounded time step for $A = \mathrm{T}$ or B)**.** *There exist $c, C \in (0, \infty)$ such that for $A \in \{\mathrm{T}, \mathrm{B}\}$, $i \in \mathbb{Z}_{>0}$, $0 \le k < \lceil 2N/\sin\alpha \rceil$, there exist random variables $\Delta^{\mathrm{IIC}} A^{(k)}(i)$ and $\Delta^{\mathrm{err}} A^{(k)}(i)$ such that a.s. for every $i \in I^{(\tau_k)}$,*

(i) $A^{(\tau_{\mathrm{end}} \wedge \tau_{k+1})}(i) - A^{(\tau_k)}(i) = \Delta^{\mathrm{IIC}} A^{(k)}(i) + \Delta^{\mathrm{err}} A^{(k)}(i)$;

(ii) $\mathbf{E}[\exp(c|\Delta^{\mathrm{IIC}} A^{(k)}(i)|)|\mathcal{F}_k] \le C$;

(iii) $\mathbf{E}[|\Delta^{\mathrm{err}} A^{(k)}(i)|\,|\mathcal{F}_k] \le C\,\mathbf{E}\Big[\sum_{s=\tau_k}^{\tau_{\mathrm{end}} \wedge \tau_{k+1}} M^{(s)}(i) \Big| \mathcal{F}_k\Big]$;

(iv) $\mathbf{E}[\Delta^{\mathrm{IIC}} A^{(k)}(i)|\mathcal{F}_k] = \begin{cases} 0 & \text{if } A^{(\tau_k)}(i) \le b(\tau_k), \\ v_A + O(e^{-c|A^{(\tau_k)}(i)-b(\tau_k)|} + \mathbf{P}[\tau_{\mathrm{end}} < \tau_{k+1}|\mathcal{F}_k]) & \text{otherwise.} \end{cases}$

Remark II.6.13. The $O(\cdot)$ quantity in (iv) comes from the fact that there are two types of errors: the first term comes from cases where $A^{(\tau_k)}(i)$ is close to the bottom $b(\tau_k)$ in which case the process described in the next proof could be stopped because the track reaches its final position, and the second from the fact that the nail i can cease to be indexed during the interval $[\tau_k, \tau_{k+1})$.

Proof. We treat the case of $A = \mathrm{T}$. The case of B is similar. In the whole proof, fix k and $i \in I^{(\tau_k)}$. To lighten the notation we omit i in the notation.

Case 1 $\mathrm{T}^{(\tau_k)} \le b(\tau_k)$**.** In this case, the coupling $\mathbf{P}$ is such that $\mathrm{T}^{(\tau_{\mathrm{end}} \wedge \tau_{k+1})} - \mathrm{T}^{(\tau_k)} = 0$ so we may define

$$\Delta^{\mathrm{IIC}} \mathrm{T}^{(k)} = \Delta^{\mathrm{err}} \mathrm{T}^{(k)} := 0.$$

Case 2 $\mathrm{T}^{(\tau_k)} > b(\tau_k)$**.** We first describe how a track-exchange at time $\tau_k \le s < \tau_{k+1}$ modifies the value of $\mathrm{T}^{(s)}$. There are three possibilities:

- $\mathrm{T}^{(s)} \notin \{h(s) - 1, h(s)\}$, in which case $\mathrm{T}^{(s)}$ is not altered;
- $\mathrm{T}^{(s)} = h(s) - 1$ which happens exactly once. In this case, T may either stay put or increase by $\sin\alpha$. In the former case, T is not altered by subsequent steps and in the latter $\mathrm{T}^{(s+1)} = h(s+1)$;
- $\mathrm{T}^{(s)} = h(s)$, which implies that either $T^{(s-1)} = h(s-1)$ and the track-exchange "dragged down" the top of the nail, or $\mathrm{T}^{(s-1)} = h(s-1) - 1$ but the track-exchange failed to increase the top. In this case, $\mathrm{T}^{(s)}$ may either increase by $\sin\alpha - 1$ in which case it will not move at subsequent steps, or decrease by -1, in which case $\mathrm{T}^{(s+1)} = h(s+1)$.

From the previous discussion, we find

$$\mathrm{T}^{(\tau_{\mathrm{end}} \wedge \tau_{k+1})} - \mathrm{T}^{(\tau_k)} = \sin\alpha - (\sigma - \tau), \tag{II.57}$$

where τ is the first (and unique) time for which $\mathrm{T}^{(\tau)} = h(\tau) - 1$ and σ is the time defined by

$$\sigma := \begin{cases} \tau & \text{if } \mathrm{T}^{(\tau+1)} = \mathrm{T}^{(\tau)} + \sin\alpha, \\ \inf\{s \in (\tau, \tau_{\mathrm{end}} \wedge \tau_{k+1}) : \mathrm{T}^{(s+1)} - \mathrm{T}^{(s)} \neq -1\} & \text{if } \mathrm{T}^{(\tau+1)} = \mathrm{T}^{(\tau)} \text{ and } s \text{ exists}, \\ \tau_{\mathrm{end}} \wedge \tau_{k+1} & \text{otherwise.} \end{cases}$$

To define $\Delta^{\mathrm{IIC}}\mathrm{T}$, we use a similar formula except that we consider the random variables $\delta_j^{\mathrm{IIC}} \mathrm{T}^{(s)}$ instead of the true increments:

$$\Delta^{\mathrm{IIC}} \mathrm{T}^{(k)} := \sin\alpha - (\sigma^{\mathrm{IIC}} - \tau), \tag{II.58}$$

where

$$\sigma^{\mathrm{IIC}} := \begin{cases} \tau & \text{if } \delta_1^{\mathrm{IIC}} \mathrm{T}^{(\tau)} = \sin\alpha, \\ \inf\{s \in (\tau, \tau_{\mathrm{end}} \wedge \tau_{k+1}) : \delta_0^{\mathrm{IIC}} \mathrm{T}^{(s)} \neq -1\} & \text{if } \delta_1^{\mathrm{IIC}} \mathrm{T}^{(\tau)} = 0 \text{ and such an } s \text{ exists}, \\ \tau_{\mathrm{end}} \wedge \tau_{k+1} & \text{otherwise} \end{cases}$$

(note that τ_{end} is still a function of the true increments).

Finally, we set

$$\Delta^{\mathrm{err}}\mathrm{T}^{(k)} := \sigma^{\mathrm{IIC}} - \sigma. \tag{II.59}$$

We are now in a position to derive our proposition. First, (i) is satisfied by construction and (II.57)–(II.59). The definition of σ^{IIC} from independent "trial" events immediately leads to (ii). For (iv), we have that

$$\begin{aligned}\mathbf{E}[\Delta^{\mathrm{IIC}}\mathrm{T}^{(k)}|\mathcal{F}_k] &= \sin\alpha - \mathbf{E}[\sigma^{\mathrm{IIC}} - \tau|\mathcal{F}_k] \\ &= \sin\alpha - \frac{\mathbf{P}[\delta_1^{\mathrm{IIC}}\mathrm{T} = 0]}{1 - \mathbf{P}[\delta_0^{\mathrm{IIC}}\mathrm{T} = -1]} + O(e^{-c|\mathrm{T}^{(t)} - b(t)|} + \mathbf{P}[\tau_{\mathrm{end}} < \tau_{k+1}|\mathcal{F}_k]),\end{aligned}$$

where the error term comes from the fact that σ^{IIC} can be equal to $\tau_{\mathrm{end}} \wedge \tau_{k+1}$. More precisely, when $\tau_{\mathrm{end}} \geq \tau_{k+1}$, we obtain the first error since $\tau_{k+1} - \tau \geq \mathrm{T}^{(t)} - b(t)$ and the difference is a geometric random variable, and when $\tau_{\mathrm{end}} < \tau_{k+1}$, we obtain the second term in the $O(\cdot)$.

It only remains to prove (iii), i.e. to bound $\mathbf{E}[|\sigma^{\mathrm{IIC}} - \sigma|\,|\mathcal{F}_k]$. In order to do it, introduce further random times defined recursively by $\sigma_0^{\mathrm{IIC}} = \sigma^{\mathrm{IIC}}$ and

$$\sigma_{\ell+1}^{\mathrm{IIC}} := \inf\{s \in (\sigma_\ell^{\mathrm{IIC}}, \tau_{\mathrm{end}}) : \delta_0^{\mathrm{IIC}}\mathrm{T}^{(s)} \neq -1\}$$

when s exists and $\sigma_{\ell+1}^{\mathrm{IIC}} = \tau_{\mathrm{end}} \wedge \tau_{k+1}$ otherwise (note that for ℓ large enough, the sequence becomes stationary at $\tau_{\mathrm{end}} \wedge \tau_{k+1}$, which is compatible with the formula below). We have

$$\sigma^{\mathrm{IIC}} - \sigma = \sum_{\tau \leq s \leq \sigma^{\mathrm{IIC}}} \mathbf{1}_{s>\sigma} - \sum_{\ell \geq 0} \sum_{s=\sigma_\ell^{\mathrm{IIC}}+1}^{\sigma_{\ell+1}^{\mathrm{IIC}}} \mathbf{1}_{s \leq \sigma}.$$

Now, let $\mathbf{X}$ denote the sum of the $|\delta^{\mathrm{err}}\mathrm{T}^{(s)}|$ for $s \in [\tau, \tau_{\mathrm{end}} \wedge \tau_{k+1}]$. On the one hand, for $\tau \leq s \leq \sigma^{\mathrm{IIC}}$ to satisfy $s > \sigma$, it must be that $\delta^{\mathrm{err}}\mathrm{T}^{(r)} \neq 0$ for some $r \in [\tau, s)$ and that $\delta_0^{\mathrm{IIC}}\mathrm{T}^{(r')} = -1$ for every $r' \in (r, s)$. Independence provided by Proposition II.6.8(ii) implies that

$$\begin{aligned}&\mathbf{E}\Big[\sum_{\tau \leq s \leq \sigma^{\mathrm{IIC}}} \mathbf{1}_{s>\sigma}\big|\mathcal{F}_k\Big] \\ &\quad\leq \sum_{s \geq r \geq \tau} \mathbf{P}[\forall r' \in (\tau, r), \delta^{\mathrm{err}}\mathrm{T}^{(r')} = 0; \delta^{\mathrm{err}}\mathrm{T}^{(r)} \neq 0; \forall s' \in (r, s), \delta_0^{\mathrm{IIC}}\mathrm{T}^{(s')} = -1|\mathcal{F}_k] \\ &\quad\leq \frac{\mathbf{P}[\mathbf{X} \geq \sin\alpha|\mathcal{F}_k]}{\mathbf{P}[\delta_0^{\mathrm{IIC}}\mathrm{T} = \sin\alpha - 1]}.\end{aligned}$$

On the other hand, for $\sigma_\ell^{\mathrm{IIC}} < s \leq \sigma_{\ell+1}^{\mathrm{IIC}}$ to be smaller than σ, it must be that $\delta^{\mathrm{err}}\mathrm{T}^{(\sigma_l^{\mathrm{IIC}})} = -\sin\alpha$ for every $0 \leq l \leq \ell$, and that $\delta_0^{\mathrm{IIC}}\mathrm{T}^{(r)} = -1$ for every $r \in [\sigma_\ell^{\mathrm{IIC}}, s]$ so that by independence of the variables $\delta_0^{\mathrm{IIC}}\mathrm{T}^{(r)}$ for $r > \sigma_\ell^{\mathrm{IIC}}$ and $\delta^{\mathrm{err}}\mathrm{T}^{(\sigma_l^{\mathrm{IIC}})}$ for $l \leq \ell$, we get in a fairly similar fashion to the previous displayed equation that

$$\begin{aligned}\mathbf{P}\Big[\sum_{s=\sigma_\ell^{\mathrm{IIC}}+1}^{\sigma_{\ell+1}^{\mathrm{IIC}}} \mathbf{1}_{s \leq \sigma}\big|\mathcal{F}_k\Big] &\leq \sum_{j \geq 0} \mathbf{P}[\delta_0^{\mathrm{IIC}}\mathrm{T} = -1]^j \mathbf{P}[\mathbf{X} \geq \ell \sin\alpha|\mathcal{F}_k] \\ &\leq C\,\mathbf{P}[\mathbf{X} \geq \ell \sin\alpha|\mathcal{F}_k].\end{aligned}$$

The claim follows by summing over ℓ. □

We now treat the impact of compounded steps on R.

Proposition II.6.14 (Compounded time step for $A = \mathrm{R}$)**.** *There exist $c, C \in (0,\infty)$ such that for $i \in \mathbb{Z}_{>0}$ and $0 \le k < \lceil 2N/\sin\alpha \rceil$, there exist random variables $\Delta^{\mathrm{IIC}}\mathrm{R}^{(k)}(i)$ and $\Delta^{\mathrm{err}}\mathrm{R}^{(k)}(i)$ such that a.s. for every $i \in I^{(\tau_k)}$,*

(i) $\mathrm{R}^{(\tau_{\mathrm{end}}\wedge\tau_{k+1})}(i) - \mathrm{R}^{(\tau_k)}(i) = \Delta^{\mathrm{IIC}}\mathrm{R}^{(k)}(i) + \Delta^{\mathrm{err}}\mathrm{R}^{(k)}(i)$*;*

(ii) $\mathbf{E}[\exp(c|\Delta^{\mathrm{IIC}}\mathrm{R}^{(k)}(i)|)|\mathcal{F}_k] \le C$*;*

(iii) $\mathbf{E}[|\Delta^{\mathrm{err}}\mathrm{R}^{(k)}(i)|\,|\mathcal{F}_k] \le C\mathbf{E}\Big[\sum_{s=t}^{\tau_{\mathrm{end}}\wedge\tau_{k+1}} M^{(s)}(i)\big|\mathcal{F}_k\Big]$*;*

(iv) $\mathbf{E}[\Delta^{\mathrm{IIC}}\mathrm{R}^{(k)}(i)|\mathcal{F}_k]$ *is equal to*

$$\begin{cases} 0 & \text{if } \mathrm{R}^{(\tau_k)}(i) \notin k\cos\alpha + \mathbb{Z}, \\ v_{\mathrm{R}} + O\Big(\mathbf{E}\Big[\sum_{s=\tau_k}^{\tau_{\mathrm{end}}\wedge\tau_{k+1}} M^{(s)}(i)\big|\mathcal{F}_k\Big] + \mathbf{P}[\tau_{\mathrm{end}} < \tau_{k+1}|\mathcal{F}_k]\Big) & \text{otherwise.} \end{cases}$$

Remark II.6.15. When $\cos\alpha \notin \mathbb{Q}$, the condition $\mathrm{R}^{(\tau_k)} \notin k\cos\alpha + \mathbb{Z}$ implies that no right-most vertex can belong to the area below the $(k+1)$-st track. The information on R therefore gives more than simply the first-coordinate of the right-most point, it also provides information on its vertical position. This is not necessary true for rational values of $\cos\alpha$. In this case, one should therefore record this information more explicitly. We chose to restrict ourselves to α with $\cos\alpha$ irrational as we will see it is sufficient to get our result.

Proof. Again, we fix k and i and drop i from the notation. We first describe how a track-exchange for $\tau_k \le s < \tau_{k+1}$ modifies the value of $\mathrm{R}^{(s)}$. There are three possibilities:

- $\mathrm{R}^{(s)} \in k\cos\alpha + \mathbb{Z}$ and $(\mathrm{R}^{(s)}, h(s))$ does not belong to the nail $\mathcal{C}(\omega^{(s)}, i)$, in such case $\mathrm{R}^{(s+1)} = \mathrm{R}^{(s)}$,
- $\mathrm{R}^{(s)} \in k\cos\alpha + \mathbb{Z}$ and $(\mathrm{R}^{(s)}, h(s))$ belongs to the cluster. In such case, the track-exchange creates a change of $\cos\alpha$, $\cos\alpha - 1$, or -1 (see Figure II.23). In the former case, $\mathrm{R}^{(s+1)} = \mathrm{R}^{(s)} + \cos\alpha$ and the next track-exchanges will not impact the maximum. In the latter, $\mathrm{R}^{(s)}$ can change by values in $[-1,0] \cap (\mathbb{Z} + \{0,\dots,k-2,k-1,k+1\}\cos\alpha)$ due to the possible existence of other vertices that are not affected by the track-exchange but had almost-maximal first coordinate[12].
- $\mathrm{R}^{(s)} \notin k\cos\alpha + \mathbb{Z}$. In such a case, there is only one possibility for $\mathrm{R}^{(s+1)}$ not to be equal to $\mathrm{R}^{(s)}$, which is that there exists a fake right s-extremum and that the track-exchange implies an increase of $\cos\alpha$ locally, which leads to $\mathrm{R}^{(s+1)} = x_1 + \cos\alpha$ and no further change can occur.

[12] In fact, essentially the only other two values that are possible are 0 if there is another extremum of the cluster in the square region below $t^-_{j(s)}$, or $\cos\alpha - 1$ if there is a "near" extremum in the square region above height $h(s)$ that becomes the right-most point after the transformation. For the increment to be different from 0, $\cos\alpha - 1$ or -1, it must be that $\mathcal{C}(\omega^{(s)}, i)$ contains a vertex below $b(t)$ with first coordinate in $(\mathrm{R}^{(s)} - 1, \mathrm{R}^{(s)})$, which has small probability as shown in Lemma II.6.10.

Now, recall the definition of $X_H^{(s)} = X_H^{(s)}(i)$ from the previous section, and introduce

$$\Delta^{\mathrm{IIC}}\mathrm{R}^{(k)} := \sum_{\tau_k \le s \le \sigma^{\mathrm{IIC}}} X^{(s)}_{\mathcal{H}^{(s)}} \delta^{\mathrm{IIC}}\mathrm{R}^{(s)},$$

where

$$\sigma^{\mathrm{IIC}} := \begin{cases} \min\{s \in [\tau_k, \tau_{\mathrm{end}} \wedge \tau_{k+1}) : \delta^{\mathrm{IIC}}\mathrm{R}^{(s)} \in \{\cos\alpha, \cos\alpha - 1\} \text{ and } X^{(s)}_{\mathcal{H}^{(s)}} = 1\} & \text{if } s \text{ exists,} \\ \tau_{\mathrm{end}} \wedge \tau_{k+1} & \text{otherwise,} \end{cases}$$

and

$$\Delta^{\mathrm{err}}\mathrm{R}^{(k)} := \mathrm{R}^{(\tau_{\mathrm{end}} \wedge \tau_{k+1})} - \mathrm{R}^{(\tau_k)} - \Delta^{\mathrm{IIC}}\mathrm{R}^{(k)}\,.$$

By definition, (i) and (ii) are satisfied. The proof of (iii) follows the same steps as the proof of (iii) in Proposition II.6.12 (we leave the details to the reader), except in the case corresponding to the third bullet above, i.e. that $\mathrm{R}^{(s)} \notin k\cos\alpha + \mathbb{Z}$ but $\mathrm{R}^{(s+1)} \neq \mathrm{R}^{(s)}$. Yet, in this case $M^{(s)} \neq 0$ and no further error is made at later times.

For (iv), note that if $R^{(\tau_k)} \notin k\cos\alpha + \mathbb{Z}$, then $X^{(s)}_{\mathcal{H}^{(s)}}$ is always equal to 0 and $\Delta^{\mathrm{IIC}}\mathrm{R} = 0$. If, on the contrary, $R^{(\tau_k)} \in k\cos\alpha + \mathbb{Z}$, define

$$\widetilde{\sigma}^{\mathrm{IIC}} := \min\{s \ge \tau_k : \delta^{\mathrm{IIC}}\mathrm{R}^{(s)} \in \{\cos\alpha, \cos\alpha - 1\} \text{ and } Y^{(s)} = 1\},$$

where $Y^{(s)} = X^{(s)}_{\mathcal{H}^{(s)}}$ for $s \le \tau_{\mathrm{end}} \wedge \tau_{k+1}$ and 1 for $s > \tau_{\mathrm{end}} \wedge \tau_{k+1}$. Also define $\widetilde{\Delta}^{\mathrm{IIC}}\mathrm{R}^{(k)}$ using the same formulas as for $\Delta^{\mathrm{IIC}}\mathrm{R}^{(k)}$ but with $\widetilde{\sigma}^{\mathrm{IIC}}$ instead of σ^{IIC}. Then, a direct computation gives

$$\mathbf{E}[\widetilde{\Delta}^{\mathrm{IIC}}\mathrm{R}^{(k)}|\mathcal{F}_k] = v_{\mathrm{R}}.$$

Moreover,

$$\begin{aligned} |\mathbf{E}[\Delta^{\mathrm{IIC}}\mathrm{R}^{(k)}|\mathcal{F}_k] - v_{\mathrm{R}}| &\le \mathbf{E}[\widetilde{\sigma}^{\mathrm{IIC}} - \sigma^{\mathrm{IIC}}|\mathcal{F}_k] \le C_0\mathbf{P}[\widetilde{\sigma}^{\mathrm{IIC}} \neq \sigma^{\mathrm{IIC}}|\mathcal{F}_k] \\ &\le C_0\mathbf{P}[\forall s \le \tau_{\mathrm{end}} \wedge \tau_{k+1} : X^{(s)}_{\mathcal{H}^{(s)}} = 1, \delta^{\mathrm{IIC}}R^{(s)} = -1|\mathcal{F}_k]. \end{aligned}$$

To estimate the probability on the right, observe that if $\tau_{\mathrm{end}} \ge \tau_{k+1}$ and $\delta^{\mathrm{IIC}}R^{(s)} = -1$ for every s such that $X^{(s)}_{\mathcal{H}^{(s)}} = 1$, it must be that $M^{(s)} \neq 0$ for at least one s since otherwise $\mathrm{R}^{(\tau_{k+1})} \in \mathrm{R}^{(\tau_k)} + \mathbb{Z}$, which is impossible. We therefore obtain that

$$\begin{aligned} &\mathbf{P}[\forall s \le \tau_{\mathrm{end}} \wedge \tau_{k+1} : X^{(s)}_{\mathcal{H}^{(s)}} = 1, \delta^{\mathrm{IIC}}R^{(s)} = -1|\mathcal{F}_k] \\ &\qquad\qquad \le \mathbf{P}[\tau_{\mathrm{end}} < \tau_{k+1}|\mathcal{F}_k] + \mathbf{E}\Big[\sum_{s=\tau_k}^{\tau_{\mathrm{end}}\wedge\tau_{k+1}} M^{(s)}\Big|\mathcal{F}_k\Big]. \end{aligned}$$

This concludes the proof of the proposition. □

II.6.5 Speed of the drift

In this section, we compute v_A for $A = \mathrm{T}, \mathrm{B}, \mathrm{R}$. We start with the first two.

Proposition II.6.16. *We have* $v_{\mathrm{T}} = v_{\mathrm{B}} = 0$.

Proof. We treat the case of v_{T} (the case of v_{B} is the same). Introduce $\mathbf{l}_N := \mathrm{lmax}((0,-N))$ (i.e. the left-most highest vertex in the cluster of $(0,-N)$) and let $\mathbf{E}$ be the coupling between $\omega_1 \sim \phi_{\mathbb{L}_1}$ and $\omega_0 \sim \phi_{\mathbb{L}_0}$ obtained by setting $\omega_0 = \mathbf{T}_1(\omega_1)$. Also, let $\Delta\mathrm{T}$ be the difference between the top height of the cluster of $(0,-N)$ in ω_1 and in ω_0.

We find that

$$\begin{aligned}\phi_{\mathbb{L}_0}[\mathbf{l}_N \in t_1^-] &= \mathbf{P}[\mathbf{l}_N \in t_1^- \text{ in } \omega_0] \\ &= \mathbf{P}[\mathbf{l}_N \in t_1^- \text{ in } \omega_1 \text{ and } \Delta\mathrm{T} = \sin\alpha - 1] + \mathbf{P}[\mathbf{l}_N \in t_0^- \text{ in } \omega_1 \text{ and } \Delta\mathrm{T} = \sin\alpha] \\ &= \phi_{\mathbb{L}_1}[\mathbf{l}_N \in t_1^-]\mathbf{P}[\delta_0^{\mathrm{IIC}} = \sin\alpha - 1] + \phi_{\mathbb{L}_1}[\mathbf{l}_N \in t_0^-]\mathbf{P}[\delta_1^{\mathrm{IIC}} = \sin\alpha] + o_N(1),\end{aligned} \tag{II.60}$$

where in the second step we used that we may couple the increment $\Delta\mathrm{T}$ with an IIC increment exactly as we did in the previous section (to estimate the error, one needs to perform a reasoning similar to the error in the top extremum in Case 1 of the coupling).

Using the same coupling, we also see that $\mathbf{l}_N \in t_0^- \cup t_1^-$ in ω_0 if and only if it does in ω_1, so we get that

$$\phi_{\mathbb{L}_0}[\mathbf{l}_N \in t_0^- \cup t_1^-] = \phi_{\mathbb{L}_1}[\mathbf{l}_N \in t_0^- \cup t_1^-]. \tag{II.61}$$

Decomposing on the possible values of $\mathbf{l}_N$ (like in the proof of Proposition II.2.6) and using the mixing of the IIC (Proposition II.3.9), we also find that for $i = 0, 1$,

$$\phi_{\mathbb{L}_i}[\mathbf{l}_N \in t_1^- | \mathbf{l}_N \in t_0^- \cup t_1^-] = \mathfrak{M}_i^2[\mathrm{lmax}(\infty) = 0^+] + o_N(1). \tag{II.62}$$

Dividing (II.60) by (II.61) and plugging (II.62) into it, we find that

$$\begin{aligned}&\mathfrak{M}_0^2[\mathrm{lmax}(\infty) = 0^+] \\ &\quad = \mathfrak{M}_1^2[\mathrm{lmax}(\infty) = 0^+]\mathbf{P}[\delta_0^{\mathrm{IIC}} = \sin\alpha - 1] + \mathfrak{M}_1^2[\mathrm{lmax}(\infty) = 0]\mathbf{P}[\delta_1^{\mathrm{IIC}} = \sin\alpha].\end{aligned} \tag{II.63}$$

Theorem II.2.4 applied to $\beta = \frac{\pi}{2}$ gives

$$\mathfrak{M}_0^2[\mathrm{lmax}(\infty) = 0^+] = \mathfrak{M}_1^2[\mathrm{lmax}(\infty) = 0] = 1 - \mathfrak{M}_1^2[\mathrm{lmax}(\infty) = 0^+] = \frac{1}{1+\sin\alpha},$$

which, when inserted in (II.63) and multiplied by $1 + \sin\alpha$, gives $v_{\mathrm{T}} = 0$. □

Next, we turn to the lateral speed v_{R}, whose value is deduced from the one of v_{T}.

Proposition II.6.17. *We have* $v_{\mathrm{R}} = 0$.

The idea of the proof is to obtain the right displacement of the cluster as the top displacement in a rotated version of the process. Below, we mention not only horizontal tracks but also vertical tracks and their track-exchanges. We believe that at this point the reader may easily make sense of these transformations so we omit the details of the definitions. Also, we refer to [DCLM18] for more information.

Proof. We refer to Figure II.27 for an illustration. Consider M and N two integers satisfying $M = N^2$. Consider the graph $\mathbb{B}^{(0)}$ formed of $2M+2$ "horizontal" tracks $t_{-M}, \dots, t_M, t_\alpha$ of transverse angles $\pi/2$ for the first $2M+1$ and transverse angle

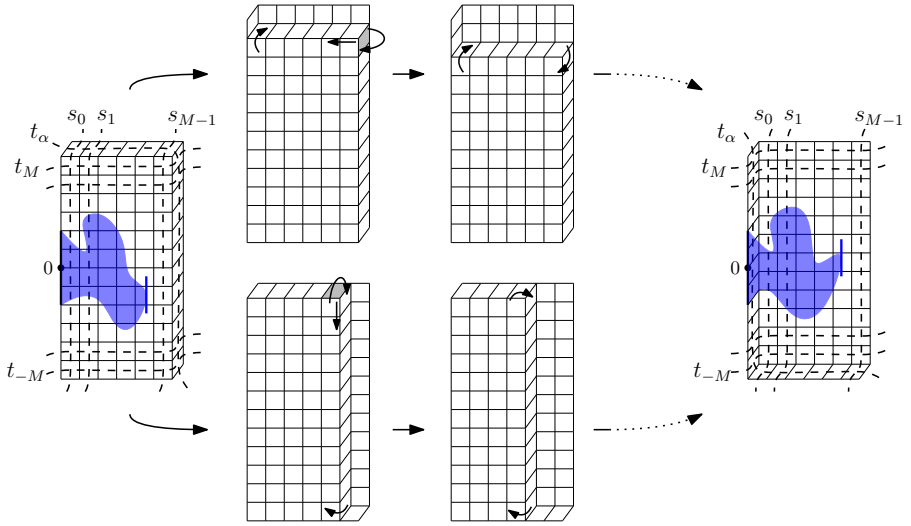

Figure II.27: The initial and final graphs $\mathbb{B}^{(0)}$ and $\mathbb{B}^{(2M+1)}$ of the two processes are the same, but the intermediate graphs $(\mathbb{B}^{(t)})_{0<t\leq 2M}$ (top) and $(\widetilde{\mathbb{B}}^{(t)})_{0<t<M}$ (bottom) are different (the figure depicts the diamond graphs). In the top process, horizontal tracks are exchanged successively, by pushing the gray rhombus from right to left; in the bottom process, the rhombus is pushed downwards, effectively exchanging vertical tracks. Throughout the two processes, we record the right-most coordinate of the union of all the clusters intersecting the base.

α for t_α and M "vertical" tracks $s_0, \dots, s_{M-1}$ of transverse angle 0. In addition to the intersection between the vertical and horizontal tracks, $\mathbb{B}^{(0)}$ contains also the intersection of tracks $t_{-M}, \dots, t_M$ with t_α; these occur at the right side of the graph (note that t_α is not straight and does a sharp turn at the top-right corner of the rectangle). Translate $\mathbb{B}^{(0)}$ so that 0 is the vertex left of s_0 and below t_0.

We perform track-exchanges via star-triangle transformations applied to the graph $\mathbb{B}^{(0)}$. Contrary to the other parts of the paper, where exchanged tracks change name, here the tracks will conserve their indexing during track-exchanges. Define recursively $\mathbb{B}^{(t+1)}$ for $0 \leq t \leq 2M$ as obtained from $\mathbb{B}^{(t)}$ by performing the track-exchange $\mathbf{T}_{M-t}$ between t_{M-t} and t_α which is a composition of M star-triangle transformations.

We follow the extrema of the set $\mathcal{C}_{\text{base}}$ obtained as the union of the primal clusters intersecting the *base* $\{0\} \times [-N, N]$. Let $(\omega^{(t)}, \mathrm{R}^{(t)})_{0\leq t\leq 2M+1}$ be obtained as follows:

- the initial step is defined by sampling $\omega^{(0)}$ according to $\phi^0_{\mathbb{B}^{(0)}}$ and setting $\mathrm{R}^{(0)}$ to be the maximal first coordinate of vertices in $\mathcal{C}_{\text{base}}$;
- at time $0 \leq t \leq 2M$, sample a configuration

$$\omega^{(t+1/2)} \sim \phi^0_{\mathbb{B}^{(t)}}[\,\cdot\,|\mathrm{R}(\mathcal{C}_{\text{base}}) = \mathrm{R}^{(t)}],$$

  let $\omega^{(t+1)} := \mathbf{T}_{M-t}(\omega^{(t)})$, and set $\mathrm{R}^{(t+1)}$ to be the maximal first coordinate of a vertex in $\mathcal{C}_{\text{base}}$.

Following the proofs of the previous sections (with some additional simplifications in this context, for instance τ_{end} does not need to be introduced) we find that

$$\mathrm{R}^{(2M+1)} - \mathrm{R}^{(0)} = \Delta^{\mathrm{IIC}}\mathrm{R} + \Delta^{\mathrm{err}}\mathrm{R}, \tag{II.64}$$

with the equivalent of (iii) and (iv) of Proposition II.6.14 being that a.s.,

$$\mathbf{E}[|\Delta^{\mathrm{err}}\mathrm{R}|\,|\mathcal{F}_0] \le C\,\mathbf{E}\Big[\sum_{t=0}^{2M} \mathrm{Err}^{(t)}\big|\mathcal{F}_0\Big],$$

$$\mathbf{E}[\Delta^{\mathrm{IIC}}\mathrm{R}|\mathcal{F}_0] = v_{\mathrm{R}} + O\Big(\mathbf{E}\Big[\sum_{t=0}^{2M} \mathrm{Err}^{(t)}\big|\mathcal{F}_0\Big]\Big),$$

where $\mathrm{Err}^{(t)}$ is defined in a similar fashion to Proposition II.6.14, but with $\mathcal{C}_{\text{base}}$ playing the role of the union of the nails now.

Let $h(t)$ be the height of the bottom of t_α at time t, $d(t) := \min\{M - h(t), h(t) + M\}$. Following an argument similar to the proof of Proposition II.6.8, the mistake contributing to $\mathrm{Err}^{(t)}$ can be of three types:

- (i) $(\mathrm{R}^{(t)}, h(t)) \in \mathcal{C}_{\text{base}}$ and $\mathrm{R}^{(t)} \le \sqrt{N}$,
- (ii) $(\mathrm{R}^{(t)}, h(t)) \in \mathcal{C}_{\text{base}}$ and $\mathrm{R}^{(t)} \ge M - \sqrt{N}$,
- (iii) $(\mathrm{R}^{(t)}, h(t)) \in \mathcal{C}_{\text{base}}$ and $\sqrt{N} \le \mathrm{R}^{(t)} \le M - \sqrt{N}$, but the true configuration and the IIC configurations are not coupled in the box of radius $\min\{d(t), N\}^{1/4}$ around $(\mathrm{R}^{(t)}, h(t))$,
- (iv) $(\mathrm{R}^{(t)}, h(t)) \in \mathcal{C}_{\text{base}}$ and there is a vertex $x = (x_1, x_2) \in \mathcal{C}_{\text{base}}$ with $x_1 \in (\mathrm{R}^{(t)} - 1, \mathrm{R}^{(t)}]$ and $|x_2 - h(t)| \ge d(t)^{1/5}$.

Recalling that the error is deterministically bounded by 2, we therefore have that

$$\mathbf{E}[\mathrm{Err}^{(t)}] \le 2(\mathbf{P}[(i)] + \mathbf{P}[(ii)] + \mathbf{P}[(iii)] + \mathbf{P}[(iv)]). \tag{II.65}$$

We now bound the probabilities of the events (i), (ii), and (iii) separately. For (i), (RSW) immediately implies the existence of $c > 0$ such that for every $0 \le t \le 2M$,

$$\mathbf{P}[(i)] = \phi^0_{\mathbb{B}^{(t)}}[(i)] \le \phi^0_{\mathbb{B}^{(t)}}[\mathrm{R}^{(t)} \le \sqrt{N}] \le \exp[-c\sqrt{N}].$$

To estimate (ii) and (iii), let us first estimate, for $x \in t^+_{M-t}$, the probability of the event $E(x)$ that $(\mathrm{R}^{(t)}, h(t)) = x$ and base $\longleftrightarrow x$. Let $s(x)$ be the distance between x and $\partial\mathbb{B}^{(t)}$. We have that

$$\phi^0_{\mathbb{B}^{(t)}}[E(x)] \le \phi_{\mathbb{B}^{(t)}}\Big[\{\text{base} \longleftrightarrow \partial\Lambda_{d(t)}(x)\} \cap A^{\mathrm{R}}_{010,x}(s(x), \tfrac{d(t)}{2}) \cap A^{\mathrm{R}}_{010,x}(0, \tfrac{s(x)}{2})\Big], \tag{II.66}$$

where $A^{\mathrm{R}}_{010,x}(r, R)$ is the translate of $A^{\mathrm{R}}_{010}(r, R)$ by x. Using the mixing property, (RSW) for the first event on the right-hand side, an argument similar to (II.11) for the third, and (II.14) for the fourth, we obtain that

$$\phi^0_{\mathbb{B}^{(t)}}[E(x)] \le C\big(\frac{N}{\max\{N, |x|\}}\big)^c \times \big(\frac{d(t)}{|x|}\big)^c \times \big(\frac{s(x)}{d(t)}\big)^{1+c} \times \big(\frac{1}{s(x)}\big)^2.$$

Summing over the $x \in t^+_{M-t}$ that are at a distance at most $\sqrt{N}$ from the right-hand side of $\mathbb{B}^{(t)}$, we obtain that

$$\mathbf{P}[(ii)] = \phi^0_{\mathbb{B}^{(t)}}[(ii)] \leq C\big(\frac{N}{M}\big)^{2c} \times \frac{1}{d(t)}. \tag{II.67}$$

For (iii), using the same argument as in Proposition II.6.8 in the first step and summing over x in the second

$$\mathbf{P}[(iii)] \leq \frac{C}{\min\{d(t), N\}^c} \sum_{x \in t^+_{M-t}} \phi^0_{\mathbb{B}^{(t)}}[E(x)] \leq \frac{C}{\min\{d(t), N\}^c} \times \frac{1}{M^c d(t)^{1-c}}. \tag{II.68}$$

The bound on (iv) can be obtained as in Lemma II.6.10:

$$\mathbf{P}[(iv)] \leq \frac{C}{d(t)M^c}. \tag{II.69}$$

Plugging (II.66)–(II.69) into (II.65) gives

$$\mathbf{E}[\mathrm{Err}^{(t)}] = O\big(\exp(-c\sqrt{N}) + \frac{1}{d(t)}\big(\frac{N}{M}\big)^{2c} + \frac{1}{\min\{d(t), N\}^c d(t)^{1-c} M^c} + \frac{1}{d(t)M^c}\big). \tag{II.70}$$

When summing over t and using that $M = N^2$, we deduce that

$$\mathbf{E}\Big[\sum_t \mathrm{Err}^{(t)}\Big] = O(N^{-c}).$$

Overall, we find that

$$\mathbf{E}[\mathrm{R}^{(2M+1)}] - \mathbf{E}[\mathrm{R}^{(0)}] = \mathbf{E}[\Delta^{\mathrm{err}}\mathrm{R}] + \mathbf{E}[\Delta^{\mathrm{IIC}}\mathrm{R}] = v_{\mathrm{R}} + O(N^{-c}).$$

Now, define a similar sequence of graphs $\widetilde{\mathbb{B}}^{(t)}$ for $0 \leq t \leq M$ by setting $\widetilde{\mathbb{B}}^{(0)} = \mathbb{B}^{(0)}$ and obtaining $\widetilde{\mathbb{B}}^{(t+1)}$ from $\widetilde{\mathbb{B}}^{(t)}$ by performing the track-exchange between s_{M-1-t} and t_α. Also, define a Markov chain $(\widetilde{\mathrm{R}}^{(t)})_{0 \leq t \leq M}$ as before. Following again the same reasoning as in the previous sections, and observing that the behaviour of $\widetilde{\mathrm{R}}^{(t)}$ under the track-exchange of vertical tracks is the same as the behaviour of the top of a cluster when exchanging horizontal tracks, we obtain using a reasoning similar to Propositions II.6.12 and II.6.8 (with the same adaptation as above) that

$$\mathbf{E}[\widetilde{\mathrm{R}}^{(M)}] - \mathbf{E}[\widetilde{\mathrm{R}}^{(0)}] = v_{\mathrm{T}} + O(N^{-c}) + O(\phi^0_{\mathbb{B}^{(0)}}[e^{-c|\mathrm{R}^{(0)}|}]) = v_{\mathrm{T}} + O(N^{-c})$$

(in the second equality we used (II.66)). Here v_{T} refers to passing a track with transverse angle $\alpha + \pi/2$, or equivalently $\pi/2 - \alpha$ by symmetry.

By definition, $\mathrm{R}^{(0)}$ and $\widetilde{\mathrm{R}}^{(0)}$ have the same law. Observe that $\mathbb{B}^{(2M+1)} = \widetilde{\mathbb{B}}^{(M)}$ and since our transformations ensure that the random-cluster law is preserved, $\widetilde{\mathrm{R}}^{(M)}$ has the same law as $\mathrm{R}^{(2M+1)}$. Thus,

$$v_{\mathrm{R}} = v_{\mathrm{T}} + O(N^{-c}) = O(N^{-c}),$$

where in the last equality we used Proposition II.6.16. Letting N go to infinity concludes the proof. □

II.6.6 Proof of Theorem II.2.3

We start with a lemma gathering the estimates obtained on the increments of the extrema.

Lemma II.6.18 (Nails do not move)**.** *There exist $c_0, C_0 \in (0,\infty)$ such that for every N,*

$$\mathbf{P}[\exists i \in I^{(0)}, \exists t \le \tau_{\mathrm{end}}(i), \exists A \in \{\mathrm{T},\mathrm{B},\mathrm{R}\}, |A^{(t)}(i) - A^{(0)}(i)| \ge N^{1-c_0}] \le \frac{C_0}{N^{c_0}}.$$

Proof. First of all, observe that it is sufficient to control the increments at compounded steps τ_k since $A^{(t)}(i)$ is between $A^{(\tau_k)}(i)$ and $A^{(\tau_{k+1}\wedge\tau_{\mathrm{end}}(i))}(i)$ for every $t \in [\tau_k, \tau_{k+1}]$. For this reason, we only focus on compounded steps and introduce the time $\tau'_{\mathrm{end}}(i)$ denoting the integer k such that $\tau_k \le \tau_{\mathrm{end}}(i) < \tau_{k+1}$. For each $i \in I^{(0)}$, introduce the processes indexed by integer times $0 \le K < \lceil 2N/\sin\alpha \rceil$,

$$\begin{aligned}
\mathbf{\Sigma}_{A,i}(K) &:= \sum_{k=0}^{K\wedge\tau'_{\mathrm{end}}(i)} \mathbf{E}[\Delta^{\mathrm{IIC}} A^{(k)}(i) | \mathcal{F}_k],\\
\mathbf{M}_{A,i}(K) &:= \sum_{k=0}^{K\wedge\tau'_{\mathrm{end}}(i)} \Delta^{\mathrm{IIC}} A^{(k)}(i) - \mathbf{\Sigma}_{A,i}(K),\\
\mathbf{\Delta}^{\mathrm{err}} A(i,K) &:= \sum_{k=0}^{K\wedge\tau'_{\mathrm{end}}(i)} |\Delta^{\mathrm{err}} A^{(k)}(i)|.
\end{aligned}$$

We now bound the probability that each one of these processes is large, which by (i) of Propositions II.6.12–II.6.14 will bound the probability that $|A^{(\tau_{K+1})} - A^{(0)}|$ is large.

Below, the constants $c, C \in (0,\infty)$ are introduced to satisfy Propositions II.3.4, II.6.8, II.6.12, and II.6.14. They are fixed all along the proof. The other constants c_i, C_i are independent of everything and should be thought of as being respectively much smaller than c and much larger than C.

We start with the easiest process, which is the last one. Note that the process is increasing and non-negative. Markov's inequality and Propositions II.6.12–II.6.14(iii) imply that for every $i \in I^{(0)}$,

$$\begin{aligned}
\mathbf{P}[\mathbf{\Delta}^{\mathrm{err}} A(i, \lceil 2N/\sin\alpha\rceil - 1) \ge N^{1-c_0} | \mathcal{F}_0] &\le \frac{1}{N^{1-c_0}} \mathbf{E}[\mathbf{\Delta}^{\mathrm{err}} A(i, \lceil 2N/\sin\alpha\rceil - 1) | \mathcal{F}_0]\\
&\le \frac{C}{N^{1-c_0}} \mathbf{E}\big[\sum_{0\le t<T} M^{(t)}(i) \big| \mathcal{F}_0\big].
\end{aligned}$$

Summing over on $i \in I^{(0)}$, averaging on $\mathcal{F}_0$ gives that

$$\mathbf{P}\Big[\exists A, \exists i \in I^{(0)}, \exists K : \mathbf{\Delta}^{\mathrm{err}} A(i,K) \ge N^{1-c_0}\Big] \le \frac{C}{N^{1-c_0}} \mathbf{E}\Big[\sum_{0\le t<T} \mathrm{Err}^{(t)}\Big] \le \frac{C_1 \log N}{N^{c-c_0}}, \tag{II.71}$$

where in the second inequality we used Proposition II.6.8(iii).

Let us now turn to the second process, which is a martingale with increments that have uniform exponential moments because of Propositions II.6.12–II.6.14(ii). We deduce from a trivial modification of the Azuma-Hoeffding inequality (to accommodate the unbounded increments, simply truncate the martingale increments at N^{c_1} and bound the error by the probability that there exists a single increment larger than N^{c_1}) that for every $i \in I^{(0)}$,

$$\mathbf{P}\big[\exists A : \max_K |\mathbf{M}_{A,i}(K)| > N^{3/4} \,\big|\, \mathcal{F}_0\big] \leq \exp[-c_2 N^{c_2}].$$

By averaging on $\mathcal{F}_0$ and using that $|I^{(0)}|$ has uniformly bounded expectation (by Proposition II.3.7), we deduce that

$$\mathbf{P}\big[\exists A, \exists i \in I^{(0)} : \max_K |\mathbf{M}_{A,i}(K)| > N^{3/4}\big] \leq \exp[-c_3 N^{c_3}].$$

It only remains to prove the following inequality:

$$\mathbf{P}[\exists A, \exists i \in I^{(0)}, \max_K |\mathbf{\Sigma}_{A,i}(K)| \geq \tfrac{1}{2} N^{1-c_0}] \leq N^{-c_4}. \tag{II.72}$$

In order to prove this, let $\mathbf{N}_1$ be the number k such that there exists $i \in I^{(\tau_k)}$ and $A \in \{\mathrm{T}, \mathrm{B}\}$ such that $|A^{(\tau_k)}(i) - b(\tau_k)| \leq N^{c_5}$, and $\mathbf{N}_2$ the number of k such that $I^{(\tau_k)} \not\subset I^{(\tau_k+1)}$.

Propositions II.6.12–II.6.14(iv) give that for every A, i, and K,

$$|\mathbf{\Sigma}_{A,i}(K)| \leq N \exp(-cN^{c_5}) + C_1 \mathbf{N}_1 + C_1 \sum_{0 \leq k < \lceil 2N/\sin\alpha \rceil} \mathbf{P}[\tau'_{\mathrm{end}} = k | \mathcal{F}_k].$$

Since the last term on the right has an expectation which is bounded by the expectation of $\mathbf{N}_2$, the Markov property implies that for $c_0 < c$ and N large enough,

$$\mathbf{P}[\exists A, \exists i \in I^{(0)}, \max_K |\mathbf{\Sigma}_{A,i}(K)| \geq \tfrac{1}{2} N^{1-c_0}] \leq \frac{2C_1 \mathbf{E}[\mathbf{N}_1 + \mathbf{N}_2]}{N^{1-c_0}} + 2N^{c_0} \exp(-cN^{c_5}). \tag{II.73}$$

Yet, for each time t it is a direct consequence of Propositions II.3.4 that for c_5 sufficiently small,

$$\mathbf{P}[\exists i \in I^{(t)}, \exists A \in \{\mathrm{T}, \mathrm{B}\} : |A^{(t)}(i) - b(t)| \leq N^{c_5}] \leq C_2 N^{c_5 - c}$$

so $\mathbf{E}[\mathbf{N}_1] \leq C_3 N^{1+c_5-c}$.

Now, pick $c_6 < c/2$. To have $I^{(\tau_k)} \not\subset I^{(\tau_{k+1})}$, it must be that one of the following three things occurs:

- there exists $i \in I^{(\tau_k)}$ with $\mathrm{Vspan}^{(\tau_k)}(i) \leq \varepsilon N + 2N^{1-c_6}$ or $\max\{|\mathrm{T}^{(\tau_k)}(i) - x_2|, |\mathrm{B}^{(\tau_k)} - x_2|, |\mathrm{R}^{(\tau_k)}(i) - x_1|\} \geq \sqrt{\eta\varepsilon} N - 2N^{1-c_6}$,
- $\Delta^{\mathrm{err}} A^{(k)}(i) \geq N^{1-c_6}$ for some A and $i \in I^{(\tau_k)}$,
- $\Delta^{\mathrm{IIC}} A^{(k)}(i) \geq N^{1-c_6}$ for some A and $i \in I^{(\tau_k)}$.

Using Propositions II.3.4 again, the first item occurs with probability $O(N^{c_6-c})$. The second item occurs with probability $O(N^{c_6-c})$ by the same computation as

(II.71). The last item occurs with probability $O(\exp(-cN^{1-c_6}))$ by (ii) of Propositions II.6.12 and II.6.14. The bound $c_6 < c/2$ gives

$$\mathbf{E}[\mathbf{N}_2] \leq C_4 N^{1-c_6}.$$

Moreover, by picking $c_0 \ll c_i$ small enough and plugging the two expectation estimates into (II.73) implies (II.72). This concludes the proof. □

We now turn to a second lemma stating that with large probability, marked nails exist near every $x \in \mathbb{B}_\eta(N)$ at time 0, or in other words when defining $I_\bullet$ at the first step of the coupling, we get $|I_\bullet| = |\mathbb{B}_\eta(N)|$.

Lemma II.6.19 (Nails exist)**.** *There exist $c, C \in (0,\infty)$ such that for every $0 < \varepsilon \ll \eta$,*

$$\mathbf{P}[|I_\bullet| = |\mathbb{B}_\eta(N)|] \geq 1 - \frac{C}{\eta^2}\big(\frac{\varepsilon}{\eta}\big)^c.$$

Proof. Set $\kappa := (\eta\varepsilon^3)^{1/4}$. There are $O(1/\eta^2)$ elements in $\mathbb{B}_\eta(N)$. Furthermore, for fixed $x \in \mathbb{B}_\eta(N)$, the non-existence of a "markable" nail near x requires the existence of a dual path from $\Lambda_{2\varepsilon N}(x)$ to $\Lambda_{\kappa N}(x)$ or a primal path from $\Lambda_{\kappa N}(x)$ to $\Lambda_{((\eta\varepsilon)^{1/2}-\varepsilon)N}(x)$ (otherwise there exists a primal circuit in the annulus $\Lambda_{\kappa N}(x) \setminus \Lambda_{2\varepsilon N}(x)$ that is not connected to $\partial\Lambda_{((\eta\varepsilon)^{1/2}-\varepsilon)N}(x)$ and therefore constitutes a nail at x that we may mark. Using (II.8) and the assumption that $\varepsilon \ll \eta$ concludes the proof. □

Proof of Theorem II.2.3. We start by assuming that $\cos\alpha \notin \mathbb{Q}$. Consider $1 \gg \eta \gg \varepsilon > 0$ and assume in particular that $C\varepsilon^c/\eta^{2+c} \leq \eta/2$, where c and C are the constants of Lemma II.6.19. Also, we assume N is large enough that $C_0/N^{c_0} \leq \eta/2$, where c_0 and C_0 are the constants of Lemma II.6.18.

The two previous lemmata imply immediately that provided that ε is sufficiently small with probability $1-\eta$, marked nails exist near all points in $\mathbb{B}_\eta(N)$ and belong to $I^{(t)}$ for every $0 \leq t < T$. By Proposition II.6.8(i), we deduce that $([\cdot]^{(T)}_{\bullet,0}, [\cdot]^{(T)}_{\bullet,1}) = ([\cdot]^{(0)}_{\bullet,0}, [\cdot]^{(0)}_{\bullet,1})$.

Now, the homotopy classes with respect to $\mathbb{B}_\eta(N)$ and with respect to marked nails are equal for any loop that remains at a distance $\sqrt{\eta\varepsilon}N$ of $\mathbb{B}_\eta(N)$. Since all loops (in $\overline{\omega}^{(0)}$ and $\overline{\omega}^{(T)}$) surrounding at least two but not all points in $\mathbb{B}_\eta(N)$ have a diameter which is larger than ηN, (RSW) immediately implies that they satisfy the previous property with probability larger than $1-\eta$ provided $\varepsilon = \varepsilon(\eta) > 0$ is chosen small enough.

In particular, when setting $\eta_0 = \sqrt{\eta}$ and assuming that $2\eta \leq \eta_0$, we obtain that the rescaled configurations $\omega^{(0)}_\delta$ and $\omega^{(T)}_\delta$ satisfy

$$\mathbf{P}[d_{\mathbf{H}}(\omega^{(0)}_\delta, \omega^{(T)}_\delta) \leq \eta_0] \leq 2\eta \leq \eta_0.$$

It remains to observe that thanks to properties of the track-exchange operators (see Remark II.3.12), the law of the homotopy classes around $\mathbb{B}_\eta(N)$ is the same under $\phi_{\mathbb{L}(\pi/2)}$ and $\phi_{\mathbb{L}^{(0)}}$ (and similarly under $\phi_{\mathbb{L}(\alpha)}$ and $\phi_{\mathbb{L}^{(T)}}$). As a consequence, we may construct a coupling between $\widetilde{\omega}_\delta \sim \phi_{\delta\mathbb{L}(\pi/2)}$ and $\widetilde{\omega}'_\delta \sim \phi_{\delta\mathbb{L}(\pi/2)}$ by first using Remark II.3.12 to couple ω_δ and $\omega^{(0)}_\delta$ in such a way that the homotopy classes of

loops surrounding one but not all points in $\mathbb{B}_\eta$ are the same, then use the coupling constructed above, and finally couple $\omega_\delta^{(T)}$ with ω'_δ using Remark II.3.12 again. Overall, we exactly proved that the rescaled version of $\mathbf{P}$ satisfies the properties of the statement of our theorem for η_0, so the proof is finished.

To get the result for $\cos\alpha$ rational, simply take the coupling obtained as the weak limit of couplings with α_n satisfying $\cos\alpha_n \notin \mathbb{Q}$ and tending to α. One easily checks that the limit makes sense and satisfies all the requested properties as the bounds are continuous in α (note that one may also directly define the coupling in this setting, being careful with the vertical position of right-most points, see Remark II.6.15 again). We insist that this limit should be taken at N (or equivalently $\delta > 0$) fixed. □

II.7 Proofs of the main theorems

II.7.1 Proofs of the results for the random-cluster model

Proof of Theorem II.1.2. We prove the result for the Schramm-Smirnov topology but a similar proof works for the Camia-Newman one. By Theorem II.2.2, it suffices to construct a coupling of $(\omega_\delta, \omega'_\delta)$ with $\omega, \omega' \sim \phi_{\delta\mathbb{L}(\pi/2)}$ for which the distance $d_{\mathbf{H}}(\omega_\delta, e^{i\alpha}\omega'_\delta)$ is typically small.

Case of $\Omega = \mathbb{R}^2$ We start with a coupling on the full space $\delta\mathbb{L}(\pi/2)$. Let σ_u be the reflection with respect to the line $e^{iu}\mathbb{R}$.

Fix $\varepsilon > 0$ and choose $\eta \leq \varepsilon/4$ so that Theorem II.2.2 implies that for every coupling of $\omega_\delta \sim \phi_{\delta\mathbb{L}(\pi/2)}$ and $\omega'_\delta \sim \phi_{\delta\mathbb{L}(\pi/2)}$, we have

$$\mathbf{P}[d_{\mathbf{H}}(\omega_\delta, e^{i\alpha}\omega'_\delta) \leq \eta, d_{\mathbf{SS}}(\omega_\delta, e^{i\alpha}\omega'_\delta) > \tfrac{\varepsilon}{2}] \leq \tfrac{\varepsilon}{4}. \tag{II.74}$$

Now, construct an explicit coupling $\mathbb{P}$ between $\omega_\delta \sim \phi_{\delta\mathbb{L}(\pi/2)}$ and $\omega'_\delta \sim \phi_{\delta\mathbb{L}(\pi/2)}$ as follows: sample $\omega'_\delta \sim \phi_{\delta\mathbb{L}(\pi/2)}$ and couple $\sigma_0\omega'_\delta$ with $\omega_\delta^\alpha \sim \phi_{\delta\mathbb{L}(\alpha)}$ using Theorems II.2.2 and II.2.3 (this is doable since $\sigma_0\omega'_\delta \sim \phi_{\delta\mathbb{L}(\pi/2)}$) and (II.74) in such a way that

$$\mathbb{P}[d_{\mathbf{SS}}(\sigma_0\omega'_\delta, \omega_\delta^\alpha) \geq \tfrac{\varepsilon}{2}] \leq \tfrac{\varepsilon}{2}, \tag{II.75}$$

then, couple $\sigma_{\alpha/2}\omega_\delta^\alpha$ with $\omega_\delta \sim \phi_{\delta\mathbb{L}(\pi/2)}$ by Theorems II.2.2 and II.2.3 (this is doable since $\sigma_{\alpha/2}\omega_\delta^\alpha \sim \phi_{\delta\mathbb{L}(\alpha)}$) in such a way that

$$\mathbb{P}[d_{\mathbf{SS}}(\omega_\delta, \sigma_{\alpha/2}\omega_\delta^\alpha) \geq \tfrac{\varepsilon}{2}] \leq \tfrac{\varepsilon}{2}. \tag{II.76}$$

Since

$$\begin{aligned} d_{\mathbf{SS}}(\omega_\delta, e^{i\alpha}\omega'_\delta) &= d_{\mathbf{SS}}(\omega_\delta, \sigma_{\alpha/2}\sigma_0\omega'_\delta) = d_{\mathbf{SS}}(\sigma_{\alpha/2}\omega_\delta, \sigma_0\omega'_\delta) \qquad \text{(II.77)} \\ &\leq d_{\mathbf{SS}}(\sigma_{\alpha/2}\omega_\delta, \omega_\delta^\alpha) + d_{\mathbf{SS}}(\omega_\delta^\alpha, \sigma_0\omega'_\delta) = d_{\mathbf{SS}}(\omega_\delta, \sigma_{\alpha/2}\omega_\delta^\alpha) + d_{\mathbf{SS}}(\omega_\delta^\alpha, \sigma_0\omega'_\delta). \end{aligned}$$

The result then follows by combining (II.75)–(II.77).

Case of a bounded simply connected domain Ω with C^1-smooth boundary To obtain the result in a finite domain, we use the domain Markov property and the fact that one may approximate $\phi^0_{\Omega_\delta}$ by asking that there exists a loop Γ within distance η of $\partial\Omega$ in the infinite-volume measure. More precisely, let $A(\Omega,\eta)$ be the event that there exists a loop $\mathbf{\Gamma} \in \mathcal{F}_0(\omega_\delta)$ which is included in Ω and such that $d(\mathbf{\Gamma},\partial\Omega) \le \eta$ (d is the distance between loops defined in the introduction). Note that whether $A(\Omega,\eta)$ occurs or not can be measured in the Schramm-Smirnov topology (we leave this as an exercise).

Now, fix $\varepsilon_0 > 0$. We use the characterization of the Schramm-Smirnov distance provided in [GPS18, Proposition 3.9]. There exists a family of non-degenerate quads $Q_1,\dots,Q_n$ in Ω such that if the sets of quads in $Q_1,\dots,Q_n$ that are crossed are the same in ω_δ and ω'_δ, then $d_{\mathbf{SS}}(\omega_\delta,\omega'_\delta) \le \varepsilon_0$. In particular, we deduce that if $H_{\vec{Q}}(I)$ denotes the event that Q_i is crossed if and only if $i \in I$, then there exists a coupling $\mathbf{P}$ between $\omega_\delta \sim \phi^0_{\Omega_\delta}$ and $\omega'_\delta \sim \phi^0_{e^{i\alpha}\Omega_\delta}$ such that

$$\mathbf{P}[d_{\mathbf{SS}}(\omega_\delta,\omega'_\delta) \ge \varepsilon_0] \le \varepsilon_0$$

if and only if for every $I \subset \{1,\dots,n\}$,

$$|\phi^0_{\Omega_\delta}[H_{\vec{Q}}(I)] - \phi^0_{e^{i\alpha}\Omega_\delta}[H_{e^{i\alpha}\vec{Q}}(I)]| \le \varepsilon_0/2^n =: \varepsilon. \tag{II.78}$$

Now, the infinite volume result above implies that for every $\delta < \delta_0(\Omega,\eta,\varepsilon)$,

$$|\phi_{\delta\mathbb{Z}^2}[H_{\vec{Q}}(I)|A(\Omega,\eta)] - \phi_{\delta\mathbb{Z}^2}[H_{e^{i\alpha}\vec{Q}}(I)|A(e^{i\alpha}\Omega,\eta)]| \le \tfrac{1}{2}\varepsilon. \tag{II.79}$$

We therefore wish to prove that

$$|\phi^0_{\Omega_\delta}[H_{\vec{Q}}(I)] - \phi_{\delta\mathbb{Z}^2}[H_{\vec{Q}}(I)|A(\Omega,\eta)]| \le \tfrac{1}{2}\varepsilon. \tag{II.80}$$

The same can be done for the rotated version, so that the previous displayed equations imply (II.78) and conclude the proof.

To get (II.80), let $\mathbf{\Omega}_\delta$ be the interior of the outer-most loop in $\mathcal{F}_0(\omega)$ satisfying the conditions of $A(\Omega,\eta)$. Using the spatial Markov property, it suffices to show that

$$|\phi^0_{\Omega_\delta}[H_{\vec{Q}}(I)] - \phi^0_{\mathbf{\Omega}_\delta}[H_{\vec{Q}}(I))]| \le \tfrac{1}{2}\varepsilon. \tag{II.81}$$

Note that there is a clear increasing coupling between $\boldsymbol{\omega}_\delta \sim \phi^0_{\mathbf{\Omega}_\delta}$ and $\omega_\delta \sim \phi^0_{\Omega_\delta}$ ($\boldsymbol{\omega}_\delta \le \omega_\delta$ because of $\mathbf{\Omega}_\delta \subset \Omega_\delta$), so that for ω_δ to belong to $H_{\vec{Q}}(I)$ but not $\boldsymbol{\omega}_\delta$ or vice versa, it must be that one of the quads Q_i must be crossed in one but not in the other. We deduce that it suffices to show that for every possible realization of $\mathbf{\Omega}_\delta$,

$$\phi^0_{\Omega_\delta}[\mathcal{C}(Q_i)] - \phi^0_{\mathbf{\Omega}_\delta}[\mathcal{C}(Q_i)] \le \tfrac{1}{2n}\varepsilon. \tag{II.82}$$

Therefore, the result boils down to the following.

Claim *For every $\epsilon > 0$, every bounded simply connected domain Ω with C^1-smooth boundary, and every quad Q inside Ω, there exists $\eta = \eta(\Omega,Q,\epsilon) > 0$ such that for every $\Omega' \subset \Omega$ with $d(\partial\Omega',\partial\Omega) \le \eta$,*

$$\phi^0_{\Omega_\delta}[\mathcal{C}(Q)] \le \phi^0_{\Omega'_\delta}[\mathcal{C}(Q)] + \epsilon$$

for δ small enough.

Proof. We only sketch the proof. Consider first the "epigraph" domains indexed by continuous functions f from $[-2,2]$ to $\mathbb{R}$ given by

$$\Omega(f) := \{x = (x_1, x_2) \in \mathbb{R}^2 : x_1 \in (-2,2), f(x_1) < x_2 < 2\}$$

(see Figure II.28). Define $\Lambda := [-1,1]^2$. For $\alpha > 0$, a straightforward yet quite lengthy application of the techniques developed[13] in [DCM20, Lemma 5.3] implies that for every $f \leq -2$ and $1 \leq k \leq \frac{1}{2}\lfloor 1/\alpha \rfloor =: K$,

$$\phi^0_{\Omega(f)_\delta}[\mathcal{C}(\Lambda)] - \phi^0_{\Omega(f+\alpha)_\delta}[\mathcal{C}(\Lambda)] \leq C\big(\phi^0_{\Omega(f+k\alpha)_\delta}[\mathcal{C}(\Lambda)] - \phi^0_{\Omega(f+(k+1)\alpha)_\delta}[\mathcal{C}(\Lambda)]\big).$$

Summing over $1 \leq k \leq K$, we deduce that

$$\phi^0_{\Omega(f)_\delta}[\mathcal{C}(\Lambda)] - \phi^0_{\Omega(f+\alpha)_\delta}[\mathcal{C}(\Lambda)] \leq \frac{C}{K}\big(\phi^0_{\Omega(f)_\delta}[\mathcal{C}(\Lambda)] - \phi^0_{\Omega(f+K\alpha)_\delta}[\mathcal{C}(\Lambda)]\big) \leq \frac{C}{K} \leq 4C\alpha. \tag{II.83}$$

Note that a similar argument works for any rotation, translate, or rescaling of the domains above.

We now use our assumption that $\partial\Omega$ is C^1-smooth. Since $\partial\Omega$ is given by a curve γ which is C^1 and has non-vanishing differential, one may find (see Figure II.28) constants $\kappa = \kappa(\Omega) > 0$ and $C = C(\Omega) > 0$, functions $f_s : [-2,2] \to (-\infty, -2]$ and $T_s : \mathbb{R}^2 \to \mathbb{R}^2$ for $1 \leq s \leq S$, where S depends on Ω (through the modulus of continuity of the derivative for the function parametrizing $\partial\Omega$) but not on η, satisfying the following properties:

- T_s is the composition of a rotation, a translation, and the multiplication by κ;
- $T_s(\Omega(f_s))$ is included in Ω for every s;
- for all η small enough, $\{x \in \Omega : d(x, \Omega^c) \leq \eta\}$ is included in the union of the sets

$$A_s := T_s(\{x = (x_1, x_2) : x_1 \in [-1,1], f(x_1) < x_2 < f(x_1) + C\eta\}).$$

Introducing the domains $\Omega_s := \Omega \setminus \bigcup_{t=1}^s A_t$, and using again [DCM20] for the first and second inequalities, one can prove the existence of $C_i = C_i(\Omega, Q, \kappa) > 0$ such that

$$\begin{aligned} \phi^0_{\Omega_{s-1}}[\mathcal{C}(Q)] - \phi^0_{\Omega_s}[\mathcal{C}(Q)] &\leq C_1\big(\phi^0_{\Omega_{s-1}}[\mathcal{C}(T_s(\Lambda))] - \phi^0_{\Omega_s}[\mathcal{C}(T_s(\Lambda))]\big) \\ &\leq C_2\big(\phi^0_{\Omega(f_s)}[\mathcal{C}(\Lambda)] - \phi^0_{\Omega(f_s+C\eta)}[\mathcal{C}(\Lambda)]\big) \\ &\leq C_3\eta, \end{aligned} \tag{II.84}$$

where the last line is due to (II.83) applied to $\alpha = C\eta$.

Choose $\eta = \eta(\Omega, \epsilon, S) > 0$ small enough. Summing (II.84) over s gives

$$\phi^0_{\Omega_\delta}[\mathcal{C}(Q)] - \phi^0_{\Omega'_\delta}[\mathcal{C}(Q)] \leq \sum_{s=0}^{S-1} \phi^0_{\Omega_{s-1}}[\mathcal{C}(Q)] - \phi^0_{\Omega_s}[\mathcal{C}(Q)] \leq \epsilon.$$

□

[13] The whole fo Section 4 of [DCM20] should be adapted to finite domains and considering the covariance of crossing events with edges on the boundary of the domain.

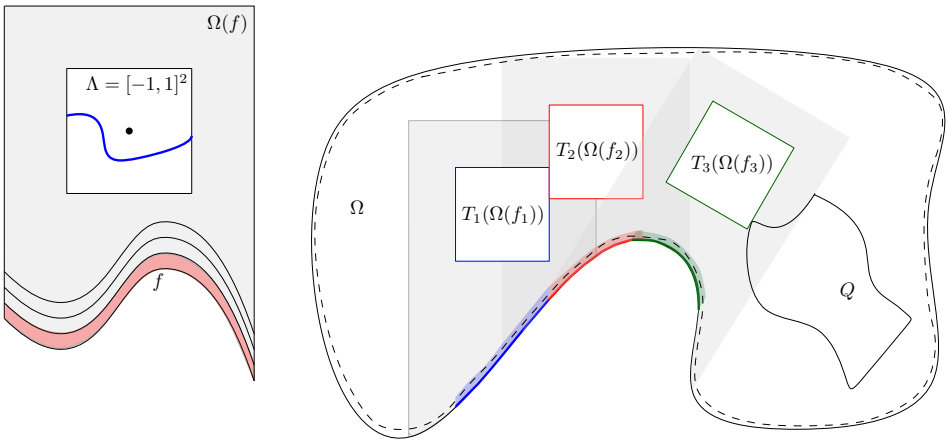

Figure II.28: On the left, an example of a domain $\Omega(f)$. Note that the sets $\Omega(f+k\alpha)$ have a nested structure (the red part denotes $\Omega(f) \setminus \Omega(f+\alpha)$). On the right, the impact of changing the boundary is compared with the impact of changing the boundary in a family of subdomains which are images by simple transformations of domains $\Omega(f)$ (with potentially different functions f). The existence of such a decomposition is made possible by the fact that the boundary of Ω is C^1.

Case of a (possibly unbounded) simply connected domain Ω with C^1-smooth boundary For every $\varepsilon > 0$, to determine the Schramm-Smirnov distance up to a precision of $\varepsilon > 0$, only quads in $B(0, 1/\varepsilon)$ need to be considered. Consider a bounded domain $\Omega^{(\varepsilon)}$ that coincides with Ω on $B(0, 1/\varepsilon^C)$. By the mixing property, one has that for every $\delta > 0$ and every event E depending on edges in $\delta\mathbb{Z}^2 \cap B(0, 1/\varepsilon)$ only,

$$|\phi_{\Omega_\delta^{(\varepsilon)}}[E] - \phi_{\Omega_\delta}[E]| \leq C_{\text{mix}} \varepsilon^{c_{\text{mix}}(C-1)} \phi_{\Omega_\delta}[E].$$

Now, take the domain $\Omega^{(\varepsilon)}$ very large but finite, equal to Ω up to large distance. Using the invariance by rotation in $\Omega_\delta^{(\varepsilon)}$ and taking δ to 0 then ε to 0 concludes the proof. □

Proof of Corollary II.1.3. When one considers a quad Q that remains at a distance at least ε of the boundary of Ω, the result follows directly from Theorem II.1.2 and the measurability of $\mathcal{C}(Q)$ in the Schramm-Smirnov topology (note that the event gets rewritten as $Q \in \omega$ when ω is seen as an element of $\mathcal{H}$).

Now, when $1 \leq q < 4$, to get the result without any assumption on the distance to the boundary, note that for a quad Q, there exists a quad Q' that is such that its distance to $\partial\Omega$ is at least ε, and which is in Hausdorff distance at a distance at most 2ε from Q. Using the strong version of crossing estimates from [DCMT21], we obtain easily (this type of reasoning is now classical, see for instance [DCM20, Lemma 3.12] for an example) that

$$|\phi_{\Omega_\delta}[\mathcal{C}(Q)] - \phi_{\Omega_\delta}[\mathcal{C}(Q')]| \leq C\varepsilon^c$$

for two constants $C > 0$ and $c > 0$. The result follows readily by first choosing ε small enough and then letting δ tend to zero and use the rotational invariance result for Q'. □

Proof of Corollary II.1.4. We use a conditional mixing argument due to Garban, Pete, and Schramm [GPS13a, Section 3] in the case of Bernoulli percolation and that can be extended to the random-cluster model using crossing estimates. Consider the *Euclidean* ball B_n of radius n, and its boundary ∂B_n. Introduce the quantities

$$\epsilon(n,N) := \phi^0_{\mathbb{Z}^2}[0 \longleftrightarrow B_N^c | B_n \longleftrightarrow B_N^c] \quad \text{and} \quad \epsilon(n) := \lim_{N\to\infty} \epsilon(n,N).$$

The statement of conditional mixing from [GPS13a] implies the following claim (in [GPS13a] it is stated for the four-arm event, but a similar – in fact simpler – argument can be performed for the one-arm event, see e.g. Proposition 5.3 of the same paper). For every $\beta, \varepsilon > 0$, there exists $\eta = \eta(\beta,\varepsilon) > 0$ such that for every Ω and every $x_1, \dots, x_n$ at a distance ε of each other and of the boundary, and every partition P of $(x_1, \dots, x_n)$,

$$\left|\phi^0_{\Omega_\delta}[\mathcal{E}(P, x_1, \dots, x_n)] - \epsilon(\tfrac{\eta}{\delta})^n \phi^0_{\Omega_\delta}[\mathcal{E}(P, B_{\eta/\delta}(x_1), \dots, B_{\eta/\delta}(x_n))]\right| \leq \beta \phi^0_{\Omega_\delta}[\mathcal{E}(P, x_1, \dots, x_n)],$$

where $\mathcal{E}(P, B_{\eta/\delta}(x_1), \dots, B_{\eta/\delta}(x_n))$ is the event that the balls $B_{\eta/\delta}(x_i)$ are connected to each other if and only if they belong to the same element of the partition P. The same formula applies in the rotated measure.

We conclude, by observing that $e^{i\alpha} B_{\eta/\delta}(x_i)$ and $B_{\eta/\delta}(e^{i\alpha} x_i)$ are equal, and that the event $\mathcal{E}(P, B_{\eta/\delta}(x_1), \dots, B_{\eta/\delta}(x_n))$ is measurable in the Schramm-Smirnov topology, so that its probability or the probability of its rotation by an angle of α are close to each other by Theorem II.1.2. □

III | Delocalization of the height function of the six-vertex model

Joint work with Hugo Duminil-Copin, Alex Karrila, Ioan Manolescu.

III.1 Introduction

III.1.1 Motivation

The six-vertex model was initially proposed by Pauling in 1935 in order to study the thermodynamic properties of ice [Pau35]. It became the archetypical example of a planar integrable model after Lieb's solution of the model in 1967 in its anti-ferroelectric and ferroelectric phases [Lie67b, Lie67c, Lie67a] using the Bethe ansatz (see [DCGH$^+$18] and references therein for an introduction). In the last fifty years, further analysis of the model has provided deep insight into the subtle structure of two-dimensional integrable systems, for instance with the development of the Yang-Baxter equation, quantum groups, and transfer matrices; see e.g. [Bax82, Res10].

The six-vertex model lies at the crossroads of a vast family of two-dimensional lattice models. Among others, it has been related to the dimer model, the Ising and Potts models, the critical random-cluster model, the loop $O(n)$ models, the Ashkin-Teller models, random permutations, stochastic growth model, and quantum spin chains, to cite but a few examples (see references below). In recent years, the interplay between all these models has been used to prove a number of new results on the behaviour of each one of them. Let us mention here the extensive study of the free fermion point in relation to dimers [BK18, FS06, Ken00]; the analysis of critical points of random-cluster models and loop $O(n)$ models [Nie82, RS20]; the development of parafermionic observables based on the six-vertex model, culminating with the proof of conformal invariance of the Ising model [CS12, Smi10][1]; the understanding of dimerization properties of the anti-ferromagnetic Heisenberg chain [ADCW20]; and the relation between Kardar–Parisi–Zhang equation and the stochastic six-vertex model [BCG16].

While the use of the six-vertex model's integrable properties has been extraordinarily fruitful to understand its free energy, the analysis of the model's correlation functions and the associated stochastic processes have been particularly limited (with some notable exceptions like the free fermion point). For instance, the exact integrability provides strong evidence of a Berezinskii–Kosterlitz–Thouless phase transition of the antiferroelectric model between a regime in which correlations de-

[1] See [IWWZJ13, IC09] for examples of constructions, [DC17] for a review, and [BDCS15, DCS12] for other examples of simple mathematical applications.

cay polynomially fast and a regime where they decay exponentially fast. However, proving mathematically that this is indeed the case remains an open problem with today's techniques.

Another example of a property of the six-vertex model that seemed to elude mathematicians for many years is the rigorous understanding of its height function representation (see definition below). Indeed, the six-vertex model produces one of the most natural models of random height functions. This interpretation of the model plays an important role for at least two reasons. First, special cases include the height function of the dimer model (when considering the free fermion point) and the uniformly chosen graph homomorphisms from $\mathbb{Z}^2$ to $\mathbb{Z}$ (when considering the original square-ice model), which are models of independent interest. Second, the height function interpretation has been at the center of the bozonization of 2D lattice models, an extremely powerful tool introduced in the physics literature and enabling the use of the Coulomb gas formalism to understand (as of today non-rigorously) the behaviour of correlations (see e.g. [Dub11, Nie84, ZI77]).

One of the most fundamental questions one can ask about a model of a random height function h is whether the height function fluctuates or not. More precisely, does the height variance $\mathrm{Var}[h(x)-h(y)]$ between two points x and y remain bounded uniformly in x and y, or does it on the contrary grow to infinity as the distance between x and y goes to infinity? In the former scenario, we say that the height function model is *localized* or *smooth*, and in the latter one, that it is *delocalized* or *rough*. On which side (localized/delocalized) of the dichotomy the model lies is a crucial question which can be understood as an analogue, for spin or percolation systems, of determining whether long-range order occurs or not at criticality. The answer can be quite subtle and seemingly similar models can exhibit very different behaviours.

As mentioned above, most of the currently known exact results on the six-vertex model seem to provide little rigorous information on the behaviour of the height function, in particular they do not directly answer the question of localization/delocalization. In this paper, we provide the first full description of which parameters $\mathbf{c}$ are such that the six-vertex height function is localized/delocalized, in the regime corresponding to Rys' model of hydrogen bonded ferroelectrics [Rys63] where the parameters of the six-vertex model, as defined in the next subsection, are $\mathbf{a} = \mathbf{b} = 1$ and $\mathbf{c} \geq 1$ [2].

III.1.2 Definitions and main result on the torus

The six-vertex model on the torus is defined as follows. For $N > 0$ even, let $\mathbb{T}_N := (V(\mathbb{T}_N), E(\mathbb{T}_N))$ be the toroidal square grid graph with $N \times N$ vertices. An *arrow configuration* ω on $\mathbb{T}_N$ is the choice of an orientation for every edge of $E(\mathbb{T}_N)$. We say that ω satisfies the *ice rule*, or equivalently that it is a *six-vertex configuration*, if every vertex of $V(\mathbb{T}_N)$ has two incoming and two outgoing incident edges in ω. These edges can be arranged in six different ways around each vertex as depicted in Figure III.1, hence the name of the model. For parameters

[2] Various predictions for the six-vertex model are formulated in terms of the parameter $\Delta = (\mathbf{a}^2+\mathbf{b}^2-\mathbf{c}^2)/(2\mathbf{ab})$. The six-vertex models with $\mathbf{a} = \mathbf{b} = 1$ and $\mathbf{c} \geq 1$ are equivalently determined by $\mathbf{a} = \mathbf{b}$ and $\Delta \leq 1/2$; as we shall soon see, in terms of the latter formulation, we have localization for $\Delta < -1$ and delocalization for $\Delta \in [-1, 1/2]$.

$\mathbf{a}_1, \mathbf{a}_2, \mathbf{b}_1, \mathbf{b}_2, \mathbf{c}_1, \mathbf{c}_2 \geq 0$, define the *weight* of a configuration ω to be

$$W_{6\mathrm{V}}(\omega) = \mathbf{a}_1^{n_1}\mathbf{a}_2^{n_2}\mathbf{b}_1^{n_3}\mathbf{b}_2^{n_4}\mathbf{c}_1^{n_5}\mathbf{c}_2^{n_6},$$

where n_i is the number of vertices of $V(\mathbb{T}_N)$ having type i in ω. In this paper, we will not study the model in its full generality of parameters, and focus on the special choice given by $\mathbf{a}_1 = \mathbf{a}_2 = \mathbf{b}_1 = \mathbf{b}_2 = 1$ and $\mathbf{c}_1 = \mathbf{c}_2 = \mathbf{c} \geq 1$, which corresponds to *isotropic*[3] parameters.

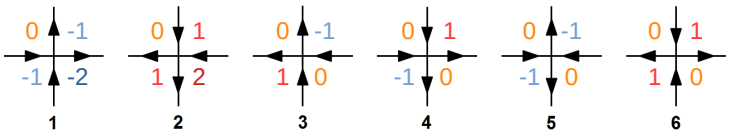

Figure III.1: The 6 *types* of vertices in the six-vertex model together with the corresponding height function values on the four squares touching this vertex (we set $h = 0$ on the upper-left square). Each type comes with a weight $\mathbf{a}_1, \mathbf{a}_2, \mathbf{b}_1, \mathbf{b}_2, \mathbf{c}_1, \mathbf{c}_2$.

The weights induce a probability measure on the set $\Omega_{6V}(\mathbb{T}_N)$ of six-vertex configurations ω on $\mathbb{T}_N$ given by

$$\mathbb{P}_{\mathbb{T}_N}[\{\omega\}] = \frac{W_{6\mathrm{V}}(\omega)}{Z(\mathbb{T}_N)},$$

where $Z(\mathbb{T}_N) := \sum_{\omega \in \Omega_{6V}(\mathbb{T}_N)} W_{6\mathrm{V}}(\omega)$ is the partition function. Below, we write $\mathbb{E}_{\mathbb{T}_N}$ for the associated expectation.

Write $\mathbb{T}_N^*$ for the dual graph of $\mathbb{T}_N$: its vertices are the faces of $\mathbb{T}_N$ and two vertices of $\mathbb{T}_N^*$ are connected by an edge of $\mathbb{T}_N^*$ if the corresponding faces of $\mathbb{T}_N$ share an edge. As mentioned in Section III.1.1, the six-vertex model and its ice-rule naturally emerge when studying *graph homomorphisms* from $\mathbb{T}_N^*$ into $\mathbb{Z}$, i.e., maps h from the faces $F(\mathbb{T}_N)$ of $\mathbb{T}_N$ to $\mathbb{Z}$ which satisfy $|h(x) - h(y)| = 1$ for all neighbouring faces $x, y \in F(\mathbb{T}_N)$. We call such graph homomorphisms *height functions*. To avoid certain technical difficulties, we will assume that N is even and partition the faces of $\mathbb{T}_N$ in a bipartite fashion into odd and even faces, and will hereafter additionally impose that a height function h is odd on odd faces and even on even faces.

For a given height function h, introduce the *six-vertex configuration ω associated to h* by orienting each edge e so that out of the two faces bordering e, the one on the left of e (in the sense of this orientation) has the larger value of h. Note that two height functions h and h' give rise to the same six-vertex configuration ω if and only if $h - h'$ is a constant function. In the converse direction, it is not always true that a six-vertex configuration gives rise to a graph homomorphism on the faces of the torus (it only defines the gradient and may lead to inconsistencies when wrapping around the torus). However, for *balanced* configurations ω such that any row (resp. column) of faces around $\mathbb{T}_N$ is crossed by as many up (resp. right) as down (resp. left) arrows, there exists a height function h associated with ω, which is

[3] The reader may verify from Figure III.1 that given $\mathbf{a}_1 = \mathbf{a}_2 = \mathbf{b}_1 = \mathbf{b}_2$ and $\mathbf{c}_1 = \mathbf{c}_2$, the weight of a vertex does not change under symmetries of the square lattice.

unique up to additive constant. From now on, let $\Omega_{6V}^{(\mathrm{bal})}(\mathbb{T}_N)$ be the set of balanced configurations and

$$\mathbb{P}_{\mathbb{T}_N}^{(\mathrm{bal})} := \mathbb{P}_{\mathbb{T}_N}[\,\cdot\,|\,\omega \in \Omega_{6V}^{(\mathrm{bal})}(\mathbb{T}_N)].$$

When ω is chosen according to $\mathbb{P}_{\mathbb{T}_N}^{(\mathrm{bal})}$, write h for the height function associated to it (to fix the additive constant choose a root face and impose that h is null on that face). Observe that the increments $h(x) - h(y)$ do not depend on the choice of the additive constant and thus on the root face. Also note that $\mathbb{E}_{\mathbb{T}_N}^{(\mathrm{bal})}[h(x) - h(y)] = 0$ by symmetry under a global arrow flip and thus we have

$$\mathbb{E}_{\mathbb{T}_N}^{(\mathrm{bal})}[(h(x) - h(y))^2] = \mathrm{Var}_{\mathbb{T}_N}^{(\mathrm{bal})}(h(x) - h(y)),$$

where $\mathrm{Var}_{\mathbb{T}_N}^{(\mathrm{bal})}$ denotes variance under $\mathbb{P}_{\mathbb{T}_N}^{(\mathrm{bal})}$. The goal of this paper is to study the behaviour of this variance as x and y are distant vertices in a large torus. Below, d denotes the graph distance on the dual graph $\mathbb{T}_N^*$.

Theorem III.1.1 (Delocalized phase)**.** *Fix $1 \le \mathbf{c} \le 2$. There exist $c, C > 0$ such that for every N even and every $x, y \in F(\mathbb{T}_N)$ with $d(x, y) \ge 2$, we have*

$$c \log d(x, y) \le \mathbb{E}_{\mathbb{T}_N}^{(\mathrm{bal})}[(h(x) - h(y))^2] \le C \log d(x, y)$$

Remark III.1.2. Instead of an $N \times N$ square torus as here, one may more generally study the balanced six-vertex model on an $N \times M$ torus with even dimensions. For $M \ge N$ the variance of $h(x) - h(y)$ behaves like $\log d(x, y) + d(x, y)/N$ up to multiplicative constants, and the results of the present paper may be used to show this.

The previous result was known in three special cases, namely for square-ice, i.e. $\mathbf{c} = 1$ [CPST21, DCHL$^+$19, She05], for the free fermion point $\mathbf{c} = \sqrt{2}$ [BK18, FS06, Ken00], and for $\mathbf{c} = 2$ [GP19]. During the writing of this paper, Marcin Lis produced a proof for $\sqrt{2 + \sqrt{2}} \le \mathbf{c} \le 2$ based on different techniques than ours [Lis21]. To the best of our knowledge, the result is new for other parameters $\mathbf{c} \ge 1$. This result offers a complete picture of the behaviour of the height function of the six-vertex model in the range of parameters $\mathbf{a} = \mathbf{b} = 1$ and $\mathbf{c} \ge 1$ as it complements the following result for $\mathbf{c} > 2$, proved in [GP19] (as a consequence of [DCGH$^+$16, RS20]).

Theorem III.1.3 (Localized phase)**.** *Fix $\mathbf{c} > 2$. There exists $C \in (0, \infty)$ such that for every N even and every $x, y \in F(\mathbb{T}_N)$,*

$$\mathbb{E}_{\mathbb{T}_N}^{(\mathrm{bal})}[(h(x) - h(y))^2] \le C.$$

In the regime $1 \le \mathbf{c} \le 2$, the model is predicted to have Gaussian behaviour and to converge in the sense of distributions in the scaling limit to (a scaling of) the Gaussian Free Field (GFF) on the two-dimensional torus. The only case for which this is known is the free fermion point $\mathbf{c} = \sqrt{2}$ (see [Ken00] and reference therein; cf. also [GMT17]). The logarithmic divergence of the variance proved here is consistent with this behaviour, but not sufficient to determine it. We do however mention [DCKK$^+$20a], whose result may be loosely reformulated as "any sub-sequential scaling limit of height functions obtained for $\sqrt{3} \le \mathbf{c} \le 2$ is invariant under rotation".

III.1.3 Main results in planar domains

In this section, we develop the theory of the six-vertex model in finite domains and present our main results in this context. Due to the six-vertex model's spatial Markov property (see Section III.2.1 for the precise definition), these results have strong implications for the six-vertex model on the torus discussed in the previous section.

Equip $\mathbb{Z}^2$ with the square grid graph structure and let $(\mathbb{Z}^2)^* = (\frac{1}{2}, \frac{1}{2}) + \mathbb{Z}^2$ denote the dual of $\mathbb{Z}^2$; its vertices are identified with the faces of $\mathbb{Z}^2$. As before, we partition $\mathbb{Z}^2$ in a bipartite fashion into odd and even faces. Let V be a finite connected set of vertices of the graph $\mathbb{Z}^2$, and let E be the edges incident to them. The height function model related to arrow configurations on E with ice rule on V is defined on the subgraph D of $(\mathbb{Z}^2)^*$ consisting of the faces of $\mathbb{Z}^2$ with at least one corner in V and the dual edges of $\mathbb{Z}^2$ that cross a primal edge in E. We say that such a subgraph D is a *discrete domain*, and denote $V = V(D)$ and $E = E(D)$. The faces of $\mathbb{Z}^2$ in D with at least one corner not in V are called the *boundary* ∂D *of* D (see Figure III.2).

A *boundary condition* on D is given by a function $\xi : \partial D \to \mathbb{Z}$; we say that ξ is *admissible* if there exists a graph homomorphism $h : D \to \mathbb{Z}$ with $h_{|\partial D} = \xi$ and if ξ is odd on odd faces (and therefore even on even faces). Let $\Omega_{6V}(D, \xi)$ be the set of arrow configurations on E, associated with graph homomorphisms $h : D \to \mathbb{Z}$ with $h_{|\partial D} = \xi$. The map from these graph homomorphisms to the associated six-vertex configurations in $\Omega_{6V}(D, \xi)$ is bijective, and hence we will often identify them, and call h height functions. Introduce the probability measure on $\Omega_{6V}(D, \xi)$ given by

$$\mathbb{P}_D^{\xi}[\{\omega\}] = \frac{W_{6\mathrm{V}}(\omega)}{Z(D, \xi)},$$

where $W_{6\mathrm{V}}$ is the six-vertex weight from the vertices of $V(D)$ and $Z(D, \xi)$ is the partition function defined by $\sum_{\omega \in \Omega_{6V}(D,\xi)} W_{6\mathrm{V}}(\omega)$[4].

For integers $0 < n < N$, define $\Lambda_n := (-n, n)^2$ and $A(n, N) = \Lambda_N \setminus \Lambda_n$; denote $\Lambda_n \subset D$ if $\Lambda_n \cap \mathbb{Z}^2 \subset V(D)$ and similarly for $A(n, N)$, and equip Λ_n and $A(n, N)$ with the obvious structure of a discrete domain. Let $\mathcal{O}_{h \geq k}(n, N)$ be the event that there exists a circuit of adjacent faces with $h(x) \geq k$ in $A(n, N)$ that surrounds Λ_n.

Theorem III.1.4 (Uniformly positive annulus circuit probabilities)**.** *Fix* $\mathbf{c} \in [1, 2]$. *For every* $k, \ell > 0$*, there exists* $c = c(\mathbf{c}, \ell, k) > 0$ *such that for every* n *large enough, every discrete domain* $D \supset \Lambda_{2n}$*, and every admissible boundary condition* ξ *on* ∂D *(or a subset of it) with* $|\xi| \leq \ell$*, we have*

$$\mathbb{P}_D^{\xi}[\mathcal{O}_{h \geq k}(n, 2n)] \geq c. \tag{III.1}$$

An important aspect of the previous estimate is that it is uniform over the scales n of the annulus in which the circuit occurs, as well as over the domains D. This allows one to combine it with the spatial Markov and FKG properties of the model (see Sections III.2.1–III.2.2) to deduce the other main theorems of this paper. Note also that the "flatness" $|\xi| \leq \ell$ of the boundary condition is crucial, and

[4] In later sections, we will use the notation $\mathbb{P}_D^{\xi}$ for height assignments ξ on other supports than ∂D; the concepts above readily generalize to these cases.

the statement above is expected to fail otherwise. An extreme example is given by "sloped" boundary conditions, that may be chosen in such a way as to completely freeze the configuration inside the domain (see Figure III.2 for an example), thus preventing the event $\mathcal{O}_{h\geq k}(n, 2n)$ from occurring.

Theorem III.1.4 may be used to derive estimates similar to (III.1) for annuli with any outer to inner radius ratio, with the constant c depending on this ratio. This can be shown with standard RSW-type techniques, by building a big circuit out of many small ones. Two extensions of the result above will be discussed in Lemmas III.5.2 and III.5.4. They are concerned with how the probability of events $\mathcal{O}_{|h|\geq k}(n, N)$ evolves as N/n tends to infinity, and as k tends to infinity, respectively. The upshot is that the probability then converges to 1 polynomially in n/N, and to 0 exponentially in k, respectively.

As a consequence of Theorem III.1.4, we obtain the following bounds on the variance of the height function. Below, d denotes the graph distance on $(\mathbb{Z}^2)^*$.

Corollary III.1.5 (Logarithmic variance in planar domains)**.** *Fix $1 \leq \mathbf{c} \leq 2$. There exist $c, C > 0$ such that for every discrete domain D, every admissible boundary condition ξ on ∂D, and every face x of $D \setminus \partial D$, if we set $\max_{y\in\partial D} |\xi(y)| = \ell$, then*

$$c \log d(x, \partial D) - 4\ell^2 \leq \mathrm{Var}_D^{\xi}(h(x)) \leq C \log d(x, \partial D) + 4\ell^2.$$

It is quite standard for percolation models that Theorem III.1.4 along with positive association and the spatial Markov property imply results such as Corollary III.1.5 and Theorem III.1.1. However, we warn the reader of subtleties in their proofs due to the particular forms of the spatial Markov property (Proposition III.2.1) and the pushing of boundary conditions (Proposition III.2.6) in this height-function model.

III.1.4 Some core ideas of the proof

As already mentioned, the key to all the results discussed so far is the circuit probability estimate of Theorem III.1.4. Its proof relies on three main inputs. First, Theorem III.1.6 below estimates certain free energies associated to the six-vertex model on a cylinder; it was obtained in [DCKK$^+$20b] using the Bethe ansatz[5]. The second is contained in the proof of Theorem III.1.7, and is way to relate the estimates of the free energy obtained above to a certain behaviour of the height function on the cylinder. This is the main innovation of the present work. The third central input, also contained in the proof of Theorem III.1.7, is a Russo–Seymour–Welsh (RSW) type theory for the level sets of the height function. Below, we briefly introduce these three results in this order.

Let $\mathbb{O}_{N,M}$ denote the cylindrical square lattice with a height of M faces and a perimeter of N faces. The six-vertex configurations on (the $N \times (M-1)$ degree 4 vertices of) $\mathbb{O}_{N,M}$ and their six-vertex weights are then defined as straightforward generalizations of the toroidal and finite planar cases. Let N be even and, for $s \in [-N/2, N/2]$, denote by $\Omega_{6V}^{(s)}$ the set of six-vertex configurations on $\mathbb{O}_{N,M}$ such

[5]The central role of this input is highlighted by the fact that it is the only place in this paper that differentiates between the phases $\mathbf{c} > 2$ and $1 \leq \mathbf{c} \leq 2$.

that every row of N faces around $\mathbb{O}_{N,M}$ is crossed by $2\lceil s\rceil$ more up arrows than down arrows. Let

$$Z_{N,M}^{(s)} := \sum_{\omega\in\Omega_{6V}^{(s)}} W_{6\mathrm{V}}(\omega).$$

Theorem III.1.6 (Free energy on the cylinder; [DCKK$^+$20b])**.** *Fix $\mathbf{c} > 0$. There exists a function $f_{\mathbf{c}} : (-1/2, 1/2) \to \mathbb{R}^+$ such that*

$$\lim_{\substack{N\to\infty\\ N\text{ even}}} \lim_{M\to\infty} \frac{1}{NM} \log Z_{N,M}^{(\alpha N)} = f_{\mathbf{c}}(\alpha).$$

Moreover, for $0 < \mathbf{c} \le 2$ there exists $C = C(\mathbf{c}) > 0$ such that for every $\alpha \in (-1/2, 1/2)$,

$$f_{\mathbf{c}}(\alpha) \le f_{\mathbf{c}}(0) - C\alpha^2. \tag{III.2}$$

The function $f_{\mathbf{c}}(\alpha)$ is called the *free energy* of the cylindrical six-vertex model at unbalance α. The previous theorem has an appealing physical intuition: the free energy $f_{\mathbf{c}}(\alpha)$ is differentiable at 0 as a function of α, for all $0 < \mathbf{c} \le 2$.

The objective of the second main ingredient, Theorem III.1.7, is to deduce the annulus circuit probabilities, and thus ultimately the delocalization of the height function, from the differentiability of $f_{\mathbf{c}}$. Let us mention that [DCKK$^+$20b] also shows that the free energy is non-differentiable at 0 when $\mathbf{c} > 2$, which corresponds to the regime where the height function is localised (see Theorem III.1.3). As such, we have a direct correspondence between differentiability/non-differentiability of $f_{\mathbf{c}}(\alpha)$ at 0 and delocalization/localization of the height function with slope 0; this correspondence is expected to apply in great generality, in particular for other slopes [She05].

Theorem III.1.7. *There exist $\eta, c, C > 0$ such that, for all integers $k \le r$ with k large enough and all $\mathbf{c} \ge 1$, we have*

$$\mathbb{P}^{0,1}_{\Lambda_{12r}}[\mathcal{O}_{h\ge ck}(12r, 6r)] \ge c \exp\big[Cr^2\big(f_{\mathbf{c}}(\eta k/r) - f_{\mathbf{c}}(0)\big)\big], \tag{III.3}$$

where $0, 1$ denotes the admissible boundary condition on $\partial\Lambda_{12r}$ taking values 0 and 1 only.

Theorems III.1.6 and III.1.7 readily imply Theorem III.1.4.

Our third main step, the RSW theory, follows ideas that were created initially in the context of two-dimensional Bernoulli percolation [Rus78, SW78], and were instrumental for instance in the computation of its critical point. To date, RSW type results are understood as comparing crossing probabilities in domains of different shape but similar size scale. In the past decade, the theory has been extended to a wide variety of percolation models [BDC12, BR10, Tas16, DCHN11, DCST17, DCGPS20, KST20b], and more recently to level sets of height function models on planar graphs, see e.g. [DCHL$^+$19, GM21].

In our main RSW type result, Theorem III.3.1, the careful reader will observe a twist compared to the existing such statements on height function models: we bound the probability of having crossings of height larger than ck of long domains by the probability of having crossings of height k of short domains, where $c > 0$

is a small constant. Such a loss in the height would prove very problematic for the renormalization arguments usually performed in percolation models. Indeed, Theorem III.3.1 does not a priori suffice to prove a dichotomy theorem as that of [DCST17] or [DCT19]. In our setting, Theorem III.1.6 provides an input which renders the renormalization superfluous.

III.1.5 Further questions

Infinite volume limits and mixing A reader familiar with the random surface theory of [She05] will notice that the delocalization proven in this paper, together with an application of that theory[6], shows the local convergence of the balanced six-vertex arrow configurations, for $\mathbf{c} \in [1, 2]$, on the torus $\mathbb{T}_N$ as $N \to \infty$. More delicate questions address the infinite-volume limit of the model in planar domains, and the rate at which the effect of different boundary conditions dies out, i.e., the mixing rate. Analogous infinite volume limits and mixing properties are fundamental, e.g., in the study of the Ising and FK Ising models. For $\mathbf{c} \in [\sqrt{3}, 2]$, such properties have been established also for the six-vertex model in [Lis21]. We plan to discuss these topics in the full range $\mathbf{c} \in [1, 2]$ in a later publication.

Different model parameters The reader will notice that our main results, Theorems III.1.4 and its consequences, Theorem III.1.1 and Corollary III.1.5, are valid only for $\mathbf{c} \in [1, 2]$. That $\mathbf{c} \leq 2$ is required is unsurprising since the model exhibits a different behaviour when $\mathbf{c} > 2$, as illustrated by Theorem III.1.3. The difference in behaviour may be traced back to the behaviour of the free energy of Theorem III.1.6; recall that this is the only point in our proof differentiating between $\mathbf{c} \in [1, 2]$ and $\mathbf{c} > 2$.

When $\mathbf{c} \in (0, 1)$, the Bethe ansatz computation of Theorem III.1.6 still applies and provides a differentiable free energy at $\alpha = 0$. Moreover, the height model is expected to have a similar behaviour to when $\mathbf{c} \in [1, 2]$. However, all the other main arguments of this paper fail in the range $\mathbf{c} \in (0, 1)$, due to the lack of positive association which is ubiquitously applied in our proofs. Indeed, when $\mathbf{c} < 1$, the FKG property fails, both for the height function and its absolute value.

In a more general context, it is natural to consider the model with arbitrary positive weights $\mathbf{a}_1 = \mathbf{a}_2 = \mathbf{a}$, $\mathbf{b}_1 = \mathbf{b}_2 = \mathbf{b}$, and $\mathbf{c}_1 = \mathbf{c}_2 = \mathbf{c}$; recall that it is expected that the behaviour of the model depends only on $\Delta = (\mathbf{a}^2+\mathbf{b}^2-\mathbf{c}^2)/(2\mathbf{ab})$, and thus delocalization results similar to ours should hold for all parameters $(\mathbf{a}, \mathbf{b}, \mathbf{c})$ with $\Delta \in [-1, 1/2]$. As regards this case, we leave it to the reader to verify that our combinatorial tools of Section III.2 and Appendix III.6, in particular the positive association properties of the model, remain valid with analogous proofs whenever $\max\{\mathbf{a}, \mathbf{b}\} \leq \mathbf{c}$. Consequently, it also holds that *if* Theorem III.1.4 remains true for $\max\{\mathbf{a}, \mathbf{b}\} \leq \mathbf{c}$, then so do Theorem III.1.1 and Corollary III.1.5 (the proof of this implication is only based on the tools of Section III.2). Unfortunately, the geometric RSW theory (and more precisely, the proof of Proposition III.3.4) in this paper relies on the model being invariant under both vertical and diagonal reflections, hence requiring $\mathbf{a} = \mathbf{b}$.

[6] See [LT20] on the validity of [She05] on the six-vertex model.

Sloped boundary conditions Let $\xi : (\mathbb{Z}^2)^* \to \mathbb{Z}$ be a fixed height function and study the measures $\mathbb{P}_D^{\xi_{|\partial D}}$ in growing domains $D \nearrow \mathbb{Z}^2$. Corollary III.1.5 gives the height variance for flat enough boundary conditions: for instance if $\xi(x) - \xi(0) = O(1)$, we have $\mathrm{Var}_D^{\xi_{|\partial D}}(h(x)) \sim \log d(x, \partial D)$. One may also study boundary conditions that are not flat, most interestingly boundary conditions with a given slope: take a fixed ice-rule arrow configuration in an $N \times M$ torus, embed it periodically in the plane, and let ξ be the corresponding height function on the faces of $\mathbb{Z}^2$. The *slope* of ξ is then the vector $s = ((\xi(y+(N,0)) - \xi(y))/N, (\xi(y+(0,M)) - \xi(y))/M)$ (which is independent of $y \in (\mathbb{Z}^2)^*$); note that

$$\xi(x) - \xi(0) = \langle x, s \rangle + O(1).$$

With different choices of M, N, ξ in the above, the possible slopes s are exactly the rational points of $[-1,1] \times [-1,1]$.

It is expected that a result similar to Corollary III.1.5 holds under the measure $\mathbb{P}_D^{\xi_{|\partial D}}$, whenever the slope of ξ is in the interior[7] of $[-1,1]^2$ (Corollary III.1.5 treats the zero-slope case). For such boundary conditions, the RSW result is also expected to apply for $h - \xi$ instead of h, at sufficiently large scales. Indeed, in a slightly different context, it was shown in [She05] that the height function delocalizes for non-zero slopes in $(-1,1)^2$. Then, the height function in finite domains is expected to converge to the unique infinite-volume one, and to delocalize logarithmically.

Organization of the paper

Section III.2 introduces a toolbox of fundamental combinatorial properties of six-vertex height functions, which will be constantly applied in the sequel. Section III.3 presents crossing probability estimates, in particular the RSW-type result of Theorem III.3.1; these do not rely on (III.2) and are valid for all $\mathbf{c} \geq 1$. Section III.4 contains the proofs of Theorems III.1.7 and III.1.4. The estimates on the variance of the height function of Theorem III.1.1 and Corollary III.1.5 are proved in Section III.5.

III.2 Basic properties

This section studies six-vertex height functions in (discrete domains embedded in) the plane, torus, or cylinder, with parameter $\mathbf{c} \geq 1$. As mentioned in the introduction, all the results in this section also hold for the three-parameter model when $\max\{\mathbf{a}, \mathbf{b}\} \leq \mathbf{c}$.

On setup and notation We denote by $\mathbb{G}$ an "ambient space graph" that can be taken to be either the torus $\mathbb{T}_N$, the cylinder $\mathbb{O}_{N,M}$, or the whole plane $\mathbb{Z}^2$. By the terms vertex, edge, face, and dual edge we will always refer to those structures of $\mathbb{G}$. We will always assume that N is even and hence the faces of $\mathbb{G}$ can be bipartitioned into *even* and *odd* faces, such that no odd (resp. even) face shares an edge with another odd (resp. even) face.

[7] For slopes on the boundary of $[-1,1]^2$ one readily shows that the configuration inside D freezes completely.

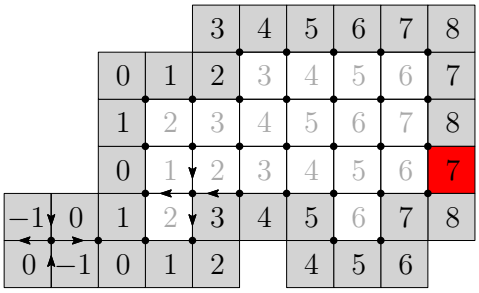

Figure III.2: A discrete domain D generated by the marked vertices. The boundary ∂D is represented in grey and some of the arrows of the associated 6-vertex configuration are shown. The boundary condition is such that there exists a unique height function inside D consistent with it (we say that the height function is frozen). If the red square were to contain a 9 instead of a 7, the boundary condition would become non-admissible.

A discrete domain $D \subset \mathbb{G}^*$ is defined for $\mathbb{G} = \mathbb{T}_N$ and $\mathbb{G} = \mathbb{O}_{N,M}$ similarly to the planar case in Section III.1.3. Recall that a function $h : D \to \mathbb{Z}$ is a *height function* if for any two adjacent faces x and y in D, we have $|h(x) - h(y)| = 1$, and h is even on even faces and odd on odd faces. Let $\mathcal{H}_D$ denote the set of such height functions on D.

Finally, recall from the introduction that a boundary condition ξ (and thus its induced measure $\mathbb{P}^{\xi}_{D}$) may be defined on any nonempty set of faces $B \subset D$.

III.2.1 Spatial Markov property

Proposition III.2.1 (Spatial Markov property (SMP))**.** *Let $D \subset D'$ be two domains of $\mathbb{G}$ and ξ be an admissible boundary condition on $\partial D'$. Then for any realisation ζ of a height function chosen according to $\mathbb{P}^{\xi}_{D'}$, we have*

$$\mathbb{P}^{\xi}_{D'}[\,\cdot \mid h = \zeta \text{ on } D^c \cup \partial D] = \mathbb{P}^{\zeta_{|\partial D}}_{D}. \tag{SMP}$$

Above, the left-hand side refers to the law of the height function restricted to D, written $h_{|D}$, when h is sampled according to $\mathbb{P}^{\xi}_{D'}$. Observe that the right-hand side of (SMP) only depends on the values of ζ on ∂D. In particular, this proves that conditionally on the values of h on ∂D, the restrictions of the height function to D and D^c are independent.

Proof. For any height function h equal to ζ on $D^c \cup \partial D$,

$$\mathbb{P}^{\xi}_{D'}[h] = \tfrac{1}{Z(D',\xi)} \prod_{v \in V(D)} \mathbf{c}^{\mathbb{1}\{v \text{ is of type 5 or 6 in } h\}} \prod_{v \in V(D') \setminus V(D)} \mathbf{c}^{\mathbb{1}\{v \text{ is of type 5 or 6 in } h\}}.$$

The second product above only depends on ζ, since it only involves vertices for which all four surrounding faces have height prescribed by ζ. Thus, the law of $h_{|D}$ under $\mathbb{P}^{\xi}_{D'}[\,\cdot \mid h = \zeta \text{ on } D^c \cup \partial D]$ has probabilities proportional to the first product above, and therefore to $\mathbb{P}^{\zeta_{|\partial D}}_{D}[h_{|D}]$, with a factor of proportionality that depends on $\zeta_{|D^c \cup \partial D}$. As these two measures are supported on the same set of height configurations, we conclude that they are equal. □

III.2.2 Monotonicity properties and correlation inequalities

The six-vertex model enjoys useful monotonicity properties with respect to its height function representation when $\mathbf{a} = \mathbf{b} = 1$ and $\mathbf{c} \geq 1$ (or in more general when $\max\{\mathbf{a}, \mathbf{b}\} \leq \mathbf{c}$). We now state these properties. Proofs are given in Appendix III.6 since they are all not explicitly present in the literature[8].

An important concept in the study of both height functions and boundary conditions is the *partial order relation* $\preceq$ on $\mathcal{H}_D$. For two height functions $h, h' \in \mathcal{H}_D$, we set $h \preceq h'$ if and only if $h(x) \leq h'(x)$ for all faces x in D. An analogous partial order is defined between boundary conditions.

A function $F : \mathcal{H}_D \to \mathbb{R}$ is *increasing* if $h \preceq h'$ implies that $F(h) \leq F(h')$. An event A is *increasing* if its indicator function $\mathbb{1}_A$ is an increasing function, and *decreasing* if its complement A^c is increasing. The results below are stated in terms of expectations of increasing functions, but we will mostly apply them to probabilities of increasing events.

Proposition III.2.2. *Fix a discrete domain D, any two admissible boundary conditions $\xi \preceq \xi'$ and any two increasing functions $F, G : \mathcal{H}_D \to \mathbb{R}$. Then, we have*

$$\mathbb{E}_D^{\xi}[F(h)G(h)] \geq \mathbb{E}_D^{\xi}[F(h)]\mathbb{E}_D^{\xi}[G(h)], \tag{FKG}$$

$$\mathbb{E}_D^{\xi'}[F(h)] \geq \mathbb{E}_D^{\xi}[F(h)]. \tag{CBC}$$

The proof of Propositions III.2.2 is in Appendix III.6. For now, let us prove the following elementary corollary of (CBC).

Corollary III.2.3. *Let D be a discrete domain and ξ an admissible boundary condition. If $\xi \geq m$ (resp. $\xi \leq M$) then for any face x of D, we have*

$$\mathbb{E}_D^{\xi}[h(x)] \geq m \qquad (\textit{resp. } \mathbb{E}_D^{\xi}[h(x)] \leq M).$$

Proof. It suffices to prove the first bound for $m = 0$ (the rest follows readily). The comparison between boundary conditions and the invariance of weight under sign flip $W_{6\mathrm{V}}(h) = W_{6\mathrm{V}}(-h)$ give

$$2\mathbb{E}_D^{\xi}[h(x)] \geq \mathbb{E}_D^{\xi}[h(x)] + \mathbb{E}_D^{-\xi}[h(x)] = 0,$$

which is what we wanted to prove. □

Crucially, our model enjoys an additional monotonicity property for the absolute value of the height function.

Proposition III.2.4. *Fix a discrete domain D, $\xi' \succeq \xi \geq 0$ two admissible boundary conditions on ∂D, a (possibly empty) set of faces $B \subset D$, and two height-functions $\zeta' \succeq \zeta \geq 0$ on B achievable under $\mathbb{P}_D^{\xi'}$ and $\mathbb{P}_D^{\xi}$, respectively. Then, for any two increasing function $F, G : \mathcal{H}_D \to \mathbb{R}$, we have*

$$\mathbb{E}_D^{\xi'}\big[F(|h|) \,\big|\, |h| = \zeta' \text{ on } B\big] \geq \mathbb{E}_D^{\xi}\big[F(|h|) \,\big|\, |h| = \zeta \text{ on } B\big], \tag{CBC-|h|}$$

$$\mathbb{E}_D^{\xi}\big[F(|h|)G(|h|)\big] \geq \mathbb{E}_D^{\xi}\big[F(|h|)\big]\mathbb{E}_D^{\xi}\big[G(|h|)\big]. \tag{FKG-|h|}$$

Remark III.2.5. The inequality (FKG-|h|) also holds for the conditional measure $\mathbb{P}_D^{\xi}[. \,|\, |h| = \zeta \text{ on } B]$ by the same proof.

[8] It is also worthwhile to point out that the computations would yield counterexamples for these monotonicity results when $\mathbf{c} \in (0, 1)$, or $\max\{\mathbf{a}, \mathbf{b}\} > \mathbf{c}$.

III.2.3 Boundary pulling and pushing

In models with the spatial Markov property and monotonicity properties, a useful tool is the comparison of probabilities of certain events in different domains. This is sometimes referred to as the pushing/pulling of boundary conditions. In our model, it is achieved through the FKG inequality for the absolute value of the height function.

In order to state the pushing/pulling property, we need the concept of minimal height functions. Let $D \subset \mathbb{G}^*$ be a discrete domain and ξ be an admissible boundary condition defined on $B \subset D$. The reader may verify that

$$\underline{h}(x) = \max_{y \in B}(\xi(y) - d_D(x, y)),$$

where d_D denotes the graph distance on $D \subset \mathbb{G}^*$, is the unique minimal height function h with $h_{|B} = \xi$. That is, for any other such h, we have $\underline{h} \preceq h$. Similarly, if h_m is the height function taking only values m and $m+1$, it holds that $h(\cdot) = \max\{\underline{h}(\cdot), h_m(\cdot)\}$ is the unique minimal height function h with $h_{|B} = \xi$ with $h \geq m$. Maximal extensions can be constructed similarly.

Proposition III.2.6. *Fix integers $k > m$. Let $D \subset \mathbb{G}^*$ be a discrete domain, ξ be an admissible boundary condition on $B \subset D$ with $\xi \geq m$ and $\zeta \in \mathcal{H}_D$ the minimal height function with boundary conditions ξ and with $\zeta \geq m-1$. Then, for any $B' \supset B$, we have*

$$\mathbb{P}_D^{\zeta_{|B'}}[\exists C \in \mathcal{C} \text{ with } h_{|C} \geq k] \leq 2\,\mathbb{P}_D^{\xi}[\exists C \in \mathcal{C} \text{ with } h_{|C} \geq k], \tag{III.4}$$

for any collection $\mathcal{C}$ of connected subsets of D. When each set in $\mathcal{C}$ intersects B, then the factor 2 may be removed.

The above will mostly be used in the form of the following corollary.

Corollary III.2.7. *Let $D \subset D'$ be two discrete domains, ξ' be an admissible boundary condition for $\mathcal{H}_{D'}$ on $\partial D'$, with $\xi' \geq m$ for some m. Let ξ be the minimal admissible boundary condition for $\mathcal{H}_D$ on ∂D, that coincides with ξ' on $\partial D \cap \partial D'$ and satisfies $\xi \geq m$. Then, for any $k > m$,*

$$\mathbb{P}_D^{\xi}[\exists C \in \mathcal{C} \text{ with } h_{|C} \geq k+2] \leq 2\,\mathbb{P}_{D'}^{\xi'}[\exists C \in \mathcal{C} \text{ with } h_{|C} \geq k], \tag{III.5}$$

for any collection $\mathcal{C}$ of connected subsets of D. When each set in $\mathcal{C}$ intersects $\partial D'$, then the factor 2 may be removed.

The corollary will be applied to the existence of certain paths, most commonly crossings of certain domains. Two things should be kept in mind when applying Corollary III.2.7. First, due to (CBC), (III.5) also applies to pairs of boundary conditions $\tilde{\xi}, \tilde{\xi}'$ with $\tilde{\xi} \preceq \xi$ and $\xi' \preceq \tilde{\xi}'$. Second, even though the statement suggests that ξ is chosen in terms of ξ', we will sometimes start with a boundary condition ξ, then construct a boundary condition ξ' for which (III.5) holds. The two cases correspond to boundary pushing and pulling.

Proposition III.2.6. Since the model is invariant under the addition of a constant, we may limit ourselves to the case $m = 0$. Fix a set $\mathcal{C}$ of connected subsets of D. Write $\mathcal{A} = \{h : \exists C \in \mathcal{C} \text{ with } h_{|C} \geq k\}$.

Since $k > 0$, if $|h| \in \mathcal{A}$, then there exits $C \in \mathcal{C}$ on which $|h| \geq k$ and in particular h is of constant sign. As a consequence

$$\mathbb{P}_D^\xi[h \in \mathcal{A}] + \mathbb{P}_D^\xi[-h \in \mathcal{A}] \geq \mathbb{P}_D^\xi[|h| \in \mathcal{A}].$$

By sign flip symmetry and comparison between boundary conditions (CBC) (recall that $\xi \geq 0$, and hence $-\xi \preceq \xi$), we find that

$$2\mathbb{P}_D^\xi[h \in \mathcal{A}] \geq \mathbb{P}_D^\xi[|h| \in \mathcal{A}]. \tag{III.6}$$

It remains to lower bound the right-hand side. Observe that the lowest possible values of $|h|$ on B are given by $|\zeta|$. By (FKG-|h|),

$$\begin{aligned}\mathbb{P}_D^\xi[|h| \in \mathcal{A}] &\geq \mathbb{P}_D^\xi[|h| \in \mathcal{A} \,|\, |h| = |\zeta| \text{ on } B] \\ &\geq \min\left\{\mathbb{P}_D^\xi[h \in \mathcal{A} \,|\, h = \zeta' \text{ on } B] : \zeta' \text{ admissible s.t. } |\zeta'| = |\zeta|\right\}.\end{aligned}$$

Due to (FKG) and to the fact that $\mathcal{A}$ is increasing, the minimum above is realised by the lowest configuration ζ' satisfying the condition above. The choice of ζ as lowest among the realisations of h on B with $\zeta \geq -1$ guarantees that the minimum in the above is obtained when $\zeta' = \zeta$. Combining this observation with (III.6) provides the desired bound.

Finally, if $\mathcal{C}$ is such that all $C \in \mathcal{C}$ intersect ∂D, then $\mathbb{P}_D^\xi[h \in \mathcal{A}] = \mathbb{P}_D^\xi[|h| \in \mathcal{A}]$. Indeed, when $|h| \in \mathcal{A}$, the sign of h on any set $C \in \mathcal{C}$ realising $\mathcal{A}$ is necessarily $+$, due to its intersection with ∂D and to the fact that $\xi \geq 0$ (since $k > 0$, C intersects the boundary only on faces where $\xi > 0$). Thus, in this particular case, the factor 2 may be removed from (III.4). □

Corollary III.2.7. Fix $D \subset D'$, ξ and ξ' as in the statement. Let ζ be the smallest realisation of a height function on D' with boundary conditions ξ' and with $\zeta \geq m - 1$. Then, due to Proposition III.2.6 and (SMP),

$$\mathbb{P}_{D'}^{\xi'}[\exists C \in \mathcal{C} \text{ with } h_{|C} \geq k] \geq \tfrac{1}{2}\mathbb{P}_D^{\zeta_{|\partial D}}[\exists C \in \mathcal{C} \text{ with } h_{|C} \geq k].$$

Notice now that, by choice of ξ, we have $\zeta_{|\partial D} \succeq \xi - 2$, and (CBC) thus gives

$$\mathbb{P}_D^{\zeta_{|\partial D}}[\exists C \in \mathcal{C} \text{ with } h_{|C} \geq k] \geq \mathbb{P}_D^{\xi-2}[\exists C \in \mathcal{C} \text{ with } h_{|C} \geq k] = \mathbb{P}_D^\xi[\exists C \in \mathcal{C} \text{ with } h_{|C} \geq k + 2].$$

The claim follows. When all sets in $\mathcal{C}$ intersect $\partial D'$, the factor $1/2$ disappears in the first equation displayed above. □

III.3 RSW theory

This section introduces tools of a geometric nature for the six-vertex height functions, related to crossings of domains by height function level sets. The main result is the Russo–Seymour–Welsh (RSW) Theorem III.3.1. An intermediate result, Proposition III.3.4 will also be used later, in Section III.4. In this section, we only work in the plane.

The results in this section work for all $\mathbf{c} \geq 1$, i.e., they do not differentiate between the localized and delocalized phases. However, as discussed in Section III.1.5, they do *not* directly generalize for the six-vertex model with three parameters $\mathbf{a}, \mathbf{b}, \mathbf{c}$. The reader will also notice that various inexplicit constants appear in the statements of this section. Explicit values for these constants could be worked out by carefully tracing through the proofs, but this is not needed for the purpose of this paper. An interesting consequence is nevertheless that the inexplicit constants may be chosen uniformly in $\mathbf{c} \geq 1$.

III.3.1 The main RSW result

Given a discrete domain D and sets A, B of faces of D, write $A \xleftrightarrow{h \geq k \text{ in } D} B$ for the event that there exists a path of faces $u_0, \dots, u_n$ of D with $u_0 \in A$, $u_n \in B$, u_i adjacent to u_{i+1} in D for all i and $h(u_i) \geq k$ for all i. When no ambiguity is possible, we remove the mention to D from the notation. The same notation applies with $h \leq k$ and $|h|$ instead of h.

For convenience, we will work here with the following measures in infinite horizontal strips. Fix $n \geq 2$ and set Strip $:= \mathbb{Z} \times [0, n]$ seen as a subgraph of $\mathbb{Z}^2$. Its boundary ∂Strip is formed of the faces in $\mathbb{Z} \times ([0, 1] \cup [n-1, n])$; the notion of admissible boundary condition on ∂Strip adapts readily from that on (finite) domains. Fix an admissible boundary condition ξ on Strip with $|\xi| \preceq M$ for some $M \geq 1$. The measure $\mathbb{P}^{\xi}_{\text{Strip}}$ is defined as the weak limit of measures $\mathbb{P}^{\xi_m}_{[-m,m]\times[0,n]}$ as $m \to \infty$, where ξ_m is the minimal boundary condition on $\partial[-m, m] \times [0, n]$ which is equal to ξ on $\partial\text{Strip} \cap \partial[-m, m] \times [0, n]$. It is an immediate consequence of the finite energy of the model that $\mathbb{P}^{\xi}_{\text{Strip}}$ exists. Furthermore, by the same argument, $\mathbb{P}^{\xi}_{\text{Strip}}$ is the limit of any sequence of measures $\mathbb{P}^{\zeta_m}_{D_m}$, where D_m is any increasing sequence of domains with $\bigcup_{m\geq 1} D_m = \text{Strip}$ and ζ_m is any sequence of boundary conditions on ∂D_m that are equal to ξ on $\partial\text{Strip} \cap \partial D_m$.

Note that as a consequence of this construction, the spatial Markov property (SMP), the FKG inequalities (FKG) and (FKG-|h|), the comparison of boundary conditions (CBC) and (CBC-|h|) and the pushing of boundary conditions (III.5) apply to $\mathbb{P}^{\xi}_{\text{Strip}}$.

We are now ready to state the main result of this section.

Theorem III.3.1 (RSW)**.** *There exist absolute constants $\delta, c, C > 0$ such that for any $k \geq 1/c$ and any n, we have*

$$\mathbb{P}^{0,1}_{\Lambda_{12n}}[\mathcal{O}_{h\geq ck}(6n, 12n)] \geq c\big(\mathbb{P}^{0,1}_{\mathbb{Z}\times[-n,2n]}\big[[0, \lfloor \delta n \rfloor] \times \{0\} \xleftrightarrow{h\geq k \text{ in } \mathbb{Z}\times[0,n]} \mathbb{Z} \times \{n\}\big]\big)^C \tag{III.7}$$

where $0, 1$ denotes the admissible boundary condition on $\partial\Lambda_{12n}$ taking values 0 and 1 only.

The right-hand side above should be interpreted as zero if $\lfloor \delta n \rfloor = 0$.

The rest of this section is organised as follows. In Section III.3.2, we discuss duality properties and crossings of certain symmetric domains. In Section III.3.3, we prove a result about vertical crossings of a strip with endpoints contained in small intervals. This result is used to prove to Theorem III.3.1 and will also be

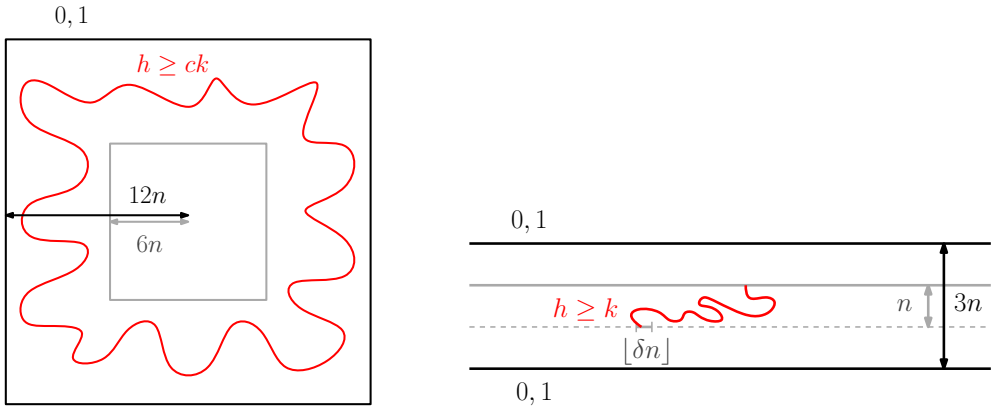

Figure III.3: Theorem III.3.1 lower-bounds the probability of a large-height circuit around an annulus (left) in terms of that of a vertical crossing of the middle third of a strip, starting from a given narrow window of length $\lfloor \delta n \rfloor$ (right).

used in Section III.4. In Section III.3.4 we use the result of Section III.3.3 to bound the probability of horizontal crossings of long rectangles in a strip. Then, in Section III.3.5, the previous bounds are extended to circuits in annuli, thus proving Theorem III.3.1.

III.3.2 Crossings of symmetric quadrilaterals

A discrete domain D is said to be *simply-connected* if it is the subgraph of $(\mathbb{Z}^2)^*$ bounded on or inside a simple loop on $(\mathbb{Z}^2)^*$. (The corresponding primal vertices $V(D) \subset \mathbb{Z}^2$ are hence those inside the loop.) When four (different) faces a, b, c, d in counter-clockwise order on the bounding loop are fixed, $(D; a, b, c, d)$ is called a *(discrete) quad*. The boundary of a quad is divided into four arcs (ab), (bc), (cd), and (da), that are paths on $(\mathbb{Z}^2)^*$ intersecting at their extremities.

For a discrete domain D, we say that two faces u and v are $\times$-*adjacent* in D if $d_D(u, v) = 2$ and u and v share a corner; a $\times$-*path* in D is a sequence of $\times$-adjacent faces. For sets A, B of faces of D we write $A \overset{h\geq k \text{ in } D}{\longleftrightarrow}_\times B$ for the event that there exists a $\times$-path $u_0, \dots, u_n \in D$ with $u_0 \in A$, $u_n \in B$ and $h(u_i) \geq k$ for all i; similar notations are used for $h \geq k$ and $|h|$, and "in D" is omitted if clear.

Remark III.3.2. The $\times$-paths are the dual of ordinary paths, in the sense that for a quad $(D; a, b, c, d)$, we have

$$\{(ab) \overset{h\geq k}{\longleftrightarrow} (cd)\}^c = \{(bc) \overset{h<k}{\longleftrightarrow}_\times (da)\}. \tag{III.8}$$

See Figure III.4 for an explanation. Furthermore, we have

$$\{(bc) \overset{h\leq k-2}{\longleftrightarrow} (da)\} \subset \{(bc) \overset{h<k}{\longleftrightarrow}_\times (da)\} \subset \{(bc) \overset{h\leq k}{\longleftrightarrow} (da)\}. \tag{III.9}$$

A *symmetry* σ of $\mathbb{Z}^2$ is a graph isomorphism from $\mathbb{Z}^2$ to itself that fixes the bipartition of $F(\mathbb{Z}^2)$ (even faces are sent to even faces, and odd faces to odd faces). Given an admissible boundary condition ξ on D, we denote by $\sigma\xi$ the admissible boundary condition $\xi \circ \sigma^{-1}$ on $\sigma(D)$. A discrete quad $(D; a, b, c, d)$ is said to be

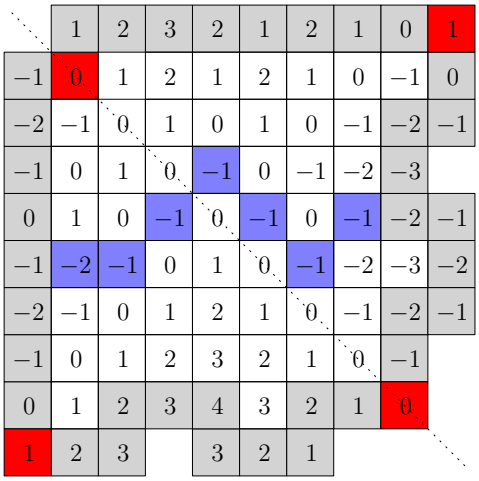

Figure III.4: A quad (with marked faces at its corners) which is symmetric with respect to the reflection σ along the diagonal. The boundary condition ξ is such that $-\xi \preceq \sigma\xi$, as required in Lemma III.3.3. This domain contains no path of non-negative height from top to bottom, but contains a negative $\times$-crossing from left to right. This path is not unique; one may be found by following the contour of the connected component of non-negative faces of the bottom arc.

symmetric if there exists a symmetry $\sigma : \mathbb{Z}^2 \to \mathbb{Z}^2$ such that $\sigma(D) = D$ and σ maps the boundary arcs (ab) and (cd) of D to (bc) and (da).

Lemma III.3.3 (Crossing probability in symmetric domains)**.** *Let $(D; a, b, c, d)$ be a discrete quad which is symmetric with respect to a symmetry σ. For any boundary condition ξ on ∂D such that $\sigma\xi \succeq -\xi$, we have*

$$\mathbb{P}_D^{\xi}[(ab) \overset{h\geq 0}{\longleftrightarrow} (cd)] \geq \tfrac{1}{2}.$$

Proof. Using first (III.8) and then (III.9), we deduce that

$$1 - \mathbb{P}_D^{\xi}[(ab) \overset{h\geq 0}{\longleftrightarrow} (cd)] = \mathbb{P}_D^{\xi}[(bc) \overset{h<0}{\longleftrightarrow}_{\times} (da)] \leq \mathbb{P}_D^{\xi}[(bc) \overset{h\leq 0}{\longleftrightarrow} (da)].$$

Applying the symmetry σ (and the fact that symmetries preserve six-vertex weights in our parameter range) we get

$$\mathbb{P}_D^{\xi}[(bc) \overset{h\leq 0}{\longleftrightarrow} (da)] = \mathbb{P}_D^{\sigma\xi}[(ab) \overset{h\leq 0}{\longleftrightarrow} (cd)] \leq \mathbb{P}_D^{-\xi}[(ab) \overset{h\leq 0}{\longleftrightarrow} (cd)] = \mathbb{P}_D^{\xi}[(ab) \overset{h\geq 0}{\longleftrightarrow} (cd)],$$

where the inequality follows from the comparison of boundary conditions of Proposition III.2.2 since $\sigma\xi \succeq -\xi$ and the event $(ab) \overset{h\leq 0}{\longleftrightarrow} (cd)$ is decreasing. The claim follows by combining the two displayed equations above. □

III.3.3 No crossings between slits

For the rest of this section, aiming to prove Theorem III.3.1, we omit the integer roundings in $\lfloor \delta n \rfloor$ to streamline the notation; δn thus always represents an integer.

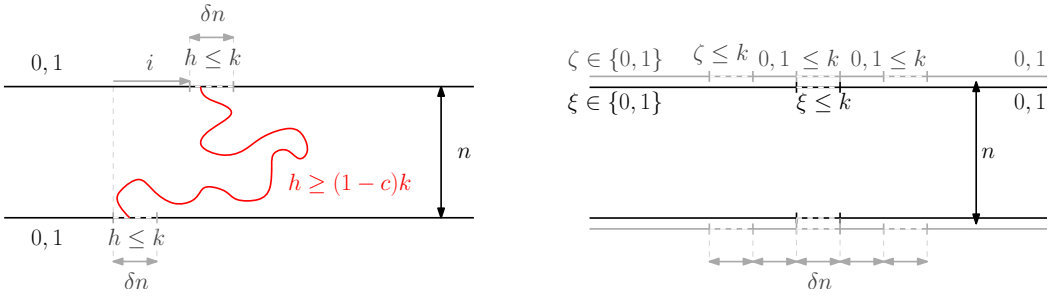

Figure III.5: Left: an illustration of the boundary condition and the crossing event in Proposition III.3.4. In the top and bottom intervals of length δn (which we call slits) the boundary conditions are $k, k-1$, except at their ends, where they progressively decrease to 0. One should think of δn as being much larger than k. Right: illustration for the proof in the case $i = 0$: the boundary conditions ξ (black) and ζ (gray) – the same color code as in the left picture applies. The geometry and the definition of boundary conditions are similar on the lower and upper boundaries of the strip.

Proposition III.3.4. *There exist constants $\delta, c > 0$ such that the following holds. For any $k \geq 1/c$, any n and any $i \in \mathbb{Z}$*

$$\mathbb{P}^{\xi}_{\mathbb{Z}\times[0,n]}\big[[0,\delta n]\times\{0\} \xleftrightarrow{h\geq(1-c)k} [i,i+\delta n]\times\{n\}\big] < 1-c, \tag{III.10}$$

where ξ is the largest boundary condition on $\partial\mathbb{Z}\times[0,n]$ which is at most k and has values $0,1$ on $(\mathbb{Z}\setminus[0,\delta n])\times\{0\}$ and $(\mathbb{Z}\setminus[i,i+\delta n])\times\{n\}$.

See Figure III.5(left) for an illustration.

The proposition above will be used twice: once as the key step in the proof of Theorem III.3.1 and again to build so-called "fences" in Section III.4. It may be useful to adopt a dual view of the result above. Indeed, due to Remark III.3.2, the above shows that, in spite of the large boundary conditions (roughly) k on the slits $(\mathbb{Z}\setminus[0,\delta n])\times\{0\}$ and $(\mathbb{Z}\setminus[i,i+\delta n])\times\{n\}$, one may construct with positive probability a path of at most $(1-c)k$ disconnecting these slits from each other.

Proposition III.3.4. We will start by proving the statement for $i = 0$; the statement for general i follows by a simple manipulation. For the rest of this subsection, we omit the subscripts $\mathbb{Z}\times[0,n]$ in the strip measures.

Case $i = 0$: Fix $\delta = 1/17$ and integers k and n with $kc \geq 1$, where $c > 0$ is a constant whose value will be specified later and will not depend on k or n. For $j \in \mathbb{Z}$, write L_j for the vertical line $\{j\delta n\}\times\mathbb{R}$,

$$I_j := [j\delta n, (j+1)\delta n]\times\{0\} \quad \text{and} \quad \tilde{I}_j := [j\delta n, (j+1)\delta n]\times\{n\}.$$

Then, for $\alpha \in \{0,+,-\}$ and $k \geq 1$, define $\mathcal{E}_{h\geq k}(j,\alpha)$ as the event that there exists a path of $h \geq k$ from I_j to $\tilde{I}_j$ in the strip $\mathbb{R}\times[0,n]$, and furthermore

- if $\alpha = 0$, the path intersects neither L_{j-5} nor L_{j+6},
- if $\alpha = +$, the path intersects L_{j+6};
- if $\alpha = -$, the path intersects L_{j-5}.

Similar notations apply for $h \le k$ and for $|h|$. Notice that the events $\mathcal{E}_{h\ge k}(j,\alpha)$ for $\alpha \in \{0,+,-\}$ are all increasing, they are not mutually exclusive, and we have

$$\bigcup_{\alpha\in\{-,0,+\}} \mathcal{E}_{h\ge k}(j,\alpha) \;=\; \{I_j \xleftrightarrow{h\ge k \text{ in } \mathbb{R}\times[0,n]} \tilde{I}_j\}. \tag{III.11}$$

Write ζ for the largest boundary condition for the strip $\mathbb{Z}\times[0,n]$, which takes values at most k and values in $\{0,1\}$ outside of I_{-2}, I_0, I_2 and their top counterparts $\tilde{I}_{-2}$, $\tilde{I}_0$ and $\tilde{I}_2$; see Figure III.5(right) for an illustration. Next we state a lemma that will quickly imply the desired result.

Lemma III.3.5. *For $c = 1/4$, any $k \ge 36$, and any $\alpha \in \{0,+,-\}$, we have*

$$\mathbb{P}^{\xi}[I_0 \xleftrightarrow{h\ge(1-c)k} \tilde{I}_0] \le 1 - \tfrac{1}{6}\mathbb{P}^{\zeta}[\mathcal{E}_{h\le ck}(-3,\alpha)\cap\mathcal{E}_{h\le ck}(-1,\alpha)\cap\mathcal{E}_{h\le ck}(1,\alpha)\cap\mathcal{E}_{h\le ck}(3,\alpha)], \tag{III.12}$$

with ξ the boundary conditions defined in Proposition III.3.4 for $i = 0$.

Before proving the lemma, let us see how it allows us to conclude the proof of Proposition III.3.4. For an integer j, let $\tau_j\xi$ be the horizontal shift of the boundary condition ξ by $j\delta n$, and remark that by definition of ξ and ζ, if j is an odd integer we have $\tau_j\xi \le k - \zeta$. Using first the sign flip invariance of the height function and then the (CBC) inequality and the horizontal shift symmetry[9], we have, for all $j \in \{\pm3,\pm1\}$ and $\alpha \in \{-,0,+\}$,

$$\mathbb{P}^{\zeta}[\mathcal{E}_{h\le ck}(j,\alpha)] = \mathbb{P}^{k-\zeta}[\mathcal{E}_{h\ge(1-c)k}(j,\alpha)] \ge \mathbb{P}^{\xi}[\mathcal{E}_{h\ge(1-c)k}(0,\alpha)].$$

By (III.11), we conclude that there exists $\alpha_0 \in \{-,0,+\}$ such that

$$\mathbb{P}^{\xi}[\mathcal{E}_{h\ge(1-c)k}(0,\alpha_0)] \ge \tfrac{1}{3}\mathbb{P}^{\xi}[I_0 \xleftrightarrow{h\ge(1-c)k} \tilde{I}_0].$$

Using first the FKG inequality for the decreasing events $\mathcal{E}_{h\le ck}(j,\alpha_0)$, and then the two previously displayed equations, we get

$$\begin{aligned}\mathbb{P}^{\zeta}[\mathcal{E}_{h\le ck}(-3,\alpha_0)\cap\mathcal{E}_{h\le ck}(-1,\alpha_0)\cap\mathcal{E}_{h\le ck}(1,\alpha_0)\cap\mathcal{E}_{h\le ck}(3,\alpha_0)] &\ge \prod_{j\in\{\pm3,\pm1\}} \mathbb{P}^{\zeta}[\mathcal{E}_{h\le ck}(j,\alpha_0)]\\ &\ge \Big(\tfrac{1}{3}\mathbb{P}^{\xi}[I_0 \xleftrightarrow{h\ge(1-c)k} \tilde{I}_0]\Big)^4.\end{aligned}$$

Injecting this into (III.12), we conclude that for $c = 1/4$, $\mathbb{P}^{\xi}[I_0 \xleftrightarrow{h\ge(1-c)k} \tilde{I}_0]$ is bounded above by an absolute constant strictly smaller than 1. Adjusting the value of c to a smaller constant if need be, we find (III.10) with $i = 0$.

Case $i \ne 0$: Fix constants δ and c so that (III.10) holds for $i = 0$ with these constants. Define $\delta' = \delta/3$; we will prove Proposition III.3.4 for δ' instead of

[9] Note that we shift the boundary condition by k, which swaps the odd and even faces in case k is odd. They can be swapped back by shifting the strip horizontally by $(1,0)$; alternatively, the reader may observe that it suffices to prove the claim for even k here. We will keep these manipulations implicit in the subsequent parity swaps occurring in the rest of the article.

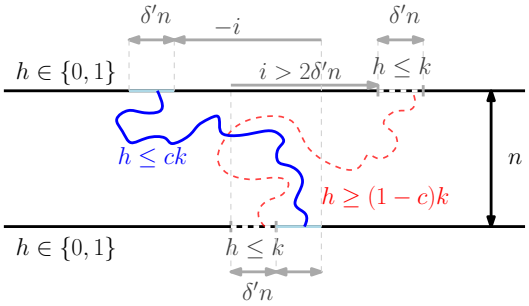

Figure III.6: A geometric argument in the end of the proof of Proposition III.3.4. The light-blue and dashed boundary segments are reflection symmetric. The small-height crossing between the light-blue boundary segments (in blue) excludes the large-height crossing between the dashed boundary segments (in dashed red). Solid-line boundaries represent here boundary conditions $0, 1$ and dashed boundaries represent their maximal extensions smaller or equal to k.

δ, and omit integer roundings also in $\lfloor \delta' n \rfloor$. By the (CBC) inequality, for any $i \in [-2\delta' n, 2\delta' n]$,

$$\mathbb{P}^{\xi'}\big[[0,\delta' n]\times\{0\} \overset{h\ge(1-c)k}{\longleftrightarrow} [i, i+\delta' n]\times\{n\}\big] \\ \le \mathbb{P}^{\xi}\big[[0,\delta n]\times\{0\} \overset{h\ge(1-c)k}{\longleftrightarrow} [0,\delta n]\times\{n\}\big] < (1-c),$$

where $\xi' \le \xi$ are the boundary conditions on $\partial\mathbb{Z}\times[0,n]$ defined in the statement of Proposition III.3.4 for δ' and δ, respectively, and for $i = 0$ for the latter.

It thus remains to prove Proposition III.3.4 for $|i| > 2\delta' n$. By vertical reflection symmetry of the model, we may assume $i > 2\delta' n$. Now, using first the sign flip invariance of the height function and then the (CBC) inequality and the vertical reflection symmetry (see Figure III.6), we compute

$$\begin{aligned}
&\mathbb{P}^{\xi'}\big[[\delta' n, 2\delta' n]\times\{0\} \overset{h\le ck}{\longleftrightarrow} [-i+\delta' n, -i+2\delta' n]\times\{n\}\big] \\
&\quad = \mathbb{P}^{k-\xi'}\big[[\delta' n, 2\delta' n]\times\{0\} \overset{h\ge(1-c)k}{\longleftrightarrow} [-i+\delta' n, -i+2\delta' n]\times\{n\}\big] \\
&\quad \ge \mathbb{P}^{\xi'}\big[[0,\delta' n]\times\{0\} \overset{h\ge(1-c)k}{\longleftrightarrow} [i, i+\delta' n]\times\{n\}\big].
\end{aligned}$$

Moreover, notice that as $c \le 1/4$ (due to the assumption of previous lemma) and $k \ge 1/c \ge 4$, the event on the left hand side above excludes the one on the right-hand side (see Figure III.6 again). We conclude that

$$\mathbb{P}^{\xi'}\big[[0,\delta' n]\times\{0\} \overset{h\ge(1-c)k}{\longleftrightarrow} [i, i+\delta' n]\times\{n\}\big] \le \tfrac{1}{2}.$$

□

We now give the proof of Lemma III.3.5.

Lemma III.3.5. Fix $\alpha \in \{0, -, +\}$. Set

$$\mathcal{S} := \mathcal{E}_{h\le ck}(-3,\alpha)\cap\mathcal{E}_{h\le ck}(-1,\alpha)\cap\mathcal{E}_{h\le ck}(1,\alpha)\cap\mathcal{E}_{h\le ck}(3,\alpha)\cap\{I_{-2} \overset{h\ge(1-c)k}{\longleftrightarrow} \tilde{I}_{-2}\}\cap\{I_2 \overset{h\ge(1-c)k}{\longleftrightarrow} \tilde{I}_2\}.$$

We first claim that it suffices to prove that

$$\mathbb{P}^{\zeta}[I_0 \xleftrightarrow{h\geq(1-c)k} \tilde{I}_0 \,|\, \mathcal{S}] \leq 1/2. \tag{III.13}$$

Indeed, (III.13) implies that

$$\mathbb{P}^{\zeta}\Big[\Big(\bigcap_{j\in\{0,\pm2\}} \{I_j \xleftrightarrow{h\geq(1-c)k} \tilde{I}_j\}\Big)^c\Big] \geq \tfrac{1}{2}\mathbb{P}^{\zeta}[\mathcal{E}_{h\leq ck}(-3,\alpha)\cap\mathcal{E}_{h\leq ck}(-1,\alpha)\cap\mathcal{E}_{h\leq ck}(1,\alpha)\cap\mathcal{E}_{h\leq ck}(3,\alpha)],$$

and therefore there exists $j_0 \in \{0,\pm2\}$ such that

$$\mathbb{P}^{\zeta}\Big[I_{j_0} \xleftrightarrow{h\geq(1-c)k} \tilde{I}_{j_0}\Big] \leq 1 - \tfrac{1}{6}\mathbb{P}^{\zeta}[\mathcal{E}_{h\leq ck}(-3,\alpha)\cap\mathcal{E}_{h\leq ck}(-1,\alpha)\cap\mathcal{E}_{h\leq ck}(1,\alpha)\cap\mathcal{E}_{h\leq ck}(3,\alpha)].$$

Finally, observe that the boundary conditions ζ are such that

$$\mathbb{P}^{\xi}[I_0 \xleftrightarrow{h\geq(1-c)k} \tilde{I}_0] \leq \mathbb{P}^{\zeta}[I_j \xleftrightarrow{h\geq(1-c)k} \tilde{I}_j] \quad \text{for every } j\in\{-2,0,2\}.$$

In conclusion, (III.12) is indeed implied by (III.13), and we will focus on proving the latter.

For $h\in\mathcal{S}$, the fact that $\mathcal{E}_{h\leq ck}(-3,\alpha)$, $\mathcal{E}_{h\leq ck}(-1,\alpha)$ and $I_{-2} \xleftrightarrow{h\geq(1-c)k} \tilde{I}_{-2}$ occur, induces the existence of a leftmost crossing γ_L of $h\leq ck$ from I_{-1} to $\tilde{I}_{-1}$. Similarly, there exists a rightmost crossing γ_R of $h\leq ck$ from I_1 to $\tilde{I}_1$.

Let D be the discrete domain made of faces of $\mathbb{Z}\times[0,n]$ that are between γ_L and γ_R, or on γ_L and γ_R. Notice that the event $\mathcal{S}$ and the paths γ_L and γ_R are measurable in terms of the values of the height function on $D^c\cup\partial D$. Moreover, when $\mathcal{S}$ occurs, all faces on γ_L and γ_R have height ck or $ck-1$ [10]. See Figure III.7.

Thus, conditionally on a realisation of γ_L, γ_R and h on $D^c\cup\partial D$, the height function in D is distributed according to $\mathbb{P}_D^{\chi}$, where χ is identical to ζ on the boundary of the strip $\mathbb{Z}\times[0,n]$ and is equal to ck or $ck-1$ on γ_L and γ_R. Let $\mathcal{X}$ be the set of possible realisations of (D,χ) such that $\mathcal{S}$ occurs. Then

$$\mathbb{P}^{\zeta}[\mathcal{S}] = \sum_{(D,\chi)\in\mathcal{X}} \mathbb{P}^{\zeta}[\gamma_L,\gamma_R \text{ bound } D] \qquad \text{and}$$

$$\mathbb{P}^{\zeta}[\{I_0 \xleftrightarrow{h\geq(1-c)k} \tilde{I}_0\}\cap\mathcal{S}] = \sum_{(D,\chi)\in\mathcal{X}} \mathbb{P}_D^{\chi}[I_0 \xleftrightarrow{h\geq(1-c)k} \tilde{I}_0]\,\mathbb{P}^{\zeta}[\gamma_L,\gamma_R \text{ bound } D].$$

To prove (III.13), it thus suffices to show that for every $(D,\chi)\in\mathcal{X}$,

$$\mathbb{P}_D^{\chi}[I_0 \xleftrightarrow{h\geq(1-c)k} \tilde{I}_0] \leq \tfrac{1}{2}. \tag{III.14}$$

If γ_L and γ_R intersect, then the left-hand side is equal to 0 and there is nothing to do, so we restrict ourselves to domains D for which γ_L and γ_R do not intersect. In the rest of the proof we show (III.14) by distinguishing between the different values of α. We only describe the proof for $\alpha=0$ and $\alpha=+$; the proof for $\alpha=-$ is the same as that for $\alpha=+$.

[10] In this sentence and for the rest of this proof we suppress for the sake of streamlined writing two minor details. First, we omit the integer roundings from $\lfloor ck\rfloor$ when it appears in exact height function values. Second, as γ_L ends on I_{-1} and $\tilde{I}_{-1}$ where the boundary condition is $0,1$ the height value at the endpoints and close to them is not ck or $ck-1$. Due to being leftmost, γ_L actually slides directly to the left from both end points, to reach the height ck or $ck-1$ in I_{-2} and $\tilde{I}_{-2}$, respectively, and then connects these "left-pushed endpoints" by a curve on which the height indeed is ck or $ck-1$.

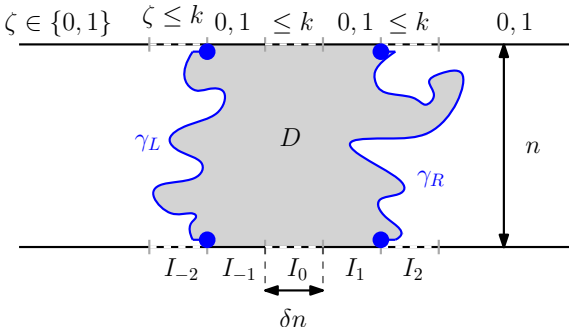

Figure III.7: Illustration for the proof of Lemma III.3.5. The curves γ_L and γ_R (blue) and the boundary segments of the strip between them define the quad D. Solid-line boundaries represent here boundary conditions $\zeta \in \{0,1\}$, and dashed lines represent maximal extensions of boundary conditions remaining at most k.

Case of $\alpha = 0$: Since $\mathcal{S}$ occurs, γ_L and γ_R are contained between any path of height $h \le ck$ from I_{-3} to $\tilde{I}_{-3}$ and from I_3 to $\tilde{I}_3$. As we are in the case $\alpha = 0$, such paths exist left of L_{-8} and right of L_9. Thus D is necessarily contained in a $n \times n$ square $D' \supset [-8\delta n, 9\delta n] \times [0, n]$ (recall that $17\delta n \le n$).

Denote by $\{ck, ck-1\}$ the boundary condition on ∂D taking only values ck and $ck-1$, and by $\chi \vee \{ck, ck-1\}$ the pointwise maximum of the two; by (CBC),

$$\mathbb{P}_D^{\chi}[I_0 \xleftrightarrow{h \ge (1-c)k} \tilde{I}_0] \le \mathbb{P}_D^{\chi \vee \{ck, ck-1\}}[I_0 \xleftrightarrow{h \ge (1-c)k} \tilde{I}_0].$$

Note that on the left and right sides of D, χ (and thus also $\chi \vee \{ck, ck-1\}$) takes values ck and $ck-1$. Let χ' be the boundary condition for $\mathcal{H}_{D'}$ on $\partial D'$ which is equal to $\chi \vee \{ck, ck-1\}$ on $\partial D \cap \partial D'$ and on the faces of $\partial D'$ left or right of D takes values ck and $ck-1$. By definition, $ck - 1 \le \chi' \le k$, and we can apply the boundary pushing of Corollary III.2.7 (recall that $c = 1/4$ so $ck - 1 < (1-c)k$) to get

$$\mathbb{P}_D^{\chi \vee \{ck, ck-1\}}[I_0 \xleftrightarrow{h \ge (1-c)k} \tilde{I}_0] \le \mathbb{P}_{D'}^{\chi'}[I_0 \xleftrightarrow{h \ge (1-c)k-2 \text{ in } D} \tilde{I}_0] \le \mathbb{P}_{D'}^{\chi'}[\mathcal{V}_{h \ge (1-c)k-2}(D')],$$

where $\mathcal{V}_{h \ge (1-c)k-2}(D')$ denotes the existence of a path of $h \ge (1-c)k - 2$ crossing D' vertically. Recall from Remark III.3.2 that $\mathcal{V}_{h \ge (1-c)k-2}(D') \subset \mathcal{H}_{h \le (1-c)k-3}(D')^c$, where $\mathcal{H}$ refers to horizontal crossings. Apply now Lemma III.3.3 to the symmetric domain D', with the boundary conditions $(1-c)k - 3 - \chi'$, to conclude that

$$\mathbb{P}_{D'}^{\chi'}[\mathcal{V}_{h \ge (1-c)k-2}(D')] \le 1 - \mathbb{P}_{D'}^{\chi'}[\mathcal{H}_{h \le (1-c)k-3}(D')] \le \tfrac{1}{2},$$

for all $k \ge 20$.

Case of $\alpha = +$: Since $\mathcal{E}_{h \le ck}(-3, +)$ and $I_{-2} \xleftrightarrow{h \ge (1-c)k} \tilde{I}_{-2}$ occur, γ_L necessarily intersects the vertical line L_3 (see Figure III.8). Orient γ_L from bottom to top and let γ_1 be its subpath up to its first intersection with L_3. Write a for the starting point of γ_L and B for the segment of $\mathbb{Z} \times \{0\}$ between a and $(3\delta n, 0)$. Let σ be the reflection with respect to the line of faces touching L_3 on the left (σ thus preserves

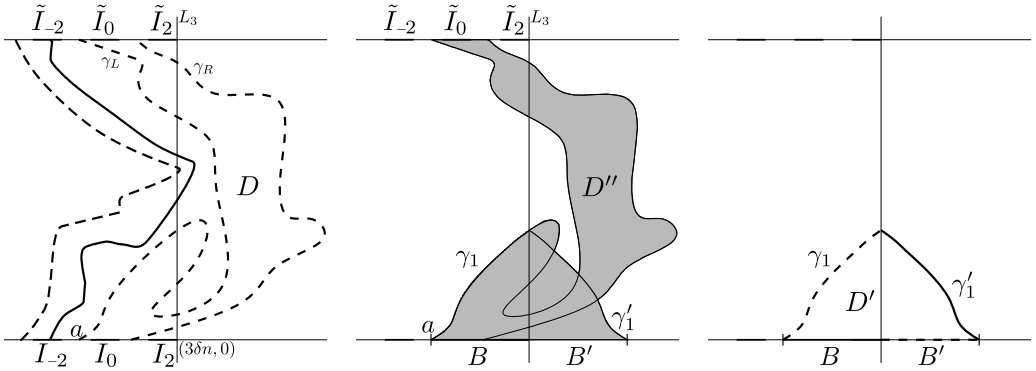

Figure III.8: The dashed lines represent boundary conditions $ck, ck-1$, while the thick ones are boundary conditions $k, k-1$ (up to interpolations at the ends of the intervals). The segments at the bottom and top have length δn. *Left:* the domain D formed of faces contained between γ_L and γ_R. *Middle:* the domain D is extended into D'' by pushing away the (small) boundary conditions $ck, ck-1$. The probability of existence of a crossing from I_0 to $\tilde{I}_0$ of large height increases. *Right:* the domain D'' is shrunk to D' by pulling closer the (large) boundary conditions $k, k-1$. The probability of existence of a crossing from γ_1 to B' of low height decreases.

parity); define $\gamma_1' = \sigma(\gamma_1)$ and $B' = \sigma(B)$. Set D' to be the simply connected domain bounded by B, B', γ_1' and γ_1; let $D'' = D' \cup D$; see Figure III.8 for an illustration.

Let $\chi \vee \{ck, ck-1\}$ be as above and write χ'' for the lowest boundary conditions on $\partial D''$ which are identical to ξ on $\partial D'' \cap \partial D$ and $\{ck, ck-1\}$ on the right or left of D. Applying (CBC) and (III.5) we find,

$$\mathbb{P}_D^{\xi}[I_0 \xleftrightarrow{h \geq (1-c)k} \tilde{I}_0] \leq \mathbb{P}_D^{\xi \vee \{ck, ck-1\}}[I_0 \xleftrightarrow{h \geq (1-c)k} \tilde{I}_0] \leq \mathbb{P}_{D''}^{\xi''}[I_0 \xleftrightarrow{h \geq (1-c)k-2} \tilde{I}_0].$$

As stated in Remark III.3.2, the event $I_0 \xleftrightarrow{h \geq (1-c)k-2} \tilde{I}_0$ is incompatible with the event $\gamma_1 \xleftrightarrow{h \leq (1-c)k-3 \text{ in } D''} B'$, so

$$\mathbb{P}_{D''}^{\xi''}[I_0 \xleftrightarrow{h \geq (1-c)k-2} \tilde{I}_0] \leq 1 - \mathbb{P}_{D''}^{\xi''}[\gamma_1 \xleftrightarrow{h \leq (1-c)k-3} B'].$$

Next, write ξ' for the largest boundary conditions on $\partial D'$ which is smaller or equal to k and equal to ξ'' on $\partial D' \cap \partial D''$. Applying (III.5) to $-h$, we get

$$\mathbb{P}_{D''}^{\xi''}[\gamma_1 \xleftrightarrow{h \leq (1-c)k-3} B'] \geq \mathbb{P}_{D'}^{\xi'}[\gamma_1 \xleftrightarrow{h \leq (1-c)k-5} B'].$$

Observe that D' is invariant under σ. Apply Lemma III.3.3 to the boundary condition $(1-c)k - 5 - \xi'$ to find that

$$\mathbb{P}_{D'}^{\xi'}[\gamma_L \xleftrightarrow{h \leq (1-c)k-5 \text{ in } D'} B'] \geq \tfrac{1}{2},$$

for $k \geq 36$. The four equations displayed above imply (III.14). □

III.3.4 Long crossings in a strip

In our proof of Theorem III.3.1, the intermediate result below refers to crossings of long rectangles in a strip. We remind the reader that we still omit the integer roundings in $\lfloor \delta n \rfloor$.

Proposition III.3.6. *There exist constants $\delta, c, C > 0$ such that the following holds. For any $k \geq 1/c$, any n, and any $\rho \geq 1$,*

$$\mathbb{P}^{0,1}_{\mathbb{Z}\times[-n,2n]}\big[\{0\}\times[-n,2n] \xleftarrow{h\geq ck \text{ in } \mathbb{Z}\times[0,n]} \{\rho\delta n\}\times[-n,2n]\big] \\ \geq \big(c\,\mathbb{P}^{0,1}_{\mathbb{Z}\times[-n,2n]}\big[[0,\delta n]\times\{0\} \xleftarrow{h\geq k \text{ in } \mathbb{Z}\times[0,n]} \mathbb{Z}\times\{n\}\big]\big)^{C\rho}. \quad \text{(III.15)}$$

Let us prepare for the proof of Proposition III.3.6 by fixing $\delta > 0$ such that Proposition III.3.4 applies for 3δ, and the constant $c_0 > 0$ appearing soon, which is given by the same proposition so that (III.18) below holds. For notation, as in the proof of Proposition III.3.4, we denote

$$I_j := [j\delta n, (j+1)\delta n]\times\{0\} \quad \text{and} \quad \tilde{I}_j := [j\delta n, (j+1)\delta n]\times\{n\}.$$

Moreover, let $\mathcal{B}_{h\geq\ell}(j)$ denote the "bridging" between I_{j-1} and I_{j+1} in $\mathbb{Z}\times[0,n]$:

$$\mathcal{B}_{h\geq\ell}(j) := \big\{I_{j-1} \xleftarrow{h\geq\ell \text{ in } \mathbb{Z}\times[0,n]} I_{j+1}\big\},$$

and define $\mathcal{B}_{|h|\geq\ell}(j)$ analogously. The following lemma is the key step in the proof of Proposition III.3.6.

Lemma III.3.7. *With the notation above,*

$$\mathbb{P}^{0,1}_{\mathbb{Z}\times[-n,2n]}[\mathcal{B}_{h\geq c_0k}(0)] \geq \tfrac{c_0}{8}\big(\mathbb{P}^{0,1}_{\mathbb{Z}\times[-n,2n]}\big[I_0 \xleftarrow{h\geq k \text{ in } \mathbb{Z}\times[0,n]} \tilde{I}_0\big]\big)^2. \quad \text{(III.16)}$$

The idea behind the proof of this lemma is simple: condition on the left- and right-most crossings of height greater than k from I_{-1} to $\tilde{I}_{-1}$ and from I_1 to $\tilde{I}_1$, respectively, then use Proposition III.3.4 to connect these two paths by a path of height at least ck. However, there are problems arising when pushing away boundary conditions; to overcome these we will need to use the FKG property for the absolute value of the height function (FKG-|h|).

Proof. We start by transferring the question to crossings in the absolute value of the height function. First, by the comparison between boundary conditions for h, we have

$$\mathbb{P}^{0,1}_{\mathbb{Z}\times[-n,2n]}[\mathcal{B}_{h\geq c_0k}(0)] \geq \tfrac{1}{2}\mathbb{P}^{0,1}_{\mathbb{Z}\times[-n,2n]}[\mathcal{B}_{|h|\geq c_0k}(0)].$$

Now, if we define

$$\mathcal{T} := \{I_{-1} \xleftarrow{|h|\geq k \text{ in } \mathbb{Z}\times[0,n]} \tilde{I}_{-1}\} \cap \{I_1 \xleftarrow{|h|\geq k \text{ in } \mathbb{Z}\times[0,n]} \tilde{I}_1\},$$

we have, due to the inclusion of events and the FKG inequality

$$\mathbb{P}^{0,1}_{\mathbb{Z}\times[-n,2n]}[\mathcal{T}] \geq \big(\mathbb{P}^{0,1}_{\mathbb{Z}\times[-n,2n]}\big[I_0 \xleftarrow{h\geq k \text{ in } \mathbb{Z}\times[0,n]} \tilde{I}_0\big]\big)^2.$$

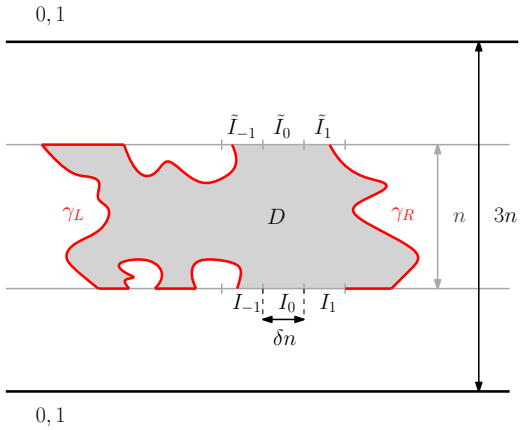

Figure III.9: An illustration for the proof of Lemma III.3.7. The red paths γ_L and γ_R have $|h| \geq k$ and are measurable in terms of the value of $|h|$ on them and on the faces to their left and right, respectively.

It thus suffices to prove

$$\mathbb{P}^{0,1}_{\mathbb{Z}\times[-n,2n]}[\mathcal{B}_{|h|\geq c_0 k}(0) \mid \mathcal{T}] \geq c_0/4. \tag{III.17}$$

When $\mathcal{T}$ occurs, write γ_L for the left-most path in $\mathbb{Z} \times [0, n]$ with $|h| \geq k$ connecting I_{-1} to $\tilde{I}_{-1}$. Similarly, let γ_R be the right-most path in $\mathbb{Z} \times [0, n]$ with $|h| \geq k$ connecting I_1 to $\tilde{I}_1$. (By finite energy, such paths exist almost surely.) Write D for the discrete sub-domain $\mathbb{Z} \times [0, n]$ of faces between or on the paths γ_L and γ_R. (See Figure III.9 for an illustration.) Notice that γ_L and γ_R are measurable in terms of the absolute value of the height function on $D^{\text{out}} = (\mathbb{Z}\times[-n, 2n]\setminus D)\cup\partial D$. Equip D with the structure of a quad with γ_L and γ_R being two sides and the remaining two contained in $\mathbb{Z} \times [0, 1]$ and $\mathbb{Z} \times [n - 1, n]$, respectively, and denote as earlier $\mathcal{V}(D)$ and $\mathcal{H}(D)$ for vertical and horizontal crossing events, respectively.

By inclusion of events, the (CBC-|h|) inequality, and inclusion again, we have

$$\begin{aligned}
\mathbb{P}^{0,1}_{\mathbb{Z}\times[-n,2n]}\big[\mathcal{B}_{|h|\geq c_0 k}(0) \,\big|\, |h| \text{ on } D^{\text{out}}\big] &\geq \mathbb{P}^{0,1}_{\mathbb{Z}\times[-n,2n]}\big[\mathcal{H}_{|h|\geq c_0 k}(D) \,\big|\, |h| \text{ on } D^{\text{out}}\big] \\
&\geq \mathbb{P}^{0,1}_{\mathbb{Z}\times[-n,2n]}\big[\mathcal{H}_{|h|\geq c_0 k}(D) \,\big|\, |h| = \zeta \text{ on } D^{\text{out}}\big], \\
&\geq \mathbb{P}^{0,1}_{\mathbb{Z}\times[-n,2n]}\big[\mathcal{H}_{h\geq c_0 k}(D) \,\big|\, |h| = \zeta \text{ on } D^{\text{out}}\big],
\end{aligned}$$

where $\zeta \geq 0$ is the minimal configuration on D^c which is equal to k and $k+1$ on γ_L and γ_R.

Now, it holds true that conditionally on the fact that $|h| = \zeta$ on D^{out}, there is a probability at least $1/4$ that h is equal to k and $k + 1$ on both γ_L and γ_R [11]. In that case, the boundary condition for h on ∂D, induced by $|h| = \zeta$, dominates the minimal boundary condition ξ on ∂D with $\xi \geq -1$ and which is equal to k and $k+1$

[11] This follows from the observation in Section III.6.1 that given the absolute value, the signs of a height function are given by a (ferromagnetic) Ising model. The positive association of the Ising model and the positive boundary signs in $\mathbb{P}^{0,1}_{\mathbb{Z}\times[-n,2n]}$ thus make two plus signs the most probable one out of the four possible sign combination on the curves γ_L and γ_R.

on γ_L and γ_R. Thus,

$$\begin{aligned}\mathbb{P}^{0,1}_{\mathbb{Z}\times[-n,2n]}\big[\mathcal{H}_{h\geq c_0k}(D)\,\big|\,|h|=\zeta \text{ on } D^{\text{out}}\big] &\geq \tfrac{1}{4}\mathbb{P}^{\xi}_{D}\big[\mathcal{H}_{h\geq c_0k}(D)\big]\\ &= \tfrac{1}{4}\mathbb{P}^{k-\xi}_{D}\big[\mathcal{H}_{h\leq(1-c_0)k}(D)\big]\\ &\geq \tfrac{1}{4}\big(1-\mathbb{P}^{k-\xi}_{D}\big[\mathcal{V}_{h\geq(1-c_0)k}(D)\big]\big),\end{aligned}$$

where the last line is due to Remark III.3.2.

Notice now that the boundary conditions $k-\xi$ are bounded above by $k+1$ and are equal to 0 and -1 on γ_R and γ_L. Using boundary pushing (Proposition III.2.6), we may now compare to $\mathbb{P}^{\xi'}_{\mathbb{Z}\times[0,n]}$ where ξ' is the largest boundary condition smaller than $k+1$ and which is equal to 0 and 1 on $(\mathbb{Z}\setminus[-\delta n,2\delta n])\times\{0,n\}$. We obtain

$$\begin{aligned}\mathbb{P}^{k-\xi}_{D}\big[\mathcal{V}_{h\geq(1-c_0)k}(D)\big] &\leq \mathbb{P}^{\xi'}_{\mathbb{Z}\times[0,n]}\big[\mathcal{V}_{h\geq(1-c_0)k}(D)\big]\\ &\leq \mathbb{P}^{\xi'}_{\mathbb{Z}\times[0,n]}\big[[-\delta n,2\delta n]\times\{0\}\xleftrightarrow{h\geq(1-c_0)k}[-\delta n,2\delta n]\times\{n\}\big],\end{aligned}$$

where the latter inequality used the fact that the bottom and top boundary segments of the quad D contain the intervals $[-\delta n,2\delta n]\times\{0\}$ and $[-\delta n,2\delta n]\times\{n\}$.

Finally, Proposition III.3.4 proves that

$$\mathbb{P}^{\xi'}_{\mathbb{Z}\times[0,n]}\big[[-\delta n,2\delta n]\times\{0\}\xleftrightarrow{h\geq(1-c_0)k}[-\delta n,2\delta n]\times\{n\}\big]\leq 1-c_0 \tag{III.18}$$

(as such, with the boundary conditions ξ', Proposition III.3.4 addresses crossings of $h\geq(1-c_0)(k+1)$ but the choice of c_0 allows us to ignore this difference).

The four previously displayed inequalities yield for any D^{out}

$$\mathbb{P}^{0,1}_{\mathbb{Z}\times[-n,2n]}\big[\mathcal{B}_{|h|\geq c_0k}\,\big|\,|h| \text{ on } D^{\text{out}}\big]\geq\tfrac{1}{4}c_0.$$

This finishes the proof of (III.17) and the entire lemma. □

Proposition III.3.6. It suffices to give the proof when ρ is an integer. When the events $\mathcal{B}_{h\geq c_0k}(j)$ with $0\leq j<\rho$ occur, they induce the existence of a path from $\{0\}\times[-n,2n]$ to $\{\rho\delta n\}\times[-n,2n]$ of height at least c_0k. Moreover, this path is contained in the central strip $\mathbb{Z}\times[0,n]$. Due to the FKG inequality, the invariance of $\mathbb{P}^{0,1}_{\mathbb{Z}\times[-n,2n]}$ under horizontal translations and Lemma III.3.7, we find

$$\begin{aligned}\mathbb{P}^{0,1}_{\mathbb{Z}\times[-n,2n]}\big[\{0\}\times[-n,2n]\xleftrightarrow{h\geq c_0k \text{ in } \mathbb{Z}\times[0,n]}\{\rho\delta n\}\times[-n,2n]\big]&\\ \geq \mathbb{P}^{0,1}_{\mathbb{Z}\times[-n,2n]}[\mathcal{B}_{h\geq c_0k}(j)]^{\rho}&\\ \geq \Big[\tfrac{c_0}{8}\mathbb{P}^{0,1}_{\mathbb{Z}\times[-n,2n]}\big[I_0\xleftrightarrow{h\geq k \text{ in } \mathbb{Z}\times[0,n]}\tilde{I}_0\big]^2\Big]^{\rho}.&\end{aligned}\tag{III.19}$$

We now claim that

$$\mathbb{P}^{0,1}_{\mathbb{Z}\times[-n,2n]}\big[I_0\xleftrightarrow{h\geq k \text{ in } \mathbb{Z}\times[0,n]}\tilde{I}_0\big]\geq\Big(\tfrac{1}{3}\mathbb{P}^{0,1}_{\mathbb{Z}\times[-n,2n]}\big[I_0\xleftrightarrow{h\geq k \text{ in } \mathbb{Z}\times[0,n]}\mathbb{Z}\times\{n\}\big]\Big)^2,\tag{III.20}$$

which together with (III.19) completes the proof. To prove (III.20), observe that if the event on the right-hand side occurs, then I_0 is either connected by $h\geq k$

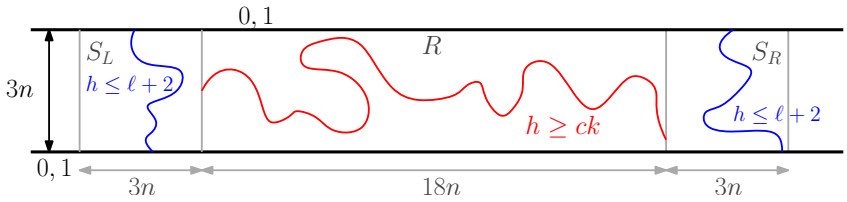

Figure III.10: The last step in the proof of Theorem III.3.1 is based on the Bayes formula for the events of the horizontal crossing $\mathcal{H}_{h\ge ck}(R)$ and the two vertical crossings $\mathcal{V}_{h\le\ell}(S_L)$ and $\mathcal{V}_{h\le\ell}(S_R)$.

to either to $\tilde{I}_0$, to $(-\infty, 0] \times \{n\}$ or to $[\delta n, \infty) \times \{n\}$. It follows that at least one of these connections has probability $\frac{1}{3}\mathbb{P}^{0,1}_{\mathbb{Z}\times[-n,2n]}\big[I_0 \xleftrightarrow{h\ge k \text{ in } \mathbb{Z}\times[0,n]} \mathbb{Z}\times\{n\}\big]$; if it is the connection to $\tilde{I}_0$, (III.20) follows immediately, so assume next that it is the connection to $[\delta n, \infty) \times \{n\}$ (the third case is symmetric).

Now, if I_0 is connected to $[\delta n, \infty) \times \{n\}$ and $\tilde{I}_0$ to $[\delta n, \infty) \times \{0\}$ by paths of height at least k simultaneously, then I_0 and $\tilde{I}_0$ are connected to each other by such paths. Thus, using the vertical symmetry and the FKG inequality,

$$\mathbb{P}^{0,1}_{\mathbb{Z}\times[-n,2n]}\big[I_0 \xleftrightarrow{h\ge k \text{ in } \mathbb{Z}\times[0,n]} \tilde{I}_0\big] \ge \mathbb{P}^{0,1}_{\mathbb{Z}\times[-n,2n]}\big[I_0 \xleftrightarrow{h\ge k \text{ in } \mathbb{Z}\times[0,n]} [\delta n, \infty) \times \{n\}\big]^2,$$

and (III.20) follows from the assumption of the previous paragraph. □

III.3.5 From strip to annulus

In this section we conclude the proof of Theorem III.3.1. The fairly classic argument consists in combining different crossings in rectangles and using the proper comparison between boundary conditions.

Theorem III.3.1. Write $\mathcal{H}_{h\ge\ell}(R)$ for the event that the rectangle $R := [0, 18n] \times [-n, 2n]$ contains a horizontal crossing of height at least ℓ, that is a path of $h \ge \ell$ from $\{0\}\times[-n, 2n]$ to $\{18n\}\times[-n, 2n]$. By Proposition III.3.6, we may fix constants c, C, δ such that

$$\mathbb{P}^{0,1}_{\mathbb{Z}\times[-n,2n]}[\mathcal{H}_{h\ge ck}(R)] \ge c\,\mathbb{P}^{0,1}_{\mathbb{Z}\times[-n,2n]}\big[[0, \delta n] \times \{0\} \xleftrightarrow{h\ge k \text{ in } \mathbb{Z}\times[0,n]} \mathbb{Z}\times\{n\}\big]^C.$$

Let $S_L = [-3n, 0] \times [-n, 2n]$ and $S_R = [18n, 21n] \times [-n, 2n]$ be the two squares to the left and right of R, respectively. Write $\mathcal{V}_{h\le\ell}(S_L)$ for the event that there exists a path from the top $[-3n, 0] \times \{2n\}$ to the bottom $[-3n, 0] \times \{-n\}$ of S_L formed of faces with height at most ℓ. The same notation applies to S_R. See Figure III.10.

When $\mathcal{H}_{h\ge ck}(R)$ occurs, let Γ be the lowest path connecting the left and right sides of R which is of height greater or equal to ck. Notice that Γ may be explored by revealing a random set of faces $F \subset R$, all of whose heights are at most $ck+1$ (here and below, we omit integer roundings of $\lceil ck\rceil$ and treat ck as an integer). Denote also $\ell = \lceil (ck+1)/2\rceil$. We have for any possible realisation γ of Γ, using (III.5) for $-h$,

$$\mathbb{P}^{0,1}_{\mathbb{Z}\times[-n,2n]}[\mathcal{V}_{h\le\ell+2}(S_L) \cap \mathcal{V}_{h\le\ell+2}(S_R) | \,\Gamma = \gamma] \ge \mathbb{P}^{\xi_L}_{S_L}[\mathcal{V}_{h\le\ell}(S_L)]\mathbb{P}^{\xi_R}_{S_R}[\mathcal{V}_{h\le\ell}(S_R)],$$

where ξ_L and ξ_R are the largest boundary conditions on ∂S_L and ∂S_R, respectively, that are everywhere at most $ck+1$ and equal to 0 and 1 on $\mathbb{Z}\times\{-n,3n\}$. Now, due to Lemma III.3.3, each of the probabilities of the right-hand side above is at least $1/2$. In conclusion,

$$\begin{aligned}\mathbb{P}^{0,1}_{\mathbb{Z}\times[-n,2n]}&[\mathcal{H}_{h\geq ck}(R)\,|\,\mathcal{V}_{h\leq \ell+2}(S_L)\cap\mathcal{V}_{h\leq\ell+2}(S_R)]\\ &\geq \mathbb{P}^{0,1}_{\mathbb{Z}\times[-n,2n]}[\mathcal{H}_{h\geq ck}(R)\cap\mathcal{V}_{h\leq \ell+2}(S_L)\cap\mathcal{V}_{h\leq\ell+2}(S_R)]\\ &\geq \tfrac{c}{4}\mathbb{P}^{0,1}_{\mathbb{Z}\times[-n,2n]}\big[[0,\delta n]\times\{0\}\xleftrightarrow{h\geq k \text{ in } \mathbb{Z}\times[0,n]}\mathbb{Z}\times\{n\}\big]^C.\end{aligned}$$

When $\mathcal{V}_{h\leq\ell+2}(S_L)\cap\mathcal{V}_{h\leq\ell+2}(S_R)$ occurs, consider the discrete domain D on and between the vertical crossings of height at most $\ell+2$ that are left-most in S_L and right-most in S_R, respectively. By the spatial Markov property, the conditional measure on the left-hand side above can be seen as a convex combination of measures on such domains D, with boundary conditions which are at most $\ell+2$. By the previous display and the (CBC) inequality, we conclude the existence of such a domain D_0 with $[0,18n]\times[-n,2n]\subset D_0\subset[-3n,21n]\times[-n,2n]$ such that

$$\mathbb{P}^{\ell+1,\ell+2}_{D_0}[\mathcal{H}_{h\geq ck}(R)]\geq \tfrac{c}{4}\mathbb{P}^{0,1}_{\mathbb{Z}\times[-n,2n]}\big[[0,\delta n]\times\{0\}\xleftrightarrow{h\geq k \text{ in } \mathbb{Z}\times[0,n]}\mathbb{Z}\times\{n\}\big]^C. \tag{III.21}$$

Finally, consider the rectangle $R_N=[-9n,9n]\times[6n,9n]$ and its rotations R_W, R_S and R_E around the origin by $\frac{\pi}{2}$, π and $\frac{3\pi}{2}$, respectively. Note that R_N is a translate of the rectangle R considered above. By (III.5), we deduce that

$$\mathbb{P}^{0,1}_{\Lambda_{12n}}[\mathcal{H}_{h\geq ck-\ell-3}(R_N)]\geq\tfrac{1}{2}\mathbb{P}^{0,1}_{D_0}[\mathcal{H}_{h\geq ck-\ell-1}(R)]=\tfrac{1}{2}\mathbb{P}^{\ell+1,\ell+2}_{D_0}[\mathcal{H}_{h\geq ck}(R)].$$

By rotational invariance, the same lower bound holds for probabilities of crossing R_W, R_S and R_E in the "long" direction. If all these crossing events occur simultaneously, then $\Lambda_{9n}\setminus\Lambda_{6n}$ contains a circuit of height at least $ck-\ell-3\geq ck/2-6$, and thus $\mathcal{O}_{h\geq ck/2-6}(6n,12n)$ occurs. Applying the FKG inequality, we find

$$\mathbb{P}^{0,1}_{\Lambda_{12n}}[\mathcal{O}_{h\geq ck/2-6}(6n,12n)]\geq\big(\tfrac{c}{8}\big)^4\,\mathbb{P}^{0,1}_{\mathbb{Z}\times[-n,2n]}\big[[0,\delta n]\times\{0\}\xleftrightarrow{h\geq k \text{ in } \mathbb{Z}\times[0,n]}\mathbb{Z}\times\{n\}\big]^{4C}.$$

The above implies (III.7) after adjustment of the constants c, C. □

III.4 From free energy to circuit probability estimate

In this section, let N be even and let $\mathbb{P}^{(0)}_{\mathbb{O}_{N,M}}$ denote the six-vertex measure on the cylinder graph $\mathbb{O}_{N,M}$ conditioned on the event that each row of N faces around $\mathbb{O}_{N,M}$ is crossed by as many up arrows as down arrows. Under $\mathbb{P}^{(0)}_{\mathbb{O}_{N,M}}$, each six-vertex configuration defines a height function on the cylindrical dual graph which is unique up to additive constant. When describing events in terms of height function, we will mean that the associated equivalence class of height functions contains a representative having the property of interest.

III.4.1 A probabilistic interpretation of free energy increments

For $k, n \geq 1$ and a set $S = \{s_0, \dots, s_{2n-1}\}$ of $2n$ faces on the bottom of $\mathbb{O}_{N,M}$ (indexed from left to right), let $\mathcal{A}(S, n, k)$ be the event that for each $0 \leq i < 2n$, there exists a vertical $\times$-crossing of the cylinder, starting at s_i, and on which $h = 0$ if i is even, and $h = k$ if i is odd. The core of this section is the proof of the following result (recall the definition of the free energy $f_{\mathbf{c}}$ from Theorem III.1.6).

Proposition III.4.1. *For every $\alpha \in (0, 1/2)$ and $k \geq 1$, for $n = \lfloor \lceil \alpha N \rceil / k \rfloor$ we have*

$$\liminf_{N\to\infty} \liminf_{M\to\infty} \tfrac{1}{NM} \log \max_S \mathbb{P}^{(0)}_{\mathbb{O}_{N,M}}[\mathcal{A}(S, n, k)] \geq f_{\mathbf{c}}(\alpha) - f_{\mathbf{c}}(0),$$

where the maximum is over sets S of $2n$ faces on the bottom of $\mathbb{O}_{N,M}$.

Relating the probability of the events $\mathcal{A}(S, n, k)$ to $f_{\mathbf{c}}$ will be done in two steps. We start by relating the free energy to the probability of the event $\mathcal{B}(L)$ that h contains two vertical $\times$-crossings of $h = 0$ and $h = L$ respectively.

Lemma III.4.2. *For every $\alpha \in (0, 1/2)$, we have*

$$\liminf_{N\to\infty} \liminf_{M\to\infty} \tfrac{1}{NM} \log \mathbb{P}^{(0)}_{N,M}[\mathcal{B}(\lceil \alpha N \rceil)] \geq f_{\mathbf{c}}(\alpha) - f_{\mathbf{c}}(0).$$

Proof. In what follows, set $L = \lceil \alpha N \rceil$. The strategy of the proof is to construct a map

$$\mathbf{T} : \Omega^{(2L)}_{6V}(\mathbb{O}_{N,M}) \longrightarrow \Omega^{(0)}_{6V}(\mathbb{O}_{N,M}) \cap \mathcal{B}(L)$$

such that

(i) for any $\omega \in \Omega^{(2L)}_{6V}(\mathbb{O}_{N,M})$, we have $W_{6\mathrm{V}}(\mathbf{T}(\omega)) \geq \mathbf{c}^{-2M/\alpha} W_{6\mathrm{V}}(\omega)$,

(ii) for any $\omega' \in \Omega^{(0)}_{6V}(\mathbb{O}_{N,M}) \cap \mathcal{B}(L)$, the number of preimages $|\mathbf{T}^{-1}(\{\omega'\})|$ is bounded by $N^2 2^{2M/\alpha}$.

Assuming for a moment that such a map $\mathbf{T}$ is constructed and using the definition of the free energy $f_{\mathbf{c}}$ in Theorem III.1.6, we find

$$\sum_{\omega' \in \mathcal{B}(L)} W_{6\mathrm{V}}(\omega') \overset{(ii)}{\geq} \sum_{\omega \in \Omega^{(2L)}_{6V}(\mathbb{O}_{N,M})} \frac{W_{6\mathrm{V}}(\mathbf{T}(\omega))}{N^2 2^{2M/\alpha}} \overset{(i)}{\geq} \frac{Z^{(2L)}_{N,M} \mathbf{c}^{-2M/\alpha}}{N^2 2^{2M/\alpha}} = \exp[f_{\mathbf{c}}(\alpha) MN(1 + o(1))],$$

where $o(1)$ denotes a quantity tending to 0 as M and then N tend to infinity. The claim thus follows by using the definition of the free energy again to give

$$Z^{(0)}_{N,M} = \exp[f_{\mathbf{c}}(0) MN(1 + o(1))].$$

We therefore turn to the construction of $\mathbf{T}$ (see Figures III.11–III.12). Consider $\omega \in \Omega^{(2L)}_{6V}(\mathbb{O}_{N,M})$. Define the associated configuration $\overrightarrow{\omega}$ of fully-packed, noncrossing oriented loops and paths on $\mathbb{O}_{N,M}$, the paths starting and ending at the bottom or top of the cylinder: $\overrightarrow{\omega}$ is obtained from ω by splitting the arrows at each vertex into noncrossing loop/path segments. This splitting done so that $\overrightarrow{\omega}$ is a deterministic function of ω (there is only one noncrossing way to split type 1–4 vertices, while for type 5–6 vertices that could be split into two left or two right-turns, we

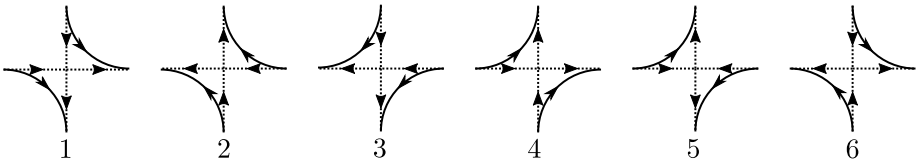

Figure III.11: A deterministic map from local 6-vertex configuration to oriented loops and paths. Vertices of types 5 and 6 could be split into non-crossing paths in two ways, but we always choose the left-turning splitting.

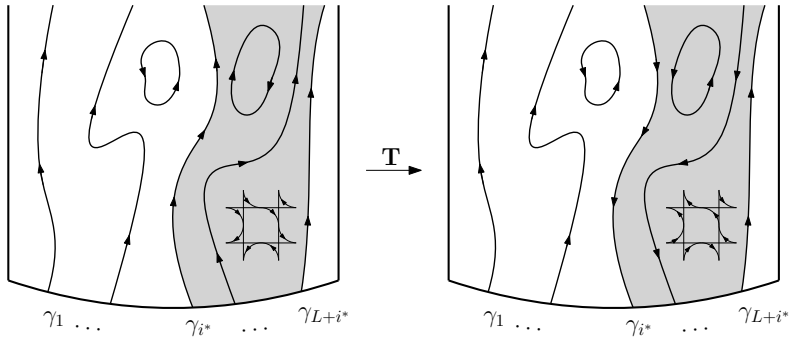

Figure III.12: The construction of $\mathbf{T}$ by reversing the orientation of all the loops (and hence the 6-vertex configuration) in the grey region.

fix an arbitrary rule, say for definiteness the left-turning splitting depicted in Figure III.11). Note that $\overrightarrow{\omega}$ must contain at least $2L$ paths between the bottom and the top of the cylinder, and that among all such paths, there are exactly $2L$ more that are oriented upward than downward.

Let $\gamma_1, \ldots, \gamma_{2L}$ be upward vertical crossing paths of $\overrightarrow{\omega}$ (indexes running from left to right) such that for $1 \leq i \leq 2L-1$, the connected component of $\mathbb{O}_{N,M} \setminus (\gamma_i \cup \gamma_{i+1})$ to the right of γ_i has an equal number of up and down vertical directed paths of $\overrightarrow{\omega}$. It is not hard to check that such crossings $\gamma_1, \ldots, \gamma_{2L}$ exist. Such a family of paths $\gamma_1, \ldots, \gamma_{2L}$ may not be unique, so in order for $\mathbf{T}$ to be well-defined, we again fix some arbitrary deterministic way to choose them.

The six-vertex configurations on $\mathbb{O}_{N,M}$ have $\leq 2NM$ oriented edges and $\gamma_1, \ldots, \gamma_{2L}$ are edge-disjoint, so for some $1 \leq i \leq L$, we must have

$$\text{length}(\gamma_i) + \text{length}(\gamma_{L+i}) \leq 2MN/L \leq 2M/\alpha.$$

Let i^* be the integer i minimizing the left-hand side above. We finally define $\mathbf{T}(\omega)$ to be the six-vertex configuration obtained by reversing the arrows of ω that are either on the path γ_{i^*} or in the connected component C of $\mathbb{O}_{N,M} \setminus (\gamma_{i^*} \cup \gamma_{L+i^*})$ to the right of γ_{i^*}[12].

We now verify that $\mathbf{T}$ sends any configuration in $\Omega_{6V}^{(2L)}(\mathbb{O}_{N,M})$ to $\Omega_{6V}^{(0)}(\mathbb{O}_{N,M}) \cap \mathcal{B}(L)$, and that it has the desired properties (i) and (ii):

[12]This can be seen as reversing some loops and paths of $\overrightarrow{\omega}$, which directly implies that $\mathbf{T}(\omega)$ indeed satisfies the ice rule.

- $\mathbf{T}(\omega) \in \Omega_{6V}^{(0)}(\mathbb{O}_{N,M}) \cap \mathcal{B}(L)$: look at the directed loops and paths of $\overrightarrow{\omega}$, after the reversal performed by $\mathbf{T}$. Among the paths between the top and bottom of $\mathbb{O}_{N,M}$, on $\mathbb{O}_{N,M} \setminus (C \cup \gamma_{i^*})$ there are L more upward than downward paths, and on $(C \cup \gamma_{i^*})$ there are L more downward than upward paths. It follows that $\mathbf{T}(\omega)$ has as many upward as downward paths, so $\mathbf{T}(\omega) \in \Omega_{6V}^{(0)}(\mathbb{O}_{N,M})$. The refinement $\mathbf{T}(\omega) \in \Omega_{6V}^{(0)}(\mathbb{O}_{N,M}) \cap \mathcal{B}(L)$ follows from the same argument, as the directed loops and paths are level lines of the height function of $\mathbf{T}(\omega)$, and vertical $\times$-paths of constant height are formed by the faces on both sides of each path $\gamma_1, \dots, \gamma_{2L}$.

- Property (i): when changing from ω to $\mathbf{T}(\omega)$, only the vertices on the paths γ_{i^*} and γ_{L+i^*} may change weight. There are at most $2M/\alpha$ such vertices, each changing the six-vertex weight by a factor at most $\mathbf{c}$.

- Property (ii): if $\omega' = \mathbf{T}(\omega)$ and we know γ_{i^*} and γ_{L+i^*}, we can reconstruct ω. Regardless of ω', there are at most $N^2 2^{M/\alpha}$ possible pairs of paths $(\gamma_{i^*}, \gamma_{L+i^*})$: at most N^2 pairs of first edges, and at most $2^{2M/\alpha}$ ways to choose the next at most $2M/\alpha$ edges of γ_{i^*} and γ_{L+i^*} (the paths turn at every vertex).

This finishes the proof. □

We now turn to the proof of Proposition III.4.1.

Proposition III.4.1. Fix a root face ρ on the bottom of $\mathbb{O}_{N,M}$ and, for integers $j \geq 0$ and $n, k \geq 1$, let $\mathcal{A}_j(n,k)$ be the event that there are $2j+2$ vertical $\times$-crossings of the cylinder $(\gamma_i, -j \leq i \leq j)$ and γ', around the cylinder in this order and such that

- γ_0 starts from ρ,
- the height h on γ_i is 0 if $|i| \leq j$ is even, and k if $|i| \leq j$ is odd,
- the height h on γ' is $(n-j)k$ if j is even and $-(n-j-1)k$ if j is odd.

We start by proving that for $0 \leq j \leq n-2$,

$$\mathbb{P}^{(0)}_{\mathbb{O}_{N,M}}[\mathcal{A}_j(n,k)] \leq \mathbb{P}^{(0)}_{\mathbb{O}_{N,M}}[\mathcal{A}_{j+1}(n,k)]. \tag{III.22}$$

In order to see this, fix $0 \leq j \leq n-2$; let us assume for definiteness that j is even (the case of odd j can be treated in a similar fashion). For $h \in \mathcal{A}_j(n,k)$ or $h \in \mathcal{A}_{j+1}(n,k)$, suppose (as the choice of the vertical $\times$-crossings inducing this event may not be unique) in the following that for $i > 0$ (resp. $i < 0$) γ_i is taken to be the left-most (resp. right-most) appropriate $\times$-crossings of $h = 0$ or $h = k$ from the root ρ. Observe that the crossings γ_{j+1} and γ_{-j-1} thus defined exist even for $h \in \mathcal{A}_j(n,k)$ due to the existence of the crossing γ' on which $h \geq 2k$. Let $X(h)$ be the portion of the cylinder on or right of γ_{-j-1} and on or left of γ_{j+1} and $\mathcal{X}$ be the set of possible values of $(X(\omega), h_{|X(\omega)})$ for ω such that $\gamma_{-j-1}, \dots, \gamma_{j+1}$ exist. We can write

$$\mathbb{P}^{(0)}_{\mathbb{O}_{N,M}}[\mathcal{A}_j(n,k)] = \sum_{(X,\xi)\in\mathcal{X}} \mathbb{P}^{(0)}_{\mathbb{O}_{N,M}}[\mathcal{V}^{\times}_{h\geq(n-j)k}(Y) \mid h_{|X} = \xi]\mathbb{P}^{(0)}_{\mathbb{O}_{N,M}}[h_{|X} = \xi],$$

$$\mathbb{P}^{(0)}_{\mathbb{O}_{N,M}}[\mathcal{A}_{j+1}(n,k)] = \sum_{(X,\xi)\in\mathcal{X}} \mathbb{P}^{(0)}_{\mathbb{O}_{N,M}}[\mathcal{V}^{\times}_{h\leq-(n-(j+1)-1)k}(Y) \mid h_{|X} = \xi]\mathbb{P}^{(0)}_{\mathbb{O}_{N,M}}[h_{|X} = \xi],$$

where the notation $\mathcal{V}^{\times}(Y)$ denotes the occurrence of a vertical $\times$-crossing of the discrete domain Y formed of faces that are in or share a corner with a face in $\mathbb{O}_{N,M} \setminus X$. Observe that by the spatial Markov property, $h_{|Y}$ under $\mathbb{P}^{(0)}_{\mathbb{O}_{N,M}}[\cdot \mid h_{|X} = \xi]$ has the law $\mathbb{P}^{B,\{k-1,k\}}_{Y}$, where the superscript denotes the boundary condition $\{k-1,k\}$ on the union B of the left and right sides of Y. From this observation, the comparison between boundary conditions and the invariance of the height function distribution between h and $2k-h$, we deduce that

$$\begin{aligned}\mathbb{P}^{(0)}_{\mathbb{O}_{N,M}}[\mathcal{V}^{\times}_{h\geq(n-j)k}(Y)|h_{|X}=\xi] &= \mathbb{P}^{B,\{k-1,k\}}_{Y}[\mathcal{V}^{\times}_{h\geq(n-j)k}(Y)]\\ &\leq \mathbb{P}^{B,\{k+1,k\}}_{Y}[\mathcal{V}^{\times}_{h\geq(n-j)k}(Y)]\\ &= \mathbb{P}^{B,\{k-1,k\}}_{Y}[\mathcal{V}^{\times}_{h\leq-(n-(j+1)-1)k}(Y)]\\ &= \mathbb{P}^{(0)}_{\mathbb{O}_{N,M}}[\mathcal{V}^{\times}_{h\leq-(n-(j+1)-1)k}(Y)|h_{|X}=\xi],\end{aligned}$$

from which (III.22) follows.

We now conclude the proof of the proposition. Set $n = \lfloor \lceil \alpha N \rceil / k \rfloor$, $\rho = s_0$ and observe that $\mathcal{B}(\lceil \alpha N \rceil) \subset \mathcal{B}(nk)$. By the rotational symmetry of the measure around the cylinder, we find that

$$\tfrac{1}{N}\mathbb{P}^{(0)}_{\mathbb{O}_{N,M}}[B(nk)] \leq \mathbb{P}^{(0)}_{\mathbb{O}_{N,M}}[\mathcal{A}_0(n,k)].$$

Using first this observation, then (III.22) iteratively $n-1$ times, and then the fact that $\mathcal{A}_{n-1}(n,k)$ is contained in the union of the $\mathcal{A}(S,n,k)$ over S, where S can be chosen in $\binom{N}{2n} \leq 2^N$ ways, we find

$$\tfrac{1}{N}\mathbb{P}^{(0)}_{\mathbb{O}_{N,M}}[B(\lceil \alpha N \rceil)] \leq \mathbb{P}^{(0)}_{\mathbb{O}_{N,M}}[\mathcal{A}_0(n,k)] \leq \mathbb{P}^{(0)}_{\mathbb{O}_{N,M}}[\mathcal{A}_{n-1}(n,k)] \leq 2^N \max_{S} \mathbb{P}^{(0)}_{\mathbb{O}_{N,M}}[\mathcal{A}(S,n,k)].$$

The claim now follows from Lemma III.4.2. □

III.4.2 Proof of Theorem III.1.7

Parameters and their relations We fix the following parameters for the rest of this subsection.

(i) The integers $r, k \geq 1$ come from the statement of Theorem III.1.7.

(ii) Let $\delta > 0$ be an absolute constant so that both Proposition III.3.4 and Theorem III.3.1 hold[13] with that δ. Set $\eta = \delta/12$ and let $c_0 > 0$ be the absolute constant given by Proposition III.3.4 in (III.28) below.

(iii) Introduce the additional parameters $N, M \in \mathbb{N}$, with N even. We will ultimately take M and N to infinity (in this order). However, given k, r, we will only work with pairs N, M and their subsequential limits such that

$$n := \eta N/r \qquad \text{and} \qquad m := M/r, \tag{III.23}$$

are integers[14] and m is divisible by 3. Finally, set $\alpha = \frac{\eta}{r/k}$ so that the relation $\lfloor \lceil \alpha N \rceil / k \rfloor = n$ of Proposition III.4.1 holds.

[13] The inequalities in Proposition III.3.4 and Theorem III.3.1 both trivially remain true if we adjust δ smaller, so there exists such δ that both hold.

[14] Similarly to the previous footnote, we assume $\delta/12 = \eta \in \mathbb{Q}$.

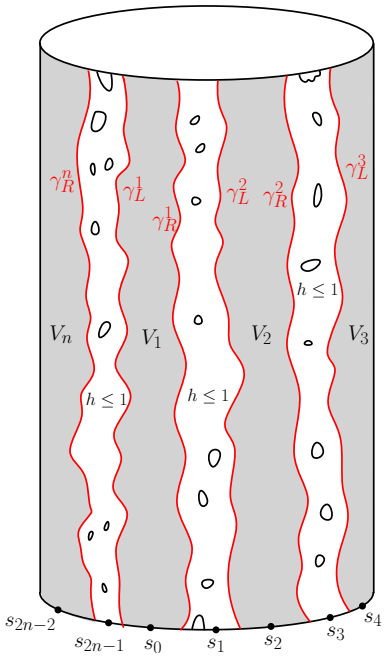

Figure III.13: An illustration of the setup of the proof of Theorem III.1.7.

Finally, we remark that we want to prove Theorem III.1.7 for $k > k_0$ and $r/k > \rho_0$ that are large enough. We will state separately any such assumptions to highlight the fact that k_0 and ρ_0 are chosen only based on parameters that are absolute constants.

The setup for the proof Let $S = \{s_0, \dots, s_{2n-1}\}$ be the set of faces, as in Proposition III.4.1, that maximizes the probability $\mathbb{P}^{(0)}_{\mathbb{O}_{N,M}}[\mathcal{A}(S, n, k)]$. Let $\mathcal{X}$ be the union of the clusters of $h \le 1$ of $s_0, s_2, \dots, s_{2n-2}$ and their bounding $\times$-paths of $h = 2$. Since

$$\mathbb{P}^{(0)}_{\mathbb{O}_{N,M}}[\mathcal{A}(S, n, k)] = \sum_X \mathbb{P}^{(0)}_{\mathbb{O}_{N,M}}[\mathcal{A}(S, n, k) \,|\, \mathcal{X} = X]\mathbb{P}^{(0)}_{\mathbb{O}_{N,M}}[\mathcal{X} = X],$$

one may find a realisation X of $\mathcal{X}$ such that

$$\mathbb{P}^{(0)}_{\mathbb{O}_{N,M}}[\mathcal{A}(S, n, k) \,|\, \mathcal{X} = X] \ge \mathbb{P}^{(0)}_{\mathbb{O}_{N,M}}[\mathcal{A}(S, n, k)]. \tag{III.24}$$

Fix X to be such a realisation.

Now, X is such that it does not exclude $\mathcal{A}(S, n, k)$. In particular, $\mathbb{O}_{N,M} \setminus X$ contains n regions $\tilde{V}_1, \dots, \tilde{V}_n$ (containing the faces $s_1, s_3, \dots s_{2n-1}$, respectively) and $\mathcal{A}(S, n, k)$ means that each of them contains a vertical $\times$-crossing of $\mathbb{O}_{N,M}$ of height at least k. Write V_i for the discrete domain formed of faces of $\mathbb{O}_{N,M}$ in $\tilde{V}_i$ or sharing a corner with a face in $\tilde{V}_i$. Note that V_i has a natural quad structure, with top and bottom sides on the top and bottom of $\mathbb{O}_{N,M}$ and left and right sides given by the faces of $X \cap V_i$ with height in $\{1, 2\}$; denote the latter two paths by γ_L^i and γ_R^i, respectively, and orient them from bottom to top. See Figure III.13.

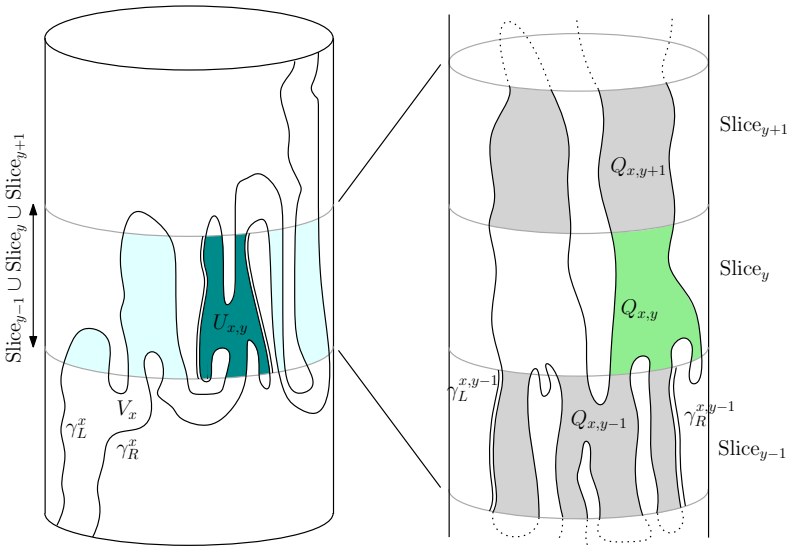

Figure III.14: Left: $V_x \bigcap (\text{Slice}_{y-1} \cup \text{Slice}_y \cup \text{Slice}_{y+1})$ may consist of several domains; $U_{x,y}$ is the bottom-most one where the top of Slice_{y+1} crosses between γ_L^x and γ_R^x. The curves $\vartheta_L^{x,y}$ and $\vartheta_R^{x,y}$ are highlighted by doubled lines. Right: $U_{x,y} \bigcap \text{Slice}_{y-1}$ may consist of several domains; those that cross the slice vertically form $Q_{x,y-1}$. The curves $\gamma_L^{x,y-1}$ and $\gamma_R^{x,y-1}$ are highlighted. For the middle slice, $Q_{x,y}$ is defined in the same way as $U_{x,y}$. It is separated inside V_x from the bottom and top of the cylinder by $Q_{x,y-1}$ and $Q_{x,y+1}$, respectively.

For $1 \leq y \leq m$ let Slice_y be the translate by $(0, (y-1)r)$ of $\mathbb{O}_{N,r}$, seen as a subset of $\mathbb{O}_{N,M}$. These horizontal slices form a partition of $\mathbb{O}_{N,M}$. For $y \equiv 2 \mod 3$, $V_x \bigcap (\text{Slice}_{y-1} \cup \text{Slice}_y \cup \text{Slice}_{y+1})$ may be formed of several domains, but in at least one of them the top of Slice_{y+1} connects γ_L^x and γ_R^x. Write $U_{x,y}$ for the bottom-most such domain in V_x (that is the one that separates all others from the bottom of V_x inside V_x). See Figure III.14 (left). For simplicity of notation, also set $U_{x,y-1} = U_{x,y+1} = U_{x,y}$. Each such domain $U_{x,y}$ contains a single sub-path of γ_L^x (resp. γ_R^x) from the bottom of Slice_{y-1} to the top of Slice_{y+1}; we call it $\vartheta_L^{x,y}$ (resp. $\vartheta_R^{x,y}$). The discrete sub-domain of $(\text{Slice}_{y-1} \cup \text{Slice}_y \cup \text{Slice}_{y+1})$ contained between $\vartheta_L^{x,y}$ and $\vartheta_R^{x,y}$ is called $\overline{U}_{x,y}$.

For $y \equiv 0$ or $1 \mod 3$, define $Q_{x,y}$ as the collection of domains of $U_{x,y} \cap \text{Slice}_y$ that connect the top and bottom of Slice_y. See Figure III.14 (right). For such y, let $\gamma_L^{x,y}$ (resp. $\gamma_R^{x,y}$) be the unique sub-path of $\vartheta_L^{x,y}$ (resp. $\vartheta_R^{x,y}$) between the top and bottom of Slice_y (where uniqueness comes from the congruence class of y modulo 3).

For $y \equiv 2 \mod 3$, define $Q_{x,y}$ similarly to $U_{x,y}$: it is the bottom-most domain of $V_x \cap \text{Slice}_y$ on which the top of Slice_y connects γ_L^x and γ_R^x *and which is contained in* $U_{x,y}$. For such y, $\gamma_L^{x,y}$ and $\gamma_R^{x,y}$ are defined similarly to $\vartheta_L^{x,y}$ and $\vartheta_R^{x,y}$; this does *not* imply $\gamma_L^{x,y} \subset \vartheta_L^{x,y}$ – see Figure III.14 (right) for an example.

For all x, y, set $\overline{Q}_{x,y}$ to be the domain of Slice_y contained between $\gamma_L^{x,y}$ and $\gamma_R^{x,y}$. Thus $Q_{x,y} \subset \overline{Q}_{x,y}$ and the latter has a natural quad structure, with two arcs formed by $\gamma_L^{x,y}$ and $\gamma_R^{x,y}$ and the two others formed by parts of the top and

bottom of Slice_y, respectively. Denote the top and bottom boundary arcs of $\overline{Q}_{x,y}$ by $\text{Top}_{x,y}$ and $\text{Bottom}_{x,y}$, respectively. We call $\overline{Q}_{x,y}$ *tight* if $\text{Top}_{x,y}$ and $\text{Bottom}_{x,y}$ each consist of at most $\lfloor \delta r \rfloor$ faces (where $\delta > 0$ is the absolute constant described above). Furthermore, for (x, y) with $y \equiv 2 \bmod 3$, we say that (x, y) is *good* if $\overline{Q}_{x,y-1}$, $\overline{Q}_{x,y}$ and $\overline{Q}_{x,y+1}$ are all tight.

Lemma III.4.3. *At least half of the pairs (x, y), with $1 \le x \le n$ and $1 \le y \le m$ and $y \equiv 2$ mod 3, are good.*

Proof. We will actually prove a slightly stronger claim: namely, at least half of the n pairs (x, y), with fixed $1 \le y \le m$, $y \equiv 2 \bmod 3$, are good.

To start, fix any $1 \le y \le m$. We claim that the quads $\overline{U}_{x,y}$ with $1 \le x \le n$ are disjoint from one another. Indeed, by construction there exists no sub-path of γ_L^x or γ_R^x crossing vertically Slice_y that lies strictly between $\vartheta_L^{x,y}$ and $\vartheta_R^{x,y}$. Thus, there are no vertical crossings of Slice_y in any other domain $V_{x'}$ with $x' \neq x$ between $\vartheta_L^{x,y}$ and $\vartheta_R^{x,y}$, which implies that the quads $\overline{U}_{x,y}$ are disjoint.

As a consequence, the quads $\overline{Q}_{x,y}$ are also disjoint, since $\overline{Q}_{x,y} \subset \overline{U}_{x,y}$. Now, the disjoint union of $\text{Bottom}_{x,y}$ for $x = 1, \dots, n$ is contained in one row of N faces of $\mathbb{O}_{N,M}$. Therefore, at least a proportion $11/12$ of the quads $(\text{Bottom}_{x,y})_{1 \le x \le n}$ contain less than $12N/n = 12\eta r = \delta r$ faces (using the relations of the various parameters). The same holds for the tops of the quads $(\overline{Q}_{x,y})_{1 \le x \le n}$, and we conclude that out of the n quads $(\overline{Q}_{x,y})_{1 \le x \le n}$, there are at most $n/6$ quads that are not tight.

Consider now a fixed $1 \le y \le m$ with $y \equiv 2 \bmod 3$. By the previous paragraph, out of the n triplets of quads $(\overline{Q}_{x,y-1}, \overline{Q}_{x,y}, \overline{Q}_{x,y+1})$, at least $n/2$ are formed exclusively of tight quads. □

Let now $\mathcal{R}$ be the "ridge event" that each $Q_{x,y}$ with $y \equiv 2 \bmod 3$ contains a $\times$-path of $h \ge k$ between $\text{Top}_{x,y}$ and $\text{Bottom}_{x,y}$. Then, we have $\mathcal{A}(S, n, k) \subset \mathcal{R}$ and

$$\mathbb{P}^{(0)}_{\mathbb{O}_{N,M}}[\mathcal{R} \,|\, \mathcal{X} = X] \ge \mathbb{P}^{(0)}_{\mathbb{O}_{N,M}}[\mathcal{A}(S, n, k) | \mathcal{X} = X]. \tag{III.25}$$

Moreover, define the "fencing event" $\mathcal{F}$ that for each (x, y) with $y \equiv 2 \bmod 3$ which is good, $Q_{x,y-1}$ and $Q_{x,y+1}$ *do not* contain $\times$-paths of $h \ge (1 - c_0)k + 1$ between the top and bottom of Slice_{y-1} and Slice_{y+1}, respectively (or equivalently, by Remark III.3.2, each component of $Q_{x,y-1}$ and $Q_{x,y+1}$ is crossed horizontally by a path of $h \le (1 - c_0)k$).

The key lemmas The proof hinges on two lemmas which we now state and prove.

Lemma III.4.4 (Building fences)**.** *With the parameters and notations above, we have for all $r > 0$ and all $k > k_0(c_0)$ large enough*

$$\mathbb{P}^{(0)}_{\mathbb{O}_{N,M}}[\mathcal{F} \,|\, \mathcal{R} \text{ and } \mathcal{X} = X] \ge c_0^{nm}.$$

Proof. The occurrence of $\mathcal{R}$ may be determined by exploring, for each y with $y \equiv 2 \bmod 3$, the component of $h \le k - 1$ in $Q_{x,y}$ that contains $\gamma_L^{x,y}$, and the $\times$-paths of $h = k$ bounding this component. Indeed, either the component of $h \le k - 1$ reaches $\gamma_R^{x,y}$, hence preventing any vertical $\times$-path of $h \ge k$, or $\gamma_L^{x,y}$ and $\gamma_R^{x,y}$ are separated in $Q_{x,y}$ by a $\times$-path of $h = k$, which due to the boundary conditions traverses from

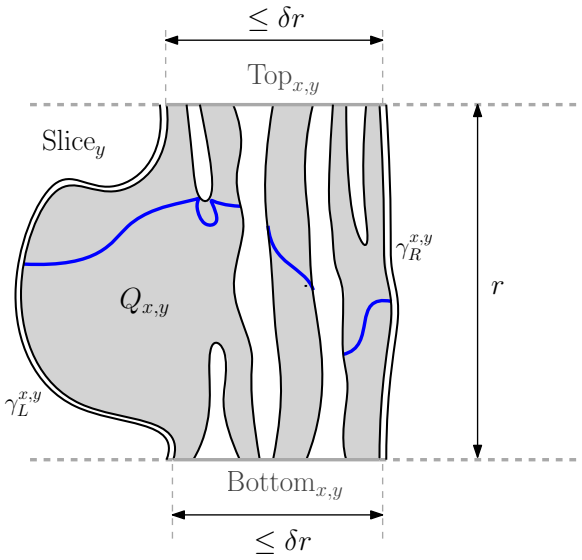

Figure III.15: An illustration for the proof of Lemma III.4.4. In every domain of $Q_{x,y}$, exactly two boundary segments in $\gamma_L^x \cup \gamma_R^x$ (in black) cross Slice_y vertically; these are called $\gamma_L^{x,y}$ and $\gamma_R^{x,y}$. The boundary condition ξ on $Q_{x,y}$ is $\{1,2\}$ on the black parts of $\partial Q_{x,y}$, and their maximal extension which is smaller or equal to k on the gray parts. The blue paths form a fence: they separate $\mathrm{Top}_{x,y}$ from $\mathrm{Bottom}_{x,y}$ inside $Q_{x,y}$ and have $h \leq (1-c_0)k$.

$\mathrm{Top}_{x,y}$ to $\mathrm{Bottom}_{x,y}$. This exploration only reveals faces in $Q_{x,y}$ with height at most k. Let Exp denote the random pair of faces and heights explored in this procedure. Then

$$\mathbb{P}^{(0)}_{\mathbb{O}_{N,M}}[\mathcal{F} \,|\, \mathcal{R} \text{ and } \mathcal{X} = X] \tag{III.26}$$
$$= \sum_{(E,h_{|E})} \mathbb{P}^{(0)}_{\mathbb{O}_{N,M}}[\mathcal{F} \,|\, \mathsf{Exp} = (E,h_{|E}) \text{ and } \mathcal{X} = X] \mathbb{P}^{(0)}_{\mathbb{O}_{N,M}}[\mathsf{Exp} = (E,h_{|E}) \,|\, \mathcal{R} \text{ and } \mathcal{X} = X],$$

where the sum is over all possible realisations $(E, h_{|E})$ of Exp such that $\mathcal{R}$ occurs.

Fix some $(E, h_{|E})$ as above such that $\mathcal{R}$ occurs, and fix (x, y) with $y \not\equiv 2 \bmod 3$, such that $\overline{Q}_{x,y}$ is tight. Recall the "dual formulation" of $\mathcal{F}$ and denote

$$\mathcal{F}_\ell^{x,y} = \{\text{there is a left-to-right crossings of } h \leq \ell \text{ in each component of } Q_{x,y}\}$$

(the meaning of "left-to-right" is explained with Figure III.15). Recall that E contains no face in $Q_{x,y}$. Due to (III.5) applied to $-h$, we now have

$$\mathbb{P}^{(0)}_{\mathbb{O}_{N,M}}[\mathcal{F}^{x,y}_{(1-c_0)k} \,|\, \mathsf{Exp} = (E,h_{|E}) \text{ and } \mathcal{X} = X] \geq \mathbb{P}^{\xi}_{Q_{x,y}}[\mathcal{F}^{x,y}_{(1-c_0)k-2}] \tag{III.27}$$

where ξ is the largest boundary conditions on $\partial Q_{x,y}$ that is at most k and takes values in $\{1,2\}$ on $\partial Q_{x,y} \setminus (\mathrm{Top}_{x,y} \cup \mathrm{Bottom}_{x,y})$.

Now, going back to the "primal formulation" of $\mathcal{F}$ and using Remark III.3.2, we have

$$\mathbb{P}^{\xi}_{Q_{x,y}}[\mathcal{F}^{x,y}_{(1-c_0)k-2}] \geq 1 - \mathbb{P}^{\xi}_{Q_{x,y}}[\mathrm{Bottom}_{x,y} \xleftrightarrow{h \geq (1-c_0)k-2 \text{ in } Q_{x,y}} \mathrm{Top}_{x,y}];$$

here and the rest of this proof, we omit integer roundings in $\lfloor (1-c_0)k \rfloor$. Then, by Corollary III.2.7 and then inclusion of events,

$$\begin{aligned}
&\mathbb{P}^{\xi}_{Q_{x,y}}[\mathrm{Top}_{x,y} \xleftarrow{h\geq(1-c_0)k-2 \text{ in } Q_{x,y}} \mathrm{Bottom}_{x,y}] \\
&\quad \leq \mathbb{P}^{\xi'}_{\mathbb{Z}\times[yr,(y+1)r]}[\mathrm{Top}_{x,y} \xleftarrow{h\geq(1-c_0)k-4 \text{ in } Q_{x,y}} \mathrm{Bottom}_{x,y}] \\
&\quad \leq \mathbb{P}^{\xi'}_{\mathbb{Z}\times[yr,(y+1)r]}[\mathrm{Top}_{x,y} \xleftarrow{h\geq(1-c_0)k-4} \mathrm{Bottom}_{x,y}],
\end{aligned}$$

where ξ' is the boundary condition on $\partial\mathbb{Z}\times[yr,(y+1)r]$ that takes values in $\{1,2\}$ outside of $\mathrm{Top}_{x,y}$ and $\mathrm{Bottom}_{x,y}$, where it is given by the maximal extension smaller or equal to k.

Now, recall that $\mathrm{Top}_{x,y}$ and $\mathrm{Bottom}_{x,y}$ both contain at most $\lfloor \delta r \rfloor$ faces. Proposition III.3.4 (and our original choice of c_0 and δ to match the below equation) guarantees [15] that

$$\mathbb{P}^{\xi'}_{\mathbb{Z}\times[yr,(y+1)r]}[\mathrm{Top}_{x,y} \xleftarrow{h\geq(1-c_0)k-4} \mathrm{Bottom}_{x,y}] \leq 1-c_0. \tag{III.28}$$

Tracing through the chain of inequalities that started from (III.27), we have

$$\mathbb{P}^{(0)}_{\mathbb{O}_{N,M}}[\gamma^{x,y}_L \xleftarrow{h\leq(1-c_0)k \text{ in } Q_{x,y}} \gamma^{x,y}_R \,|\, \mathsf{Exp} = (E, h_{|E}) \text{ and } \mathcal{X} = X] \geq c_0.$$

Finally, due to (SMP), (FKG) applies to the conditional measure $\mathbb{P}^{(0)}_{\mathbb{O}_{N,M}}[\cdot \,|\, \mathsf{Exp} = (E, h_{|E}) \text{ and } \mathcal{X} = X]$. As there are at most mn collections $Q_{x,y}$ needing to be crossed in order for $\mathcal{F}$ to occur, we conclude that

$$\mathbb{P}^{(0)}_{\mathbb{O}_{N,M}}[\mathcal{F} \,|\, \mathsf{Exp} = (E, h_{|E}) \text{ and } \mathcal{X} = X] \geq c_0^{mn}.$$

The statement then follows from (III.26). □

Lemma III.4.5 (Ridges given fences)**.** *With the parameters and notations above, we have for all $r > 0$ and all $k > k_0(c_0)$ large enough*

$$\mathbb{P}^{(0)}_{\mathbb{O}_{N,M}}[\mathcal{R} \,|\, \mathcal{F} \text{ and } \mathcal{X} = X] \leq \left(2\mathbb{P}^{0,1}_{\mathbb{Z}\times[-r,2r]}\big[[0,\delta r]\times\{0\} \xleftarrow{h\geq c_0k-2 \text{ in } \mathbb{Z}\times[0,r]} \mathbb{Z}\times\{r\}\big]\right)^{\frac{mn}{6}}.$$

Proof. When $\mathcal{F}$ occurs, for each good pair (x,y), let $\chi^{x,y}_T$ be the collection of top-most paths, in each connected component of $Q_{x,y+1}$, of height at most $(1-c_0)k$ that disconnect the bottom and top of Slice_{y+1}. Similarly, let $\chi^{x,y}_B$ be the bottom-most paths in $Q_{x,y-1}$, of height at most $(1-c_0)k$ (here and for the rest of this proof, we again omit integer roundings in $\lfloor (1-c_0)k \rfloor$). Write $D_{x,y}$ the connected component of $Q_{x,y}$ in the union of the faces of $U_{x,y}$ contained on or between the curves of $\chi^{x,y}_B$ and $\chi^{x,y}_T$.

Notice that the domains $(D_{x,y} : (x,y) \text{ good})$ are measurable in terms of the height function outside of them and on their boundaries. Thus, conditionally on any realisation of these domains and on a realisation ζ of the height function outside

[15] Strictly speaking, for the boundary condition ξ, Proposition III.3.4 addresses crossings of $h \geq (1-c_0)(k-1)+1$ but the above holds by adjusting c_0 suitably smaller and taking $k > k_0(c_0)$ large enough.

of them and on their boundaries, the height functions inside the different domains $D_{x,y}$ are independent of each other and follow laws $\mathbb{P}^{\zeta}_{D_{x,y}}$.

The definition of $D_{x,y}$ is such that the values of ζ on $\partial D_{x,y}$ are at most $(1-c_0)k$ (when $k > k_0(c_0)$ is large enough so that $(1-c_0)k \geq 2$). By (CBC), each measure $\mathbb{P}^{\zeta}_{D_{x,y}}$ is stochastically dominated by $\mathbb{P}^{(1-c_0)k-1,(1-c_0)k}_{D_{x,y}}$. Thus, for any good (x,y), using (III.5) (and $D_{x,y} \subset \mathrm{Slice}_{y-1} \cup \mathrm{Slice}_y \cup \mathrm{Slice}_{y+1}$), we have

$$\begin{aligned}
\mathbb{P}^{\zeta}_{D_{x,y}}[\mathrm{Bottom}_{x,y} \xleftrightarrow{h\geq k \text{ in } Q_{x,y}}{\times} \mathrm{Top}_{x,y}] &\leq \mathbb{P}^{(1-c_0)k-1,(1-c_0)k}_{D_{xy}}[\mathrm{Bottom}_{xy} \xleftrightarrow{h\geq k-1 \text{ in } Q_{x,y}} \mathrm{Top}_{xy}] \\
&\leq \mathbb{P}^{0,1}_{D_{x,y}}[\mathrm{Bottom}_{x,y} \xleftrightarrow{h\geq c_0 k \text{ in } Q_{x,y}} \mathrm{Top}_{x,y}] \\
&\leq 2\,\mathbb{P}^{0,1}_{\mathbb{Z}\times[(y-1)r,(y+2)r]}[\mathrm{Bottom}_{xy} \xleftrightarrow{h\geq c_0 k-2 \text{ in } Q_{x,y}} \mathrm{Top}_{x,y}] \\
&\leq 2\,\mathbb{P}^{0,1}_{\mathbb{Z}\times[-r,2r]}\big[[0,\lfloor \delta r \rfloor] \times \{0\} \xleftrightarrow{h\geq c_0 k-2 \text{ in } \mathbb{Z}\times[0,r]} \mathbb{Z}\times\{r\}\big].
\end{aligned}$$

The last inequality follows from the fact that (x,y) is good, and therefore $\overline{Q}_{x,y}$ is tight, which is to say that $\mathrm{Bottom}_{x,y}$ is shorter than δr.

Finally, since $\mathcal{R}$ imposes that $\mathrm{Bottom}_{x,y} \xleftrightarrow{h\geq k} \mathrm{Top}_{x,y}$ occurs in every domain $D_{x,y}$ and since there are at least $mn/6$ good pairs (x,y), using the independence of the measures inside the domains $D_{x,y}$ and the computation above, we find that

$$\mathbb{P}^{(0)}_{\mathbb{O}_{N,M}}[\mathcal{R} \,|\, \mathcal{F} \text{ and } \mathcal{X} = X] \leq \left(2\mathbb{P}^{0,1}_{\mathbb{Z}\times[-r,2r]}\big[[0,\lfloor \delta r \rfloor] \times \{0\} \xleftrightarrow{h\geq c_0 k-2 \text{ in } \mathbb{Z}\times[0,r]} \mathbb{Z}\times\{r\}\big]\right)^{\frac{mn}{6}},$$

as required. □

Theorem III.1.7. In this proof, we require that $k > k_0(c_0, c_1)$ is large enough so that Lemmas III.4.4 and III.4.5 and (III.31) below apply; we also assume that $r/k > \delta/24$ (the proof is thus a bit stronger than the stated assumption $r \geq k$).

Using elementary probability in the first step, and then Lemma III.4.4 as well as (III.24) and (III.25) in the second, we have

$$\begin{aligned}
\mathbb{P}^{(0)}_{\mathbb{O}_{N,M}}[\mathcal{R} \,|\, \mathcal{F} \text{ and } \mathcal{X} = X] &\geq \mathbb{P}^{(0)}_{\mathbb{O}_{N,M}}[\mathcal{F} \,|\, \mathcal{R} \text{ and } \mathcal{X} = X]\mathbb{P}^{(0)}_{\mathbb{O}_{N,M}}[\mathcal{R} \,|\, \mathcal{X} = X] \\
&\geq c_0^{nm}\mathbb{P}^{(0)}_{\mathbb{O}_{N,M}}[\mathcal{A}(S,n,k)].
\end{aligned}$$

Applying now Lemma III.4.5, we deduce that

$$\mathbb{P}^{0,1}_{\mathbb{Z}\times[-r,2r]}\big[[0,\lfloor \delta r \rfloor] \times \{0\} \xleftrightarrow{h\geq c_0 k-2 \text{ in } \mathbb{Z}\times[0,r]} \mathbb{Z}\times\{r\}\big] \geq \frac{c_0^6}{2}\,\mathbb{P}^{(0)}_{\mathbb{O}_{N,M}}[\mathcal{A}(S,n,k)]^{\frac{6}{nm}}. \tag{III.29}$$

Observe that the left-hand side does not depend on M and N, while the right-hand one does. Recall next that our choice parameter choice $\alpha = \eta k/r = \delta k/(12r)$ (which for $r/k > \delta/24$ satisfies $\alpha \in [0, 1/2)$) was matched for applying Proposition III.4.1, which gives

$$\mathbb{P}^{(0)}_{\mathbb{O}_{N,M}}[\mathcal{A}(S,n,k)] \geq \exp\big(NM(f_{\mathbf{c}}(\alpha) - f_{\mathbf{c}}(0)) + o(NM)\big)$$

as $M \to \infty$ and then $N \to \infty$. Applying this and the definitions (III.23) of m and n, the factor on the right-hand side of (III.29) becomes

$$\mathbb{P}^{(0)}_{\mathbb{O}_{N,M}}[\mathcal{A}(S,n,k)]^{\frac{6}{nm}} \geq \exp\left(\frac{6r^2}{\eta}(f_{\mathbf{c}}(\eta k/r) - f_{\mathbf{c}}(0)) + o(1)\right). \tag{III.30}$$

For the left-hand side of (III.29), we apply Theorem III.3.1 (recall that δ was chosen so that it applies) to deduce that there exist absolute constants $c_1, C_1 > 0$ such that

$$(\mathbb{P}^{0,1}_{\Lambda_{12r}}[\mathcal{O}_{h\geq c_1 k}(6r,12r)]/c_1)^{1/C_1} \geq \mathbb{P}^{0,1}_{\mathbb{Z}\times[-r,2r]}\big[[0,\lfloor \delta r\rfloor]\times\{0\} \xleftarrow{h\geq c_0 k-2 \text{ in } \mathbb{Z}\times[0,r]} \mathbb{Z}\times\{r\}\big], \tag{III.31}$$

for all $k > k_0(c_0, c_1)$ large enough.

Injecting (III.30) and (III.31) into (III.29), we get that for suitable absolute constants $c, C > 0$,

$$\mathbb{P}^{0,1}_{\Lambda_{12r}}[\mathcal{O}_{h\geq ck}(6r,12r)] \geq c\exp\big(C\, r^2[f_{\mathbf{c}}(\eta k/r) - f_{\mathbf{c}}(0)]\big).$$

This finishes the proof. □

III.4.3 Proof of Theorem III.1.4

Observe first that by inclusion of events, it suffices to prove the claim when k is larger than some constant. Second, by height shift and (CBC),

$$\mathbb{P}^{\xi}_{D}[\mathcal{O}_{h\geq k}(n,2n)] = \mathbb{P}^{\xi+\ell}_{D}[\mathcal{O}_{h\geq k+\ell}(n,2n)] \geq \mathbb{P}^{0,1}_{D}[\mathcal{O}_{h\geq k+\ell}(n,2n)],$$

so, by adjusting k, it suffices to prove the claim for $\xi = \{0,1\}$. Third, observe that by Corollary III.2.7 (or Proposition III.2.6 if the conditions ξ and $\{0,1\}$ above were only imposed on a subset of ∂D), when $D \supset \Lambda_{2n}$, we have

$$\mathbb{P}^{0,1}_{D}[\mathcal{O}_{h\geq k}(n,2n)] \geq \tfrac{1}{2}\mathbb{P}^{0,1}_{\Lambda_{2n}}[\mathcal{O}_{h\geq k+2}(n,2n)].$$

Thus, (adjusting k again) it suffices to prove claim for the $D = \Lambda_{2n}$. We thus turn to proving the claim for k large enough, $\xi = \{0,1\}$, and $D = \Lambda_{2n}$.

Fix now $\mathbf{c} \in [1,2]$ and k large enough for Theorem III.1.7 to apply; Let $\eta, c, C > 0$ and $C_0 > 0$ be the constants appearing in Theorem III.1.7 and (III.2), respectively. Applying (III.3) and (III.2) gives

$$\mathbb{P}^{0,1}_{\Lambda_{12r}}[\mathcal{O}_{h\geq ck}(6r,12r)] \geq c\exp\big[Cr^2\big(f_{\mathbf{c}}(\eta k/r) - f_{\mathbf{c}}(0)\big)\big] \geq c\exp\big[-C\eta^2 C_0 k^2\big] > 0.$$

This directly implies the claim when $n = 6r$ is a multiple of 6. For general n, let n' be the smallest multiple of 6 with $n' \geq n$. Note that under $\mathbb{P}^{0,1}_{\Lambda_{2n'}}$, we necessarily have $h \leq 11$ on $\partial\Lambda_{2n}$. Thus, by (SMP) and (CBC), we have

$$\mathbb{P}^{0,1}_{\Lambda_{2n'}}[\mathcal{O}_{h\geq k+10}(n',2n')] \leq \mathbb{P}^{10,11}_{\Lambda_{2n}}[\mathcal{O}_{h\geq k+10}(n',2n)] \leq \mathbb{P}^{0,1}_{\Lambda_{2n}}[\mathcal{O}_{h\geq k}(n,2n)],$$

where the second step used a shift of boundary conditions and inclusion of events. This concludes the proof. □

III.5 Logarithmic bounds on variance of height functions

Throughout this section, we restrict our attention to the six-vertex model with $1 \leq \mathbf{c} \leq 2$.

III.5.1 Lower bounds

Proof of the lower bound in Corollary III.1.5

The proof will be based on the following quantity:

$$v_n := \min_{\xi:\partial\Lambda_n \to \{-1,0,+1\}} \mathbb{E}^{\xi}_{\Lambda_n}[h(0)^2],$$

where the minimum is taken over all functions $\xi : \partial\Lambda_n \to \{-1, 0, +1\}$ that take odd values on odd faces and even on even faces (all such ξ are admissible boundary conditions).

Lemma III.5.1. *Fix $\mathbf{c} \in [1, 2]$. There exist $R \geq 1$ such that for every n large enough*

$$v_{Rn} \geq v_n + 1.$$

Before proving this lemma, let us explain how it implies the lower bound in Corollary III.1.5.

the lower bound in Corollary III.1.5. We will suppose hereafter that $x = 0$. Let D be a discrete domain D containing the box Λ_n and ξ be some boundary condition on ∂D with $|\xi| \leq \ell$. Using (CBC) and $|\mathbb{E}^{\xi+\ell}_D[h(0)]| \leq 2\ell$ (by Corollary III.2.3), we get that

$$\mathrm{Var}^{\xi}_D[h(0)] = \mathrm{Var}^{\xi+\ell}_D[h(0)] \geq \mathbb{E}^{\xi+\ell}_D[h(0)^2] - 4\ell^2. \tag{III.32}$$

Now, $\xi + \ell$ is of definite sign and we may apply (CBC-|h|) and (FKG-|h|) to find

$$\mathrm{Var}^{\xi}_D[h(0)] \geq \mathbb{E}^{0,1}_D[h(0)^2] - 4\ell^2 \geq \mathbb{E}^{0,1}_D[h(0)^2 \,|\, |h| \leq 1 \text{ on } D \setminus \Lambda_n] - 4\ell^2.$$

By the spatial Markov property, the last expectation value above is an average of quantities $\mathbb{E}^{\xi}_{\Lambda_n}[h(0)^2]$ over boundary conditions ξ with values in $\{-1, 0, 1\}$. As such, it is bounded from below by v_n.

It is an immediate consequence of Lemma III.5.1 that $v_n \geq c \log n$ for some constant $c > 0$ and all $n \geq 1$. Since n may be chosen as the distance from 0 to ∂D, this concludes the proof. □

The rest of the section is dedicated to proving Lemma III.5.1. We start by stating a consequence of Theorem III.1.4 which may also be of independent interest.

For integers $N \geq n > 0$, recall that $A(n, N) := \Lambda_N \setminus \Lambda_n$ and $\mathcal{O}_{h\geq k}(n, N)$ (resp. $\mathcal{O}_{|h|\geq k}(n, N)$) is the event that there exists a path of $h \geq k$ (resp. $|h| \geq k$) in $A(n, N)$ forming a circuit around 0.

Lemma III.5.2. *Fix $\mathbf{c} \in [1, 2]$. For every $k \geq 0$, there exist $c, C, n_0 > 0$ such that for all $N/2 \geq n > n_0$,*

$$\mathbb{P}^{0,1}_{\Lambda_N}[\mathcal{O}_{|h|\geq k}(n, N)] \geq 1 - C(n/N)^c.$$

The necessity of the lemma comes from the fact that for the proof of Lemma III.5.1, it does not suffice to show that circuits of a given height occur with positive probability in annuli (which is the conclusion of Theorem III.1.4); we need circuits to occur with high probability, when the ratio between the inner and outer radii of the annulus is large.

Proof. Let us denote $\mathbb{P}_N^{0,1} := \mathbb{P}_{\Lambda_N}^{0,1}$ for simplicity. Below, we show by induction that there exists $\delta = \delta(k) > 0$ that for every $n > n_0(k)$ and $i \geq 1$,

$$\mathbb{P}_{2^i n}^{0,1}[\mathcal{O}_{|h|\geq k}(n, 2^i n)^c] \leq (1-\delta)^i. \tag{III.33}$$

The claim for $N = 2^i n$ then directly follows from (III.33). To treat general $2^i n \leq N < 2^{i+1} n$, compute

$$\begin{aligned}
\mathbb{P}_N^{0,1}[\mathcal{O}_{|h|\geq k}(n, N)] &\geq \mathbb{P}_N^{0,1}[\mathcal{O}_{|h|\geq k}(n, 2^i n)] \qquad \text{(by inclusion)} \\
&\geq \mathbb{P}_N^{0,1}[\mathcal{O}_{|h|\geq k}(n, 2^i n) \mid |h| \leq 1 \text{ on } \partial\Lambda_{2^i n}] \qquad \text{(by (FKG-|h|))} \\
&\geq \min_{\xi:\partial\Lambda_{2^i n}\to\{0,\pm 1\}} \mathbb{P}_{2^i n}^{\xi+2}[\mathcal{O}_{|h|\geq k+2}(n, 2^i n)] \qquad \text{(by (SMP))} \\
&\geq \mathbb{P}_{2^i n}^{0,1}[\mathcal{O}_{|h|\geq k+2}(n, 2^i n)] \qquad \text{(by (CBC-|h|))},
\end{aligned}$$

and the claim follows from the case of $N = 2^i n$ by adjusting k. We thus turn to the proof of (III.33).

For $i = 1$, using the inclusion of events in the first inequality, Theorem III.1.4 implies that for $n > n_0$,

$$\mathbb{P}_{2n}^{0,1}[\mathcal{O}_{|h|\geq k}(n, 2n)] \geq \mathbb{P}_{2n}^{0,1}[\mathcal{O}_{h\geq k+2}(n, 2n)] \geq \delta$$

for some constant $\delta > 0$ depending on k only, and which we now fix. Let us now assume that (III.33) holds true for $i-1$ and then prove it for i. By inclusion of events and conditioning, we get

$$\begin{aligned}
\mathbb{P}_{2^i n}^{0,1}[\mathcal{O}_{|h|\geq k}(n, 2^i n)^c] &\leq \mathbb{P}_{2^i n}^{0,1}[\mathcal{O}_{|h|\geq k}(2n, 2^i n)^c \cap \mathcal{O}_{|h|\geq k}(n, 2n)^c] \\
&= \mathbb{P}_{2^i n}^{0,1}[\mathcal{O}_{|h|\geq k}(2n, 2^i n)^c] \underbrace{\mathbb{P}_{2^i n}^{0,1}[\mathcal{O}_{|h|\geq k}(n, 2n)^c \mid \mathcal{O}_{|h|\geq k}(2n, 2^i n)^c]}_{P}.
\end{aligned}$$

Using the inductive hypothesis, it thus suffices to show that $P \leq 1 - \delta$. Now, since $\mathcal{O}_{|h|\geq k}(2n, 2^i n)^c$ depends only on $|h|$ on $A(2n, 2^i n)$, one may further condition on the precise value of $|h|$ in $A(2n-1, 2^i n) \supset A(2n, 2^i n)$. The measure thus obtained involved only conditioning on $|h|$, except on $\partial\Lambda_{2^i n}$, where we have $h \in \{0, 1\}$. We can therefore use FKG for $|h|$ to deduce that

$$\begin{aligned}
P &\leq \mathbb{P}_{2^i n}^{0,1}[\mathcal{O}_{|h|\geq k}(n, 2n)^c \,|\, |h(x)| \leq 1, \forall x \in A(2n-1, 2^i n)] \\
&\leq \mathbb{P}_{2^i n}^{0,1}[\mathcal{O}_{h\geq k}(n, 2n)^c \,|\, |h(x)| \leq 1, \forall x \in A(2n-1, 2^i n)] \\
&\leq \mathbb{P}_{2n}^{0,-1}[\mathcal{O}_{h\geq k}(n, 2n)^c] \\
&= 1 - \mathbb{P}_{2n}^{0,1}[\mathcal{O}_{h\geq k+2}(n, 2n)] \\
&\leq 1 - \delta,
\end{aligned}$$

where the additional manipulations were based on inclusion of events, spatial Markov property and comparison of boundary conditions, shift of boundary conditions, and our choice of δ above, respectively. □

Lemma III.5.1. Fix $k = 4$ and let $R > 1$ be such that

$$\mathbb{P}^{0,1}_{\Lambda_{Rn}}[\mathcal{O}_{|h|\geq k}(n, Rn)] \geq 1/2, \tag{III.34}$$

for all n large enough.

Fix $n \geq 1$ large enough for (III.34) to hold and let ξ be a boundary condition on $\partial\Lambda_{Rn}$ taking values in $\{-1, 0, 1\}$ that minimises $\mathbb{E}^{\xi}_{\Lambda_{Rn}}[h(0)^2]$. By symmetry, we may choose ξ so that $\mathbb{E}^{\xi}_{\Lambda_{Rn}}[h(0)] \leq 0$. Then, we have

$$\begin{aligned} v_{Rn} = \mathbb{E}^{\xi}_{\Lambda_{Rn}}[h(0)^2] &\geq \mathbb{E}^{\xi}_{\Lambda_{Rn}}[(h(0)+2)^2] - 4 \\ &= \mathbb{E}^{\xi+2}_{\Lambda_{Rn}}[h(0)^2] - 4 \\ &\geq \mathbb{E}^{0,1}_{\Lambda_{Rn}}[h(0)^2] - 4, \end{aligned} \tag{III.35}$$

where the last step used (CBC-|h|).

Hereafter we focus on bounding $\mathbb{E}^{0,1}_{\Lambda_{Rn}}[h(0)^2]$. We have

$$\mathbb{E}^{0,1}_{\Lambda_{Rn}}[h(0)^2] = \mathbb{E}^{0,1}_{\Lambda_{Rn}}[h(0)^2 \mathbb{1}_{\mathcal{O}_{|h|\geq k}(n,Rn)}] + \mathbb{E}^{0,1}_{\Lambda_{Rn}}[h(0)^2 \mathbb{1}_{\mathcal{O}_{|h|\geq k}(n,Rn)^c}], \tag{III.36}$$

and we will bound separately the two terms on the right-hand side of the above.

If $\mathcal{O}_{|h|\geq k}(n, Rn)$ occurs, let Γ be the outer-most circuit with $|h| \geq k$ around Λ_{Rn}. Write $\mathcal{D}$ for the random domain formed of the faces on or surrounded by Γ. Notice that $\mathcal{D}$ is measurable in terms of the values of $|h|$ on $\Gamma = \partial\mathcal{D}$ and $\mathcal{D}^c$. As such, the measure in $\mathcal{D}$ is $\mathbb{P}^{\zeta}_{\mathcal{D}}$, with ζ taking values either k and $k+1$ or $-k$ and $-k-1$. Thus

$$\begin{aligned} \mathbb{E}^{0,1}_{\Lambda_{Rn}}[h(0)^2 \mathbb{1}_{\mathcal{O}_{|h|\geq k}(n,Rn)}] &= \sum_{D'} \mathbb{E}^{k,k+1}_{D'}[h(0)^2] \mathbb{P}^{0,1}_{\Lambda_{Rn}}[\mathcal{D} = D'] \\ &= \sum_{D'} \mathbb{E}^{0,1}_{D'}[(h(0)+k)^2] \mathbb{P}^{0,1}_{\Lambda_{Rn}}[\mathcal{D} = D'] \\ &\geq k^2 \mathbb{P}^{0,1}_{\Lambda_{Rn}}[\mathcal{O}_{|h|\geq k}(n, Rn)] + \sum_{D'} \mathbb{E}^{0,1}_{D'}[h(0)^2] \mathbb{P}^{0,1}_{\Lambda_{Rn}}[\mathcal{D} = D'] \\ &\geq (k^2 + v_n) \mathbb{P}^{0,1}_{\Lambda_{Rn}}[\mathcal{O}_{|h|\geq k}(n, Rn)]. \end{aligned} \tag{III.37}$$

In the first equality, we used the symmetry $h \leftrightarrow -h$ and in the first inequality the positivity of $\mathbb{E}^{0,1}_{D'}[h(0)]$ (see Corollary III.2.3). In the last inequality, we used (FKG-|h|) to bound $\mathbb{E}^{0,1}_{D'}[h(0)^2]$ by v_n, in the same way as after (III.32).

We turn to the second term of (III.36). This term is an average of quantities of the type $\mathbb{E}^{0,1}_{\Lambda_{Rn}}[h(0)^2 \,|\, |h| = \zeta \text{ on } \Lambda_n^c]$, where ζ runs through all values of $|h|$ outside Λ_n^c such that $\mathcal{O}_{|h|\geq k}(n, Rn)$ fails. Notice that by (FKG-|h|), for any such ζ,

$$\mathbb{E}^{0,1}_{\Lambda_{Rn}}[h(0)^2 \,|\, |h| = \zeta \text{ on } \Lambda_n^c] \geq \mathbb{E}^{0,1}_{\Lambda_{Rn}}[h(0)^2 \,|\, |h| = 0 \text{ or } 1 \text{ on } \Lambda_n^c] \geq v_n.$$

In conclusion,

$$\mathbb{E}^{0,1}_{\Lambda_{Rn}}[h(0)^2 \mathbb{1}_{\mathcal{O}_{|h|\geq k}(n,Rn)^c}] \geq v_n \mathbb{P}^{0,1}_{\Lambda_{Rn}}[\mathcal{O}_{|h|\geq k}(n, Rn)^c]. \tag{III.38}$$

Inject now (III.37) and (III.38) into (III.36), then use (III.35) to conclude that

$$v_{Rn} \geq v_n + k^2\, \mathbb{P}^{0,1}_{\Lambda_{Rn}}[\mathcal{O}_{|h|\geq k}(n, Rn)] - 4.$$

Due to (III.34) and the fact that $k = 4$, the right hand side is larger than $v_n + 1$. □

Proof of the lower bound in Theorem III.1.1

Fix N and $x, y \in F(\mathbb{T}_N)$. Fix a representative of the equivalence class of each homomorphism by setting $h(x) = 0$. Using the FKG inequality for $|h|$ (recall that it does indeed hold for the balanced six-vertex model on the torus) we find

$$\begin{aligned}\mathbb{E}^{(\mathrm{bal})}_{\mathbb{T}_N}[(h(y)-h(x))^2] &= \mathbb{E}^{(\mathrm{bal})}_{\mathbb{T}_N}[h(y)^2 | h(x)=0] \\ &\geq \mathbb{E}^{(\mathrm{bal})}_{\mathbb{T}_N}[h(y)^2 \,|\, |h(u)| \leq 1 \text{ for every } u \notin \Lambda_{\lfloor d(x,y)/2 \rfloor}(y)] \\ &\geq \min_{|\xi|\leq 1} \mathbb{E}^{\xi}_{\Lambda_{\lfloor d(x,y)/2\rfloor}}[h(y)^2] \\ &\geq c \log(d(x,y)/2).\end{aligned}$$

In the second inequality we used the spatial Markov property and in the third Lemma III.5.1. The lower bound of Theorem III.1.1 may be obtained by adapting the constant c.

III.5.2 Upper bounds

In this section we prove the logarithmic upper bounds for the variance of Corollary III.1.5 and Theorem III.1.1. We start in Section III.5.2 with the upper bound of Corollary III.1.5 for simply-connected domains. The case of the torus (Theorem III.1.1) is very similar to that of simply connected domains, but with additional technical difficulties. We sketch it in Section III.5.2. Finally, the case of non simply-connected domains follows easily from the result on the torus, as shown in Section III.5.2.

The upper bound of Corollary III.1.5 for simply-connected domains

We start by defining the counterpart of the quantity v_n of Section III.5.1. For $n \geq 1$, set

$$w_n := \sup_{\partial D \cap \Lambda_n \neq \emptyset} \mathbb{E}^{0,1}_D[h(0)^2],$$

where the supremum is taken over simply-connected discrete domains D with $\partial D \cap \Lambda_n \neq \emptyset$.

Lemma III.5.3. *Fix* $\mathbf{c} \in [1,2]$. *There exists* $C > 0$ *such that for all* $n \geq 1$,

$$w_{2n} \leq w_n + C. \tag{III.39}$$

Let us show how the above implies the upper bound in Corollary III.1.5 for simply-connected domains.

the upper bound in Corollary III.1.5 for simply-connected domains. We may assume $x = 0$. Fix a simply connected domain D containing 0 and a boundary condition ξ with $|\xi| \leq \ell$. Let n be the distance from 0 to D^c. We have

$$\mathrm{Var}^{\xi}_D(h(0)) = \mathrm{Var}^{\xi}_D(h(0)+\ell) \leq \mathbb{E}^{\xi}_D[(h(0)+\ell)^2] = \mathbb{E}^{\xi+\ell}_D[h(0)^2]$$

Then, (CBC-|h|) and Corollary III.2.3 imply that

$$\mathbb{E}_D^{\xi+\ell}[h(0)^2] \le \mathbb{E}_D^{2\ell,2\ell-1}[h(0)^2] \le \mathrm{Var}_D^{2\ell,2\ell-1}(h(0)) + 4\ell^2 = \mathrm{Var}_D^{0,1}(h(0)) + 4\ell^2 \le w_n + 4\ell^2.$$

Finally, it is a direct consequence of Lemma III.5.3 that $w_n \le C \log n$ for some constant C and $n \ge 2$ and the claim thus follows from the previous two displayed equations. □

To prove Lemma III.5.3, we will use the following result which may also be of independent interest.

Lemma III.5.4. *Fix* $\mathbf{c} \in [1,2]$. *There exist* $c, C > 0$ *such that for all* k *and* n *and any simply connected domain* D *containing* Λ_n *but not* Λ_{2n},

$$\mathbb{P}_D^{0,1}[\partial D \xleftrightarrow{|h|\le k} \Lambda_n] \ge 1 - Ce^{-ck}. \tag{III.40}$$

Remark III.5.5. It is useful to adopt the dual view of Remark III.3.2 to Lemma III.5.4: equivalently

$$\mathbb{P}_D^{0,1}[\mathcal{O}^{\times}_{|h|\ge k+1}(n)] \le Ce^{-ck},$$

where $\mathcal{O}^{\times}_{|h|\ge k+1}(n)$ denotes the event that there exists a $\times$-circuit of $|h| \ge k+1$ in D that winds around Λ_n.

Proof. First, by the union bound and (CBC)

$$\mathbb{P}_D^{0,1}[\mathcal{O}^{\times}_{|h|\ge k}(n)] \le \mathbb{P}_D^{0,1}[\mathcal{O}^{\times}_{h\ge k}(n)] + \mathbb{P}_D^{0,1}[\mathcal{O}^{\times}_{h\le -k}(n)] \le 2\mathbb{P}_D^{0,1}[\mathcal{O}^{\times}_{h\ge k}(n)].$$

We will prove that for some universal constant $c > 0$ to be chosen below

$$\mathbb{P}_D^{0,1}[\mathcal{O}^{\times}_{h\ge 2k}(n)] \le e^{-ck}, \tag{III.41}$$

for all $k \ge 0$ by induction. The statement is trivial for $k = 0$, and we focus on the inductive step. Assume that (III.41) holds for some integer k.

When $\mathcal{O}^{\times}_{h\ge 2k}(n)$ occurs, let $\mathcal{Q}$ be the random discrete domain formed of faces inside the exterior-most $\times$-loop of $h = 2k$, and the faces sharing a corner with this interior. Then,

$$\begin{aligned}\mathbb{P}_D^{0,1}[\mathcal{O}^{\times}_{h\ge 2k+2}(n) \mid \mathcal{O}^{\times}_{h\ge 2k}(n) \text{ and } \mathcal{Q} = Q] &= \mathbb{P}_Q^{2k,2k-1}[\mathcal{O}^{\times}_{h\ge 2k+2}(n)] \\ &= \mathbb{P}_Q^{1,2}[\mathcal{O}^{\times}_{h\ge 4}(n)].\end{aligned} \tag{III.42}$$

Fix now any $z \in \mathbb{Z}^2$ on the boundary of Λ_{2n} (viewed as a continuous domain) and not inside D; such a z exists as D does not contain Λ_{2n}. Remark that any circuit around Λ_n in D must cross $\partial\Lambda_n(z)$ and $\partial\Lambda_{2n}(z)$; in particular it connects them, see Figure III.16. Hence, we have

$$\mathbb{P}_Q^{1,2}[\mathcal{O}^{\times}_{h\ge 4}(n)] \le \mathbb{P}_Q^{1,2}[\partial\Lambda_n(z) \xleftrightarrow{h\ge 4}_{\times} \partial\Lambda_{2n}(z)].$$

Let R be a simply connected domain such that $Q \cup \Lambda_{2n}(z) \subset R$. Write $\mathcal{O}_{h\le 3}(A(n,2n)+z)$ for the event that there exists a circuit of faces of height at most 3 in $\Lambda_{2n}(z)$ that surrounds $\Lambda_n(z)$. By duality (Remark III.3.2) and (SMP) we then have

$$\mathbb{P}_Q^{1,2}[\partial\Lambda_n(z) \xleftrightarrow{h\ge 4}_{\times} \partial\Lambda_{2n}(z)] = 1 - \mathbb{P}_R^{1,2}[\mathcal{O}_{h\le 3}(A(n,2n)+z) \,|\, h \in \{1,2\} \text{ on } R \setminus Q].$$

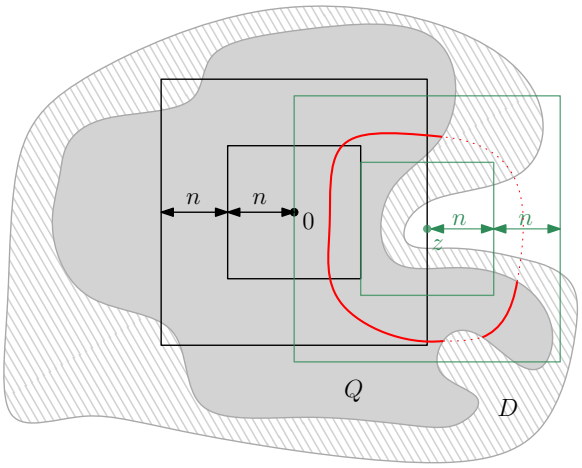

Figure III.16: The event $\mathcal{Q} = Q$ is determined by the value of h on $D \setminus Q$. For z as above, any circuit disconnecting ∂D from Λ_n must cross the annulus $A(n, 2n) + z$ from inside to outside, or, by duality, any circuit in $\Lambda_{2n}(z)$ surrounding $\Lambda_n(z)$ induces a crossing between ∂Q and Λ_n.

Let ξ be the maximal boundary condition on $\partial\Lambda_{2n}(z)$ that takes values $\{1, 2\}$ on $\partial\Lambda_{2n}(z) \setminus Q$, and that is smaller or equal to 6 overall. Then, by Proposition III.2.6 applied to $-h$,

$$\begin{aligned}&\mathbb{P}_R^{1,2}[\mathcal{O}_{h\le 3}(A(n,2n)+z) \,|\, h \in \{1,2\} \text{ on } R \setminus Q] \\ &\qquad \ge \mathbb{P}^{\xi}_{\Lambda_{2n}(z)}[\mathcal{O}_{h\le 3}(A(n,2n)+z) \,|\, h \in \{1,2\} \text{ on } \Lambda_{2n}(z) \setminus Q].\end{aligned}$$

Notice that any path realising $\mathcal{O}_{h\le 3}(A(n, 2n) + z)$ does intersect $\Lambda_{2n}(z) \setminus Q$, which ensures the absence of the multiplicative factor 2. Applying again duality, we conclude that

$$\begin{aligned}\mathbb{P}_Q^{1,2}[\partial\Lambda_n(z) \overset{h\ge 4}{\longleftrightarrow}_{\times} \partial\Lambda_{2n}(z)] &\le \mathbb{P}^{\xi}_{\Lambda_{2n}(z)}[\partial\Lambda_n(z) \overset{h\ge 4}{\longleftrightarrow}_{\times} \partial\Lambda_{2n}(z) \,|\, h \in \{1,2\} \text{ on } \Lambda_{2n}(z) \setminus Q] \\ &\le \mathbb{P}^{\xi}_{\Lambda_{2n}(z)}[\partial\Lambda_n(z) \overset{h\ge 3}{\longleftrightarrow} \partial\Lambda_{2n}(z) \,|\, h \in \{1,2\} \text{ on } \Lambda_{2n}(z) \setminus Q].\end{aligned}$$

Using (FKG) and (FKG-|h|), we find

$$\begin{aligned}&\mathbb{P}^{\xi}_{\Lambda_{2n}(z)}[\partial\Lambda_n(z) \overset{h\ge 3}{\longleftrightarrow} \partial\Lambda_{2n}(z) \,|\, h \in \{1,2\} \text{ on } \Lambda_{2n}(z) \setminus Q] \\ &\quad = \mathbb{P}^{\xi-2}_{\Lambda_{2n}(z)}[\partial\Lambda_n(z) \overset{h\ge 1}{\longleftrightarrow} \partial\Lambda_{2n}(z) \,|\, h \in \{-1,0\} \text{ on } \Lambda_{2n}(z) \setminus Q] \\ &\quad \le \mathbb{P}^{\xi-2}_{\Lambda_{2n}(z)}[\partial\Lambda_n(z) \overset{|h|\ge 1}{\longleftrightarrow} \partial\Lambda_{2n}(z) \,|\, |h| \le 1 \text{ on } \Lambda_{2n}(z) \setminus Q] \\ &\quad \le \mathbb{P}^{\xi-2}_{\Lambda_{2n}(z)}[\partial\Lambda_n(z) \overset{|h|\ge 1}{\longleftrightarrow} \partial\Lambda_{2n}(z)] \\ &\quad = \mathbb{P}^{\xi-2}_{\Lambda_{2n}(z)}[\partial\Lambda_n(z) \overset{h\ge 1}{\longleftrightarrow} \partial\Lambda_{2n}(z)],\end{aligned}$$

where for the second equality one should again keep in mind that any path realising the event above reaches $\partial\Lambda_{2n}$, and therefore its sign is determined[16]. Finally, duality

[16]For a completely formal proof, the event in the last two displays should specify that the path reaches a part of $\partial\Lambda_{2n}$ where $\xi \ge 3$; we omit this technical detail.

allows us to bound the above as

$$\mathbb{P}^{\xi-2}_{\Lambda_{2n}(z)}[\partial\Lambda_n(z) \overset{h\geq 1}{\longleftrightarrow} \partial\Lambda_{2n}(z)] \leq 1 - \mathbb{P}^{3,4}_{\Lambda_{2n}}[\mathcal{O}^{\times}_{h\leq 0}(n)] \leq 1 - \mathbb{P}^{0,1}_{\Lambda_{2n}}[\mathcal{O}_{h\geq 4}(n)] \leq e^{-c},$$

where $c > 0$ is independent of n and is generated by Theorem III.1.4. Summarizing the chain of inequalities starting from (III.42), we have

$$\mathbb{P}^{0,1}_{D}[\mathcal{O}^{\times}_{h\geq 2k+2}(n) \mid \mathcal{O}^{\times}_{h\geq 2k}(n) \text{ and } \mathcal{Q} = Q] \leq e^{-c}$$

for all Q. Using the induction hypothesis and averaging over Q, we conclude that (III.41) also holds for $k+1$, and thus for all k. This implies (III.40) after adjusting the constants. □

Lemma III.5.3. Let D be a simply-connected domain such that $\partial D \cap \Lambda_{2n} \neq \emptyset$. Define the random variable

$$K := \inf\{k \geq 1 \,:\, \partial D \overset{|h|\leq k}{\longleftrightarrow} \Lambda_n\}.$$

Denote by C_k the connected component of faces with $|h| \leq k$ of ∂D, and the $\times$-circuits of $|h| = k+1$ bounding them. Then, C_k may be determined by only exploring the faces in it. Explore C_K by revealing C_1 then C_2, etc, until the first cluster that reaches Λ_n. Write Ω for the faces in $D \setminus \mathsf{C}_K$ or sharing a corner with a face in $D \setminus \mathsf{C}_K$. Then,

$$\mathbb{E}^{0,1}_{D}[h(0)^2] = \sum_{(Q,\zeta)} \mathbb{P}^{0,1}_{D}[h(0)^2 \,|\, \Omega = Q,\, h = \zeta \text{ on } \mathsf{C}_K]\mathbb{P}^{0,1}_{D}[\Omega = Q,\, h = \zeta \text{ on } \mathsf{C}_K], \tag{III.43}$$

where the sum runs over all the possible realizations of $(\Omega, h_{|\mathsf{C}_K})$. When $0 \notin \Omega$, we have $h(0)^2 \leq K^2$. Fix now (Q,ζ) such that $0 \in \Omega$. Write k for the value of K in the realization ζ. Then the values of ζ on ∂Q are either k, $k+1$, $-k$ or $-k-1$. The sign of the boundary conditions may depend on the connected component of Q, however the quantity of interest, $h(0)^2$, is invariant under sign flip. Hence we can as well assume that ζ is positive on ∂Q. Finally, observe that, due to the definition of K, Q necessarily intersects Λ_n. Then,

$$\begin{aligned}
\mathbb{E}^{0,1}_{D}[h(0)^2 \,|\, \Omega = Q \text{ and } h = \zeta \text{ on } \mathsf{C}_K] &= \mathbb{E}^{k,k+1}_{Q}[h(0)^2] \\
&= \mathbb{E}^{0,1}_{Q}[(h(0)+k)^2] \\
&= \mathbb{E}^{0,1}_{Q}[h(0)^2] + 2k\mathbb{E}^{0,1}_{Q}[h(0)] + k^2 \\
&\leq w_n + 2k + k^2.
\end{aligned}$$

Plugging the above into (III.43), we find

$$\mathbb{E}^{0,1}_{D}[h(0)^2] \leq w_n + \mathbb{E}^{0,1}_{D}[2K + K^2].$$

Finally, Lemma III.5.4 implies that $\mathbb{E}^{0,1}_{D}[2K + K^2] \leq C$ for some constant $C > 0$ which is independent of n or D. This proves (III.39). □

The upper bound of Theorem III.1.1

Throughout this proof we fix $\mathbf{c}$ and N, and operate on the torus $\mathbb{T}_N =: \mathbb{T}$. For $B \subset F(\mathbb{T})$, denote

$$\mathbb{E}^{0,1}_{B^c}[\,\cdot\,] = \mathbb{E}^{(\mathrm{bal})}_{\mathbb{T}}[\,\cdot \mid h_{|B} \in \{0,1\}].$$

For $u \in F(\mathbb{T})$ and $1 \le n \le N/2$, write $\Lambda_n(u)$ for the lift of Λ_n to $\mathbb{T}$, translated so that it is centered at the bottom-left corner of u.

Let $x, y \in F(\mathbb{T})$ be the faces appearing in the statement. Due to the triangular inequality, it suffices to prove the bound for $d(x,y) \le N/16$, and we will assume this henceforth. Write $d = d(x,y)$ and for simplicity assume that d is a power of 2 (small adaptations allow to overcome this assumptions).

In analogy to Section III.5.2, for $n \le N/4$, define

$$w_n := \sup\{\mathbb{E}^{0,1}_{B^c}[h(x)^2] \,:\, B \subset F(\mathbb{T}) \text{ connected, intersecting } \Lambda_n(x), \text{ with diameter} \ge 4n\,\}$$
$$u_n := \sup\{\mathbb{E}^{0,1}_{B^c}[h(x)^2] \,:\, B \subset F(\mathbb{T}) \text{ connected, containing } y, \text{ and intersecting } \partial\Lambda_n(y)\}.$$

The result below controls the growth of w_n and u_n, similarly to Lemma III.5.3 in the previous section.

Lemma III.5.6. *Fix $\mathbf{c} \in [1,2]$. There exists $C > 0$ such that for all N and all $x, y \in \mathbb{T}_N$ with $d(x,y) \le N/16$, we have*

$$w_{2n} \le w_n + C \qquad \text{for all } n \le N/8, \tag{III.44}$$
$$u_n \le u_{2n} + C \qquad \text{for all } n \le N/8, \tag{III.45}$$
$$u_{4d} \le w_d. \tag{III.46}$$

Before outlining the proof of this lemma, let us see how it implies the upper bound of Theorem III.1.1.

the upper bound of Theorem III.1.1. By the definition of u_1, we have

$$\mathbb{E}^{(\mathrm{bal})}_{\mathbb{T}_N}[(h(x)-h(y))^2] \le u_1 \overset{\text{(III.45)}}{\le} u_{4d} + C\log 4d \overset{\text{(III.46)}}{\le} w_d + C\log 4d \overset{\text{(III.44)}}{\le} w_1 + 2C\log 4d.$$

Since $w_1 \le 2$, the desired bound is attained. □

Proof outline for Lemma III.5.6 The relations (III.44) and (III.45) are proved in the same way as in Lemma III.5.3 and hinge on the following two statements (which correspond to Lemma III.5.4).

- There exist $c, C > 0$ such that for all k and $n \le N/8$ and any $B \subset F(\mathbb{T})$ connected, intersecting $\Lambda_{2n}(x)$ and with diameter at least $8n$,
$$\mathbb{P}^{0,1}_{B^c}[B \overset{|h|\le k}{\longleftrightarrow} \Lambda_n(x)] \ge 1 - Ce^{-ck}.$$
- There exist $c, C > 0$ such that for all k and $n \le N/8$ and any $B \subset F(\mathbb{T})$ connected, with $y \in B$ and intersecting $\partial\Lambda_n(y)$,
$$\mathbb{P}^{0,1}_{B^c}[B \overset{|h|\le k}{\longleftrightarrow} \partial\Lambda_{2n}(y)] \ge 1 - Ce^{-ck}.$$

Both of these statements are proved in the same way as Lemma III.5.4.

Finally (III.46) follows directly from the definition of u_n and w_n, since any set appearing in the supremum defining u_{4d} also appears in that defining w_d. □

The upper bound of Corollary III.1.5 for arbitrary domains

Fix a finite planar domain D, a face x of D, and a boundary condition ξ on ∂D with $|\xi| \leq \ell$ for some ℓ. By two trivial steps and then (CBC-|h|)

$$\mathrm{Var}_D^{\xi}(h(x)) = \mathrm{Var}_D^{\xi+\ell}(h(x)) \leq \mathbb{E}_D^{\xi+\ell}[h(x)^2] \leq \mathbb{E}_D^{\zeta+2\ell}[h(x)^2] = \mathrm{Var}_D^{\zeta+2\ell}(h(x)) + \mathbb{E}_D^{\zeta+2\ell}[h(x)]^2,$$

for any boundary conditions ζ taking values -1, 0 and 1, and with the same parity as $\xi + \ell$. Let $\pm\zeta$ be the condition minimizing $\mathbb{E}_D^{\zeta}[h(x)^2]$, with the sign chosen so that $\mathbb{E}_D^{\zeta}[h(x)] \leq 0$; whence, by Corollary III.2.3 and the above, we have

$$\mathrm{Var}_D^{\xi}(h(x)) \leq \mathrm{Var}_D^{\zeta}(h(x)) + 4\ell^2.$$

Let y be the even face of ∂D closest to x; note that thus $d(x, y) \leq d(x, \partial D) + 1$. Furthermore, embed D in the torus $\mathbb{T}_N$ for some N larger than twice the diameter of D, and for $\mathbb{E}_{\mathbb{T}_N}^{(\mathrm{bal})}$ normalize height functions by $h(y) = 0$. Using the choice of ζ above and the embedding of D in $\mathbb{T}_N$, we have

$$\begin{aligned}
\mathrm{Var}_D^{\zeta}(h(x)) &\leq \mathbb{E}_{\mathbb{T}_N}^{(\mathrm{bal})}[h(x)^2 \,|\, |h| \leq 1 \text{ on } \partial D] \\
&\leq \mathbb{E}_{\mathbb{T}_N}^{(\mathrm{bal})}[h(x)^2 \,|\, h(y) = 0] && \text{by (FKG-|h|)} \\
&= \mathbb{E}_{\mathbb{T}_N}^{(\mathrm{bal})}[(h(x) - h(y))^2].
\end{aligned}$$

By Theorem III.1.3, the latter is bounded by $C \log d_{\mathbb{T}_N}(x, y)$, where $d_{\mathbb{T}_N}(x, y)$ is the distance between x and y, when embedded in the torus. Notice however that, due to our choice of N and y, $d_{\mathbb{T}_N}(x, y) = d(x, y) \leq d(x, \partial D) + 1$. The claim follows by adjusting C. □

Acknowledgements This research was funded by an IDEX Chair from Paris Saclay, by the NCCR SwissMap from the Swiss NSF and the ERC grant 757296 CRIBLAM. The second author is supported by the ERC CRIBLAM. The third author is supported by the Swiss NSF. We thank Piet Lammers for useful discussions.

III.6 Proofs of the statements in Section III.2.2

III.6.1 Preliminaries

In this preliminaries, we recall the classical Holley criterion, and also draw a connection between our model and the Ising model.

Holley and FKG criteria

Fix some discrete domain D and μ and μ' denote two probability measures on $\mathcal{H}_D$. We say that μ' *stochastically dominates* μ, denoted $\mu \leq_{st} \mu'$, if there exists a probability measure ν on $(h, h') \in \mathcal{H}_D \times \mathcal{H}_D$ such that the first and second marginal distributions are respectively μ and μ', and $\nu[h \preceq h'] = 1$. Note that if $\mu \leq_{st} \mu'$, then, for all increasing $F : \mathcal{H}_D \to \mathbb{R}$,

$$\mu[F(h)] \leq \mu'[F(h)].$$

We say that μ is *irreducible* if for any two $h, h' \in \mathcal{H}_D$ with $\mu[h] > 0$ and $\mu[h'] > 0$, there exists a finite sequence of height functions $h = h_0, h_1, \ldots, h_m = h'$, such that for every $1 \le i \le m$, $\mu[h_i] > 0$ and h_i differs from h_{i-1} on one face only.

We now recall the classical Holley and FKG criteria. For details see the extensive discussion of these criteria in [Gri04].

Lemma III.6.1 (Holley's criterion)**.** *Consider two measures μ and μ' such that*

- *μ and μ' are irreducible,*
- *there exists $h \preceq h' \in \mathcal{H}_D$ such that $\mu[h] > 0$ and $\mu'[h'] > 0$,*
- *for every face $x \in D$, every $k \in \mathbb{Z}$, μ-almost every $\chi \in \mathcal{H}_{D\setminus\{x\}}$, and μ'-almost every $\chi' \in \mathcal{H}_{D\setminus\{x\}}$ with $\chi \preceq \chi'$,*

$$\mu[h(x) \ge k \mid h_{|D\setminus\{x\}} = \chi] \le \mu'[h(x) \ge k \mid h_{|D\setminus\{x\}} = \chi'], \tag{III.47}$$

then $\mu \le_{st} \mu'$.

Lemma III.6.2 (FKG criterion)**.** *Suppose that μ is irreducible. If for every face $x \in D$, every $k \in \mathbb{Z}$, and μ-almost every $\chi \in \mathcal{H}_{D\setminus\{x\}}$ and $\chi' \in \mathcal{H}_{D\setminus\{x\}}$ with $\chi \preceq \chi'$,*

$$\mu[h(x) \ge k \mid h_{|D\setminus\{x\}} = \chi] \le \mu[h(x) \ge k \mid h_{|D\setminus\{x\}} = \chi'], \tag{III.48}$$

then for all increasing functions $F, G : \mathcal{H}_D \to \mathbb{R}$,

$$\mu[F(h)G(h)] \ge \mu[F(h)]\mu[G(h)].$$

Signs of six-vertex height functions and the Ising model

Let D be a discrete domain and $H \in \mathcal{H}_D$ be non-negative. Let $G = G(H) = (V, E)$ be the following (multi-)graph: the vertices V are labelled by the clusters of $H > 0$ on the graph D; between any two vertices $u, v \in V$ place as many edges as there are vertices of D that are adjacent to a face in each of the clusters corresponding to u and v. Notice that any vertex of D that corresponds to an edge of G necessarily has two adjacent faces for which $H = 0$. For $v \in V$, the sign of any height function $h \in \mathcal{H}_D$ with $|h| = H$ is constant on the cluster of $H > 0$ associated with v. We denote this sign as $\sigma_h(v)$, yielding a function $\sigma_h : V \to \{\pm 1\}$.

Define the Ising model on G via the following weights W_{Ising} and probability measure $\mathsf{P}_{\text{Ising}}$: for $\sigma \in \{\pm 1\}^V$,

$$W_{\text{Ising},H}(\sigma) := \prod_{e=\langle u,v\rangle \in E} \mathbf{c}^{\mathbb{1}[\sigma(u)=\sigma(v)]},$$
$$\mathsf{P}_{\text{Ising},H}[\sigma] := \tfrac{1}{Z} W_{\text{Ising},H}(\sigma).$$

Lemma III.6.3. *Let $h, H \in \mathcal{H}_D$ satisfying $|h| = H$. Then, in the above notation*

$$W_{6V}(h) = \mathbf{c}^{N(H)}\, W_{\text{Ising},H}(\sigma_h),$$

where $N(H)$ is the number of type 5–6 vertices of D in H that are not edges of G.

Proof. Any type 5–6 vertex of h is also a type 5–6 vertex in H. Conversely, any type 5–6 vertex of H which does not correspond to an edge of G is also a type 5–6 vertex in h. The other type 5–6 vertices of H however may correspond to either type 1–4 or type 5–6 vertices of h, depending on the choice of the signs in h of the two clusters of $H > 0$ meeting there. Indeed, they are of type 5–6 only if the two clusters have same sign. We deduce that

$$W_{6V}(h) := \mathbf{c}^{N(H)} \prod_{e=\langle u,v\rangle \in E} \mathbf{c}^{\mathbb{1}[\sigma_h(u)=\sigma_h(v)]} = \mathbf{c}^{N(H)}\, W_{\mathrm{Ising},H}(\sigma_h).$$

□

Let now $H, H' \in \mathcal{H}_D$ be two height functions with $H' \geq H \geq 0$. Let $G' = (V', E') = G(H')$. Note that every cluster of $H > 0$ is thus contained in a unique cluster of $H' > 0$. Let $\pi : V \to V'$ be the projection corresponding to this inclusion, and define also the preimage map π^{-1} of this projection, from V' to subsets of V.

Lemma III.6.4. *Condition the Ising model $\mathsf{P}_{\mathrm{Ising},H}$ on G on the event that $\sigma(\cdot)$ is constant on $\pi^{-1}(v)$ for every $v \in V'$; then the law of $\sigma \circ \pi^{-1}$ (this is a slight abuse of notation) is $\mathsf{P}_{\mathrm{Ising},H'}$.*

Proof. Consider an edge $e' = \langle u', v'\rangle \in E'$ corresponding to a local configuration of H' given by $\left(\begin{smallmatrix} 0 & 1 \\ 1 & 0 \end{smallmatrix}\right)$ or $\left(\begin{smallmatrix} 1 & 0 \\ 0 & 1 \end{smallmatrix}\right)$. Since $0 \leq H \preceq H'$, H has the same local configuration, and thus e' corresponds to a unique edge $e \in E$, where furthermore $e = \langle v, u\rangle$ satisfies $\pi(v) = v'$ and $\pi(u) = u'$. We denote this injective map by $\iota : E' \to E$. We claim that the restriction of ι is a bijection

$$\iota : \{e' = \langle u', v'\rangle \in E' \ : \ u' \neq v'\} \longrightarrow \{e = \langle u, v\rangle \in E \ : \ \pi(u) \neq \pi(v)\}$$

(we use a slight abuse of notation and write ι for the restriction as well). Indeed, first, for $e' = \langle u', v'\rangle \in E'$ with $u' \neq v'$ the image $\iota(e') = \langle v, u\rangle$ satisfies $\pi(v) = v'$ and $\pi(u) = u'$, so $\pi(u) \neq \pi(v)$. Second, given $e = \langle u, v\rangle \in E$, the additional condition $\pi(u) \neq \pi(v)$ implies that the local configuration $\left(\begin{smallmatrix} 0 & 1 \\ 1 & 0 \end{smallmatrix}\right)$ or $\left(\begin{smallmatrix} 1 & 0 \\ 0 & 1 \end{smallmatrix}\right)$ of H corresponding to e must be the same in H'. Hence, there exists $e' \in E'$, labelled by this local configuration of H', that maps $\iota(e') = e$. This proves the bijectivity, as ι is by construction injective.

Suppose now that $\sigma(\cdot)$ is constant on $\pi^{-1}(v)$ for every $v \in V'$. Compute

$$\begin{aligned}
W_{\mathrm{Ising},H}(\sigma) &= \prod_{e=\langle u,v\rangle \in E} \mathbf{c}^{\mathbb{1}[\sigma(u)=\sigma(v)]} \\
&= \underbrace{\Big(\prod_{\substack{e=\langle u,v\rangle \in E \\ \pi(u)=\pi(v)}} \mathbf{c} \Big)}_{K(H,H')} \times \prod_{\substack{e=\langle u,v\rangle \in E \\ \pi(u)\neq\pi(v)}} \mathbf{c}^{\mathbb{1}[\sigma(u)=\sigma(v)]} \\
&= K(H,H') \times \prod_{\substack{e'=\langle u',v'\rangle \in E' \\ u'\neq v'}} \mathbf{c}^{\mathbb{1}[\sigma\circ\pi^{-1}(u')=\sigma\circ\pi^{-1}(v')]} \\
&= K(H,H')\mathbf{c}^{-\#\{\text{loop edges of } E'\}} W_{\mathrm{Ising},H'}(\sigma \circ \pi^{-1}),
\end{aligned}$$

where in the third equality we re-labeled the product using the bijection ι, and used the observation that for an edge $\langle u', v' \rangle \in E'$ in the new labeling, the corresponding $\langle u, v \rangle \in E$, for which $\iota(\langle u, v \rangle) = \langle u', v' \rangle$, satisfies $u \in \pi^{-1}(u')$ and $v \in \pi^{-1}(v')$. The claimed equality of distributions now follows from the previous displayed equation. □

III.6.2 Proof of (FKG) and (CBC)

We will check the assumption of Lemma III.6.1 for $\mu = \mathbb{P}_D^{\xi}$ and $\mu' = \mathbb{P}_D^{\xi'}$ where $\xi \preceq \xi'$. In the special case when $\xi = \xi'$, the assumptions of Lemma III.6.1 become those of Lemma III.6.2. These two lemmas then directly imply (CBC) and (FKG), respectively.

We start by showing the irreducibility of $\mathbb{P}_D^{\xi}$. Consider two height functions h, h' which are admissible for $\mathbb{P}_D^{\xi}$. It is easy to check that their point-wise maximum $h \vee h'$ is also admissible. Thus, it suffices to consider the case $h \preceq h'$, which is what we do next.

Assuming that $h \neq h'$, the function $h' - h$ has at least one face of strictly positive value. Write $m := \max\{h'(z) - h(z) : z \in D\}$ and let x be a face of maximal h'-value among the faces z with $h'(z) - h(z) = m$. By this maximality, one readily deduces that h' takes values $h'(x) - 1$ on all faces adjacent to x. Thus, the function h_1 which is equal to h' on $D \setminus \{x\}$ and equal to $h'(x) - 2$ at x is also admissible. Applying repeatedly this type of modification, we construct a decreasing sequence of admissible height functions $h' = h_1, \dots, h_m = h$, with h_{i+1} differing from h_i at only one face. In conclusion $\mathbb{P}_D^{\xi}$ is irreducible. (The monotonicity is unimportant here, but crucial when repeating the same argument for absolute values.) The same holds for $\mathbb{P}_D^{\xi'}$.

To check the second condition of Lemma III.6.1, let h and h' be arbitrary admissible height functions for $\mathbb{P}_D^{\xi}$ and $\mathbb{P}_D^{\xi'}$, respectively. Then, the point-wise minimum and maximum $h \wedge h'$ and $h \vee h'$ are also admissible height functions for $\mathbb{P}_D^{\xi}$ and $\mathbb{P}_D^{\xi'}$, respectively. These two height functions satisfy the second condition of Lemma III.6.1.

We now check (III.47). Let χ and χ' as in the assumption of Lemma III.6.1. Let N_x be the set of faces of D adjacent to x in D (there are between 2 and 4 of them). Let $m := \min_{y \in N_x} \chi(y)$, $M := \max_{y \in N_x} \chi(y)$, and m', M' similarly defined for χ'. By assumption, we have that $m \leq m'$ and $M \leq M'$.

Moreover since χ and χ' are admissible, we have $M \in \{m, m+2\}$ and $M' \in \{m', m'+2\}$. If $M = m+2$, then $h(x) = m+1$ with $\mathbb{P}_D^{B,\xi}[\cdot | h_{|D\setminus\{x\}} = \chi]$- probability 1. Otherwise $h(x) \in \{m-1, m+1\}$. As a consequence, if either $M > m$ and $M' > m'$, then (III.47) holds trivially. The same is true when $m = M < m' = M'$.

The only remaining case is when $m = m' = M = M'$. In this case, for both measures, we know that $h(x) \in \{m-1, m+1\}$, and it thus remains to show that

$$\mathbb{P}_D^{B,\xi'}[h(x) = m+1 \mid h_{|D\setminus\{x\}} = \chi'] \geq \mathbb{P}_D^{B,\xi}[h(x) = m+1 \mid h_{|D\setminus\{x\}} = \chi].$$

Let $N_x^{\times}$ be the set of faces in $D \setminus \{x\}$ that share a corner with x. On $N_x^{\times}$, χ takes a value in $\{m-1, m, m+1\}$. Define $n_- = \#\{y \in N_x^{\times}, \chi(y) = m-1\}$, $n_+ = \#\{y \in N_x^{\times}, \chi(y) = m+1\}$ and n'_-, n'_+ similarly for χ'. By computing the

weights of the different height functions extending χ, we get

$$\mathbb{P}_D^{B,\xi}[h(x) = m+1 \mid h_{|D\setminus\{x\}} = \chi] = \frac{\mathbf{c}^{n_+}}{\mathbf{c}^{n_+} + \mathbf{c}^{n_-}},$$
$$\mathbb{P}_D^{B,\xi'}[h(x) = m+1 \mid h_{|D\setminus\{x\}} = \chi'] = \frac{\mathbf{c}^{n'_+}}{\mathbf{c}^{n'_+} + \mathbf{c}^{n'_-}}.$$

Observe that the assumption $\chi \preceq \chi'$ implies $n_+ \leq n'_+$ and $n_- \geq n'_-$, and as $\mathbf{c} \geq 1$, we thus deduce (III.47) in this case as well. □

III.6.3 Proof of (FKG-|h|) and (CBC-|h|)

As before, we focus on proving the three properties of Lemma III.6.1 for the laws μ and μ' of $|h|$ under $\mathbb{P}_D^{\xi}$ and $\mathbb{P}_D^{\xi'}$.

For irreducibility, observe that, since $\xi \succeq 0$, $\mathbb{P}_D^{\xi}[|h| = H] > 0$ if and only if $\mathbb{P}_D^{\xi}[h = H] > 0$. The irreducibility of the law of $|h|$ follows from that of $\mathbb{P}_D^{\xi}$. The same holds for $\mathbb{P}_D^{\xi'}$. The second property of Lemma III.6.1 for $|h|$ is derived in a similar way from that for the law of h.

Finally, let us prove (III.47). Fix $0 \leq \chi \preceq \chi'$. Let N_x be as in the proof of Proposition III.2.2. Let $m := \min_{y\in N_x} \chi(y)$, $M := \max_{y\in N_x} \chi(y)$, and m', M' similarly for χ'. Then, $m' \geq m \geq 0$ and $M' \geq M \geq 0$. Identically to the proof of Proposition III.2.2, one can show that the only non trivial case is $m = m' = M = M'$, which we now assume is the case. We divide the proof in three cases depending on whether the common value $m = m' = M = M'$ is equal to 0, 1 or larger than or equal to 2.

If $m = 0$, then we must have $|h(x)| = 1$ under both measures, and we therefore have nothing to prove.

Suppose now that $m \geq 2$. As in the proof of Proposition III.2.2, let $N_x^{\times}$ be set of faces sharing a corner with x and $n_- := \#\{y \in N_x^{\times} : \chi(y) = m-1\}$, $n_+ := \#\{y \in N_x^{\times} : \chi(y) = m+1\}$ and n'_-, n'_+ similarly for χ'. Given that χ and χ' only take values in $\{m-1, m, m+2\}$, the sign of h is constant on $N_x^{\times}$. In particular, the types of the vertices at the corners of the square x only depend on the absolute value $|h|$, not on the sign of h. One can thus directly compute the weights of the different possible configurations of h and obtain

$$\mathbb{P}_D^{\xi}[|h(x)| = m+1 \mid |h_{|D\setminus\{x\}}| = \chi] = \frac{\mathbf{c}^{n_+}}{\mathbf{c}^{n_+} + \mathbf{c}^{n_-}},$$
$$\mathbb{P}_D^{\xi'}[|h(x)| = m+1 \mid |h_{|D\setminus\{x\}}| = \chi'] = \frac{\mathbf{c}^{n'_+}}{\mathbf{c}^{n'_+} + \mathbf{c}^{n'_-}}.$$

As in the proof of Proposition III.2.2, $\chi \preceq \chi'$ implies $n_+ \leq n'_+$ and $n_- \geq n'_-$, which in turn implies (III.47) since $\mathbf{c} \geq 1$.

There remains the case where $m = 1$, which is the core of the proof and for which we use the connection to the Ising model mentioned in Section III.6.1. In this case, there are only two possible values for $|h(x)|$, namely 0 and 2. We wish to show

$$\mathbb{P}_D^{\xi}\big[|h(x)| = 2 \;\big|\; |h_{|D\setminus\{x\}}| = \chi\big] \leq \mathbb{P}_D^{\xi'}\big[|h(x)| = 2 \;\big|\; |h_{|D\setminus\{x\}}| = \chi'\big]. \tag{III.49}$$

Let $H_0 \in \mathcal{H}_D$ (resp. H_2) be the height functions equal to 0 (resp. 2) at x and coinciding with χ on $D \setminus \{x\}$. Define

$$Z_0 = \sum_{\substack{h \in \mathcal{H}_D \\ |h|=H_0 \\ h \geq 0 \text{ on } B}} W_{6V}(h) \qquad \text{and} \qquad Z_2 = \sum_{\substack{h \in \mathcal{H}_D \\ |h|=H_2 \\ h \geq 0 \text{ on } B}} W_{6V}(h). \tag{III.50}$$

Then

$$\mathbb{P}_D^{\xi}\big[|h(x)| = 2 \;\big|\; |h_{|D\setminus\{x\}}| = \chi\big] = \frac{Z_2}{Z_0 + Z_2}.$$

A similar formula is obtained for the "primed" configurations. To deduce (III.49), one needs to show that

$$Z_2/Z_0 \leq Z_2'/Z_0'. \tag{III.51}$$

Now follows a simple but crucial observation. There is an injection $\mathbf{T}$ from the height functions h contributing to Z_2 to the height functions h contributing to Z_0: simply change the value ± 2 of $h(x)$ to 0. The image of this injection is exactly those h contributing to Z_0 for which in addition h has constant sign[17] on N_x. Set $n_0 := \#\{y \in N_x^\times \;:\; \chi(y) = 0\}$ and $n_2 := \#\{y \in N_x^\times \;:\; \chi(y) = 2\}$. Under this injection the six-vertex weights become

$$W_{6V}(\mathbf{T}(h)) = \mathbf{c}^{n_0 - n_2} W_{6V}(h).$$

We can thus express Z_2 using this up-to-constant weight-preserving injection as

$$Z_2 = \mathbf{c}^{n_2 - n_0} \sum_{\substack{h \in \mathcal{H}_D \\ |h|=H_0 \\ h \geq 0 \text{ on } B \\ \text{sign}(h) \text{ cst. on } N_x}} W_{6V}(h),$$

and finally, using (III.50),

$$Z_2/Z_0 = \mathbf{c}^{n_2 - n_0} \mathbb{P}_D^{\xi}[\text{sign}(h) \text{ cst. on } N_x \mid |h| = H_0]. \tag{III.52}$$

A similar formula holds for the "primed" configurations.

Recall again that $\mathbf{c} \geq 1$ and that $n_2 - n_0 \leq n_2' - n_0'$. Using (III.52) and its "primed" analogue, we observe that for (III.51) to hold it thus suffices that

$$\mathbb{P}_D^{\xi}[\text{sign}(h) \text{ cst. on } N_x \mid |h| = H_0] \leq \mathbb{P}_D^{\xi'}[\text{sign}(h') \text{ cst. on } N_x \mid |h'| = H_0']. \tag{III.53}$$

Let us now study the conditional probability appearing on the left. Lemma III.6.3

[17] And this sign tells whether the preimage takes value $+2$ or -2 at x, which implies the injectivity.

gives

$$\mathbb{P}_D^{\xi}[\text{sign}(h) \text{ cst. on } N_x \mid |h| = H_0] = \sum_{\substack{h\in\mathcal{H}_D \\ |h|=H_0 \\ h\geq 0 \text{ on } B \\ \text{sign}(h) \text{ cst. on } N_x}} W_{6V}(h) \Big/ \sum_{\substack{h\in\mathcal{H}_D \\ |h|=H_0 \\ h\geq 0 \text{ on } B}} W_{6V}(h)$$

$$= \sum_{\substack{\sigma\in\{\pm1\}^V \\ \sigma=+1 \text{ on } B \\ \sigma \text{ cst. on } N_x}} W_{\text{Ising},H_0}(\sigma) \Big/ \sum_{\substack{\sigma\in\{\pm1\}^V \\ \sigma=+1 \text{ on } B}} W_{\text{Ising},H_0}(\sigma)$$

$$= \mathsf{P}_{\text{Ising},H_0}[\sigma \text{ cst. on } N_x \mid \sigma = +1 \text{ on } B].$$

where the Ising model is as in Section III.6.1, and by "σ cst. on N_x" we mean that σ is constant on the vertices of v labeled by clusters of $H_0 > 0$ intersecting N_x; "$\sigma = +1$ on B" should be interpreted analogously.

A similar reasoning together with Lemma III.6.4 applied to $H_0 \preceq H_0'$ gives that

$$\begin{aligned}
&\mathbb{P}_D^{\xi'}[\text{sign}(h') \text{ cst. on } N_x \mid |h'| = H_0'] \\
&= \mathsf{P}_{\text{Ising},H_0'}[\sigma' \text{ cst. on } N_x \mid \sigma' = +1 \text{ on } B] \\
&= \mathsf{P}_{\text{Ising},H_0}[\sigma \text{ cst. on } N_x \mid \{\sigma \text{ cst. on } \pi^{-1}(v') \text{ for each } v' \in V'\} \cap \{\sigma = +1 \text{ on } B\}].
\end{aligned}$$

Plugging the two previous displayed equations in (III.53), we see that it suffices to show that

$$\mathsf{P}_+[\sigma \text{ cst. on } N_x] \leq \mathsf{P}_+[\sigma \text{ cst. on } N_x \mid \sigma \text{ cst. on } \pi^{-1}(v') \text{ for each } v' \in V'], \quad \text{(III.54)}$$

where P_+ denotes $\mathsf{P}_{\text{Ising},H_0}[\,\cdot\,|\sigma = +1 \text{ on } B]$.

Denote by N the vertices of V that correspond to clusters intersecting N_x, and denote the sets $\pi^{-1}(v')$ by U_i. Equivalently to (III.54), we want to prove

$$\text{Cov}_{\mathsf{P}_+}\big(\mathbb{1}[\sigma \text{ cst. on } N], \prod_{i=1}^{m} \mathbb{1}[\sigma \text{ cst. on } U_i]\big) \geq 0.$$

Now, note that we have

$$\mathbb{1}\{\sigma \text{ cst. on } A\} = \prod_{u,v\in A} \frac{1+\sigma_u\sigma_v}{2} = \sum_{U\subset A} a_U \prod_{u\in U} \sigma_u,$$

where $a_U \geq 0$ for every $U \subset A$. Applying this formula for $A = N$ and $A = U_i$, we get

$$\text{Cov}_{\mathsf{P}_+}\big(\mathbb{1}[\sigma \text{ cst. on } N], \prod_{i=1}^{m} \mathbb{1}[\sigma \text{ cst. on } U_i]\big) = \sum_{U\subset V} \sum_{U'\subset N} a_U b_{U'} \text{Cov}_{\mathsf{P}_+}\big(\prod_{u'\in U'} \sigma_{u'}, \prod_{u'\in U'} \sigma_u\big) \geq 0,$$

where in the last step we observed that $a_U, b_{U'} \geq 0$ and that by Griffiths' second inequality [Gri67], each individual covariance term in the sum is non-negative. This finishes the proof.

A | Incipient Infinite Clusters in FK percolation

A.1 Introduction

The term "Incipient Infinite Cluster" (IIC) has been used since at least the mid-seventies (see e.g. [SBRN76]) in the physics literature on percolation to talk about the large clusters at or just below the critical point p_c, that are about to become the true infinite cluster once p passes p_c. In [Kes86], Kesten proposed a definition of the IIC measure as a limit of conditional percolation measures. It is the measure where the configuration around the origin of the lattice (say in $\mathbb{Z}^2$) is the typical configuration seen around a vertex lying in a large macroscopic cluster at p_c. The two proposed definitions, which are shown to be equivalent, are given by the following limits

$$(i) \quad \lim_{n\to\infty} \mathbb{P}_{p_c}(\cdot \mid 0 \leftrightarrow \partial\Lambda_n) \tag{A.1}$$

$$(ii) \quad \lim_{p\searrow p_c} \mathbb{P}_p(\cdot) \tag{A.2}$$

for events depending on finitely many edges. A true probability measure is then constructed through the Kolmogorov extension theorem.

Following these lines, Damron and Sapozhnikov [DS11] introduced the "multi-arm IIC", by taking the limit of Bernoulli percolation measure conditioned on having, not only one connection, but several primal and dual arms connected to the boundary of a large box.

The key strategy of these proofs is to show that the shape of the cluster, or the arms, decorrelates at every scale. When several arms are involved, an important ingredient is the *arm separation* : say that we have several arms reaching $\partial\Lambda_N$ from inside, and others reaching $\partial\Lambda_{2N}$ from outside, and we want to glue them. To do that with RSW-type techniques, we need the endpoints of these arms to bo well separated. Arm separation for Bernoulli percolation first appeared in [Kes87] and was developed in [Nol08]. A stronger version of this result appears in [GPS13b, Appendix A]. For critical FK percolation, the separation phenomenon was proven for $q \in [1, 4)$ successively in [CDCH16, DCMT21].

The result on arm separation was used to show the quasi-multiplicativity of arm events probabilities. In [BS17], Basu and Sapozhnikov proposed a construction of the IIC for Bernoulli percolation along the lines of Kesten, on general bounded degree graphs, assuming only the uniqueness of the infinite cluster and the quasi-multiplicativity of arm-events probabilities.

In Chapter II, we need to use a "3-arm in the half plane" IIC measure. The previous proofs of existence of IIC-type measures were written for Bernoulli percolation, hence using the independence, Reimer inequality, etc. The same strategy works for FK percolation on isoradial graphs, and we give here a self contained proof of existence that is not assuming $q = 1$. Since we want to cover $q \in [1, 4]$, we also explain how we can avoid using RSW to adverse fractal boundary condition (that holds for $q \in [1, 4)$ by [DCMT21] but not for $q = 4$). Finally, the previous statements of convergence to the IIC measure were non quantitative. Following the lines of the proof of [GPS13b, Proposition 3.1], we show that the convergence occurs at polynomial speed.

A.2 Main statements

Let $G = (V, E)$ be an isoradial lattice and $G^* = (V^*, E^*)$ be the isoradial dual of G. Let $G^\diamond = (V^\diamond, E^\diamond)$ be the diamond graph of G.

Let $q \in [1, 4]$ and Φ be the critical random cluster measure on G with parameter q. We assume that Φ verifies RSW uniformly in the plane and that 0 is a vertex of G. For any $v \in V$ we denote by v_0 and v_1 its x and y coordinates. Define the half-plane H by $H = \{(x, y) \in \mathbb{R}^2 \mid y < 0 \text{ or } y = 0 \wedge x \geq 0\}$. For any $X \subset V$, let X^* be the vertices of V^* adjacent to some $x \in X$ in $G^\diamond$.

Notice that there must exist a dual vertex $z \in V^*$ with $z_1 > 0$ and z adjacent to 0 in $G^\diamond$. For $N > 0$ and $X, Y, Z \subset \partial\Lambda_N$, denote by $\left\{0 \overset{(3)}{\longleftrightarrow} (X, Y, Z)\right\}$ the event that 0 is connected by an open path in $H \cap \Lambda_N$ to Y, and z is connected to X and Y by two disjoint dually open paths of $(H \cap \Lambda_N)^*$. One can check that this definition does not depend on the choice of z. See Figure A.1.

For any $N \geq 1$, define three sets $X_N, Y_N, Z_N \subset \partial\Lambda_N$ and an event E_N that depends only on the state of edges in $G \setminus \Lambda_N$. Let the event A_N be

$$A_N = \left\{0 \overset{(3)}{\longleftrightarrow} (X_N, Y_N, Z_N)\right\} \cap E_N.$$

Suppose that for any $n \geq 0$, $\Phi(A_N) > 0$.

Proposition A.2.1. *There exists a measure $\nu := \nu_{G,q,H}$ on $\{0, 1\}^E$ that depends only on Φ and H such that for any event B depending on finitely many edges,*

$$\lim_{N \to +\infty} \Phi(B \mid A_N) = \nu(B). \tag{A.3}$$

Proposition A.2.2. *The speed of convergence to the IIC measure is polynomial and does not depend on X_N, Y_N, Z_N, E_N. Let $\mathcal{F}_n$ be the set of events B depending only on the edges of Λ_n. There exists a constant $k := k(\Phi)$ such that for any $N > n > 0$,*

$$\sup_{B \in \mathcal{F}_n} \frac{|\nu(B) - \Phi(B|A_N)|}{\nu(B)} \leq \left(\frac{n}{N}\right)^k.$$

For any two scales $0 < N < M$, let $A(N, M)$ be the annulus $A(N, M) = \Lambda_M \setminus \Lambda_N$. Let $U_{N,M}$ be the event that there are exactly one primal and one dual crossing clusters C_p and C_d in $A(N, M)$.

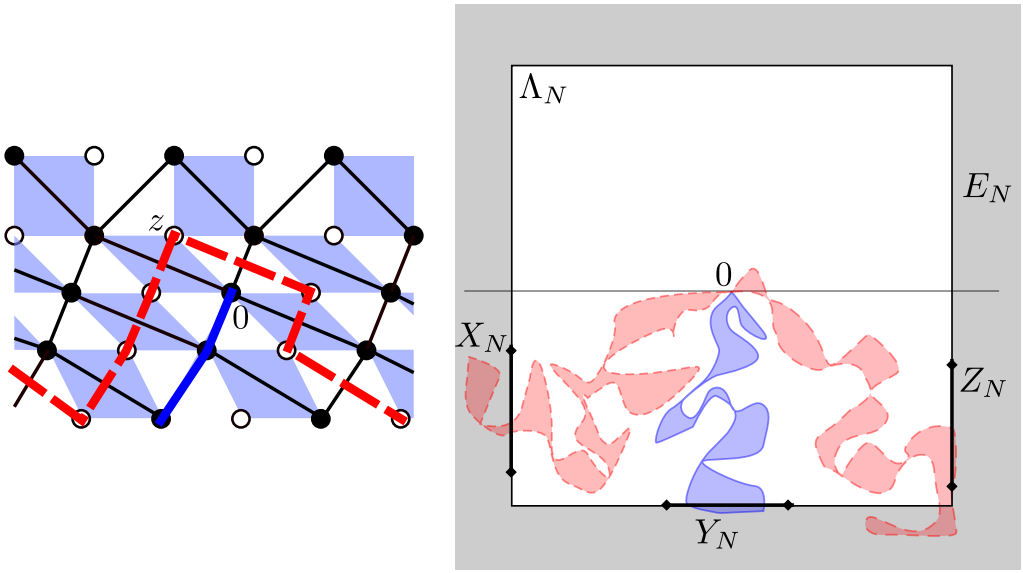

Figure A.1: On the left, we represented G in black, the dual vertices as white filled circles, the underlying lozenge graph $G^\diamond$, as well as the two red dashed dual arm end the blue primal arm. On the right, the three arm event in the half plane is represented.

If X, Y, Z are three vertex sets in $\partial\Lambda_M$, denote by $\partial\Lambda_N \overset{(3)}{\longleftrightarrow} (X, Y, Z)$ the event that there exist two dually open paths between $\partial\Lambda_N^*$ and X^*, Z^* in H^* and an open path between $\partial\Lambda_N$ and Y in H such that the primal path lies between the two dual paths in $A(N, M) \cap H$.

A.3 Strong arm separation

The main result that allows us to study the decorrelation of arm events across scales is the fact that asking the arms to be well separated on the boundary of a box does not cost more than a multiplicative constant in probability.

Let $\Gamma_{N,M}$ be the set of percolation interfaces crossing an annulus $A(N, M)$. Following the notations of [GPS13b], we define the interior quality $\mathbf{Q}(\Gamma_{N,M})$ to be the minimal distance separating the inner endpoints of the interfaces of $\Gamma_{N,M}$, and the upper half-plane, normalized by N, that is

$$\mathbf{Q}(\Gamma_{N,M}) = \frac{1}{N} \min_{i,j}(||x^i - x^j||, |x_1^i|)$$

where the minimum is over the endpoints $(x^i)_i$ of the interfaces of $\Gamma_{N,M}$ on $\partial\Lambda_N$. The separation result proven in [DS11, GPS13b] can be rephrased in our context as follows.

Proposition A.3.1. *There exists a constant $c_{\text{sep}} > 0$ such that for any $0 < N < 2N < M$,*

$$\Phi(\mathbf{Q}(\Gamma_{N,M}) > 1/3 \mid \partial\Lambda_N \overset{(3)}{\longleftrightarrow} (X_M, Y_M, Z_M), E_M) > c_{\text{sep}}.$$

We sketch the core of the proof. The idea is to start from an arbitrary quality and to improve it scale by scale, such that the cost δ of having a bad quality ρ at some scale exceeds the cost c_2 of keeping a good quality with RSW type constructions. We need the following inequalities:

(i) If the quality is not to bad, we can improve it at some positive cost. That is, for every $\rho > 0$, there exists $c_1(\rho) > 0$ such that

$$\Phi(\mathbf{Q}(\Gamma_{N,M}) > 1/3 \mid \partial\Lambda_N \overset{(3)}{\longleftrightarrow} \partial\Lambda_M) > c_1(\rho)\Phi(\mathbf{Q}(\Gamma_{2N,M}) > \rho \mid \partial\Lambda_{2N} \overset{(3)}{\longleftrightarrow} \partial\Lambda_M).$$

(ii) If we have a good quality, we can keep it at constant cost. That is, there exists some $c_2 > 0$ such that

$$\Phi(\mathbf{Q}(\Gamma_{N,M}) > 1/3 \mid \partial\Lambda_N \overset{(3)}{\longleftrightarrow} \partial\Lambda_M) > c_2\Phi(\mathbf{Q}(\Gamma_{2N,M}) > 1/3 \mid \partial\Lambda_{2N} \overset{(3)}{\longleftrightarrow} \partial\Lambda_M).$$

(iii) Low quality is unlikely. That is, for any $\delta > 0$, there exists a quality $\rho > 0$ such that

$$\Phi(\mathbf{Q}(\Gamma_{N,2N}) < \rho \mid \partial\Lambda_N \overset{(3)}{\longleftrightarrow} \partial\Lambda_M) < \delta.$$

Assume that all the scales $N, 2N, \dots, 2^j N$ have quality less than ρ. By item (iii), the probability of this happening conditionally on $\{\mathbf{Q}(\Gamma_{2^{j+1}N,M}) > \rho, \partial\Lambda_{2^{j+1}N} \overset{(3)}{\longleftrightarrow} \partial\Lambda_M\}$ has probability less than δ^j. On the other hand, conditionally on the same event, we can deduce from (i) and (ii) that

$$\Phi(\mathbf{Q}(\Gamma_{N,M}) > 1/3 \mid \partial\Lambda_N \overset{(3)}{\longleftrightarrow} \partial\Lambda_M) > c_1(\rho)c_2^{j-1}\Phi(\mathbf{Q}(\Gamma_{2^{j+1}N,M}) > \rho \mid \partial\Lambda_{2^{j+1}N} \overset{(3)}{\longleftrightarrow} \partial\Lambda_M).$$

However the argument breaks when $2^j N$ reaches M. Since we want to condition on any event outside Λ_M, we do not control the quality at this scale. Therefore, [GPS13b] introduced a *strong* arm separation proof that uses a hierarchical construction to increase step by step the relative quality of subset of the interfaces that start close to each other at scale M.

Proof of Proposition A.3.1. The proof of [GPS13b, Proposition A.1] runs with no changes. Its uses of RSW type crossing events are always to boundary of the same type (primal to primal, dual to dual), and always at macroscopic distance of the other type. The proof relies on two lemmas corresponding to the above enumerated items.

Items (i) and (ii) in our sketch correspond to [GPS13b, Lemma A.2]. The proof is a classical use of RSW, always to same type boundary (see in particular the remark just above the statement of this lemma).

Item (iii) corresponds to [GPS13b, Lemma A.3], and one should be more careful there. In addition to the references given in this paper, one can find a similar statement in [Nol08, Lemma 14]. Since we are interested in three arms in a half plane, there is a one dimensional way of exploring the interfaces (e.g, starting from the positive x-axis and exploring clockwise around the origin), so the structure of the proof of [Nol08] can apply. Moreover, our three arms are alternating (dual, primal, dual). So instead of using *shields* of the two type as described in [Nol08] (which would require a stronger version of RSW than what we have for $q = 4$), we can only use monochromatic shields : a primal shield adjacent to a primal arm will anyway prevent the next dual arm to come close. □

A.4 Proof of Proposition A.2.1

We follow the strategy of the proof of [BS17, Theorem 3]. We first prove Lemma A.4.1 stating that with a good choice of scales N, M, there is a unique primal (resp. dual) crossing cluster of the annulus $A_{N,M}$ with high probability. This allows to decouple what happens inside and outside this annulus. We then express the probability $\Phi(B \mid A_L)$ in terms of a ratio of matrix products (plus some error term), and we prove a decoupling inequality on the matrix coefficients, that is Lemma A.4.2. This decoupling result is enough to deduce the convergence of the probability, and hence the existence of the IIC measure.

Lemma A.4.1. *There exists a constant $k > 0$ such that for any integers $N < 8N < M < L$,*

$$\Phi(U_{N,M} \mid A_L) \geq 1 - \left(\frac{N}{M}\right)^k. \tag{A.4}$$

Proof. By inclusion we have that

$$\Phi(U^c_{N,M}, A_L) \leq \Phi\left(U^c_{N,8N}, U^c_{8N,8^2N}, \dots, U^c_{8^{\ell-1}N,8^\ell N}, A_L\right) \tag{A.5}$$

for $\ell := \lfloor \log_8(M/N) \rfloor$. With successive conditioning, we can write

$$\begin{aligned}\Phi(U^c_{N,M}, A_L) \leq \\ \Phi(A_L) \times \Phi(U^c_{8^{\ell-1}N,8^\ell N} \mid A_L) \times \Phi(U^c_{8^{\ell-2}N,8^{\ell-1}N} \mid U^c_{8^{\ell-1}N,8^\ell N}, A_L) \\ \times \cdots \times \Phi(U^c_{N,8N} \mid U^c_{8N,8^2N}, \dots, U^c_{8^{\ell-1}N,8^\ell N}, A_L).\end{aligned} \tag{A.6}$$

Any term of the right hand side for $0 \leq j < \ell$ is of the form

$$\Phi(U^c_{8^jN,8^{j+1}N} \mid F_j, 0 \overset{(3)}{\longleftrightarrow} (X_L, Y_L, Z_L))$$

where F_j is an event depending only on the edges of $\Lambda^c_{8^{j+1}N}$. Using the arm separation stated in Proposition A.3.1, we are going to bound below the probability

$$\Phi(U_{8^jN,8^{j+1}N}, 0 \overset{(3)}{\longleftrightarrow} (X_L, Y_L, Z_L) \mid F_j).$$

We will also need to use the outer separation quality $\mathbf{Q}'$, defined by the separation of the endpoints of the interfaces on the outer boundary of an annulus, and for which the same properties holds. There is a constant $c_{\text{sep}} > 0$ such that

$$\begin{aligned}\Phi(\mathbf{Q}(\Gamma_{4\times 8^j,L}) > 1/3 \mid \partial\Lambda_{4\times 8^j} \overset{(3)}{\longleftrightarrow} (X_L, Y_L, Z_L), F_j) \geq c_{\text{sep}} \\ \Phi(\mathbf{Q}'(\Gamma_{8^j,2\times 8^j}) > 1/3 \mid 0 \overset{(3)}{\longleftrightarrow} \partial\Lambda_{2\times 8^j}, F_j) \geq c_{\text{sep}}.\end{aligned}$$

Thanks to arm separation and using RSW constructions in the annulus $\Lambda_{4\times 8^j} \setminus \Lambda_{2\times 8^j}$, we can prove that conditionally on the events above, there is a constant probability that the annulus is dually crossed by an exteriormost dual path, and by a primal path (see Figure A.2). Up to exploring the exteriormost dual path

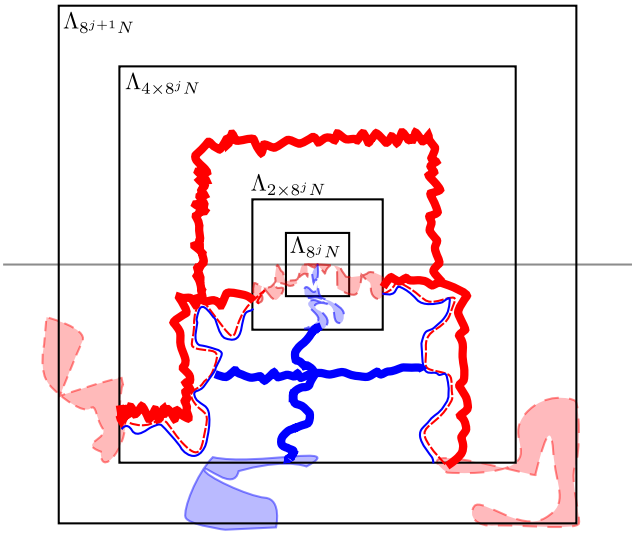

Figure A.2: The thick primal (blue) and dual (red) RSW construction ensure that there are primal and dual path realizing the three-arms event that cross the annulus only once. The two dual path are linked together, hence we can explore this dual cluster up to finding the (thin blue) primal interface. The two parts of the interface can be linked together with a RSW construction which ensures the uniqueness of the two crossing clusters.

and using RSW from primal boundary to primal boundary, there exists a constant $K > 0$ such that

$$\Phi\Big(U_{2\times 8^j N, 4\times 8^j N}, 0 \overset{(3)}{\longleftrightarrow} (X_L, Y_L, Z_L) \;\Big|\; \mathbf{Q}(\Gamma_{4\times 8^j, L}) > 1/3, \partial\Lambda_{4\times 8^j} \overset{(3)}{\longleftrightarrow} (X_L, Y_L, Z_L), \mathbf{Q}'(\Gamma_{8^j, 2\times 8^j}) > 1/3, 0 \overset{(3)}{\longleftrightarrow} \partial\Lambda_{2\times 8^j}, F_j\Big) \geq K.$$

Finally, using inclusion of events and the mixing property of the measure to decouple the interior and the exterior of the annulus $\Lambda_{4\times 8^j} \setminus \Lambda_{2\times 8^j}$ up to a constant $K' > 0$, we get

$$\Phi(U_{8^j N, 8^{j+1} N}, 0 \overset{(3)}{\longleftrightarrow} (X_L, Y_L, Z_L) \mid F_j) \geq K K'^2 c_{\text{sep}}^2 \Phi(0 \overset{(3)}{\longleftrightarrow} (X_L, Y_L, Z_L) \mid F_j).$$

That is to say, there is a constant $c_u > 0$ such that

$$\Phi(U^c_{8^j N, 8^{j+1} N} \mid F_j, 0 \overset{(3)}{\longleftrightarrow} (X_L, Y_L, Z_L)) \leq 1 - c_u.$$

Plugging this in (A.6) finishes the proof. □

Let $\Pi_{N,M}$ be the set of pairs of primal/dual crossing clusters $R = (C_p, C_d)$ and $U(R)$ be the event that $U_{N,M}$ happens with the pair R. For any two scale indices, i, j such that $i + 1 < j$, $R \in \Pi_i$, $T \in \Pi_j$, define the matrix coefficient M_{RT} by

$$M_{RT} = \Phi\left(U_i(R),\ R \overset{(3)}{\longleftrightarrow} T \mid U_j(T)\right) \tag{A.7}$$

Lemma A.4.2. *There exists a constant $\kappa > 0$ such that for any indices $i < i+1 < j$, $R, R' \in \Pi_i$, $T, T' \in \Pi_j$,*

$$\frac{M_{RT} M_{R'T'}}{M_{RT'} M_{R'T}} \leq \kappa. \tag{A.8}$$

Proof. The goal is to decouple M_{RT} as a product of two terms, one involving only on R and the other one involving only T.

Let $L > 0$ such that $2N_{i+1} < L < 8L < N_j$. Then by inclusion,

$$\Phi\left(U_i(R), R \overset{(3)}{\longleftrightarrow} T, U_j(T)\right) \leq \Phi\left(U_i(R), R \overset{(3)}{\longleftrightarrow} \partial\Lambda_L, \partial\Lambda_{4L} \overset{(3)}{\longleftrightarrow} T, U_j(T)\right) \tag{A.9}$$

$$\leq c_{\text{mix}} \Phi(U_i(R), R \overset{(3)}{\longleftrightarrow} \partial\Lambda_L) \Phi(\partial\Lambda_{4L} \overset{(3)}{\longleftrightarrow} T, U_j(T)) \tag{A.10}$$

where the last inequality and the constant c_{mix} come from the polynomial ratio mixing of FK percolation (see [DC13, Theorem 5.45]): the two events depend respectively on the edges inside Λ_L and outside Λ_{4L}, and they are hence decorrelated up to the constant c_{mix} which only depends on the RSW constant.

We want to get the reverse inequality, up to a multiplicative constant. For this we use the arm separation stated in Proposition A.3.1. There is a constant $c_{\text{sep}} > 0$ such that

$$\Phi(\mathbf{Q}(\Gamma_{4L,N_{j+1}}) > 1/3 \mid \partial\Lambda_{4L} \overset{(3)}{\longleftrightarrow} T, U_j(T)) > c_{\text{sep}}. \tag{A.11}$$

We defined the inner separation quality $\mathbf{Q}$, as well as the outer separation quality $\mathbf{Q}'$ for which similar definition and properties hold. Hence we have the similar result

$$\Phi(\mathbf{Q}'(\Gamma_{N_i,L}) > 1/3 \mid U_i(R), R \overset{(3)}{\longleftrightarrow} \partial\Lambda_L) > c_{\text{sep}}. \tag{A.12}$$

Using the two latter equation and the mixing constant of FK percolation, we have

$$\begin{aligned}
&c_{\text{sep}} \Phi(U_i(R), R \overset{(3)}{\longleftrightarrow} \partial\Lambda_L) \Phi(\partial\Lambda_{4L} \overset{(3)}{\longleftrightarrow} T, U_j(T)) \\
&\leq \Phi\left(\mathbf{Q}'(\Gamma_{N_i,L}) > 1/3, U_i(R), R \overset{(3)}{\longleftrightarrow} \partial\Lambda_L\right) \Phi\left(\mathbf{Q}(\Gamma_{4L,N_{j+1}}) > 1/3, \partial\Lambda_{4L} \overset{(3)}{\longleftrightarrow} T, U_j(T)\right) \\
&\leq c_{\text{mix}} \Phi\left(\mathbf{Q}'(\Gamma_{N_i,L}) > 1/3, U_i(R), R \overset{(3)}{\longleftrightarrow} \partial\Lambda_L, \mathbf{Q}(\Gamma_{4L,N_{j+1}}) > 1/3, \partial\Lambda_{4L} \overset{(3)}{\longleftrightarrow} T, U_j(T)\right).
\end{aligned}$$

Now, conditionally on $U_i(R)$ and $U_j(T)$, we can decompose the event along all the possible values of the interfaces $\gamma_{i,1}, \gamma_{i,2}$ from R to $\partial\Lambda_L$, and $\gamma_{j,1}, \gamma_{j,2}$ from $\partial\Lambda_{4L}$ to T. Remark that the events $\{\mathbf{Q}'(\Gamma_{N_i,L}) > 1/3\}$, $\{R \overset{(3)}{\longleftrightarrow} \partial\Lambda_L\}$, $\{\mathbf{Q}(\Gamma_{4L,N_{j+1}}) > 1/3\}$ and $\{\partial\Lambda_{4L} \overset{(3)}{\longleftrightarrow} T\}$ are measurable with respect to the events $\Gamma(\gamma_{i,1})$, $\Gamma(\gamma_{i,2})$, $\Gamma(\gamma_{j,1})$, $\Gamma(\gamma_{j,2})$. So we can just explore these interfaces, and thanks to the high quality of the separations, we can glue the interfaces arriving at scale N_i to those exiting scale N_j using standard RSW techniques. Hence there is a constant $K > 0$, depending on the RSW gluing, such that

$$\begin{aligned}
&\Phi\left(\mathbf{Q}'(\Gamma_{N_i,L}) > 1/3, U_i(R), R \overset{(3)}{\longleftrightarrow} \partial\Lambda_L, \mathbf{Q}(\Gamma_{4L,N_{j+1}}) > 1/3, \partial\Lambda_{4L} \overset{(3)}{\longleftrightarrow} T, U_j(T)\right) \\
&\qquad \leq K \Phi\left(U_i(R), R \overset{(3)}{\longleftrightarrow} T, U_j(T)\right).
\end{aligned}$$

Putting all the inequalities together, we conclude that

$$M_{R,T} \asymp \Phi\left(U_i(R), R \overset{(3)}{\longleftrightarrow} \partial\Lambda_L\right) \Phi\left(\partial\Lambda_{4L} \overset{(3)}{\longleftrightarrow} T \mid U_j(T)\right). \tag{A.13}$$

□

Proof of Proposition A.2.1. To simplify notations we assume that A_N is just $0 \overset{(3)}{\longleftrightarrow} \partial\Lambda_N$ but the same proof works exactly the same for general A_N. We now express the probabilities appearing in the Proposition in terms of the matrix coefficients (A.7). Define, for $R \in \Pi_i$, the vector coefficients

$$u_R = \Phi\left(B, 0 \overset{(3)}{\longleftrightarrow} R \mid U_i(R)\right) \tag{A.14}$$

$$\tilde{u}_R = \Phi\left(0 \overset{(3)}{\longleftrightarrow} R \mid U_i(R)\right) \tag{A.15}$$

$$v_R = \Phi\left(R \overset{(3)}{\longleftrightarrow} \partial\Lambda_N, U_i(R)\right) \tag{A.16}$$

Using the fact that the event $U_i(R)$ fixes the boundary condition outside of a topological annulus, and that Φ enjoys the Spatial Markov Property (SMP), we can write

$$\begin{aligned}
&\Phi(B, A_N, U_i, U_j) \\
&= \sum_{R\in\Pi_i} \Phi(U_i(R))\Phi\left(B, 0 \overset{(3)}{\longleftrightarrow} R, R \overset{(3)}{\longleftrightarrow} \partial\Lambda_N, U_j \mid U_i(R)\right) \\
&= \sum_{R\in\Pi_i} \Phi(U_i(R))\Phi\left(B, 0 \overset{(3)}{\longleftrightarrow} R \mid U_i(R)\right) \Phi\left(R \overset{(3)}{\longleftrightarrow} \partial\Lambda_N, U_j \mid U_i(R)\right) \\
&= \sum_{R\in\Pi_i} u_R \Phi\left(U_i(R), R \overset{(3)}{\longleftrightarrow} \partial\Lambda_N, U_j\right) \\
&= \sum_{R\in\Pi_i} u_R \sum_{R'\in\Pi_j} \Phi(U_j(R'))\Phi\left(U_i(R), R \overset{(3)}{\longleftrightarrow} R', R' \overset{(3)}{\longleftrightarrow} \partial\Lambda_N \mid U_j(R')\right) \\
&= \sum_{R\in\Pi_i, R'\in\Pi_j} u_R \Phi(U_j(R'))\Phi\left(U_i(R), R \overset{(3)}{\longleftrightarrow} R' \mid U_j(R')\right) \Phi\left(R' \overset{(3)}{\longleftrightarrow} \partial\Lambda_N \mid U_j(R')\right) \\
&= \sum_{R\in\Pi_i, R'\in\Pi_j} u_R M_{RR'} v_{R'}
\end{aligned}$$

For any sequence of scales $N_{i_1}, \dots, N_{i_\ell}$, we can repeat this decomposition and write

$$\Phi(B, A_N, U_{i_1}, \dots, U_{i_\ell}) = u^{i_1} M^{i_1,i_2} \cdots M^{i_{\ell-1},i_\ell} v^{i_\ell} \tag{A.17}$$

where we made explicit the dependency in the scale of the vectors u, v and the matrix M, and where the product is the usual matrix product over the set of indices Π_{i_j} for $j = 1, \dots, \ell$.

By union bound, we have

$$\Phi(U_{i_1}, \dots, U_{i_\ell} \mid B, A_N) \geq 1 - \sum_{j=1}^{\ell} \Phi(U_{i_j}^c \mid B, A_N) \geq 1 - \sum_{j=1}^{\ell} \left(\frac{N_{i_j}}{N_{i_j+1}}\right)^k \tag{A.18}$$

where we used Lemma A.4.1 (and the constant k is the one appearing in the lemma). Up to a good choice of scales (N_i) we can make the sum in the last term summable and of arbitrary small value. That is, for any $\varepsilon > 0$, we can choose scales such that for any ℓ,

$$e^{-\varepsilon} \leq \frac{\Phi(U_{i_1}, \dots, U_{i_\ell}, B, A_N)}{\Phi(B, A_N)} \leq e^{\varepsilon}. \tag{A.19}$$

Moreover, by the matrix decomposition, we have

$$\Phi(B \mid U_{i_1}, \dots, U_{i_\ell}, A_N) = \frac{u^{i_1} M^{i_1,i_2} \dots M^{i_{\ell-1},i_\ell} v^{i_\ell}}{\tilde{u}^{i_1} M^{i_1,i_2} \dots M^{i_{\ell-1},i_\ell} v^{i_\ell}}$$

and Lemma A.4.2 together with [Hop63, Theorem 3] cited in [BS17], imply that this ratio has a limit, i.e there exists a real $\nu(B)$ such that

$$\lim_{\ell \to \infty} \frac{u^{i_1} M^{i_1,i_2} \dots M^{i_{\ell-1},i_\ell} v^{i_\ell}}{\tilde{u}^{i_1} M^{i_1,i_2} \dots M^{i_{\ell-1},i_\ell} v^{i_\ell}} = \nu(B). \tag{A.20}$$

Putting (A.19) and (A.20) together concludes the proof. □

A.5 Proof of Proposition A.2.2

We cannot directly deduce from the proof of Proposition A.2.1 that the convergence to the IIC measure occurs at polynomial speed. Indeed, the choice of scales (N_i) that we have to make so that the sum in (A.18) converges must be a super-exponential sequence. In this section, we follow the ideas of [GPS13b, Proposition 3.1] to get a polynomial mixing rate.

Proof. Define the logarithmic scales $N_i := 8^i$. Let M, N, j, k be integers such that $N < N_j < N_{k+1} < M$. Our goal is to build a coupling of configurations $(\omega, \tilde{\omega})$ such that ω has law $\Phi(\cdot \mid 0 \overset{(3)}{\longleftrightarrow} \partial\Lambda_M)$ and $\tilde{\omega}$ has law ν. Let $(T_j, \dots, T_k)$ (resp. $(\tilde{T}_j, \dots, \tilde{T}_k)$) be the random sequence of elements of $\Pi_j, \dots \Pi_k$ such that for every $j \leq i \leq k$, either U_i does not occur in ω (resp. $\tilde{\omega}$) and $T_i = \emptyset$, or $U(T_i)$ occurs in ω (resp. $\tilde{\omega}$).

For $j \leq h < i \leq k$ we have by Lemma A.4.1, that for any event F_i that depends only on edges in $\Lambda_M \setminus \Lambda_{N_{i+1}}$, we have

$$\Phi(U_h \mid F_i, 0 \overset{(3)}{\longleftrightarrow} \partial\Lambda_M) \geq c_u.$$

Moreover, thanks to the uniformity of this bound and taking the limit $n \to \infty$ and using Proposition A.2.1, we have

$$\nu(U_h \mid F_i) \geq c_u.$$

Using this inequality twice, we can write

$$\nu(U_{h-1}, U_h \mid F_i) = \nu(U_{h-1} \mid U_h, F_i)\nu(U_h \mid F_i) \geq c_u^2 \tag{A.21}$$

and similarly for Φ. Moreover remark that for $T_h \in \Pi_h, T_{h-1} \in \Pi_{h-1}$, by the Spatial Markov property and the decoupling in a topological annulus induced by the event $U_h(T_h)$, we have

$$\begin{aligned}\nu(U_{h-1}(T_{h-1}) \mid U_h(T_h)) &= \lim_{M\to\infty} \Phi(U_{h-1}(T_{h-1}) \mid U_h(T_h), 0 \overset{(3)}{\longleftrightarrow} \partial\Lambda_M) \\ &= \lim_{M\to\infty} \Phi(U_{h-1}(T_{h-1}) \mid U_h(T_h), 0 \overset{(3)}{\longleftrightarrow} T_h) \\ &= \Phi(U_{h-1}(T_{h-1}) \mid U_h(T_h), 0 \overset{(3)}{\longleftrightarrow} T_h)\end{aligned}$$

Hence

$$\begin{aligned}\nu(U_{h-1}(T_{h-1}), U_h \mid F_i) &= \sum_{T_h\in\Pi_h} \nu(U_{h-1}(T_{h-1}), U_h(T_h) \mid F_i) \\ &= \sum_{T_h\in\Pi_h} \nu(U_{h-1}(T_{h-1}) \mid U_h(T_h))\nu(U_h(T_h) \mid F_i) \\ &= \sum_{T_h\in\Pi_h} \Phi(U_{h-1}(T_{h-1}) \mid 0 \overset{(3)}{\longleftrightarrow} T_h, U_h(T_h))\nu(U_h(T_h) \mid F_i) \\ &= \sum_{T_h\in\Pi_h} \frac{\Phi(U_{h-1}(T_{h-1}), 0 \overset{(3)}{\longleftrightarrow} T_h, U_h(T_h))}{\Phi(0 \overset{(3)}{\longleftrightarrow} T_h, U_h(T_h))}\nu(U_h(T_h) \mid F_i) \\ &= \sum_{T_h\in\Pi_h} \frac{\Phi(0 \overset{(3)}{\longleftrightarrow} T_{h-1} \mid U_{h-1}(T_{h-1}))M_{T_{h-1}T_h}}{\Phi(0 \overset{(3)}{\longleftrightarrow} T_h \mid U_h(T_h))}\nu(U_h(T_h) \mid F_i)\end{aligned}$$

and using equation A.13 where we denote by K the implicit constant, and by L a scale between N_{h-1} and $2N_{h-1}$, we can split the dependencies in T_{h-1} and T_h in the last term.

$$\begin{aligned}&\nu(U_{h-1}(T_{h-1}), U_h \mid F_i) \\ &\asymp \Phi\left(U_{h-1}(T_{h-1}), 0 \overset{(3)}{\longleftrightarrow} \partial\Lambda_L\right) \sum_{T_h\in\Pi_h} \frac{\Phi\left(\partial\Lambda_{4L} \overset{(3)}{\longleftrightarrow} T_h \mid U_h(T_h)\right)}{\Phi(0 \overset{(3)}{\longleftrightarrow} T_h \mid U_h(T_h))}\nu(U_h(T_h) \mid F_i)\end{aligned} \tag{A.22}$$

Using (A.21), we have that

$$\nu(U_{h-1}, U_h \mid F_i) = \sum_{T_{h-1}} \nu(U_{h-1}(T_{h-1}), U_h \mid F_i) \asymp 1$$

Plugging the right hand term of (A.22) in the above equality we get that

$$\nu(U_{h-1}(T_{h-1}), U_h \mid F_i) \asymp \Phi\left(U_{h-1}(T_{h-1}) \mid U_{h-1}, 0 \overset{(3)}{\longleftrightarrow} \partial\Lambda_L\right).$$

We can run exactly the same computation with the measure $\Phi(\cdot \mid 0 \overset{(3)}{\longleftrightarrow} \partial\Lambda_M)$ and find the same expression, that is to say

$$\nu(U_{h-1}(T_{h-1}), U_h \mid F_i) \asymp \Phi(U_{h-1}(T_{h-1}), U_h \mid F_i', 0 \overset{(3)}{\longleftrightarrow} \partial\Lambda_M) \tag{A.23}$$

for any two events F_i, F_i'.

Assume that k is even and j is odd. We can couple the two sequences $(T_i)_{j\leq i\leq k}$ and $(\tilde{T}_i)_{j\leq i\leq k}$. For every odd i starting from $k-1$ in decreasing order, sample (T_i, T_{i+1}) and $(\tilde{T}_i, \tilde{T}_{i+1})$ conditionally on the couples already sampled, and maximizing the probability that $(T_i, T_{i+1}) = (\tilde{T}_i, \tilde{T}_{i+1})$. We can deduce from Equations (A.21) and (A.23) that at every step, there is a positive constant $c > 0$ that bounds from below the probability that $(T_i, T_{i+1}) = (\tilde{T}_i, \tilde{T}_{i+1}) \neq (\emptyset, \emptyset)$ occurs. If this occurs then $U_i(T_i)$ imposes the same boundary condition for the two measures and by the Spatial Markov property, the distribution inside the topological annulus in both cases is equal to $\Phi(\cdot \mid U_i(T_i), 0 \overset{(3)}{\longleftrightarrow} T_i)$. In this case, we sample the same configuration inside the annulus for $\omega, \tilde{\omega}$ according to this conditional measure.

Hence, the probability that $\omega, \tilde{\omega}$ do not coincide on the box Λ_n must be smaller than $c^{(k-j)/2}$. Remembering that $k-j$ is of the order of $\log(n/N)$ concludes the proof. □

B | More on rapidity lines

In the introduction of this thesis, we defined isoradial graphs. In this chapter we introduce the train tracks and rapidity lines formalism, which is a combinatorial representation of isoradial graphs. The advantage of forgetting the geometric embedding and just remembering the combinatorics of track crossings is that it allows to consider "imaginary graphs" that would not be realizable with actual embedded isoradial graphs (e.g. see Figure B.5 and Theorem B.1.2). One could then find a relation between two genuine isoradial graphs using transformations that go through these fictitious isoradial graphs.

In this bibliographical appendix that is mostly based on [IP12], we apply the rapidity line representation to a percolation ($q = 1$) model on a strip, in order to establish the *q-deformed Knizhnik–Zamolodchikov equations* (it is not the same q as in the FK percolation definition). One can also refer to [DGP$^+$10, DF05, Pon11, ZJ07].

B.1 Tracks, Loops and Spectral Parameters

Track system representation

The representation as (train) *tracks* of a rhombic tiling was introduced by de Bruijn [dB81] in its generalization of Penrose's tiling [Pen79]. Let $G^\diamond = (V^\diamond, E^\diamond)$ be the diamond graph of an infinite isoradial graph such that $G^\diamond$ is a tiling of the plane. Let e_0 be one of its edges, it belongs to two rhombic faces of $G^\diamond$, and in each of these faces, there is one edge opposite to e_0. Call these edges e_{-1} and e_1. Again, e_1 belongs to another rhombic face. Call the opposite edge of this face e_2. Continuing this process, we end up with a doubly infinite sequence $t = \dots e_{-2}, e_{-1}, e_0, e_1, e_2 \dots$ that we call a track. The sequence of edges gives a choice of orientation of the track. It is easy to see that since the faces are rhombi, all the edges of t, seen as straight line segments oriented positively with respect to the orientation of the track, have the same angle α relative to any oriented axis $\vec{\mathcal{D}}$. We call this angle the *transverse angle* relative to $\vec{\mathcal{D}}$ (see Figure B.3). If we look at the projection of the edges of t on an axis with angle $\alpha + \pi/2$ relative to $\vec{\mathcal{D}}$, we can see that the sequence t is strictly monotonic. Hence, t does not cycle and all its edges are distinct. When the graph is finite, tracks can be defined the same way except that they are finite sequences of edges. The collection of all the tracks of $G^\diamond$ is called its track system representation.

The way we constructed tracks shows directly that every edge of $G^\diamond$ belongs to exactly one track. Oriented tracks can also be seen as oriented arcs joining the midpoints of their edges (see Figure B.1). Two tracks t, t' are said to intersect at

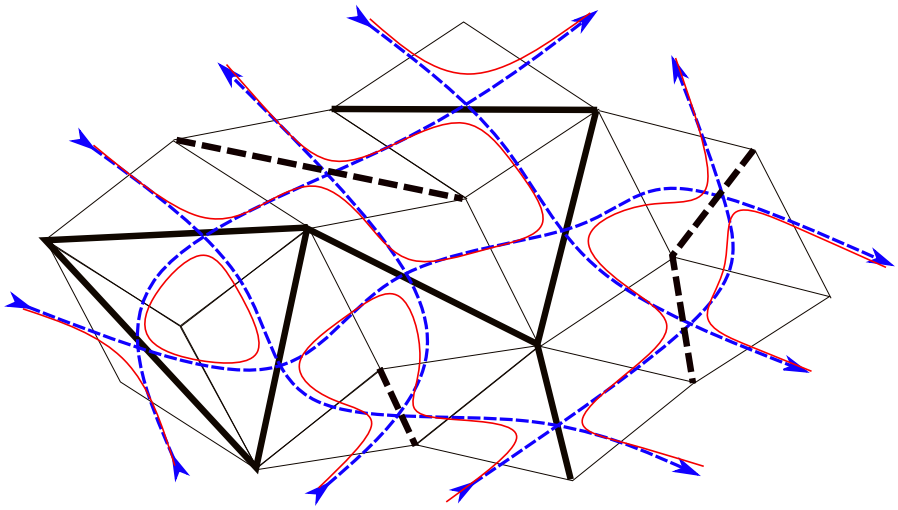

Figure B.1: A percolation configuration on an isoradial graph. The diamond graph is shown as thin black lines, open edges as thick black lines, dually open edges (i.e. duals of closed edges) as thick and dashed black lines, tracks as dashed blue curves and loops as red curves.

some rhombic face F if there are two edges $e \in t, e' \in t'$ with $e, e' \in F$. This means that the corresponding arcs intersect in the interior of F. Two tracks have at most one intersection: if they intersect once, then the potential first next intersection (say along t seen as an arc) cannot happen as the transverse angles are not compatible. This result relies on the fact that an arc separates the plane in two disjoint domains. This is not true for rhombic tilings of the torus for instance.

Loops and cluster interfaces

Given a percolation configuration on an isoradial graph, we can consider its clusters (i.e. connected components) and dual clusters (i.e. dually connected components). It is possible to define the interfaces of these clusters as non-intersecting loops and infinite paths separating every cluster from the adjacent dual clusters. We call this collection of interfaces a loop configuration. There is a bijection between percolation configurations and their loop representations. Usually the loop representation is formally defined on the medial lattice which is the dual of the diamond graph (e.g. [DC17]). However it will be more convenient for us to define it on the track system.

Let G be an isoradial graph, $G^\diamond = (V^\diamond, E^\diamond)$ its diamond graph and $\mathcal{T}$ its track system. A loop l on $\mathcal{T}$ is a finite or doubly infinite sequence of edges of $G^\diamond$ such that every two consecutive edges e, e' belong to the same rhombic face of $G^\diamond$ but are not opposite edges. In the case of a finite loop $l = e_0, \dots, e_n$, we consider that e_0 and e_n are consecutive, except if $G^\diamond$ is finite and e_0 and e_n belong to its boundary, in which case we impose no other condition. Finally we impose that every edge appears at most once in a loop. A loop can be seen as a curve living on the arc representation of the tracks that makes a left or right turn whenever it reaches an intersection between two tracks (as represented on Figure B.1). We insist on the fact that a loop can either be a proper loop or a path.

Take ω a percolation configuration on G. The loop representation of ω is a

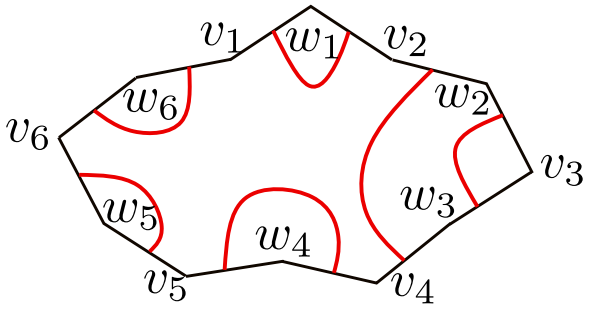

Figure B.2: Link pattern corresponding to the configuration in Figure B.1. Primal clusters are $\{v_1, v_2, v_4, v_5, v_6\}$, $\{v_3\}$, dual clusters are $\{w_1\}$, $\{w_2, w_3\}$, $\{w_4\}$, $\{w_5\}$, $\{w_6\}$.

collection ℓ of loops such that every edge $e \in G^\diamond$ belongs to exactly one $l \in \ell$, and such that loops, seen as curves, make their left or right turn so as to avoid open and dually open edges of ω (see Figure B.1). More formally, for every two consecutive edges e, e' of some $l \in \ell$, let F be the common rhombus to e and e'. Then in ω, F is split by either a primal or a dual edge g. In this case e and e' must be on the same side of g in F.

Link patterns

Suppose that G is finite, then the union of the rhombic faces of $G^\diamond$ forms a bounded simply connected domain whose boundary is a collection $\partial G^\diamond = \{e_1, \dots, e_n\}$ of edges of $G^\diamond$. As before, ω is a percolation configuration on G and ℓ its loop representation. Then ℓ induces a perfect matching of $\partial G^\diamond$ by the fact that every loop $l \in \ell$ contains either 0 or 2 edges of the boundary. This matching is called the link pattern $\lambda(\ell)$ on $\partial G^\diamond$ induced by ℓ. We denote by $\mathrm{LP}(\partial G^\diamond)$ the set of all possible link patterns on $\partial G^\diamond$. We represent in Figure B.2 the link pattern corresponding to the configuration of Figure B.1. The loops being interfaces between primal and dual clusters, it is easy to see that the link pattern contains exactly the information necessary to recover the connectivity relations between primal and dual vertices of $\partial G^\diamond$: two (dual) vertices are (dually) connected if and only if they are not separated by a link.

From isoradial graphs to rapidity lines

As we have seen, a percolation configuration on G is equivalent to a loop configuration on $\mathcal{T}$ and induces a link pattern of $\mathrm{LP}(\partial G^\diamond)$. To generate a loop configuration, one just needs to know how the tracks of $\mathcal{T}$ intersect, and what is the probability of a left or right turn of the loops at every such intersection. Moreover this probability only depends on the transverse angles of the tracks. Take two oriented tracks t_1, t_2 intersecting on a rhombus F, with transverse angles θ_1, θ_2 relative to some axis $\vec{\mathcal{D}}$ as in Figure B.3. We define the spectral parameter, or *rapidity*, of t_1 (resp. t_2) to be $z_1 = \exp(i\theta_1/3)$ (resp. $z_2 = \exp(i\theta_2/3)$). An oriented track together with its spectral parameter is called in the Physics literature a *rapidity line*. We will us the same terminology.

In a percolation configuration, the rhombus F can either be crossed by a (primal or dual) edge transverse to the direction of the tracks (this is the first case of Figure

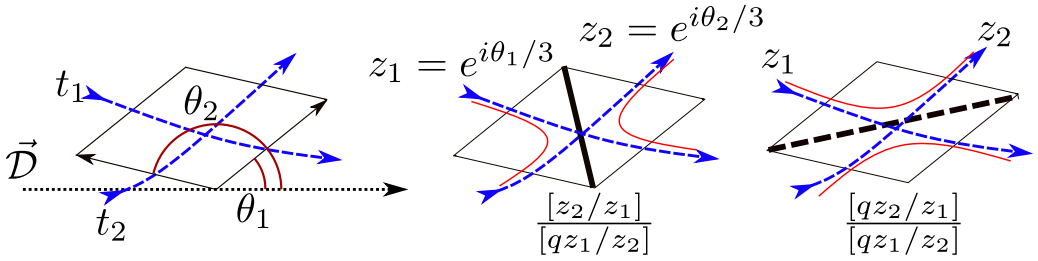

Figure B.3: The tracks t_1 and t_2, with transverse angle θ_1 and θ_2 and rapidities z_1 and z_2 intersect on a rhombus. The two possible outcomes for the loop configuration at this intersection are shown on the right, with the corresponding probabilities. $q = \exp\left(\frac{2i\pi}{3}\right)$ and $[x] = x - 1/x$.

B.3). This happens with probability $p_{\theta_2-\theta_1}$. Or it is crossed by a (primal or dual) edge in the direction of the tracks (this is the second case of Figure B.3). This happens with probability $p_{\pi-(\theta_2-\theta_1)}$. From now on we use the notation $[x] = x - 1/x$ for any scalar x, and we define $q = \exp\left(\frac{2i\pi}{3}\right)$. Remark that

$$2i \sin\left(\frac{\theta_2 - \theta_1}{3}\right) = \frac{z_2}{z_1} - \frac{z_1}{z_2} = [z_2/z_1].$$

Likewise

$$\begin{aligned} 2i \sin\left(\frac{\pi - (\theta_2 - \theta_1)}{3}\right) &= 2i \sin\left(\pi - \frac{\pi - (\theta_2 - \theta_1)}{3}\right) \\ &= 2i \sin\left(\frac{2\pi + \theta_2 - \theta_1}{3}\right) = \frac{qz_2}{z_1} - \frac{z_1}{qz_2} = [qz_2/z_1]. \end{aligned}$$

Moreover one can check that for any $w \in \mathbb{C}$, $[w] + [qw] = [q/w]$.

Hence according to Equation (I.2), we have

$$p_{\theta_2-\theta_1} = \frac{\sin\left(\frac{\theta_2-\theta_1}{3}\right)}{\sin\left(\frac{\theta_2-\theta_1}{3}\right) + \sin\left(\frac{\pi-(\theta_2-\theta_1)}{3}\right)} = \frac{[z_2/z_1]}{[qz_1/z_2]} \tag{B.1}$$

$$p_{\pi-(\theta_2-\theta_1)} = \frac{\sin\left(\frac{\pi-(\theta_2-\theta_1)}{3}\right)}{\sin\left(\frac{\theta_2-\theta_1}{3}\right) + \sin\left(\frac{\pi-(\theta_2-\theta_1)}{3}\right)} = \frac{[qz_2/z_1]}{[qz_1/z_2]}. \tag{B.2}$$

Given an isoradial graph with oriented tracks $t_1, \ldots, t_n$, it is tempting to try to reduce its study to its rapidity line configuration and to forget about the isoradial embedding. To do so, we need to choose a reference axis $\vec{\mathcal{D}}$ and a determination in $\mathbb{R}$ of the transverse angles $\theta_1, \ldots, \theta_n$ to compute the spectral parameters. Indeed, because of the division by 3 in the computation of the rapidities, it is not enough to know the angles modulo 2π. **As a result, it is not always possible to represent an isoradial graph with its oriented tracks as a rapidity line configuration.** Suppose that t_i and t_j cross in this order as in Figure B.3, then we need the following condition for Equation (B.1) to hold:

$$\theta_2 - \theta_1 \in (0, \pi) \tag{B.3}$$

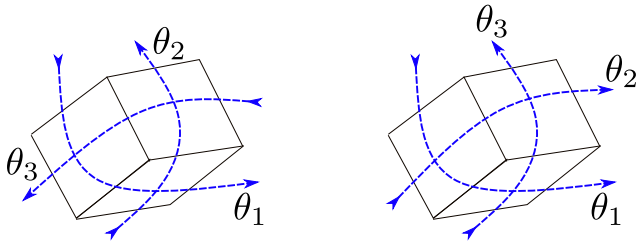

Figure B.4: For the oriented tracks on the left to be realized as rapidity lines, we need a determination in $\mathbb{R}$ of the transverse angles verifying $\theta_3 > \theta_2$, $\theta_2 > \theta_1$, $\theta_1 > \theta_3$. This is impossible. To realize the oriented tracks on the right, we just need $\theta_3 > \theta_2 > \theta_1$. Take for instance $\theta_1 = 0$, $\theta_2 = \pi/2$, $\theta_3 = 3\pi/4$.

$\frac{z_2}{z_1} = e^{i\alpha}, \alpha \in$	$[0, \pi/3]$	$(\pi/3, 2\pi/3)$	$(2\pi/3, \pi)$
$\frac{[z_2/z_1]}{[qz_1/z_2]} \in$	$[0, 1]$	$(1, +\infty)$	$(-\infty, 0)$
$\frac{[qz_2/z_1]}{[qz_1/z_2]} \in$	$[0, 1]$	$(-\infty, 0)$	$(1, +\infty)$

Table B.1: Domain of the local loop weights as functions of the spectral ratio z_2/z_1. The weights are π-periodic as functions of α.

Otherwise they do not give true probabilities (see Table B.1). Figure B.4 provides an example of a very simple graph with two orientations of its tracks. The first one cannot be realized as a rapidity line configuration. It is possible for the second one.

Abstract rapidity lines

Let us now consider arbitrary configurations of rapidity lines. In particular configurations where, unlike tracks, two rapidity lines can intersect more than once. The formulas of Figure B.3 still give weights to local loop configurations at every intersection but we must be careful as these weights are real but not necessarily probabilities in $[0, 1]$. We always have $\frac{[z_2/z_1]}{[qz_1/z_2]} + \frac{[qz_2/z_1]}{[qz_1/z_2]} = 1$, and Table B.1 gives the domain of the weights as a functions of the rapidities.

If the rapidity line configuration is finite then we can give a weight to each loop configuration by multiplying its local weights. This produces a signed measure on loop configurations. We believe that this level of formalism should be sufficient, even more so since for the sake of readability, the following proofs on rapidity lines in this text will distinguish cases graphically.

However we finish this section with a formal definition for what we intuitively see as a family of 'nice' curves in general position. If we look at the union of these curves as the trace of a graph in the plane, then the dual of this graph has quadrangular faces, like the diamond graph. Hence the following: let $H = (V, E)$ be a finite planar graph such that all its bounded faces are quadrangles (only the combinatorial structure matters here, the geometry is not relevant) and such that its outer boundary is a simple sequence of edges, or equivalently every edge $e \in E$ is adjacent to two distinct faces. A rapidity line $r = (z, e_0, \ldots, e_n)$ is defined by

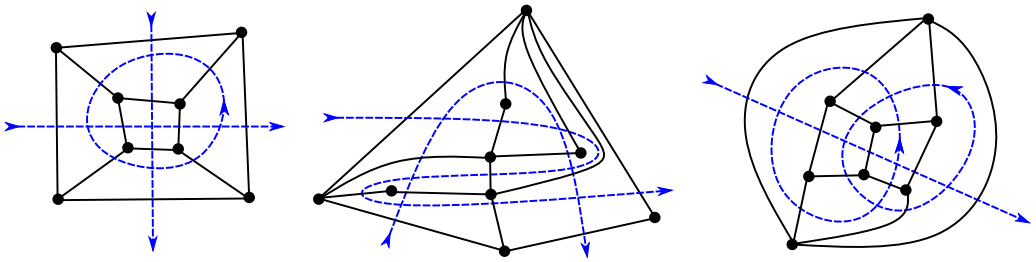

Figure B.5: Example of rapidity line configuration in blue with their quadrangular construction graph H in black.

a complex spectral parameters $z \in \mathbb{U}$ and a sequence of edges of E such that if e, e' are two consecutive edges, there exists a bounded face F of H such that e and e' belong to F but are not adjacent with each other (they are to opposite edges of F). Either e_0 and e_n both belong to the boundary ∂H, or we consider that they are consecutive. Every edge appears at most once in r. Let $\mathcal{R}$ be a collection rapidity lines on G, such that every edge appears in $\mathcal{R}$ exactly once. If $r, r' \in \mathcal{R}$, we write $r \cap r'$ for the set of faces F of H having both edges belonging to r and edges belonging to r'. Examples are given in Figure B.5.

A loop configuration ℓ on E is defined as in the beginning of the current section (B.1), changing rhombic faces to quadrangular faces. Let $\mathcal{L}$ be the set of all loop configurations. If F is a bounded face of H with boundary edges f_1, f_2, f_3, f_4 in cyclic order, these edges are paired in ℓ by appearing and being consecutive in the same loop. Denote by ℓ_F the pairing describing the configuration of ℓ on F, that is either $\{\{f_1, f_2\}, \{f_3, f_4\}\}$ or $\{\{f_1, f_4\}, \{f_2, f_3\}\}$. Define $w_{\mathcal{R}}(\ell_F) = \frac{[z_2/z_1]}{[qz_1/z_2]}$ or $\frac{[qz_2/z_1]}{[qz_1/z_2]}$ the correct weight of the pairing according to Figure B.3, where z_1, z_2 are the spectral parameters of the two rapidity lines intersecting at F with the correct orientation. Then the weight of a loop configuration is defined by

$$w_{\mathcal{R}}(\ell) = \prod_{F \text{ face of } H} w_{\mathcal{R}}(\ell_F). \tag{B.4}$$

We use the same notation for the induced weight of link patterns on ∂G. For any link $\alpha \in \mathrm{LP}(\partial H)$,

$$w_{\mathcal{R}}(\alpha) = \sum_{\ell \in \mathcal{L}, \lambda(\ell) = \alpha} w_{\mathcal{R}}(\ell). \tag{B.5}$$

B.1.1 Yang-Baxter Equation and Other Symmetries

Let $\mathcal{R}$ and $\mathcal{R}'$ be two rapidity line configurations defined on quadrangular construction graphs H and H' such that $\partial H = \partial H'$. These two configurations induce two signed measures $w_{\mathcal{R}}$ and $w_{\mathcal{R}'}$ on the same space of link patterns $\mathrm{LP}(\partial H)$. We define the equivalence relation $\simeq_{\mathrm{LP}}$ on rapidity line configurations by

$$\mathcal{R} \simeq_{\mathrm{LP}} \mathcal{R}' \iff w_{\mathcal{R}} = w_{\mathcal{R}'}. \tag{B.6}$$

This section is devoted to show the $\simeq_{\mathrm{LP}}$-equivalence of some configurations. These equivalences will be useful to transform bigger rapidity line configuration: if $\mathcal{R}, \mathcal{R}', \mathcal{R}''$

are three configurations with $\mathcal{R} \simeq_{\mathrm{LP}} \mathcal{R}'$ and $\mathcal{R}$ appears as some sub-pattern of $\mathcal{R}''$, then the link pattern distribution on $\mathcal{R}''$ depends only on the link pattern on its version of $\mathcal{R}$ and not on the particular loop configuration realizing it. This allows us to replace $\mathcal{R}$ by $\mathcal{R}'$ in $\mathcal{R}''$ and still get an $\simeq_{\mathrm{LP}}$-equivalent configuration giving the same weights to the same link patterns.

In the following results, the configurations will be defined pictorially, with a specification of the edges of ∂H. The first equivalence result just shows what happens when the orientation of a rapidity line is reversed.

Theorem B.1.1 (Crossing relation)**.**

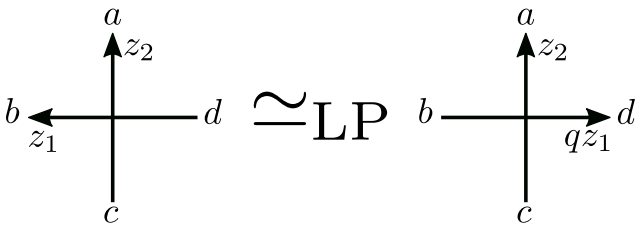

(B.7)

Where a, b, c, d are labels of the edges joined by the rapidity lines, $z_1, z_2 \in \mathbb{U}$ are rapidities.

Proof. Define $\mathcal{R}$ (resp. $\mathcal{R}'$) to be the configuration on the left hand side (resp. right hand side) of (B.7). Since $\mathrm{LP}(\{a, b, c, d\})$ has only two (non-intersecting) link patterns and since the total weight is always 1, it is enough to check the equality of the weight for one of them, say $\alpha = \{\{a, b\}, \{c, d\}\}$. We have

$$w_{\mathcal{R}}(\alpha) = \frac{[z_1/z_2]}{[qz_2/z_1]} = \frac{[z_2/z_1]}{[z_1/(qz_2)]} = \frac{[qz_2/(qz_1)]}{[q(qz_1)/z_2]} = w'_{\mathcal{R}}(\alpha).$$

□

Theorem B.1.2 (Unitary relation)**.**

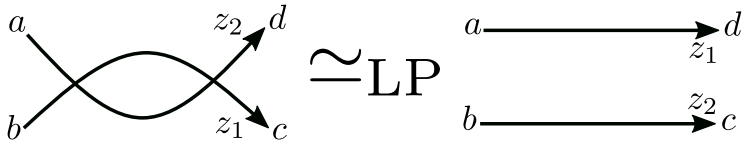

(B.8)

Where a, b, c, d are labels of the edges joined by the rapidity lines, $z_1, z_2 \in \mathbb{U}$ are rapidities.

Proof. As before let $\mathcal{R}, \mathcal{R}'$ be the two configurations, it is enough to check that weights coincides on one of the two possible link patterns. The pattern $\alpha = \{\{a, d\}, \{b, c\}\}$ is realized by only one loop configuration. Hence

$$w_{\mathcal{R}}(\alpha) = \frac{[qz_1/z_2]}{[qz_2/z_1]} \times \frac{[qz_2/z_1]}{[qz_1/z_2]} = 1 = w'_{\mathcal{R}}(\alpha).$$

□

Theorem B.1.3 (Yang-Baxter equation)**.** *We have*

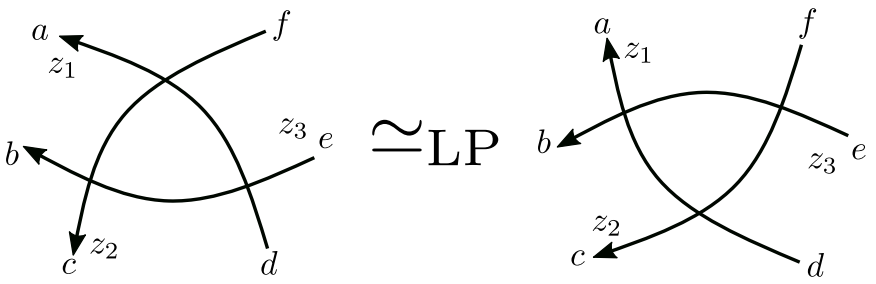

(B.9)

where a, b, c, d, e, f are labels of the edges joined by the rapidity lines, $z_1, z_2, z_3 \in \mathbb{U}$ are rapidities.

The term 'Yang-Baxter equation' was introduced by Faddeev to describe a principle of invariance appearing in a wide variety of physical systems, that can be seen as a generalization of the star-triangle transformation. The first appearance of such transformation goes back to the work of Kennelly in 1899 on electrical networks. One can refer to [PAY06] for an account on the history and the various versions of the Yang-Baxter equation.

On isoradial graphs the star-triangle transformation is just a permutation of rhombi of the diamond graph, which is exactly equivalent to sliding one of the three tracks (or rapidity lines) corresponding to these rhombi over the other two. This track transformation is exactly the one appearing in Equation (B.9).

Building on our work on the star-triangle transformation on isoradial graphs, we can give the following proof of Theorem B.1.3.

Proof. Let $\mathcal{R}, \mathcal{R}'$ be the two rapidity line configurations appearing in Equation (B.9). Let α be a link pattern with weights $w_{\mathcal{R}}(\alpha)$ and $w'_{\mathcal{R}}(\alpha)$. Figure B.4 shows that $\mathcal{R}$ can be obtained from an actual isoradial graph. In this case the weights are probabilities and we showed that $w_{\mathcal{R}}(\alpha) = w'_{\mathcal{R}}(\alpha)$. It is easy to see that if $\theta_1, \theta_2, \theta_3$ are the angles of the edges of the rhombi of the the isoradial graph, then we can slightly move one of these angles while keeping the other fixed and still having an isoradial representation (there are three degrees of freedom on these angles). This means that there exists an open set of $\mathbb{U}^3$ such that (z_1, z_2, z_3) corresponds to an isoradial graph. Moreover $w_{\mathcal{R}}(\alpha)$ and $w'_{\mathcal{R}}(\alpha)$ are rational functions of the rapidities z_1, z_2, z_3. So $w_{\mathcal{R}}(\alpha) = w'_{\mathcal{R}}(\alpha)$ in general. □

A more straightforward proof is to check that the weights of link patterns correspond. Up to symmetries, we can reduce this verification to two link patterns, namely $\alpha = \{\{a, f\}, \{b, e\}, \{c, d\}\}$ and $\beta = \{\{a, f\}, \{b, c\}, \{d, e\}\}$. α is realized by only one loop configuration in $\mathcal{R}$ and $\mathcal{R}'$, β is realized by 4 loop configurations in $\mathcal{R}$ and 1 in $\mathcal{R}'$. One can do the calculation and check $w_{\mathcal{R}}(\alpha) = w'_{\mathcal{R}}(\alpha)$ and $w_{\mathcal{R}}(\beta) = w'_{\mathcal{R}}(\beta)$.

B.2 Boundary Passage on a Strip

B.2.1 Percolation on a Strip

From now on, we will focus on a particular isoradial graph, the strip, represented in Figure B.6. The strip can be constructed from a square isoradial graph (i.e. a graph isomorphic to $\mathbb{Z}^2$) by selecting two (vertical) parallel tracks that we call the left and the right boundaries. We fix all edges of the left (resp. right) boundary to be closed (resp. open). The strip is the graph between these boundaries. Let L be the number of tracks of the strip parallel to the boundaries. We consider only the case when L is odd.

It will be convenient to take the x-axis oriented in the negative direction as a reference $\vec{\mathcal{D}}$ for transverse angles. We assume that all horizontal tracks have the same transverse angle $\frac{-\pi}{2}$, corresponding to the rapidity $w = \exp\left(-i\frac{\pi}{6}\right)$ on Figure B.6. We take the determination of the transverse angles of the vertical tracks in $(-\pi/2, \pi/2)$. Since the crossing always involve a vertical and an horizontal track, it is easy to see that the consistency condition (B.3) is verified. The percolation on a strip can hence be described by the rapidity line configuration shown in Figure B.6.

Denote by $z_1, \dots, z_L$ the rapidities of the vertical lines as in Figure B.6, and define the corresponding probabilities (or weights when the rapidities are out of the scope of isoradial graphs):

$$p_i = \frac{[qz_i/w]}{[qw/z_i]}, i = 1, \dots, L.$$

In every column of the strip, primal or dual edges in the south-west to north-east direction are open with probability p_i and closed with probability $1 - p_i$.

Define two vertices v_0 and v_1 as in Figure B.6, and B the set of vertices of the right boundary. We are interested by the computation of

$$\hat{P}_L = \mathbb{P}\left(v_0 \leftrightarrow B\right) \text{ and } P_L = \mathbb{P}\left(v_1 \leftrightarrow B\right). \tag{B.10}$$

We call them the boundary passage probabilities. They depend on the rapidities of the system, or equivalently on the probabilities $p_i, i = 1 \dots L$. We will abuse notation and see them as function, writing $P_L(z_1, \dots, z_L)$ (since w is fixed) or $P_L(p_1, \dots p_L)$, and likewise for $\hat{P}_L$.

B.2.2 The transfer matrix on link patterns

Define $\mathrm{LP}_L = \mathrm{LP}(\{1, \dots, L, \infty\})$ to be the link patterns where $1, \dots, L, \infty$ are thought of as $L+1$ points lying on a line in this order, and such that the links when drawn in one of the half-plane do not intersect. We represent these patterns as links between $1, \dots, L$ together with one path starting at a point of $1, \dots, L$ and thought of as going to ∞ (see Figure B.7).

Since the width of the strip L is odd, the loop configuration induced by a random percolation configuration is almost surely composed of finite loops and one single infinite path, that we call the interface, stretching from $-\infty$ to $+\infty$. The uniqueness of the infinite path can be deduced from the fact that almost surely, two-line configurations letting only one path to traverse them (like the one in Figure B.6.c)

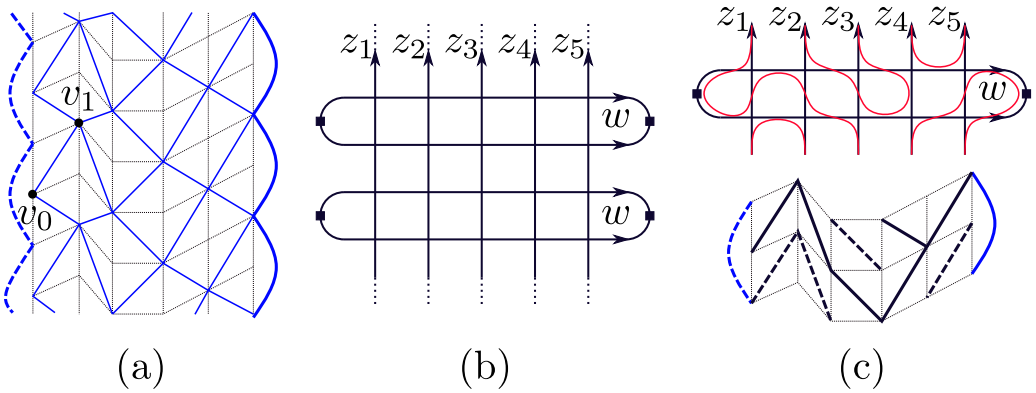

Figure B.6: (a): A section of the infinite isoradial strip with $L = 5$. The primal graph is drawn in straight blue line and the diamond graph in black dotted line. The right boundary (in thick blue line) is fixed to be open and the left boundary (in dashed thick blue line) is set to be dually open (i.e. closed). (b): The rapidity line configuration corresponding to the strip. The left and right boundary conditions translate by the fact that extremities of loops ending on the boundaries are linked two by two. This is represented by small link with a square (to distinguish from the continuation of a rapidity line). All the rapidity lines from left to right have the same spectral parameter w, vertical lines have rapidities $z_1, \dots, z_5$. (c): A percolation configuration on two lines of the strip and the corresponding loop configuration on the rapidity line configuration.

happen infinitely often. Hence, if we fix one line of the strip and look at the cut loop configuration, it induces a probability law on the upward (resp. downward) link patterns on the half plane below (resp. above) the line by linking the edges joined by a loop (and linking the remaining edge to ∞). We call $\pi_L^{\uparrow}$ (resp. $\pi_L^{\downarrow}$) this probability law on LP_L.

Let $\mathcal{L}$ be the set of loop configurations on two horizontal lines of the strip and $\ell \in \mathcal{L}$ a random configuration induced by the percolation process. It is easy to see that $\{v_0 \leftrightarrow B\}$ and $\{v_1 \leftrightarrow B\}$ are equivalent to the fact the interface passes to the left of either v_0 or v_1 (see Figure B.7). And this can be deduced from the upward link pattern, the downward link pattern, and the state of the two lines around v_0: there exist two indicator functions $I : \mathrm{LP}_L^2 \to \{0, 1\}$ and $\hat{I} : \mathrm{LP}_L \times \mathcal{L} \times \mathrm{LP}_L \to \{0, 1\}$ such that

$$P_L = \sum_{\alpha \in \mathrm{LP}_L} \sum_{\beta \in \mathrm{LP}_L} \pi_L^{\uparrow}(\alpha) \pi_L^{\downarrow}(\beta) I(\alpha, \beta) \tag{B.11}$$

$$\text{and } \hat{P}_L = \sum_{\alpha \in \mathrm{LP}_L} \sum_{l \in \mathcal{L}} \sum_{\beta \in \mathrm{LP}_L} \pi_L^{\uparrow}(\alpha) \mathbb{P}(\ell = l) \pi_L^{\downarrow}(\beta) \hat{I}(\alpha, l, \beta) \tag{B.12}$$

We can define the action of $l \in \mathcal{L}$ on $\alpha \in \mathrm{LP}_L$ by $l \uparrow \alpha$ (resp. $l \downarrow \alpha$) that consists in the link resulting from the concatenation of the loop configuration l with the link pattern α seen as an upward (resp. downward) link pattern on the strip. An example of the action $l \uparrow \alpha$ is shown in Figure B.8. The laws $\pi_L^{\uparrow}$ and $\pi_L^{\downarrow}$ are invariant by a translation of two line (we still get the same half infinite strip). This means that $\pi_L^{\uparrow}$ (resp. $\pi_L^{\downarrow}$) is the invariant distribution of the Markov chain on LP_L

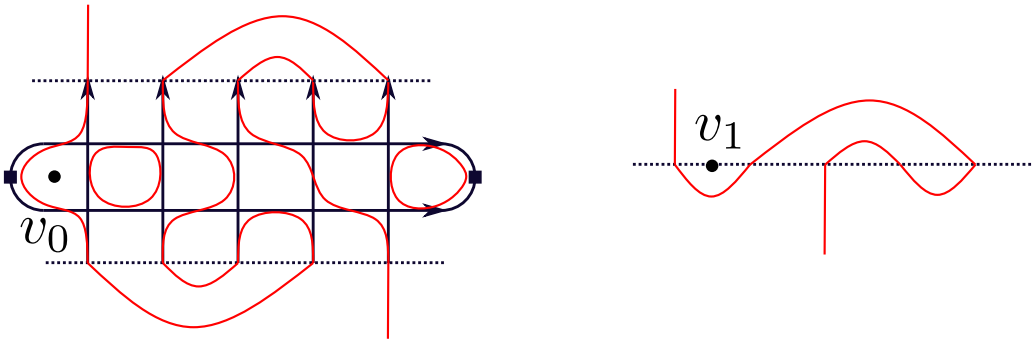

Figure B.7: Two configurations realizing respectively $\{v_0 \leftrightarrow B\}$ and $\{v_1 \leftrightarrow B\}$.

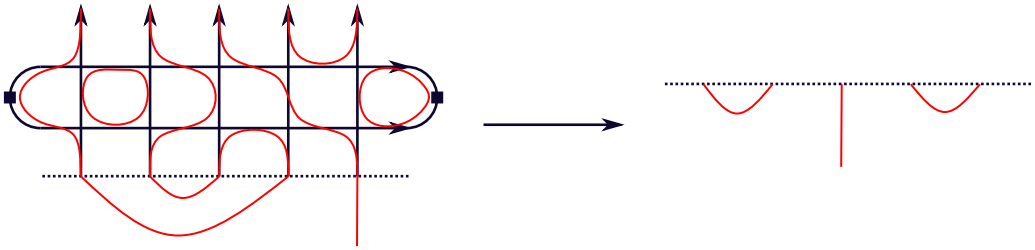

Figure B.8: The action $\uparrow$ of a loop configuration on two lines of the strip on an upward link pattern.

defined by the action of $\ell \uparrow \cdot$ (resp. $\ell \downarrow \cdot$). Indeed this Markov chain is easily shown to be irreducible and aperiodic (on its support which might not be all LP_L).

With this Markov chain interpretation, the link between the upward and the downward distribution is clearer. If we make explicit the dependency of the distribution on the p_i's, we can see that

$$\forall \alpha \in \mathrm{LP}_L, \forall p_1, \dots, p_L \in [0,1], \pi^{\downarrow}_{L,p_1\dots,p_L}(\alpha) = \pi^{\uparrow}_{L,1-p_1\dots,1-p_L}(\alpha). \tag{B.13}$$

To simplify notations, we will only consider upward link patterns. We define the transfer matrix t to be the transposed of the transition matrix of the Markov chain. When necessary we will make the dependency in $p_1, \dots, p_L$ or $z_1, \dots z_L$ explicit.

$$\forall \alpha, \beta \in \mathrm{LP}_L, t_{\beta,\alpha} = \mathbb{P}(\ell \uparrow \alpha = \beta) \tag{B.14}$$

Our goal for the rest of this text is to identify $\pi^{\uparrow}_L$ and hence the boundary passage probabilities. Here is a first result in this direction:

Theorem B.2.1. *The coefficients* $\left(\pi^{\uparrow}_L(\alpha)\right)_{\alpha \in \mathrm{LP}_L}$ *are rational functions in the parameters* $p_1, \dots, p_L$. *Hence so are* P_L *and* $\hat{P}_L$.

Proof. By definition, the coefficients of t are polynomials in $p_1, \dots, p_L$ (and hence rational functions in $z_1, \dots, z_L$). They belong to the field $\mathbb{Q}(p_1, \dots, p_L)$. Moreover $\pi^{\uparrow}_L$ can be seen as a right eigenvector of t for the eigenvalue 1. Hence, its coefficients are also defined in the field $\mathbb{Q}(p_1, \dots, p_L)$ of rational fractions in $p_1, \dots, p_L$. □

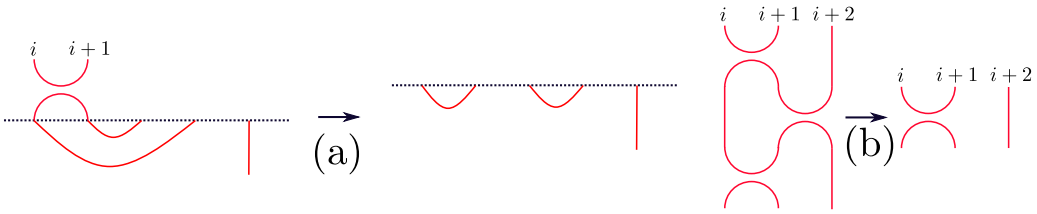

Figure B.9: (a) example of an action of e_i on a link pattern. (b) $e_i e_{i+1} e_i = e_i$.

B.3 Spectral Analysis of Link Patterns Distribution

We saw with Theorem B.2.1 that the values of $\pi_L^{\uparrow}$ are rational fractions in the variables $z_1, \ldots, z_l$. We can multiply them by the same factor and define a vector $(\Psi_\alpha)_{\alpha \in \mathrm{LP}_L}$ proportional to $\pi_L^{\uparrow}$ whose coefficients are Laurent polynomial and have no factor in common. The goal of this section is to find a set of equation, called the q-deformed Knizhnik–Zamolodchikov equations, that are sufficient to identify a particular such Ψ.

B.3.1 The Temperley-Lieb Algebra

The Temperley-Lieb algebra is generated by the collection $(e_i)_{1 \leq i \leq L-1}$ of operators acting on LP_L (seen as upward links) by applying a downward link between i and $i+1$ and then an upward link between i and $i+1$ (see Figure B.9.a). These operators verify some relations:

$$\begin{aligned} e_i^2 &= e_i \\ e_i e_{i\pm1} e_i &= e_i \text{ (see Figure B.9)} \\ e_i e_j &= e_j e_i \text{ if } |i-j| \geq 2. \end{aligned}$$

We define the canonical base of $\mathbb{C}^{\mathrm{LP}_L}$ by $(|\alpha\rangle)_{\alpha \in \mathrm{LP}_L}$ where $|\alpha\rangle$ is the vector with coefficient 1 at coordinate α and 0 otherwise. We abuse notation by also considering e_i as an operator on $\mathbb{C}^{\mathrm{LP}_L}$ defined on the base by $e_i|\alpha\rangle = |e_i \alpha\rangle$. Define the operator corresponding to the crossing of rapidity lines exiting from sites i and $i+1$:

$$\check{R}_i(w) = \frac{[q/w]}{[qw]} \mathbf{1} - \frac{[w]}{[qw]} e_i \tag{B.15}$$

The operator $\check{R}_i(z_i/z_{i+1})$ corresponds to the transformation on upward link pattern induced by

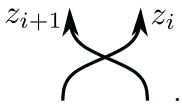

.

B.3.2 Symmetries of the Transfer Matrix

Lemma B.3.1. *The transfer matrix satisfies the interlacing relation*

$$\check{R}_i(z_i/z_{i+1}) t(z_1, \ldots, z_i, z_{i+1}, \ldots) = t(z_1, \ldots, z_{i+1}, z_i, \ldots) \check{R}_i(z_i/z_{i+1}), \tag{B.16}$$

and the boundary relations

$$t(z_1, z_2, \ldots) = t(1/z_1, z_2, \ldots) \tag{B.17}$$

$$t(z_1, \ldots, z_{L-1}, z_L) = t(z_1, \ldots, z_{L-1}, 1/z_L) \tag{B.18}$$

Proof. The left hand side and the right hand side of (B.16) correspond to the following rapidity line configurations which are $\simeq_{\mathrm{LP}}$-equivalent thanks to a repeated application of the Yang-Baxter equation (B.9).

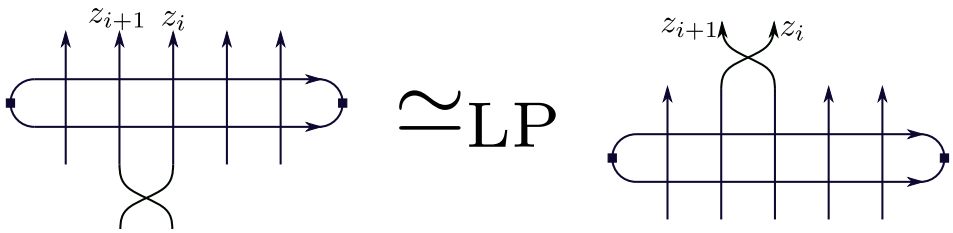

The boundary relations are easily deduced by considering all the possible tiles on the crossings of the first and the last vertical rapidity line. For instance for the first boundary relation, this loop configuration is the only one giving its link pattern on the boundary:

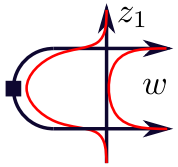

Using the fact that $w = \exp(-i\pi/6)$, it has weight

$$\frac{[qz_1/w][z_1/w]}{[qw/z_1][qw/z_1]} = \frac{[z_1/w^5][z_1/w]}{[1/(w^3 z_1)][1/(w^3 z_1)]} = \frac{[1/(z_1 w)][z_1/w]}{[z_1/w^3][1/(z_1 w^3)]}$$

which invariant under $z_1 \leftrightarrow 1/z_1$. □

For $1 \leq i \leq L-1$, define the function $\varphi_i : \mathrm{LP}_{L-2} \longrightarrow \mathrm{LP}_L$ by inserting two points at position i and a link between them. Formally, if $\alpha = \left\{\{x_1, y_1\}, \ldots, \left\{x_{\frac{L-1}{2}}, y_{\frac{L-1}{2}}\right\}\right\} \in \mathrm{LP}_{L-2}$,

$$\varphi(\alpha) = \{\{i, i+1\}\} \bigcup_{j=1}^{(L-1)/2} \{\{x_j + 2 \times 1_{x_j \geq i}, y_j + 2 \times 1_{y_j \geq i}\}\}.$$

Lemma B.3.2. *When $z_{i+1} = qz_i$, the transfer matrix verifies*

$$t_L(z_1, \ldots, z_i, qz_i, z_{i+2}, \ldots)\varphi_i = \varphi_i t_{L-2}(z_1, \ldots, z_{i-1}, z_{i+2}, \ldots) \tag{B.19}$$

where we made explicit the dependency of t in L.

Proof. If we look at the rapidity line configuration induced by φ_i on the vertical lines i and $i+1$, we can apply twice the following transformations based on the crossing relation (B.7) and the unitary relation (B.8).

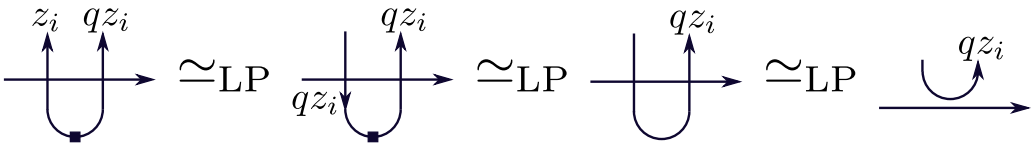

By doing so, we prove the $\simeq_{\mathrm{LP}}$-equivalence of the configurations corresponding to the two sides of the relation. □

We finish this section with a remark on the horizontal rapidity lines. We made the choice of giving the same rapidity w to the two lines of the transfer matrix and of fixing the value of $w = \exp\left(-i\frac{\pi}{6}\right)$ from the beginning. Suppose that we gave two different rapidities w and w' to the two horizontal lines of the transfer matrix. Then using the relations (B.7, B.8, B.9) and Lemma B.3.6, it is possible to show that two transfer matrices with the same value of the product ww' commute. Hence they have the same Perron-Froebenius eigenvector. This means that if we squeeze the strip like an accordion, the link pattern distribution, and hence the boundary passage probabilities, do not change.

B.3.3 The q-deformed Knizhnik–Zamolodchikov Equations

When we take the rapidities $z_1, \ldots, z_L$ to be induced from transverse angles in $(-\pi/2, \pi/2)$, $t(z_1, \ldots, z_L)$ is the transposed of the transition matrix of an irreducible aperiodic Markov chain. Hence it has a Perron-Froebenius eigenvector for the eigenvalue 1, say v. Following Theorem B.2.1, the coordinates of v are rational fractions in $z_1, \ldots, z_L$ and we can normalize this eigenvector to get another proportional Perron-Froebenius eigenvector whose coordinates are Laurent polynomials with no factor in common. The following theorem exhibits a set of relations that we will show to be sufficient to identify one such eigenvector.

Theorem B.3.3. *Let $\Psi(z_1, \ldots, z_L) \in \mathbb{C}^{\mathrm{LP}_L}$ be a vector valued function in the variables $z_1, \ldots, z_L$. Define the partition function*

$$Z(z_1, \ldots, z_L) = \sum_{\alpha \in \mathrm{LP}_L} \Psi_\alpha(z_1, \ldots, z_L).$$

Denote for any function f, $\pi_j f(\ldots, z_j, z_{j+1}, \ldots) = f(\ldots, z_{j+1}, z_j, \ldots)$. Then the following are equivalent:

(i) Ψ verifies the following relations called the qKZ equations

$$\check{R}_j(z_j/z_{j+1})\Psi = \pi_j \Psi \text{ for } 1 \leq j \leq L-1 \tag{B.20a}$$
$$\Psi(z_1, \ldots, z_L) = \Psi(1/z_1, z_2, \ldots, z_L) \tag{B.20b}$$
$$\Psi(z_1, \ldots, z_L) = \Psi(z_1, \ldots, z_{L-1}, 1/z_L). \tag{B.20c}$$

(ii) $Z(z_1, \ldots, z_L)$ is invariant under any π_i, $i = 1, \ldots, L-1$ and the transformations $z_1 \leftrightarrow 1/z_1$ and $z_L \leftrightarrow 1/z_L$, and

$$t(z_1, \ldots, z_L)\Psi(z_1, \ldots, z_L) = \Psi(z_1, \ldots, z_L).$$

In particular if Ψ is non-zero, it is a Perron-Froebenius eigenvector of t.

Proof. We first show $(ii) \implies (i)$ using Lemma B.3.1. If we apply both sides of Equation (B.16) to Ψ, we find

$$\check{R}_i(z_i/z_{i+1})\Psi = t(z_1, \ldots, z_{i+1}, z_i, \ldots)\check{R}_i(z_i/z_{i+1})\Psi.$$

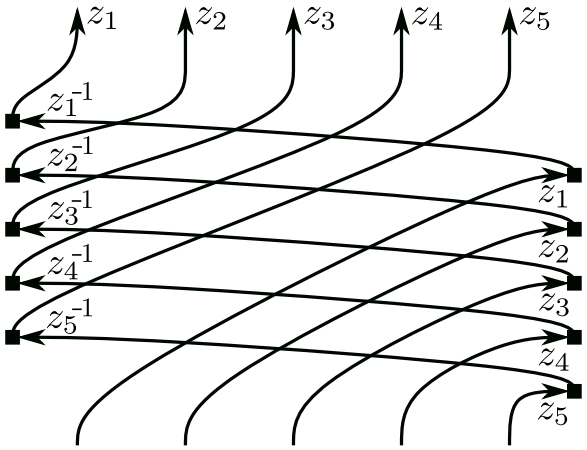

Figure B.10: Rapidity line representation of the scattering matrix S for $L = 5$. The squares represent junctions between rapidity lines with different rapidities.

The Perron-Froebenius eigenvector being unique, this tells us that $\check{R}_i(z_i/z_{i+1})\Psi$ and $\pi_i\Psi$ are proportional (they can be zero a priori). Moreover $\check{R}$ is a measure preserving transformation, hence

$$\sum_{\alpha\in \mathrm{LP}_L} \left(\check{R}_i(z_i/z_{i+1})\Psi\right)_\alpha = \sum_{\alpha\in \mathrm{LP}_L} \Psi_\alpha = Z = \pi_i Z = \sum_{\alpha\in \mathrm{LP}_L} (\pi_i\Psi)_\alpha \,.$$

So $\check{R}_i(z_i/z_{i+1})\Psi = \pi_i\Psi$. The same strategy works to equally deduce (B.20b) and (B.20c) from (B.17) and (B.18).

Now we show $(i) \implies (ii)$. The strategy of the proof is to define another matrix acting on $\mathbb{C}^{\mathrm{LP}_L}$ called the scattering matrix $S(z_1,\ldots,z_L)$, which is the transposed of an irreducible stochastic matrix. We will show that S and t commute, hence they have the same Perron-Froebenius eigenvectors. To conclude, we show that if Ψ is a vector verifying the qKZ equations, it is an eigenvector of S for the eigenvalue 1 (or zero).

The scattering matrix S is defined as the matrix representation of the action on upward link patterns LP_L of the rapidity line configuration represented in Figure B.10. Formally, it is defined by

$$S(z_1,\ldots,z_L) = \prod_{i=2}^{L}\prod_{j=1}^{i-1} \check{R}_{i-j}(z_i z_j) \times \prod_{i=2}^{L}\prod_{j=1}^{i-1} \check{R}_{j+L-i}(z_j z_j) \tag{B.21}$$

where the order of the products is very important since these operators do not commute. If $\theta_1,\ldots,\theta_L$ are the transverse angles corresponding to the vertical rapidities, we can take them to be positive and close to 0. Then the coefficients of the operators $\check{R}$ in (B.21) are positive and S is the transposed of an irreducible stochastic matrix (the irreducibility is easy to check). Let Ψ be a vector verifying the qKZ equations (B.20a, B.20b, B.20c), then by Lemma B.3.4 we have $S\Psi = \Psi$. By Lemma B.3.5, t and S commute, so they have the same Perron-Froebenius eigenvectors, hence $t\Psi = \Psi$.

Since $\check{R}$ is measure preserving, it is clear from (B.20a) that $Z = \pi_i Z$ for $i = 1,\ldots,L-1$, and from (B.20b,B.20c) that Z is invariant under $z_1 \leftrightarrow 1/z_1$ and $z_L \leftrightarrow 1/z_L$.

□

Lemma B.3.4. *Let Ψ be a vector verifying the qKZ equations (B.20a, B.20b, B.20c) then $S\Psi = \Psi$.*

Proof. A graphical way to see this is to say that on the diagram in Figure B.10, the arguments of Ψ after a sequence of upward operations are exactly the rapidities read in order on the rapidity lines just above the crossings corresponding to the sequence of operations. When two line cross, the index of their rapidities is exchanged and (B.20a) shows that it is exactly what happens to the argument of Ψ. When a rapidity line ends on the boundary and another one with inversed rapidity starts, it appears in Ψ at first or last position, and (B.20b,B.20c) show that we can apply the same inversion to the arguments of Ψ.

We show the formal computation for $L = 3$.

$$
\begin{aligned}
&S(z_1, z_3, z_3)\Psi(z_1, z_2, z_3) \\
&= \check{R}_1(z_1z_2)\check{R}_2(z_1z_3)\check{R}_1(z_2z_3)\check{R}_2(z_1z_2)\check{R}_1(z_1z_3)\check{R}_2(z_2z_3)\Psi(z_1, z_2, 1/z_3) \\
&= \check{R}_1(z_1z_2)\check{R}_2(z_1z_3)\check{R}_1(z_2z_3)\check{R}_2(z_1z_2)\check{R}_1(z_1z_3)\Psi(z_1, 1/z_3, z_2) \\
&= \check{R}_1(z_1z_2)\check{R}_2(z_1z_3)\check{R}_1(z_2z_3)\check{R}_2(z_1z_2)\Psi(1/z_3, z_1, 1/z_2) \\
&= \check{R}_1(z_1z_2)\check{R}_2(z_1z_3)\check{R}_1(z_2z_3)\Psi(z_3, 1/z_2, z_1) \\
&= \check{R}_1(z_1z_2)\check{R}_2(z_1z_3)\Psi(1/z_2, z_3, 1/z_1) \\
&= \check{R}_1(z_1z_2)\Psi(z_2, 1/z_1, z_3) = \Psi(1/z_1, z_2, z_3) = \Psi(z_1, z_2, z_3)
\end{aligned}
$$

□

Lemma B.3.5. *The transfer matrix and the scattering matrix commute:*

$$t(z_1, \dots, z_L)S(z_1, \dots, z_L) = S(z_1, \dots, z_L)t(z_1, \dots, z_L).$$

Proof. If we concatenate the rapidity line representation of t and S, we need to make the two lines with rapidity w of t cross the representation of S. Figure B.11 shows the sequence of operations for $L = 3$. The Yang-Baxter equation (B.9) shows that all the internal crossing of S can be crossed easily by t. It remains to show that t can cross the boundary points of S, that is to show the following $\simeq_{\mathrm{LP}}$-equivalences:

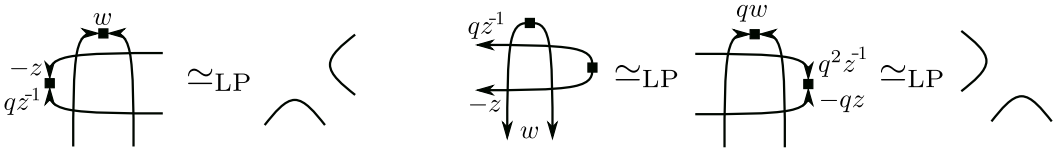

The first $\simeq_{\mathrm{LP}}$-equivalence on the right comes from two applications of (B.7), first to vertical lines and then to the horizontal lines. On the left, $-z \times qz^{-1} = -q = w \times w$. On the right, $-qz \times q^2z^{-1} = -1 = qw \times qw$. Hence we can conclude using Lemma B.3.6. □

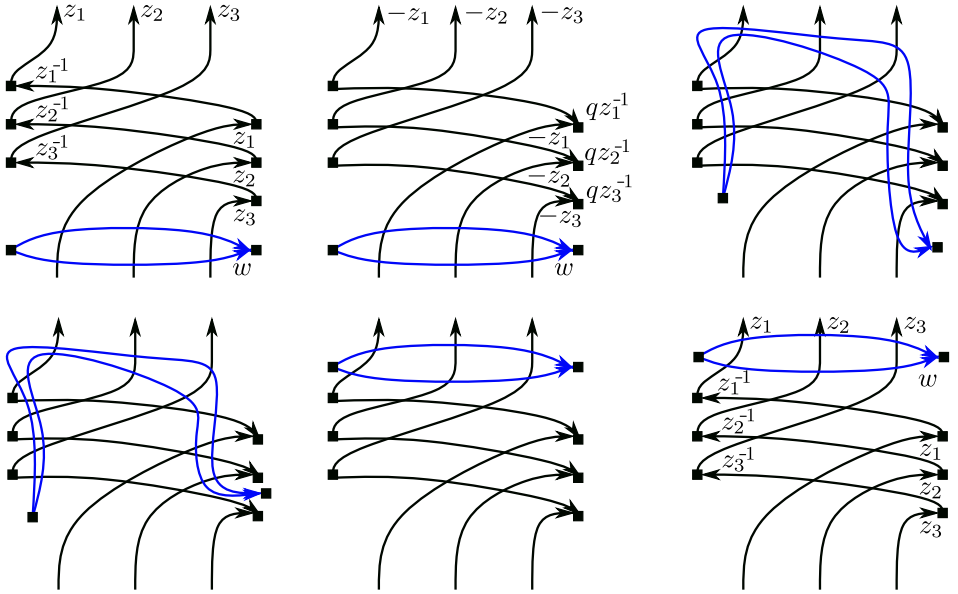

Figure B.11: Graphical proof that $tS = St$ for $L = 3$. This shows a sequence of $\simeq_{\mathrm{LP}}$-preserving transformation. We first change the rapidities on some lines using (B.7) and the fact that the weights are invariant if we replace a rapidity by its opposite. The next step is done via a repetition of the Yang-Baxter equation. The next one relies on the boundary result in the proof of Lemma B.3.5, and it is repeated to get the final rapidity line configuration corresponding to tS, where we replace the rapidities by the original ones.

Lemma B.3.6 (Boundary decoupling)**.** *If x, x', y, y' are rapidities such that $xx' = yy'$, then we have the following $\simeq_{\mathrm{LP}}$-equivalence:*

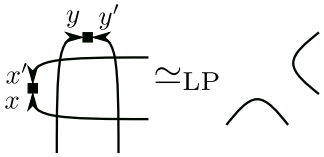

Proof. The loop configurations not equivalent to the right hand sides are the following:

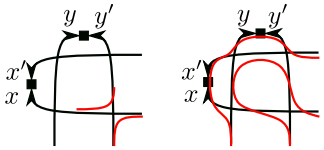

The two configurations have weight

$$\begin{aligned}
&\frac{[x/y']}{[qy'/x]} + \frac{[qx/y'][qx'/y'][qx/y][x'/y]}{[qy'/x][qy'/x'][qy/x][qy/x']} \\
&\qquad = \frac{[x/y'][qy'/x'][qy/x][qy/x'] + [qx/y'][qx'/y'][qx/y][x'/y]}{[qy'/x][qy'/x'][qy/x][qy/x']} \\
&\qquad\qquad = \frac{[y/x'][qx/y][qx'/y'][qx/y'] + [qx/y'][qx'/y'][qx/y][x'/y]}{[qy'/x][qy'/x'][qy/x][qy/x']} = 0.
\end{aligned}$$

□

Bibliography

[ADCW20] Michael Aizenman, Hugo Duminil-Copin, and Simone Warzel. Dimerization and néel order in different quantum spin chains through a shared loop representation. In *Annales Henri Poincare*, volume 21, pages 2737–2774. Springer, 2020.

[Bat19] Robert W Batterman. Universality and rg explanations. *Perspectives on Science*, 27(1):26–47, 2019.

[Bax78] Rodney James Baxter. Solvable eight-vertex model on an arbitrary planar lattice. *Philosophical Transactions of the Royal Society of London. Series A, Mathematical and Physical Sciences*, 289(1359):315–346, 1978.

[Bax82] R. J. Baxter. *Exactly solved models in statistical mechanics*. 1982.

[BCG16] Alexei Borodin, Ivan Corwin, and Vadim Gorin. Stochastic six-vertex model. *Duke Mathematical Journal*, 165(3):563–624, 2016.

[BDC12] Vincent Beffara and Hugo Duminil-Copin. The self-dual point of the two-dimensional random-cluster model is critical for $q \geq 1$. *Probability Theory and Related Fields*, 153(3-4):511–542, 2012.

[BDCS15] Vincent Beffara, Hugo Duminil-Copin, and Stanislav Smirnov. On the critical parameters of the $q \leq 4$ random-cluster model on isoradial graphs. *Journal of Physics A: Mathematical and Theoretical*, 48(48):484003, 2015.

[BdT12] Cédric Boutillier and Béatrice de Tilière. Statistical mechanics on isoradial graphs. In *Probability in Complex Physical Systems*, pages 491–512. Springer, 2012.

[BH57] Simon R Broadbent and John M Hammersley. Percolation processes: I. crystals and mazes. In *Mathematical proceedings of the Cambridge philosophical society*, volume 53, pages 629–641. Cambridge University Press, 1957.

[BH19] Stéphane Benoist and Clément Hongler. The scaling limit of critical ising interfaces is $cle(3)$. *The Annals of Probability*, 47(4):2049–2086, 2019.

[BK18] Alexey Bufetov and Alisa Knizel. Asymptotics of random domino tilings of rectangular aztec diamonds. In *Annales de l'Institut Henri Poincaré, Probabilités et Statistiques*, volume 54, pages 1250–1290. Institut Henri Poincaré, 2018.

[BKW76] Rodney J Baxter, Stewart B Kelland, and Frank Y Wu. Equivalence of the potts model or whitney polynomial with an ice-type model. *Journal of Physics A: Mathematical and General*, 9(3):397, 1976.

[BPZ84a] Alexander A Belavin, Alexander M Polyakov, and Alexander B Zamolodchikov. Infinite conformal symmetry in two-dimensional quantum field theory. *Nuclear Physics B*, 241(2):333–380, 1984.

[BPZ84b] Alexander A Belavin, Alexander M Polyakov, and Alexander B Zamolodchikov. Infinite conformal symmetry of critical fluctuations in two dimensions. *Journal of Statistical Physics*, 34(5):763–774, 1984.

[BR10] Béla Bollobás and Oliver Riordan. Percolation on self-dual polygon configurations. In *An irregular mind*, pages 131–217. Springer, 2010.

[BS17] Deepan Basu and Artem Sapozhnikov. Kesten's incipient infinite cluster and quasi-multiplicativity of crossing probabilities. *Electronic Communications in Probability*, 22:1–12, 2017.

[CDCH$^+$14] Dmitry Chelkak, Hugo Duminil-Copin, Clément Hongler, Antti Kemppainen, and Stanislav Smirnov. Convergence of ising interfaces to schramm's sle curves. *Comptes Rendus Mathematique*, 352(2):157–161, 2014.

[CDCH16] Dmitry Chelkak, Hugo Duminil-Copin, and Clément Hongler. Crossing probabilities in topological rectangles for the critical planar FK-Ising model. *Electronic Journal of Probability*, 21(none):1 – 28, 2016.

[CHI15] Dmitry Chelkak, Clément Hongler, and Konstantin Izyurov. Conformal invariance of spin correlations in the planar ising model. *Annals of mathematics*, pages 1087–1138, 2015.

[CN06a] Federico Camia and Charles M Newman. Sle (6) and cle (6) from critical percolation. *arXiv preprint math/0611116*, 2006.

[CN06b] Federico Camia and Charles M Newman. Two-dimensional critical percolation: the full scaling limit. *Communications in Mathematical Physics*, 268(1):1–38, 2006.

[CN07] Federico Camia and Charles M Newman. Critical percolation exploration path and sle 6: a proof of convergence. *Probability theory and related fields*, 139(3-4):473–519, 2007.

[CPST21] Nishant Chandgotia, Ron Peled, Scott Sheffield, and Martin Tassy. Delocalization of uniform graph homomorphisms from $\mathbb{Z}^2$ to $\mathbb{Z}$. *Communications in Mathematical Physics*, 387(2):621–647, 2021.

[CS12] Dmitry Chelkak and Stanislav Smirnov. Universality in the 2d ising model and conformal invariance of fermionic observables. *Inventiones mathematicae*, 189(3):515–580, 2012.

[dB81] Nicolaas Govert de Bruijn. Algebraic theory of penrose's non-periodic tilings of the plane. *Kon. Nederl. Akad. Wetensch. Proc. Ser. A*, 43(84):1–7, 1981.

[DC13] Hugo Duminil-Copin. Parafermionic observables and their applications to planar statistical physics models. *Ensaios Matematicos*, 25:1–371, 2013.

[DC17] Hugo Duminil-Copin. Lectures on the ising and potts models on the hypercubic lattice. In *PIMS-CRM Summer School in Probability*, pages 35–161. Springer, 2017.

[DCGH$^+$16] Hugo Duminil-Copin, Maxime Gagnebin, Matan Harel, Ioan Manolescu, and Vincent Tassion. Discontinuity of the phase transition for the planar random-cluster and potts models with $q > 4$. *arXiv preprint arXiv:1611.09877*, 2016.

[DCGH$^+$18] Hugo Duminil-Copin, Maxime Gagnebin, Matan Harel, Ioan Manolescu, and Vincent Tassion. The bethe ansatz for the six-vertex and xxz models: An exposition. *Probability Surveys*, 15:102–130, 2018.

[DCGPS20] Hugo Duminil-Copin, Alexander Glazman, Ron Peled, and Yinon Spinka. Macroscopic loops in the loop $o(n)$ model at nienhuis' critical point. *Journal of the European Mathematical Society*, 23(1):315–347, 2020.

[DCHL$^+$19] Hugo Duminil-Copin, Matan Harel, Benoit Laslier, Aran Raoufi, and Gourab Ray. Logarithmic variance for the height function of square-ice. *arXiv preprint arXiv:1911.00092*, 2019.

[DCHN11] Hugo Duminil-Copin, Clément Hongler, and Pierre Nolin. Connection probabilities and rsw-type bounds for the two-dimensional fk ising model. *Communications on pure and applied mathematics*, 64(9):1165–1198, 2011.

[DCKK$^+$20a] Hugo Duminil-Copin, Karol Kajetan Kozlowski, Dmitry Krachun, Ioan Manolescu, and Mendes Oulamara. Rotational invariance in critical planar lattice models. *arXiv preprint arXiv:2012.11672*, 2020.

[DCKK$^+$20b] Hugo Duminil-Copin, Karol Kajetan Kozlowski, Dmitry Krachun, Ioan Manolescu, and Tatiana Tikhonovskaia. On the six-vertex model's free energy. *arXiv preprint arXiv:2012.11675*, 2020.

[DCKMO20] Hugo Duminil-Copin, Alex Karrila, Ioan Manolescu, and Mendes Oulamara. Delocalization of the height function of the six-vertex model. *arXiv preprint arXiv:2012.13750*, 2020.

[DCLM18] Hugo Duminil-Copin, Jhih-Huang Li, and Ioan Manolescu. Universality for the random-cluster model on isoradial graphs. *Electronic Journal of Probability*, 23:1–70, 2018.

[DCM20] Hugo Duminil-Copin and Ioan Manolescu. Planar random-cluster model: scaling relations. *arXiv preprint arXiv:2011.15090*, 2020.

[DCMT21] Hugo Duminil-Copin, Ioan Manolescu, and Vincent Tassion. Planar random-cluster model: fractal properties of the critical phase. *Probability Theory and Related Fields*, pages 1–49, 2021.

[DCRT19] Hugo Duminil-Copin, Aran Raoufi, and Vincent Tassion. Sharp phase transition for the random-cluster and potts models via decision trees. *Annals of Mathematics*, 189(1):75–99, 2019.

[DCS12] Hugo Duminil-Copin and Stanislav Smirnov. The connective constant of the honeycomb lattice equals $\sqrt{2+\sqrt{2}}$. *Annals of Mathematics*, pages 1653–1665, 2012.

[DCST17] Hugo Duminil-Copin, Vladas Sidoravicius, and Vincent Tassion. Continuity of the phase transition for planar random-cluster and potts models with $q \leq 4$. *Communications in Mathematical Physics*, 349(1):47–107, 2017.

[DCT19] Hugo Duminil-Copin and Vincent Tassion. Renormalization of crossing probabilities in the planar random-cluster model. *arXiv preprint arXiv:1901.08294*, 2019.

[DF05] Philippe Di Francesco. Inhomogeneous loop models with open boundaries. *Journal of Physics A: Mathematical and General*, 38(27):6091, 2005.

[DGP+10] Jan De Gier, Pavel Pyatov, et al. Factorised solutions of temperley-lieb *qkz* equations on a segment. *Advances in Theoretical and Mathematical Physics*, 14(3):795–878, 2010.

[DS11] Michael Damron and Artëm Sapozhnikov. Outlets of 2d invasion percolation and multiple-armed incipient infinite clusters. *Probability theory and related fields*, 150(1):257–294, 2011.

[Dub11] Julien Dubédat. Exact bosonization of the ising model. *arXiv preprint arXiv:1112.4399*, 2011.

[Duf68] Richard James Duffin. Potential theory on a rhombic lattice. *Journal of Combinatorial Theory*, 5(3):258–272, 1968.

[ES64] John W Essam and MF Sykes. Exact critical percolation probabilities for site and bond problem in two dimensions. *J. Math. Phys*, 5:1117–1127, 1964.

[Fis98] Michael E Fisher. Renormalization group theory: Its basis and formulation in statistical physics. *Reviews of Modern Physics*, 70(2):653, 1998.

[FK72] Cornelius Marius Fortuin and Piet W Kasteleyn. On the random-cluster model: I. introduction and relation to other models. *Physica*, 57(4):536–564, 1972.

[FKG71] Cees M Fortuin, Pieter W Kasteleyn, and Jean Ginibre. Correlation inequalities on some partially ordered sets. *Communications in Mathematical Physics*, 22(2):89–103, 1971.

[For71] Cornelius Marius Fortuin. On the Random-Cluster model. *Doctoral thesis, University of Leiden*, 1971.

[FS06] Patrik L Ferrari and Herbert Spohn. Domino tilings and the six-vertex model at its free-fermion point. *Journal of Physics A: Mathematical and General*, 39(33):10297, 2006.

[Gib02] Josiah Willard Gibbs. *Elementary principles in statistical mechanics: developed with especial reference to the rational foundations of thermodynamics*. C. Scribner's sons, 1902.

[GM13a] Geoffrey R Grimmett and Ioan Manolescu. Inhomogeneous bond percolation on square, triangular and hexagonal lattices. *The Annals of Probability*, 41(4):2990–3025, 2013.

[GM13b] Geoffrey R Grimmett and Ioan Manolescu. Universality for bond percolation in two dimensions. *The Annals of Probability*, 41(5):3261–3283, 2013.

[GM14] Geoffrey R Grimmett and Ioan Manolescu. Bond percolation on isoradial graphs: criticality and universality. *Probability Theory and Related Fields*, 159(1):273–327, 2014.

[GM21] Alexander Glazman and Ioan Manolescu. Uniform lipschitz functions on the triangular lattice have logarithmic variations. *Communications in Mathematical Physics*, 381(3):1153–1221, 2021.

[GMT17] Alessandro Giuliani, Vieri Mastropietro, and Fabio Lucio Toninelli. Height fluctuations in interacting dimers. In *Annales de l'Institut Henri Poincaré, Probabilités et Statistiques*, volume 53, pages 98–168. Institut Henri Poincaré, 2017.

[GP19] Alexander Glazman and Ron Peled. On the transition between the disordered and antiferroelectric phases of the 6-vertex model. *arXiv preprint arXiv:1909.03436*, 2019.

[GPS13a] Christophe Garban, Gábor Pete, and Oded Schramm. Pivotal, cluster, and interface measures for critical planar percolation. *Journal of the American Mathematical Society*, 26(4):939–1024, 2013.

[GPS13b] Christophe Garban, Gábor Pete, and Oded Schramm. Pivotal, cluster, and interface measures for critical planar percolation. *Journal of the American Mathematical Society*, 26(4):939–1024, 2013.

[GPS18] Christophe Garban, Gábor Pete, and Oded Schramm. The scaling limits of near-critical and dynamical percolation. *Journal of the European Mathematical Society*, 20(5):1195–1268, 2018.

[Gri67] Robert B Griffiths. Correlations in ising ferromagnets. i. *Journal of Mathematical Physics*, 8(3):478–483, 1967.

[Gri99] Geoffrey Grimmett. Percolation. Springer, 1999.

[Gri04] Geoffrey Grimmett. The random-cluster model. In *Probability on discrete structures*, pages 73–123. Springer, 2004.

[Gri14] Geoffrey R Grimmett. Criticality, universality, and isoradiality. *arXiv preprint arXiv:1404.2831*, 2014.

[Har01] Peter JF Harris. Rosalind franklin's work on coal, carbon, and graphite. *Interdisciplinary Science Reviews*, 26(3):204–210, 2001.

[Hop63] Eberhard Hopf. An inequality for positive linear integral operators. *Journal of Mathematics and Mechanics*, 12(5):683–692, 1963.

[HS13] Clément Hongler and Stanislav Smirnov. The energy density in the planar ising model. *Acta mathematica*, 211(2):191–225, 2013.

[HW80] JM Hammersley and DJA Welsh. Percolation theory and its ramifications. *Contemporary Physics*, 21(6):593–605, 1980.

[IC09] Yacine Ikhlef and John Cardy. Discretely holomorphic parafermions and integrable loop models. *Journal of Physics A: Mathematical and Theoretical*, 42(10):102001, 2009.

[IP12] Yacine Ikhlef and Anita K Ponsaing. Finite-size left-passage probability in percolation. *Journal of Statistical Physics*, 149(1):10–36, 2012.

[IWWZJ13] Yacine Ikhlef, Robert Weston, Michael Wheeler, and Paul Zinn-Justin. Discrete holomorphicity and quantized affine algebras. *Journal of Physics A: Mathematical and Theoretical*, 46(26):265205, 2013.

[Jár03] Antal A Járai. Invasion percolation and the incipient infinite cluster in 2d. *Communications in mathematical physics*, 236(2):311–334, 2003.

[K$^+$80] Harry Kesten et al. The critical probability of bond percolation on the square lattice equals 1/2. *Communications in mathematical physics*, 74(1):41–59, 1980.

[Ken99a] Arthur Edwin Kennelly. The equivalence of triangles and three-pointed stars in conducting networks. *Electrical world and engineer*, 34(12):413–414, 1899.

[Ken99b] Arthur Edwin Kennelly. The equivalence of triangles and three-pointed stars in conducting networks. *Electrical world and engineer*, 34(12):413–414, 1899.

[Ken00] Richard Kenyon. Conformal invariance of domino tiling. *Annals of probability*, pages 759–795, 2000.

[Ken02] Richard Kenyon. The laplacian and dirac operators on critical planar graphs. *Inventiones mathematicae*, 150(2):409–439, 2002.

[Ken03] Richard Kenyon. An introduction to the dimer model. *arXiv preprint math/0310326*, 2003.

[Kes86] Harry Kesten. The incipient infinite cluster in two-dimensional percolation. *Probability theory and related fields*, 73(3):369–394, 1986.

[Kes87] Harry Kesten. Scaling relations for 2d-percolation. *Communications in Mathematical Physics*, 109(1):109–156, 1987.

[KS05] Richard Kenyon and Jean-Marc Schlenker. Rhombic embeddings of planar quad-graphs. *Transactions of the American Mathematical Society*, 357(9):3443–3458, 2005.

[KST20a] Laurin Köhler-Schindler and Vincent Tassion. Crossing probabilities for planar percolation. *arXiv preprint arXiv:2011.04618*, 2020.

[KST20b] Laurin Köhler-Schindler and Vincent Tassion. Crossing probabilities for planar percolation. *arXiv preprint arXiv:2011.04618*, 2020.

[Law08] Gregory F Lawler. *Conformally invariant processes in the plane.* Number 114. American Mathematical Soc., 2008.

[Lie67a] Elliott H. Lieb. Exact solution of the f model of an antiferroelectric. *Phys. Rev. Lett.*, 18:1046–1048, Jun 1967.

[Lie67b] Elliott H. Lieb. Exact solution of the two-dimensional slater kdp model of a ferroelectric. *Phys. Rev. Lett.*, 19:108–110, Jul 1967.

[Lie67c] Elliott H. Lieb. Residual entropy of square ice. *Phys. Rev.*, 162:162–172, Oct 1967.

[Lis21] Marcin Lis. On delocalization in the six-vertex model. *Communications in Mathematical Physics*, 383(2):1181–1205, 2021.

[LT20] Piet Lammers and Martin Tassy. Macroscopic behavior of lipschitz random surfaces. *arXiv preprint arXiv:2004.15025*, 2020.

[Mel19] Paul Melotti. *Modèles intégrables de spins, vertex et boucles.* PhD thesis, Sorbonne université, 2019.

[Mer01] Christian Mercat. Discrete riemann surfaces and the ising model. *Communications in Mathematical Physics*, 218(1):177–216, 2001.

[Nie82] B Nienhuis. Exact critical point and critical exponents. *Phys. Rev. Lett*, 49:1062–1065, 1982.

[Nie84] Bernard Nienhuis. Coulomb gas description of 2-d critical behaviour. *J. Stat. Phys*, 34:731–761, 1984.

[Nol08] Pierre Nolin. Near-critical percolation in two dimensions. *Electronic Journal of Probability*, 13:1562–1623, 2008.

[Ons44] L Onsager. A two-dimensional model with an order-disorder transition (crystal statistics i). *Phys. Rev*, 65(3-4):117–149, 1944.

[Pau35] Linus Pauling. The structure and entropy of ice and of other crystals with some randomness of atomic arrangement. *Journal of the American Chemical Society*, 57(12):2680–2684, 1935.

[PAY06] Jacques HH Perk and Helen Au-Yang. Yang-baxter equations. *arXiv preprint math-ph/0606053*, 2006.

[Pen79] Roger Penrose. Pentaplexity a class of non-periodic tilings of the plane. *The mathematical intelligencer*, 2(1):32–37, 1979.

[Pol70] Alexander M Polyakov. Conformal symmetry of critical fluctuations. *JETP Lett.*, 12:381–383, 1970.

[Pon11] Anita Kristine Ponsaing. Finite size lattice results for the two-boundary temperley–lieb loop model. *PhD Thesis, arXiv:1109.0374*, 2011.

[PR15] Ron Peled and Dan Romik. Bijective combinatorial proof of the commutation of transfer matrices in the dense $o(1)$ loop model. *Séminaire Lotharingien de Combinatoire*, 73:B73b, 2015.

[Res10] N Reshetikhin. Lectures on the integrability of the six-vertex model. *Exact methods in low-dimensional statistical physics and quantum computing*, pages 197–266, 2010.

[ros] The rosalind franklin papers - the holes in coal: Research at bcura and in paris, 1942-1951. `https://profiles.nlm.nih.gov/spotlight/kr/feature/coal`. Accessed: 2022-01-17.

[RS20] Gourab Ray and Yinon Spinka. A short proof of the discontinuity of phase transition in the planar random-cluster model with $q > 4$. *Communications in Mathematical Physics*, 378(3):1977–1988, 2020.

[Rus78] Lucio Russo. A note on percolation. *Zeitschrift für Wahrscheinlichkeitstheorie und verwandte Gebiete*, 43(1):39–48, 1978.

[Rys63] Franz Rys. Uber ein zweidimensionales klassisches konfigurationsmodell. In *Helvetica Physica Acta*, volume 36, page 537. BIRKHAUSER VERLAG AG VIADUKSTRASSE 40-44, PO BOX 133, CH-4010 BASEL, SWITZERLAND, 1963.

[SBRN76] H E Stanley, R J Birgeneau, P J Reynolds, and J F Nicoll. Thermally driven phase transitions near the percolation threshold in two dimensions. *Journal of Physics C: Solid State Physics*, 9(20):L553–L560, oct 1976.

[Sch00] Oded Schramm. Scaling limits of loop-erased random walks and uniform spanning trees. *Israel Journal of Mathematics*, 118(1):221–288, 2000.

[She05] Scott Sheffield. *Random surfaces*. Société mathématique de France, 2005.

[Smi01] Stanislav Smirnov. Critical percolation in the plane: conformal invariance, cardy's formula, scaling limits. *Comptes Rendus de l'Académie des Sciences-Series I-Mathematics*, 333(3):239–244, 2001.

[Smi10] Stanislav Smirnov. Conformal invariance in random cluster models. i. holmorphic fermions in the ising model. *Annals of mathematics*, pages 1435–1467, 2010.

[SS09] Oded Schramm and Scott Sheffield. Contour lines of the two-dimensional discrete gaussian free field. *Acta mathematica*, 202(1):21–137, 2009.

[SSG11] Oded Schramm, Stanislav Smirnov, and Christophe Garban. On the scaling limits of planar percolation. *The Annals of Probability*, 39(5):1768–1814, 2011.

[SW78] Paul D Seymour and Dominic JA Welsh. Percolation probabilities on the square lattice. In *Annals of Discrete Mathematics*, volume 3, pages 227–245. Elsevier, 1978.

[Tas16] Vincent Tassion. Crossing probabilities for voronoi percolation. *The Annals of Probability*, 44(5):3385–3398, 2016.

[vK82] Dirk W van Krevelen. Development of coal research—a review. *Fuel*, 61(9):786–790, 1982.

[Wu18] Hao Wu. Polychromatic arm exponents for the critical planar fk-ising model. *Journal of Statistical Physics*, 170(6):1177–1196, 2018.

[ZI77] Jean-Bernard Zuber and Claude Itzykson. Quantum field theory and the two-dimensional ising model. *Physical Review D*, 15(10):2875, 1977.

[ZJ07] Paul Zinn-Justin. Loop model with mixed boundary conditions, qkz equation and alternating sign matrices. *Journal of Statistical Mechanics: Theory and Experiment*, 2007(01):P01007, 2007.